Capillary Zone Electrophoresis, Capillary Isoelectric Focusing, and Ion Exchange Chromatography for the Separation of Antibody Variants on the Intact and Subunit Level with Online Mass Spectrometric Characterization

Dissertation

der Mathematisch-Naturwissenschaftlichen Fakultät

der Eberhard Karls Universität Tübingen

zur Erlangung des Grades eines

Doktors der Naturwissenschaften

(Dr. rer. nat.)

vorgelegt von

Jasmin Schairer

aus Sindelfingen

Tübingen

2025

Gedruckt mit Genehmigung der Mathematisch-Naturwissenschaftlichen Fakultät
der Eberhard Karls Universität Tübingen.

Tag der mündlichen Qualifikation:	26.11.2025
Dekan:	Prof. Dr. Thilo Stehle
1. Berichterstatter/-in:	Prof. Dr. Christian Neusüß
2. Berichterstatter/-in:	Prof. Dr. Michael Lämmerhofer

“As someone told me lately, "Everyone deserves the chance to fly” ”

Stephen Lawrence Schwartz – Defying Gravity - Wicked

Acknowledgment

An dieser Stelle möchte ich mich bei all den Menschen bedanken, die die letzten Jahre an meiner Seite waren und mich unterstützt haben.

Besonderer Dank geht an Prof. Dr. Christian Neusüß. Nicht nur für die initiale Frage in Coronazeiten, ob ich „denn schon einmal über die Promotionsmöglichkeit nachgedacht habe“, sondern auch für die Betreuung, die Gespräche, die Korrekturen und natürlich die Möglichkeit, an so vielen Konferenzen teilzunehmen. Des Weiteren geht ein besonderer Dank an Prof. Dr. Michael Lämmerhofer für die Betreuung der Arbeit vonseiten der Universität Tübingen.

Ein weiterer Dank gilt Jennifer Römer, Dietmar Lang und dem ganzen Team bei Rentschler Biopharma SE, ohne die dieses Projekt gar nicht existiert hätte.

Ein großer Dank gilt Lukas Naumann, Alexander Stolz und Johannes Schlecht, die ihr Wissen im Labor als „alte Hasen“ an mich weitergaben, mir halfen, wenn die Geräte nicht so wollten, wie ich, und die generell immer für Fragen und Diskussionen offen waren. Danke, dass ihr den Start für mich einfach gemacht habt.

Großer Dank gilt auch all den Leuten des in der Zwischenzeit relativ großen AKCN. Alisa Höchsmann, Tobias Waldmann. Lena Kruse, Ann-Katrin Schwenzer, Marcel Hübner, Volker Höfer, Nadine Pejs und Florian Plathe: Ihr wart Leidensgenossen, Diskussionspartner, Ideengeber, Inspiration und manchmal einfach nur ein verrückter Haufen. Aber ich habe gern mit euch die Zeit verbracht.

Danke an Svenja Stocker und Vanessa Fischer für die „Quartalstreffen“ in der Therme, in Restaurants, im Musical oder einfach mal so, die mir immer geholfen haben, zu entspannen und mich daran zu erinnern, dass es auch ein anderes Leben als die Promotion gibt.

Danke an die anderen Mädels, ihr wisst, wer ihr seid (aka Fehler 404), für Musical, Konzert und Kinobesuche, Urlaub und Quatschabende mit Käsefondue.

Ein finaler und besonderer Dank geht an meine Mama und meinen Bruder. Ihr habt mir zugehört, obwohl ihr sicher oft kein Wort von dem verstanden habt, worüber ich da geredet habe. Und vermutlich habt ihr beide euch ab und an gefragt, warum ich das alles überhaupt mache.

Und ganz zum Schluss danke an all die Menschen, die nicht mehr da sind, mich aber zu dem Menschen gemacht haben, der ich heute bin.

Contents

Abbreviations

ACN	Acetonitrile
BGE	Background electrolyte
BPE	Base peak electropherogram
C_H / C_L	Constant subdomains of heavy chain and light chain
CID	Collision-induced dissociation
CIEF	Capillary isoelectric focusing
CRM	Charge residue mode
CZE	Capillary zone electrophoresis
DTT	Dithiothreitol
EACA	6-aminocaproic acid
EIE	Extracted ion electropherogram
EOF	Electroosmotic flow
ESI	Electrospray ionization
ETD	Electron-transfer dissociation
EThcD	ETD and HCD combined
$F(ab')_2$	Antigen-binding fragment
FA	Formic acid
Fc/2	C-terminal half of heavy chain
Fd	N-terminal half of the heavy chain
HAc	Acetic acid
HC	Heavy chain
HCD	Higher-energy collisional dissociation
HIC	Hydrophobic interaction liquid chromatography
HILIC	Hydrophilic interaction liquid chromatography
ICIEF	Imaged capillary isoelectric focusing
IdeS	Immunoglobulin G-degrading enzyme of *Streptococcus pyogenes*
IEX	Ion exchange chromatography
Ig	Immunoglobin
IM	Ion mobility
IRM	Ion routing multipole

LC	Light chain
mAbs	Monoclonal antibodies
MES	2-(N-morpholino)ethane sulfonic acid
MS	Mass spectrometry
Mw	Molecular weight
PEO	Polyethylenoxide
pI	Isoelectric point
PTMs	Posttranslational modifications
PVA	Polyvinyl alcohol
RPLC	Reversed-phase liquid chromatography
SCX	Strong cation exchange chromatography
SEC	Size exclusion chromatography
SL	Sheath liquid
SMIL	Successive multiple ionic-polymer layer
TETA	Triethylenetetramine
TIC	Total ion chromatogram
TIE	Total ion electropherogram
TIMS	Trapped ion mobility spectrometry
TOF	Time of flight
UV	Ultraviolet
V_H / V_L	Variable subdomains of heavy chain (H) and light chain (L)
WCX	Weak cation exchange chromatography

Abstract

The analysis of monoclonal antibodies (mAbs) is an ever-evolving field of research. Depending on the host cell, the purification process, or different storage conditions, mAbs can differ, for example in their glycosylation profile or have alterations of amino acids. The analysis of these post-translational modifications (PTMs) is therefore quite complex and time-consuming and can generally be performed on an intact, subunit, or peptide level by coupling a separation technique with mass spectrometry (MS). The analysis of intact mAbs provides information on the overall variant composition and requires minimal sample preparation, however, it does not allow for detailed information on the position of the protein modification. Analysis at the subunit level enables detailed mass spectrometric characterization by fragmentation experiments and provides valuable information about the position of the modification in the molecule. However, the sample preparation must be carefully examined to guarantee proper sample reduction and to reduce the risk of generating artifacts. Separation is the key to detailed and unambiguous MS analysis of mAb variants, and various separation principles are used in the literature for this purpose.

The general object of this thesis was to investigate capillary zone electrophoresis (CZE), capillary isoelectric focusing (CIEF), and ion exchange chromatography (IEX) coupled with MS for their performance in analyzing charge variants of antibodies at the intact and subunit level. The newly developed CZE-MS method at the subunit level enabled the selective separation of several size variants (e.g. glycosylation variants) and charge variants (e.g. c-terminal lysine clipping) as well as multiple other variants (e.g. additional glycation) and reduced variants. Initially, the subunits were incompletely reduced, which caused a large heterogeneity of different subunit moieties, various reduction states, and positional isomers of these partly-reduced subunit moieties. This artificial heterogeneity could be separated by the new CZE method and the location of the variants was determined by middle-down electron transfer higher energy collisional dissociation (EThcD) experiments. Middle-down fragmentation was crucial for detecting the site specificity of the incompletely reduced subunit moieties, especially for the CZE-separated positional isomers. Overall fragmentation coverages between 10% (incompletely reduced subunit) and 30% (completely reduced subunit) could be obtained. Fragmentation

was also valuable for the determination of other site-specific mAb variants. The informational output was limited when positional isomers of mAb variants were not previously separated. Subunit moieties were additionally analyzed by ion mobility (IM) -MS and different ion mobilities for the different variants were obtained. CZE and IM were so far scarcely coupled most likely because the separation of these techniques is based on similar separation mechanisms. For the first time, the orthogonality of CZE and IM was therefore evaluated by analyzing a complex peptide mixture (tryptic digest of HeLa proteins), and a very high orthogonality of around 80% was obtained. The artificial heterogeneity caused by incomplete sample reduction complicated the charge variant analysis of mAb subunits which was solved by the addition of urea as a chaotropic salt in the reduction step. Depending on the mAb this urea addition led to full sample reduction and the identification of 10 – 40 mAb variants.

Additionally, to the successful CZE-MS subunit approach, CZE-MS was performed on the intact level. CIEF-MS and IEX-MS were both performed on an intact level only. CZE-MS enabled the selective separation of several size variants (e.g. glycosylation variants) and charge variants (e.g. C-terminal lysine) as well as multiple other variants (e.g. additional glycation) and reduced variants. IEX-MS and CIEF-MS enabled the separation and detection of several size variants (e.g. glycosylation variants) and charge variants (e.g. C-terminal lysine) as well as the detection of some minor mass changes of the antibody compared to the main form on the intact mAb level. The high resolving power of all three methods was evaluated based on the lysine variant of several mAbs and the different method selectivities were revealed by the monoglycosylation, which was found in the main peak of CEX and CIEF, while it was separated from the main peak by CZE. Even though CIEF-MS using online ultraviolet (UV) detection proved to selectively separate multiple mAb variants, CIEF-MS needs further improvement since some mAbs in the sample set encountered solubility problems when the near-native mAb was mixed with acidic sheath liquid for MS ionization. IEX-MS suffered from high ion suppression but the selective variant separation detected by online UV detection could be contained towards the MS.

Overall, the presented separation methods show a separation of acidic and basic variants from the main form of the mAb. The methods were tested using a sample

set of ten mAbs without any mAb-specific method optimization. This highlights the generic application of these methods within the tested pI range. The online UV detection was supplemented by detailed variant characterization and identification using mass spectrometry and ion mobility. This combination of techniques allowed an in-depth analysis of the variants of the mAb samples.

Zusammenfassung

Die Analyse monoklonaler Antikörper (mAbs) ist ein sich ständig weiterentwickelndes Forschungsgebiet. Je nach Wirtszelle, Reinigungsverfahren oder Lagerungsbedingungen können sich mAbs zum Beispiel in ihrem Glykosylierungsprofil unterscheiden oder Veränderungen der Aminosäuren aufweisen. Die Analyse dieser posttranslationalen Modifikationen (PTMs) ist daher komplex und zeitaufwändig. Sie kann im Allgemeinen auf intakter, Untereinheiten- oder Peptidebene durchgeführt werden, indem man eine geeignete Trenntechnik mit der Massenspektrometrie (MS) koppelt. Die Analytik intakter mAbs liefert Informationen über die Gesamtzusammensetzung der Varianten und erfordert nur eine minimale Probenvorbereitung, jedoch wird auf der intakten Ebene keine detaillierte Information über die Position der Proteinmodifikation erhalten. Die Analyse auf Untereinheitsebene ermöglicht eine detaillierte massenspektrometrische Charakterisierung durch Fragmentierungsexperimente und liefert wertvolle Informationen über die Position der Modifikation im Molekül. Die Probenvorbereitung muss jedoch sorgfältig durchgeführt werden, um eine ordnungsgemäße Probenreduktion zu gewährleisten und das Risiko der Artefaktbildung zu verringern. Die Trennung von mAb-Varianten ist essentiell für eine detaillierte und eindeutige MS-Analyse. In der Literatur werden zu diesem Zweck verschiedene Trennungsprinzipien verwendet.

Das Ziel dieser Arbeit war, die Kapillarzonenelektrophorese (CZE), die kapillare isoelektrische Fokussierung (CIEF) und die Ionenaustauschchromatographie (IEX) in Kopplung mit MS auf ihre Leistungsfähigkeit bei der Analyse von Ladungsvarianten von Antikörpern auf intakter und Untereinheitenebene zu untersuchen. Die neu entwickelte CZE-MS-Methode auf Untereinheitenebene ermöglichte die selektive Trennung mehrerer Größenvarianten (z. B. Glykosylierungsvarianten) und Ladungsvarianten (z. B. C-terminales Lysin) sowie mehrerer anderer Varianten (z. B. zusätzliche Glykierung) und reduzierter Varianten. Initial waren die Untereinheiten unvollständig reduziert, was zu einer großen Heterogenität aus verschiedenen Untereinheiten, verschiedenen Reduktionszuständen und Positionsisomeren führte. Diese künstliche Heterogenität konnte durch die neue CZE-Methode getrennt und die Position der Varianten durch middle-down Fragmentierungsexperimente bestimmt werden. Die

Fragmentierung war entscheidend für den Nachweis der Ortsspezifität, insbesondere der getrennten Positionsisomere und insgesamt konnten Fragmentierungsabdeckungen zwischen 10 % (unvollständig reduzierte Untereinheit) und 30 % (vollständig reduzierte Untereinheit) erzielt werden. Die Fragmentierung war auch für die Bestimmung anderer ortsspezifischer mAb-Varianten wertvoll und nur dann begrenzt, wenn die Positionsisomere der mAb-Varianten nicht vorher getrennt wurden. Die Untereinheiten wurden zusätzlich erstmals mittels Ionenmobilitäts-Massenspektrometrie (IM-MS) analysiert. Die Ergebnisse zeigen unterschiedliche Ionenmobilitäten für die verschiedenen Varianten. CZE und IM wurden bisher kaum gekoppelt, vermutlich aufgrund der ähnlichen Trennmechanismen beider Techniken. Zum ersten Mal wurde daher die Orthogonalität von CZE und IM durch die Analyse eines komplexen Peptidgemischs (tryptischer Verdau von HeLa-Proteinen) evaluiert. Eine sehr hohe Orthogonalität von etwa 80% wurde dabei erzielt. Die Heterogenität, die durch die unvollständige Probenreduktion verursacht wird, erschwerte die Analyse der Ladungsvarianten der mAb-Untereinheiten. Dies wurde durch die Zugabe von Harnstoff als chaotropes Salz im Reduktionsschritt behoben und führte je nach mAb zur Identifikation von 10 - 40 mAb-Varianten.

Zusätzlich zum erfolgreichen CZE-MS-Untereinheiten-Ansatz wurde CZE-MS auf intakter Ebene durchgeführt. CIEF-MS und IEX-MS wurden beide nur auf intakter Ebene durchgeführt. CZE-MS ermöglichte die selektive Trennung mehrerer Größenvarianten (z. B. Glykosylierungsvarianten) und Ladungsvarianten (z. B. C-terminales Lysin) sowie mehrerer anderer Varianten (z. B. zusätzliche Glykierung) und reduzierter Varianten. IEX-MS und CIEF-MS ermöglichten die Trennung und den Nachweis mehrerer Größenvarianten (z. B. Glykosylierungsvarianten) und Ladungsvarianten (z. B. C-terminales Lysin) sowie den Nachweis einiger geringfügiger Massenänderungen des Antikörpers. Das hohe Auflösungsvermögen aller Methoden wurde anhand der Lysin-Variante berechnet. Die unterschiedlichen Selektivitäten der Methoden wurden anhand der Monoglykosylierung deutlich, die bei CEX und CIEF im Hauptpeak detektiert wurde, während sie bei CZE vom Hauptpeak getrennt wurde. Obwohl die CIEF-MS mit Online-UV-Detektion eine selektive Trennung mehrerer mAb-Varianten ermöglichte, muss die CIEF-MS weiter verbessert werden, da einige mAbs

Löslichkeitsprobleme aufwiesen, wenn der nahezu native mAb für die MS-Ionisierung mit saurer Schleierflüssigkeit gemischt wurde. IEX-MS litt zwar unter einer hohen Ionensuppression, aber die selektive Trennung der Varianten, wurde sowohl online-UV als auch im MS detektiert.

Insgesamt zeigen die vorgestellten Trennmethoden eine Trennung der sauren und basischen Varianten von der Hauptform des mAbs. Zehn mAbs wurden ohne eine mAb-spezifische Methodenoptimierung mit jeder Methode gemessen. Dies unterstreicht die generische Anwendbarkeit dieser Methoden innerhalb des getesteten pI-Bereichs. Die Online-UV-Detektion wurde durch detaillierte Charakterisierung und Identifizierung mittels Massenspektrometrie und Ionenmobilität ergänzt. Diese Kombination von Techniken ermöglichte eine tiefgreifende Analyse der mAb Varianten.

List of Publications

Accepted Manuscripts

I. CE-MS/MS and CE-timsTOF to separate and characterize intramolecular disulfide bridges of monoclonal antibody subunits and their application for the assessment of subunit reduction protocols
Jasmin Schairer, Jennifer Römer, Dietmar Lang, Christian Neusüß
Analytical and Bioanalytical Chemistry. 2024; 416: 1599–612
DOI: 10.1007/s00216-024-05161-8

II. Ion mobility in gas and liquid phases: How much orthogonality is obtained in capillary electrophoresis-ion mobility-mass spectrometry?
Jasmin Schairer, Florian Plathe, Sonja Hudelmaier, Eckhard Belau, Stuart Pengelley, Lena Kruse, Christian Neusüß
Electrophoresis. 2024; 45: 735-742. DOI: 10.1002/elps.202300210

III. CE-MS and CE-MS/MS for the multiattribute analysis of monoclonal antibody variants at the subunit level
Jasmin Schairer, Jennifer Römer, Christian Neusüß
Journal of pharmaceutical and biomedical analysis. 2025; 252: 116495. DOI: 10.1016/j.jpba.2024.116495

IV. Ion-exchange chromatography, capillary isoelectric focusing, and capillary zone electrophoresis coupled to mass spectrometry for charge variant analysis of monoclonal antibodies
Jasmin Schairer, Alisa Höchsmann, Benedikt Bauer, Volker Höfer, Jennifer Römer, Christian Neusüß
mAbs. 2025; 17: 2537116. DOI: 10.1080/19420862.2025.2537116

Other contributions not included in this thesis:

- Capillary Electrophoresis–Mass Spectrometry Interfacing: Principles and Recent Developments In: R Ramautar, DDY Chen, editors. Capillary electrophoresis mass spectrometry for proteomics and metabolomics
Lukas Naumann, Jasmin Schairer, Alisa Höchsmann, Elahe Naghdi, Christian Neusüß
Weinheim:Wiley-VCH. 2022; p. 1–33. DOI: https://doi.org/10.1002/9783527833092.ch1

- Flow rate determination of the nanoflow sheath liquid CE-MS-coupling applying the nanoCEasy interface
  Alisa Höchsmann, Jasmin Schairer, Oliver Schott, Ralf Höneise, Christian Neusüß
  Electrophoresis. 2024; https://doi.org/10.1002/elps.202400191

Author Contribution

Manuscript I

CE-MS/MS and CE-timsTOF to separate and characterize intramolecular disulfide bridges of monoclonal antibody subunits and their application for the assessment of subunit reduction protocols

Jasmin Schairer: Conceptualization, Data curation, Formal analysis, Investigation, Methodology, Visualization, Writing – original draft

Jennifer Römer: Project administration, Resources, Supervision, Writing – review & editing

Dietmar Lang: Project administration, Resources, Supervision, Writing – review & editing

Christian Neusüß: Corresponding author, Conceptualization, Funding acquisition, Project administration, Resources, Supervision, Writing – review & editing

Manuscript II

Ion mobility in gas and liquid phases: How much orthogonality is obtained in capillary electrophoresis-ion mobility-mass spectrometry?

Jasmin Schairer: Conceptualization, Data curation, Formal analysis, Investigation, Methodology, Visualization, Writing – original draft

Florian Plathe: Data curation, Visualisation

Sonja Hudelmaier: Data curation, Visualisation

Eckard Belau: Data curation, Supervision

Stuart Pengelley: Data curation, Supervision, Writing – review & editing

Lena Kruse: Formal analysis, Writing – review & editing

Christian Neusüß: Corresponding author, Conceptualization, Project administration, Resources, Supervision, Writing – original draft; Writing – review & editing

Manuscript III

CE-MS and CE-MS/MS for the multiattribute analysis of monoclonal antibody variants at the subunit level

Jasmin Schairer: Conceptualization, Data curation, Formal analysis, Investigation, Methodology, Visualization, Writing – original draft

Jennifer Römer: Project administration, Resources, Supervision, Writing – review & editing

Christian Neusüß: Corresponding author, Conceptualization, Funding acquisition, Project administration, Resources, Supervision, Writing – review & editing

Manuscript IV

Ion-exchange chromatography, capillary isoelectric focusing, and capillary zone electrophoresis coupled to mass spectrometry for charge variant analysis of monoclonal antibodies

Jasmin Schairer: Conceptualization, Data curation, Formal analysis, Investigation, CIEF-MS/ IEX-MS methodology, Visualization, Writing – original draft

Alisa Höchsmann: CZE-MS methodology

Benedikt Bauer: IEX-MS methodology

Volker Höfer: CIEF-MS methodology

Jennifer Römer: Project administration, Resources, Supervision, Writing – review & editing

Christian Neusüß: Corresponding author, Conceptualization, Funding acquisition, Project administration, Resources, Supervision, Writing – review & editing

List of oral presentations at scientific conferences

The presenting author is underlined.

I. Characterization of the nanoCEasy CE-MS interface: Analytical properties and flow rates of the nanoflow sheath liquid coupling
Jasmin Schairer, Alexander Stolz, Johannes Schlecht, Christian Neusüß
24th IMSC, Maastricht (Netherlands), August 27th – September 2nd, 2022

II. Capillary electrophoresis coupled to TIMS-TOF mass spectrometry using the NanoCEasy interface
Jasmin Schairer, Lukas Naumann, Stuart Pengelley, Eckhard Belau, Christian Albers, Christian Neusüß
24th IMSC, Maastricht (Netherlands), August 27th – September 2nd, 2022

III. Disulfide characterization of trastuzumab subunits with CE-tims-TOF MS and CE-MS/MS
Jasmin Schairer, Christian Neusüß
33rd Ph.D. meeting on separation science (Doktorandenseminar des AK Separation Science), Hohenroda (Germany), January 8th - January 10th, 2023

IV. Intramolecular disulfide separation and characterization of trastuzumab subunits with CE-MS/MS
Jasmin Schairer, Jennifer Römer, Dietmar Lang, Christian Neusüß
54th Annual Conference of the DGMS, Dortmund (Germany), May 14th -May 17th, 2023

V. Intramolecular disulfide and charge variant separation and characterization of various antibody subunits with CE-MS/MS
Jasmin Schairer, Jennifer Römer, Christian Neusüß
40th MSB, Brno (Czech Republic), May 19th – May 22nd, 2024

VI. Charge variant separation and characterization of various antibodies using CZE-MS, cIEF-MS, and IEX-MS on intact and subunit level
Jasmin Schairer, Christian Neusüß
34th PBA, Geneva (Suisse), September 9th September 12th, 2024

List of poster participations at scientific conferences

The presenting author is underlined.

I. Capillary electrophoresis coupled to timsTOF Mass Spectrometry using the nanoCEasy interface
Lukas Naumann, Jasmin Schairer, Stuart Pengelley, Eckhard Belau, Christian Albers, Yun Yang, Christian Neusüß
70th ASMS, Minneapolis (USA), June 5th – June 9th, 2022

II. Coupling capillary electrophoresis with timsTOF Mass Spectrometry using the nanoCEasy interface
Jasmin Schairer**,** Lukas Naumann, Lena Kruse, Stuart Pengelley, Eckhard Belau, Christian Albers, Christian Neusüß
ANAKON 2023, Vienna (Austria), April 11th – April 14th, 2023

III. Coupling capillary electrophoresis with timsTOF Mass Spectrometry using the nanoCEasy interface
Jasmin Schairer**,** Florian Plathe, Sonja Hudelmaire, Lukas Naumann, Lena Kruse, Stuart Pengelley, Eckhard Belau, Christian Albers, Christian Neusüß
54th Annual Conference of the DGMS, Dortmund (Germany), May 14th - May 17th, 2023

IV. Coupling CZE with TIMS-TOF mass spectrometry - Creation of a fast data analysis workflow for PASEF data
Florian Plathe, Sonja Hudelmaier, Jasmin Schairer, Christian Neusüß
13th CE Forum, Aalen (Germany), February 28th – February 29th, 2024

V. Charge variant separation and characterization of various antibodies using CZE-MS, cIEF-MS, and IEX-MS on intact and subunit level
Jasmin Schairer, Christian Neusüß
34th ISC, Liverpool (Great Britain), October 6th -October 10th, 2024

List of Awards

I. Poster Award for “Coupling Capillary Electrophoresis with timsTOF Mass Spectrometry using the nanoCEasy interface”
ANAKON 2023, Wien (Austria), April 11th – April 14th, 2023

II. Young Scientists Award for the oral presentation entitled “Intramolecular disulfide and charge variant separation and characterization of various antibody subunits with CE-MS/MS”
MSB 2024, Brno (Czech Republic), May 19th – May 22nd, 2024

1. Introduction

In the past decade, sales of biopharmaceuticals, especially monoclonal antibodies (mAbs), have continuously increased, and more than 50% of biopharmaceuticals approved for the first time were mAbs [1]. This shows the enormous interest in mAbs but also raises the need for thorough testing and characterization before they can be administered to a patient. Multiple methods are available for the characterization of mAbs, and this thesis aims to have a closer look at three separation approaches coupled with mass spectrometry (MS) for the identification of mAb variants. In the following introduction, an overview is provided of what an antibody is, what modifications can occur, and how these modifications are separated and analyzed. The information given here will help to understand the following investigations of this thesis in the results and discussion section.

1.1 Monoclonal antibodies and variants

1.1.1 Monoclonal antibodies

Monoclonal antibodies are large and complex, y-shaped immunoglobins (Ig) built from four individual protein chains, connected and stabilized by inter- and intra-chain disulfide bridges, and modified by posttranslational modifications (PTMs). The combination of these modalities creates the specific affinity of mAbs against certain antigens. Depending on their heavy chain mAbs can be divided into five classes namely IgA, IgD, IgG, IgE, and IgM [2]. IgG, as the most abundant mAb class, is further divided into subclasses IgG1 to IgG4 according to their relative abundance [2]. Figure 1.1 illustrates a schematic IgG1 (Molecular weight (Mw): ~150 kDa) consisting of two identical heavy chains (HC; Mw: ~50 kDa) and two identical light chains (LC; Mw: ~25 kDa) connected by four interchain disulfide bridges.

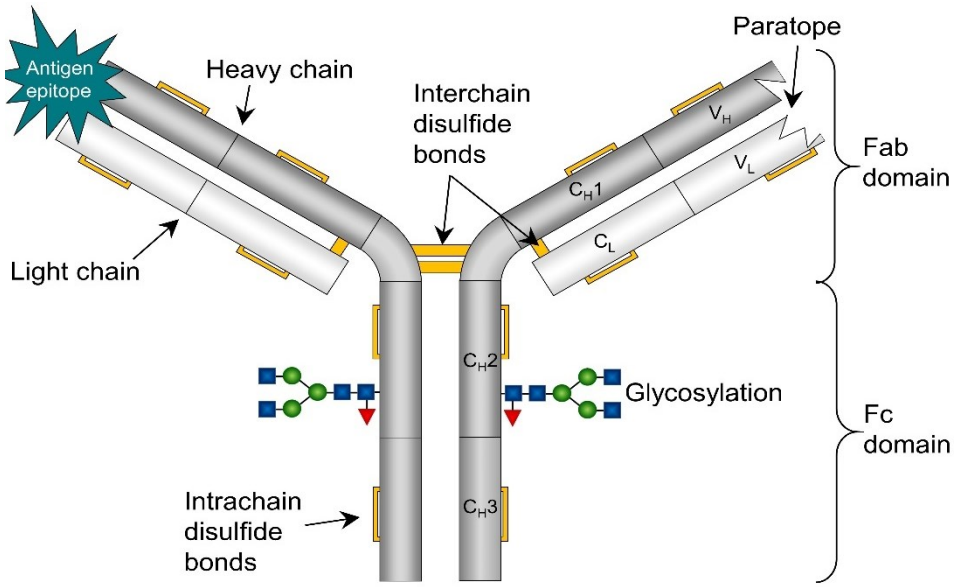

Figure 1.1: Schematic illustration of IgG1 mAb with two identical heavy chains and two identical light chains all connected via four interchain disulfide bridges. The intrachain disulfide bridge at each subdomain results in a total of 16 disulfide bridges in an IgG1 antibody. Fc: C-terminal half of heavy chain, Fab: antigen-binding fragment.

The HC consists of three constant subdomains (C_H1-C_H3) and one variable domain (V_H) while the LC has one constant and one variable subdomain (C_L1 and V_L) [3]. Each subdomain has an additional intrachain disulfide bridge which sums up to a total of 16 disulfide bridges (inter- and intrachain disulfide bridges) within an IgG antibody. The antibody's functionality and safety rely on the amino acid sequence, the protein folding including all essential disulfide bridges, and the PTMs. This requires transcriptional, translational, and post-translational accuracy. Nevertheless, even if the production process is highly controlled mAb variants can be found within biopharmaceuticals which will be discussed in the following chapter.

1.1.2 Monoclonal antibody variants

Monoclonal antibody variants can occur due to different conditions during the production, purification, or storage of the mAb and range from incompletely assembled antibodies to changes in post-translational modifications as shown in Figure 1.2 [4, 5]. While antibody fragments and aggregates can be removed from the biopharmaceutical during downstream processing using ion exchange chromatography (IEX) or affinity chromatography [6] mAb variants are harder to remove.

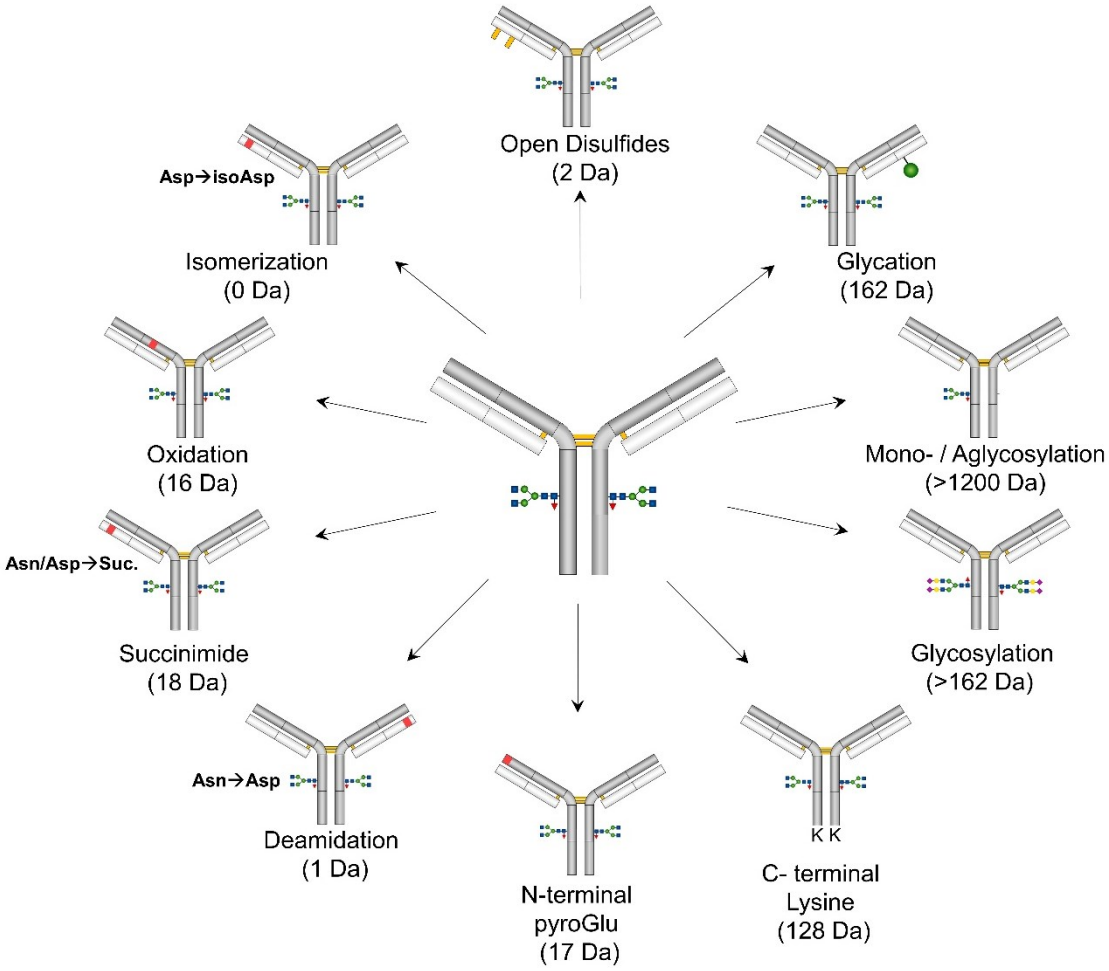

Figure 1.2: Overview of several mAb variants. The modification of specific amino acids is illustrated as a red dot on the mAb. The mass difference induced by the modification is indicated in brackets.

Some PTMs are relatively easy to analyze because they cause a relatively large change in antibody mass, such as the introduction or loss of a hexose unit (e.g. glycosylation and glycation), an incompletely truncated amino acid (e.g. lysine variant) or the introduction of a sugar acid (e.g. sialic acids). Other variants only marginally change the antibody mass due to alterations of amino acids (e.g. pyroGlu formation, oxidation, isomerization, succinimide, deamidation), or errors in the disulfide bridge formation and are therefore much harder to determine. Variants can be classified as acidic or basic depending on their change in isoelectric point (pI). For example, lysine variants introduce a positive charge and therefore lead to basic variants [7]. Deamidations, where the net charge is reduced, lead to acidic variants [8] and other modifications like pyroGlu, oxidations, succinimide formations, or isomerizations can be acidic or basic depending on the amino acid the modification is present [9]. All PTMs potentially have effects on the stability, functionality, or safety of the mAb. The mAb glycosylation profile can differ

depending on the expression host and play a critical role in mAb structure, stability, and functions [10, 11]. Oxidations at specific methionine moieties result in a destabilization of the C_H2 domain and decrease neonatal fragment crystallizable receptor binding [12, 13]. Deamidation can decrease the antibody-dependent cellular cytotoxicity activity [14], and reduced disulfide bridges affect the mAbs thermal stability and domain stability [15, 16]. Even though C-terminal lysin [17] and N-terminal pyroGlu [18] have no impact on mAb structure and function, these variants are also closely monitored, especially between batches, to detect changes in the heterogeneity profile and to guarantee product safety.

1.2 Strategies for the characterization of monoclonal antibodies

Monoclonal antibodies can be analyzed on multiple levels with different amounts of sample preparation. Especially when coupled with MS (detailed information in chapter 1.4), sample preparation can be crucial regarding the informational output.

The intact level allows the determination of the overall mAb composition including all modifications. The analysis of mAbs and mAb variants at an intact level is a relatively fast approach. As illustrated in Figure 1.3 no sample preparation is needed except that sometimes mAbs are rebuffered before the analysis [19–21]. Due to the minimal sample preparation, artifact formation is low. However, the informational output of the intact approach is limited since the separation of mAb variants is more challenging especially whenever multiple variants are present on the mAb. Unseparated variants can cause ion suppression in the MS and reduced spectral quality especially if the overall mass of the variant is not significantly different from the main form. For more information fragmentation of the intact mAb is possible, however it requires special instrumentation and the fragmentation coverages are limited [22–24].

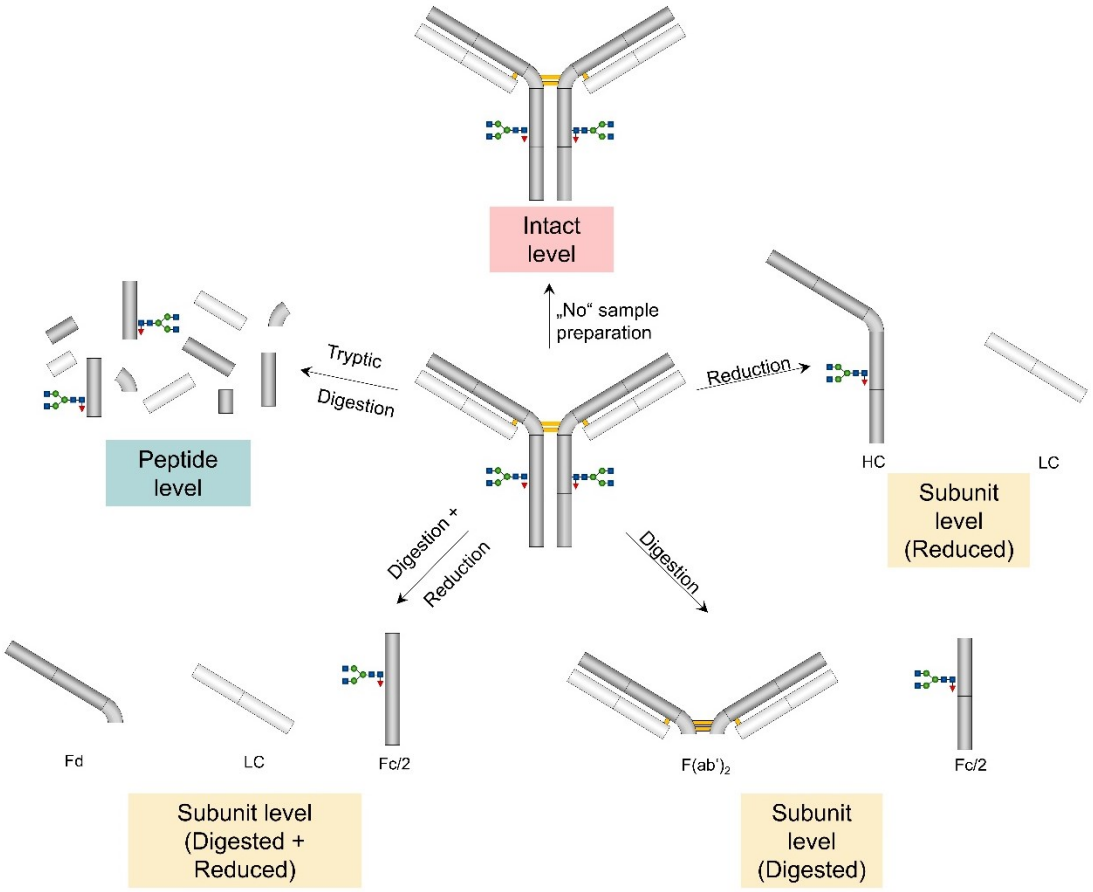

Figure 1.3: Different sample preparation approaches for mAb analysis. Each approach takes a different amount of time (intact level<subunit level< peptide level) and can provide different informational output. HC: heavy chain, LC: light chain, Fd: N-terminal half of the heavy chain, Fc/2: C-terminal half of heavy chain, $F(ab')_2$: antigen-binding fragment.

Compared to the intact level the peptide level shown in Figure 1.3 allows the exact determination of the mAb variant within the peptide. This approach is time-consuming, requires the most sample preparation steps, and artifacts can be introduced during the sample preparation if not executed properly [25, 26]. The sample preparation procedure involves five general steps; cleanup and initial sample dilution are not counted. The steps are (I) protein denaturation, (II) protein reduction, (III) protein alkylation, (IV) tryptic digest, and (V) sample cleanup, quench, or dilution [25, 27–29]. Especially the tryptic digest is time-consuming, increasing sample preparation time to hours [29] or even days [25, 27, 28]. Although sample preparation is excessive and the overall mAb information is lost, detailed mAb variant information is gained because peptides can be easily fragmented in the MS. Additionally, the complexity of the whole mAb is reduced, and the peptides can be analyzed by standard reversed-phase liquid chromatography (RPLC) using a relatively simple C18 RPLC-MS and MS/MS

approach [25, 26, 29]. A compromise and a combination of the benefits of the intact and peptide levels is the subunit level. Similar to the peptide level, this approach reduces sample complexity by digesting the mAb to smaller subunits, making them more accessible for fragmentation and simplifying the separation. Similar to the intact approach the sample preparation is kept to a minimum to prevent artifact formation and to reduce sample preparation time to a few hours. As shown in Figure 1.3 the subunit level is reached whenever a mAb is either enzymatically digested [30, 31], reduced [32, 33], or a combination of both [30, 34–36]. Depending on the approach, the 150 kDa mAb is broken down to 25 kDa – 100 kDa subunit moieties. The final approach has to be chosen based on the analytical question. In this thesis, mAbs were analyzed on the intact and subunit level (enzymatically digested and reduced) to keep sample preparation to a minimum and prevent artifact formation.

1.3 Separation approaches

Separation is key for ultraviolet (UV) or MS detection and identification of mAb variants. Antibody variants can be analyzed with almost every liquid-based separation technique as long as the selectivity of the separation is sufficient. Variants can be analyzed using RPLC, hydrophilic interaction liquid chromatography (HILIC), hydrophobic interaction liquid chromatography (HIC), size exclusion chromatography (SEC), ion exchange chromatography (IEX), capillary zone electrophoresis (CZE), capillary isoelectric focusing (CIEF), and in various combinations including multidimensional approaches [37]. This chapter aims to introduce the three separation techniques CZE, IEX, and CIEF used for mAb charge variant separation in this thesis.

1.3.1 Capillary zone electrophoresis

As discussed in chapter 1.1.2 many mAb variants are size and charge modifications which make them prone to CZE separation. A widely applied, generic, selective, and efficient CZE-UV system for mAb variant separation was published a decade ago by He et al. [38]. A typical CZE set-up consists of a capillary filled with a conductive liquid, the so-called background electrolyte (BGE), whose ends are immersed in vials of BGE (inlet and outlet reservoirs). Detection is mostly done using UV or MS. A schematic CZE-UV setup is shown in Figure 1.4.

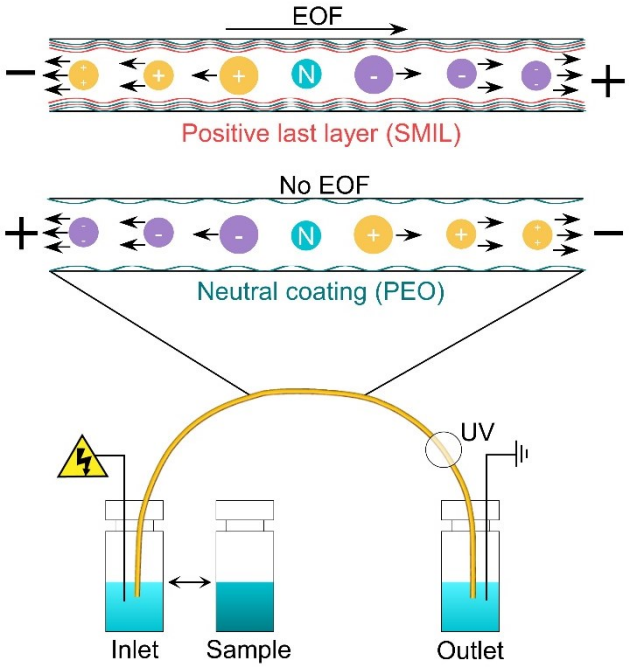

Figure 1.4: Simple capillary electrophoresis setup using an UV detector. Both capillary ends are immersed in BGE to close the electric circuit. Capillaries are coated to prevent protein adsorption to the capillary wall. Migration order neutral coated capillary (no electroosmotic flow (EOF)): positively charged species (neutral and negatively charged analytes do not reach the detector); Migration order positive last layer coated capillary (strong EOF): negative>neutral>positive species.

Samples are either injected electrokinetically or hydrodynamically from a sample reservoir [39]. For electrokinetic injection, a voltage is applied to a sample reservoir while hydrodynamic injection uses pressure to inject the sample [40]. After injection, the separation voltage is applied to the inlet and outlet reservoir via the electrodes. In CZE molecules are separated based on their mobility in an electric field. Small, highly charged species have a higher mobility and migrate faster compared to large, minimally charged species [39]. This can be used for mAb variant separation. However, proteins can not be analyzed in a fused silica capillary since they tend to stick to the silica surface. Therefore, the capillary wall is coated for mAb variant analysis [41]. Neutral coatings like polyethylene oxide (PEO) suppress protein adsorption [42] and the migration is solely based on the mobility of the variants in the electric field (compare Figure 1.4; neutral coating (PEO)). As a result, in an acidic BGE, negatively charged and neutral components will not be detected since they either migrate to the inlet reservoir (negatively charged components) or do not migrate at all (neutral components). Positively charged mAbs and mAb variants on the other hand migrate towards the detector and can therefore be separated and analyzed. E.g. mAbs with sialylated glycans will migrate later (acidic variants) compared to other variants since the overall positive

charge of the protein is reduced by the sialic acid and the molecule size is slightly increased. Other capillary coatings like the successive multiple ionic-polymer layer (SMIL) provide a strong electroosmotic flow (EOF, compare Figure 1.4; positive last layer (SMIL)). The EOF is a bulk flow that develops when the electric field is applied and a diffuse double layer is created [39]. The EOF is strongly pH-dependent and varies based on the capillary coating [39, 43]. In EOF-based separation systems using an acidic BGE, the migration behavior is therefore highly influenced by that EOF and the migration order is reversed compared to the PEO-coated capillary [44]. Negatively charged components are migrating first because they are migrating with the EOF, followed by neutral species which are transported by the EOF. Positively charged mAbs and mAb variants migrate against the EOF. E.g. sialylated glycans will now elute earlier compared to other variants since the reduced positive charge reduces the ability of the variant to migrate against the EOF. By adjusting the EOF strength the resolution can therefore be optimized to a certain extent [43]. Both neutral and positive last-layer coated capillaries were used in this thesis for mAb variant analysis.

1.3.2 Ion exchange chromatography

Charge differences of mAb variants can also be separated by IEX. In IEX, charged and immobilized stationary phases are used, and the separation is achieved due to electrostatic interactions of the molecules with that stationary phase. Even though anion exchange columns can be used for the separation of mAb variants [45, 46] this chapter will focus on the more commonly applied cation exchange columns. Cation exchange columns have a negatively charged stationary phase material mostly sulfopropyl or carboxymethyl for strong and weak cation exchange respectively, which interacts with the cations in the sample [47]. Strong cation exchange chromatography (SCX) and weak cation exchange chromatography (WCX) can be used, however, SCX columns are fully ionized over a broad pH range while WCX columns are only partially ionized over a narrow pH range [47]. As a result, stronger eluents might have to be applied to the SCX column. Figure 1.5 shows the cation exchange chromatography principle.

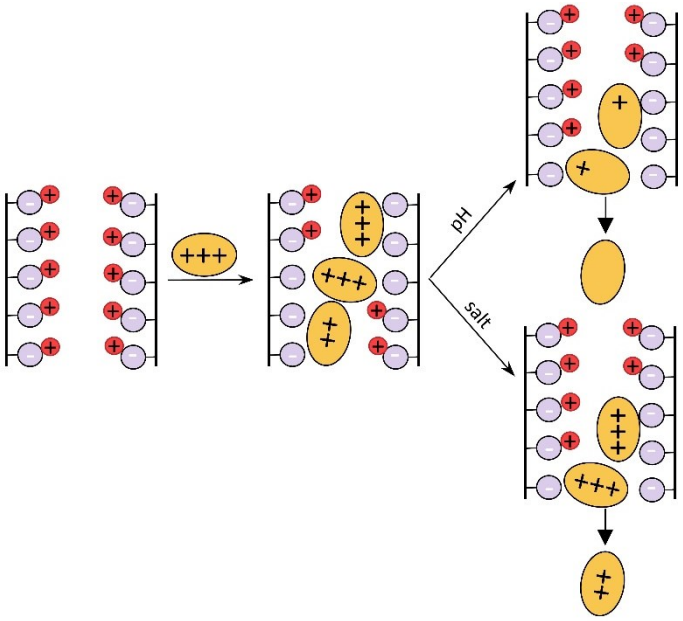

Figure 1.5: Cation exchange principle. First positively charged molecules interact with the stationary phase of the column. The elution is done by changing the pH (reducing the positive charge of the molecule) or introducing salts (displacement of molecules from the column). A combination of both elution mechanisms can be used.

The positively charged proteins bind via the electrostatic interaction to the negatively charged column material. The strength of this bond depends on the PTMs of the mAb and on the pH of the eluents which both directly affect the charge of the protein. For example, on a cation exchange column, mAbs with sialylated glycans will elute earlier (acidic variants) compared to other mAbs since the overall positive charge of the protein is reduced by the sialic acid. Proteins are eluted from the strong cation exchange column by either increasing the pH and therefore reducing the charge of the protein or by adding salts that displace the proteins from the column (compare elution principles in Figure 1.5). Studies compared pH and salt-based elution gradients and showed good separation of mAb variants no matter which approach was used [48–50]. However, especially salt gradients are often a problem when it comes to MS detection due to the use of involatile substances like 2-(N-morpholino)ethanesulfonic acid (MES) [48, 50] or sodium chloride [49]. This is why MS-based separation approaches mainly work with ammonium acetate-based eluents which are often used as combined salt and pH gradients [31, 51].

1.3.3 Capillary isoelectric focusing

The differences in mAb variant pI values can be used to separate them in the pH gradient and electric field of a CIEF method. This approach, done in neutrally coated capillaries to prevent protein adsorption and EOF formation, consists of two distinct steps which are illustrated in Figure 1.6.

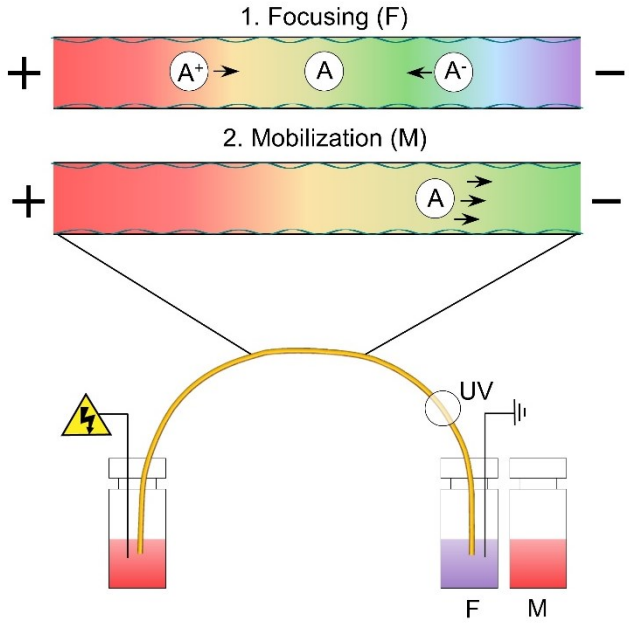

Figure 1.6: Simple capillary isoelectric focusing setup using UV detection. First step: Focusing (F). The capillary is fully flushed with antibody (A) and ampholyte solution. Negative species migrate to the anode and positive ones toward the cathode when a separation voltage is applied. Second step: Chemical mobilization (M). The cathode vial is switched from an alkaline to an acidic solution which successively dissolves the pH gradient.

For the first step, the focusing step, a homogeneous pH gradient is needed. This homogenous pH gradient is achieved by first fully flushing the capillary with an antibody-ampholyte mixture, followed by dipping the ends in acidic and alkaline solutions and applying a separation voltage. In the beginning, the ampholytes are cationic or anionic depending on their pI values and the pH of the antibody-ampholyte mixture. After the voltage is applied, the ampholytes start to separate. Negatively charged ampholytes migrate toward the positive electrode (anode) and positively charged ampholytes toward the negative electrode (cathode) which causes a high pH at the cathode and a low pH at the anode [52]. Ampholytes will stop moving in the electric field at their respective pI and are ideally evenly distributed over the whole pH range [53]. The establishment of the pH gradient and the focusing of the antibody are done at the same time [52]. The antibody will stop

migrating, similar to the ampholytes, once it reaches its pI. The second step, the mobilization step, transfers the focused antibodies to the UV detector. For this pressure can be applied (hydrodynamic mobilization) or the pH gradient can be dissolved (chemical mobilization) by exchanging the alkaline solution for an acidic solution [54]. When pressure is used for the mobilization, the hydrodynamic flow profile can lead to peak broadening which can be counteracted by applying the focusing voltage during mobilization [52]. Nevertheless, pressure-driven mobilization often reduces the resolution. The chemical mobilization prevents peak broadening since there is no hydrodynamic flow or EOF and the focused antibodies migrate according to the charge they get due to the dissolving of the pH gradient [54]. Still, some resolution might be lost whenever focused analytes are mobilized. There are CIEF systems available, that do not mobilize the separated mAbs at all which provides faster and higher resolved analysis results. These imaged capillary isoelectric focusing (ICIEF) systems monitor the whole separation channel via UV which makes mobilization redundant [55, 56]. Even though CIEF and ICIEF are great methods for variant separation when UV detection is used, MS detection is still challenging due to the mostly non-volatile ampholytes and the necessary mobilization. However, in recent years approaches have shown that CIEF and ICIEF can successfully be coupled to MS [21, 57–59].

1.4 Mass spectrometry

After the mAb variant separation using one of the previously discussed techniques, mAb variants must be identified and characterized. UV enables the visualization of charge variant separation and the analysis of a relative charge variant distribution, however, lacks any information on the nature of a separated variant. Therefore, MS is highly desirable to characterize charge variants in detail. The overall antibody composition as well as changes in mass due to mAb variants can be identified using MS. For site-specific information, the mAb has to be further fragmented using MS/MS experiments. The following chapter will briefly introduce the electrospray ionization (ESI) process, the CZE-MS and CIEF-MS coupling using the nanoCEasy interface (IEX was coupled using a standard ESI source), and the mass spectrometers and fragmentation approaches used in this thesis.

1.4.1 Electrospray ionization of proteins

Whenever a liquid-based separation system is coupled to MS, the ions have to be transferred from the liquid to the gas phase, for which the ESI process is widely used. The ESI process consists of three steps: (I) droplet creation in an electric field, (II) desolvation and shrinking of droplets, and (III) formation of charged gas-phase ions [60]. In the first step, the so-called Taylor Cone is formed. This happens as soon as the critical field strength is reached and the surface tension is overcome by the electrostatic forces [61]. This leads to a fine jet of charged droplets. On their way to the counter electrode, the charged droplets get dried, for which a dry gas can be used. The shrinking of the droplets increases the charge density on the surface. As soon as the surface charge density overcomes the surface tension (Rayleigh limit), Coulomb repulsions occur, resulting in smaller but still charged droplets. This process is repeated several times until, in the last step, charged gas phase ions remain [60, 61]. For this last step, two main models are accepted, the ion evaporation model and the charge residue model (CRM) [60, 61]. Antibodies follow the CRM (compare Figure 1.7). This model assumes that at the end of a cascade of Coulomb repulsions, a sufficiently small droplet remains that only contains one analyte molecule [61]. This molecule then retains part of the droplet charge and becomes a free gas-phase ion [60].

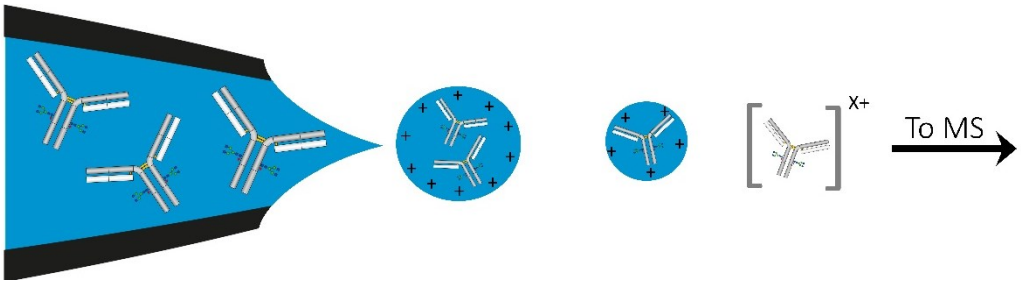

Figure 1.7: Charge residue model (CRM) of the ESI process.

1.4.2 CZE-MS coupling

CZE-MS coupling is challenging due to two aspects. First, the CZE effluent is variable depending on the EOF, and second, both CZE and MS require a specific voltage in different orders of magnitude. Various concepts are available which were discussed by Naumann et al. [62], but here only a short introduction is given. Some interfaces are commercially available, but they all suffer from drawbacks. The coaxial sheath flow ESI-MS interface (Agilent: triple tube sprayer) suffers from high

sample dilution because the full sheath liquid (SL) flow has to go to the MS [63]. Porous Tip interfaces are limited in BGE composition because the BGE is also used as a conductive liquid and therefore must be a compromise between the optimal conditions for the CZE separation and the ESI process [63]. Interfaces commercialized by specific vendors are often only applicable to specific MS instruments. A few years ago, the working group of Christian Neusüß came up with the nanoCEasy interface, a universally applicable interface that reduces sample dilution while being fully flexible [64]. A schematic of the interface setup can be found in Figure 1.8.

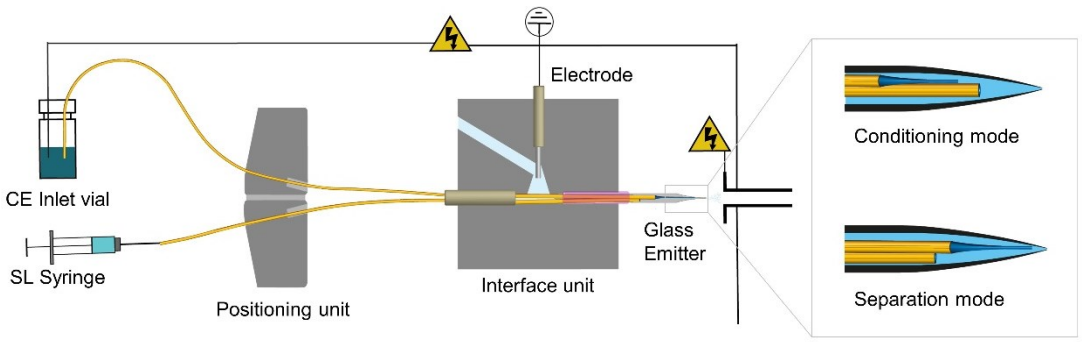

Figure 1.8: Basic setup of the nanoCEasy CE-MS coupling. The two capillaries are introduced to the glass emitter in the interface unit via the positioning unit. The platinum electrode closes the electric circuits and enables the application of up to 30 kV separation voltage while using 1500 V ES voltage.

The interface consists of two 3D-printed polymer blocks, the interface and the positioning unit [64]. A glass emitter is introduced into the interface unit and the separation and SL capillary are placed at the tip of that glass emitter via the positioning unit. The setup is completed by a platinum electrode and a PEEK tubing for the drain. This plug-and-play design enables fast and easy interface setup [64]. The nanoCEasy interface can e.g. significantly increase the signal intensity of HC and LC of mAbs compared to the coaxial sheath flow ESI-MS interface which was shown by Höcker et al. [63]. The interface is flexible in BGE choice as it was applied for multiple separation systems [43, 58, 65, 66] and can be coupled so far to MS instruments from Thermo and Bruker [64]. Additionally, MS contamination can be reduced because the interface has a kind of valving functionality given by the movable SL and CZE capillary [67]. In the conditioning mode, the CZE capillary is positioned behind the SL capillary and the CZE effluent is flushed into the drain. This prevents MS contamination with incompatible solutions like capillary coating reagents or sample matrix components. In the separation mode, the capillary

positions are switched. Recently the interface was tested for robustness regarding the applied electrospray voltage, emitter distance, and capillary distance [64] and was even further characterized regarding its total flow rate in the context of sample dilution [68].

1.4.3 Time of flight mass spectrometry

The time of flight (TOF) principle is fairly simple. As shown in Figure 1.9 all ions from the ion source are forced into a beam which enters the orthogonal accelerator if no fragmentation or precursor selection is done in the quadrupole or collision cell of the instrument. A package of this beam is then orthogonally accelerated (pulsed) into the flight tube. While this ion package covers the distance of the flight tube the orthogonal accelerator can be filled with ions again [61]. In the flight tube, the ions travel the distance according to their mass. The velocity of the ions (v) is inversely proportional to the square root of their mass (m) as given by Equation (1) meaning that lighter molecules will reach the detector faster compared to heavier masses [61].

$$v = \sqrt{\frac{2ezU}{m}} \qquad (1)$$

This difference in time is measured at the detector and translated to the mass of the ion. As soon as the last ion has reached the detector the next ion package can be pulsed into the flight tube. TOF-MS are high-resolution devices with theoretically no m/z limit [69, 70]. Especially the introduced IEX separation of mAb variants under native conditions (compare chapter 1.3.2) results in a mAb charge envelope of 4000-7000 m/z which can not be measured with e.g. the Orbitrap fusion Lumos that only covers an m/z range up to 6000 m/z [71] (for more information on the orbitrap compare chapter 1.4.4). In this work, a MaXis QTOF from Bruker Daltonics was mostly used.

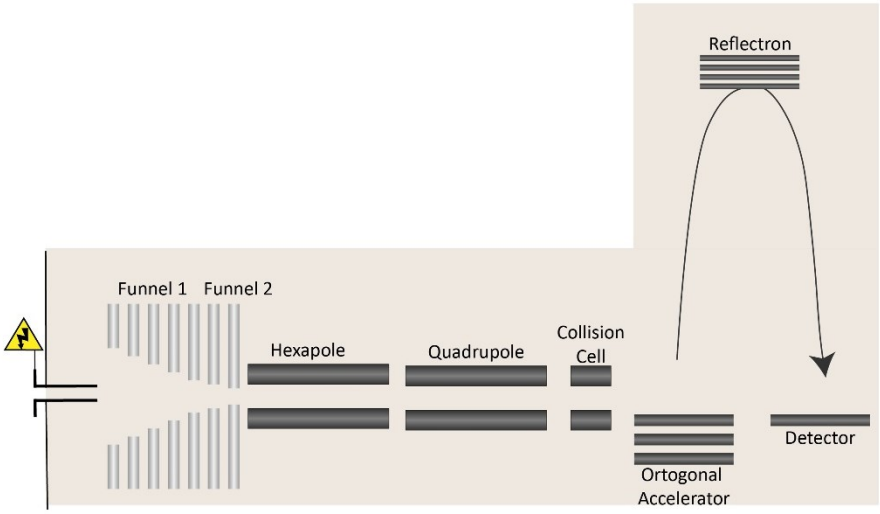

Figure 1.9: Simplified TOF setup equipped with a reflectron to prolong the flight distance without enlarging the flight tube.

1.4.4 Orbitrap mass spectrometry and fragmentation mechanisms

The orbitrap mass analyzer basically consists of three electrodes, the two outer, cup-shaped electrodes separated by a dielectric ring and the inner, spindle-shaped electrode as schematically illustrated in Figure 1.10 [72]. The outer electrodes are held at a fixed potential, while a potential is applied to the inner electrode [72]. When ions enter the orbitrap, they start a radial movement around the central electrode as well as an axial movement along the z-axis due to the shape of the orbitrap [73]. Stable trajectories are obtained because the electrostatic attraction toward the center is counteracted by the centrifugal force from the rotational movement [72]. Theoretically, the three frequencies of radial oscillation, axial oscillation, and rotation frequency could be used for detection. Since the radial oscillation and the rotation frequency depend on the energy and the position of the ion only the axial frequency is used for detection [74]. The axial movement induces an image current in the outer electrodes which is detected by a differential amplifier [75]. A frequency spectrum is then obtained via Fourier transformation and the frequencies are converted to m/z values [73].

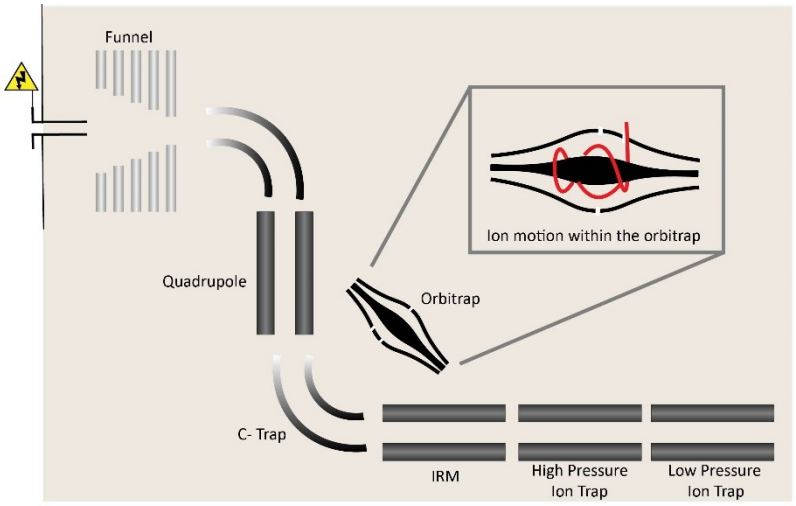

Figure 1.10: Simplified orbitrap setup only showing the main parts of the instrument including a schematic illustration of the ion motion within the orbitrap. IRM: Ion routing multipole.

The Orbitrap fusion Lumos provides multiple fragmentation options that can be used to identify proteins and determine site-specificities of mAb variants. Four fragmentation options namely collision-induced dissociation (CID), electron-transfer dissociation (ETD), higher-energy collisional dissociation (HCD), and combined ETD and HCD (EThcD) fragmentation were applied in this thesis. CID is done in the high-pressure cell [71] of the Orbitrap fusion Lumos where the ions collide with helium ions and get fragmented [61]. With CID the weakest bond breaks resulting mostly in the generation of b- and y-ions. The ETD fragmentation is also done in the high-pressure cell [71] but fragmentation is achieved differently. First fluoranthen is ionized via electron capture chemical ionization with methane. The positively charged peptide and negatively charged fluoranthen are then accumulated in the ion trap and the peptides are fragmented by the electron transfer to the peptide [61]. In ETD mostly, c- and z-ions are generated. The orbitrap also offers a special collision-induced dissociation method the HCD mechanism. Compared to the CID this fragmentation is done in the ion routing multipole (IRM) [71]. Ions are accelerated into the IRM and collide with the nitrogen atoms which results in mainly b- and y-ions [61]. EThcD combines ETD and HCD and therefore occurs in both the ion trap and the IRM [71]. Ions are first fragmented by ETD in the ion trap and then in addition to that by HCD in the IRM. Depending on the predominant fragmentation type b-, c-, y-, and z-ions are received. Depending on the fragmentation technique, the precursor selection, and the fragmentation parameters different fragmentation coverages can be achieved [76].

1.4.5 Ion mobility mass spectrometry

Ion mobility (IM) mass spectrometry devices have gained massive attention in the last few years. More importantly, trapped ion mobility spectrometry (TIMS) separates ions based on their size and charge in the gas phase and therefore adds another separation dimension to the already chromatographically or electrophoretically separated mAb variants. The schematic illustration of the timsTOF SCP including the dual-TIMS technology is shown in Figure 1.11.

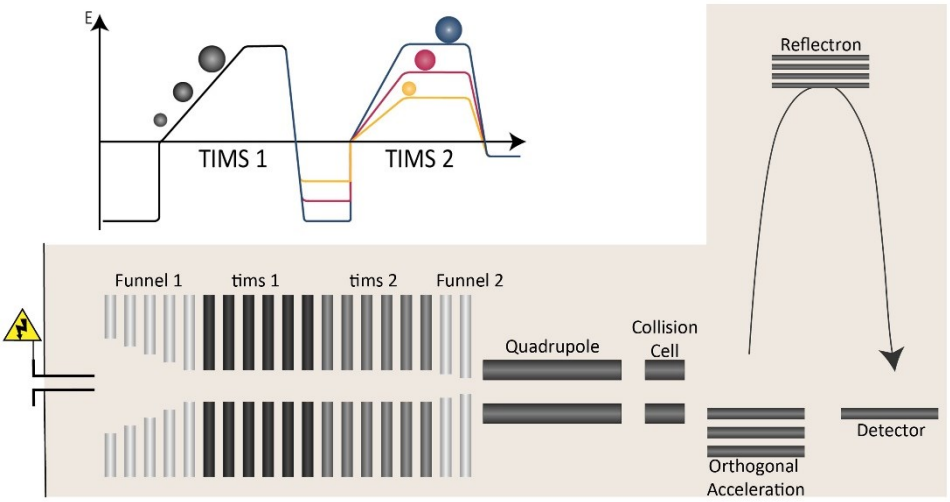

Figure 1.11: Simplified timsTOF setup only showing the main parts of the instrument including a schematic illustration of the TIMS separation principle.

The TIMS cell is composed of stacked ring electrodes and ions entering the tunnel experience two forces [77]. The ions are dragged into the TIMS tunnel by a gas flow (e.g. nitrogen) while at the same time, a counteracting electric field is applied [78, 79]. The electric field strength is increasing over the TIMS tunnel length. How far ions migrate into the TIMS tunnel is based on their size and charge in the gas phase. Ions are trapped at the position where the ion drift velocity (v_d) is large enough to prevent the ions from being further dragged into the tunnel by the gas flow velocity (v_g) as given by Equation *(2)* [78].

$$vd + vg = 0 \qquad (2)$$

The ion drift velocity (v_d) depends on the mobility of the ion (K) and the electric field strength (E) as given by Equation *(3)* [78].

$$vd = K * E \qquad (3)$$

Based on these two equations large ions with a low mobility and therefore a low velocity get dragged far into the TIMS tunnel if the electric field strength is low (like at the beginning of the TIMS tunnel). Small ions with a high mobility and therefore a high velocity get trapped at the beginning of the TIMS tunnel. To release ions from the TIMS tunnel the electric field strength only has to be reduced below this trapping field strength. The dual-TIMS technology of the timsTOF SCP allows the accumulation in the first section, while ions are sequentially released from the second TIMS which results in a near 100% duty cycle [80]. RPLC and TIMS were already studied regarding their orthogonality and showed a quite good orthogonality value [81–83]. So far a few studies combined CZE with IM-MS [84–96], only one of them dealing with protein separation [95] and none of them doing a systematic evaluation of liquid and gas phase mobility and orthogonality.

2 Aim of this work

Many mAb variants can be present within one mAb sample and separation and identification are of utmost importance. The key to unequivocal identification of mAb variants with MS is a generic, selective, and efficient separation technique. Therefore, the overall aim of this thesis was the development and evaluation of several separation techniques (CZE, IEX, and CIEF) directly coupled with MS for the characterization of mAb variants.

mAb variants were analyzed on the subunit level using CZE-MS. The sample complexity was reduced, by mAb digestion and reduction, to gain detailed site-specific information on the mAb variant by MS/MS fragmentation. Additionally, the generic application of the developed method was evaluated by measuring a set of ten mAb samples. The development of a generic sample preparation approach and the results for mAb variant evaluation are described in **manuscripts I** and **III**.

Ion mobility is known to enhance separation however it has so far rarely been used coupled to CZE since the separation principles are similar. This thesis aimed to evaluate the orthogonality of CZE and trapped ion mobility mass spectrometry. For this, a tryptic HeLa digest was used and the results are summarized in **manuscript II**. The IM was used to separate mAb variants as shown in **manuscript I.**

In addition to the subunit level mAbs variants were also analyzed on the intact level. For this, an IEX-MS and a CIEF-MS method were developed for selective and generic mAb variant separation. Similar to the subunit approach generic application was evaluated by measuring a set of ten mAb samples. The advantages and drawbacks of the two methods were systematically evaluated and compared to a new intact CZE-MS approach under acidic conditions. The individual method discussions and the overall method comparisons are described in **manuscript IV**.

3 Results and Discussion

The analysis of mAb variants, especially the detection of small mass differences on the intact mAb level is challenging and no site-specific information of the variant can be obtained. Therefore, mAbs were first analyzed on the subunit level (chapter 3.1) including fragmentation experiments for mAb variant localization and ion mobility as an additional separation dimension. Intact analysis, however, can minimize sample preparation time and reduce artifact formation. Based on the commonly applied CZE-UV system for the separation of charge variants of intact mAb by He et al. [38] (chapter 3.2) the benefits and drawbacks of CZE-UV systems are discussed. Following this, intact CZE-, IEX-, and CIEF-MS approaches are presented and discussed individually and comparatively (chapter 3.3). Finally, the results from the intact approaches are compared with the results from the subunit approach.

3.1 CZE-MS and MS/MS of mAb subunits

3.1.1 Initial sample preparation

As described in chapter 1.2 three general subunit states can be generated depending on the digestion and reduction approach. For this thesis, the mAb was digested and reduced to 25 kDa subunits by enzymatic digestion followed by reduction. While antibody digestion using the immunoglobulin G-degrading enzyme of *Streptococcus pyogenes* (IdeS) is very well established the reduction is not uniformly done. Different reduction chemicals are used and the reduction is carried out at room temperature or elevated temperatures, with or without chaotropic salt, for 5-60 min (for detailed information compare **manuscript I**). The reduction is sometimes followed by further steps like acidification, rebuffering, and desalting. Since no uniform sample reduction is available the initial sample reduction in **manuscript I** was done using dithiothreitol (DTT) in water at 37°C for 1 hour. The separation of the subunits was carried out in a PEO-coated capillary using an acidic BGE. The total ion electropherogram (TIE) and the subunit-specific extracted ion electropherograms (EIE) in Figure 3.1A show several separate signals for each subunit moiety. However, the deconvolution of the individual signals does not show mAb variants but instead indicates incomplete sample reduction using the initial sample reduction approach. This is also indicated by a

shift in the m/z charge envelope towards lower m/z values over time which is exemplarily shown for the LC subunit in Figure 3.1B. (same MS spectra for the N-terminal half of the heavy chain (Fd) and the C-terminal half of heavy chain (Fc/2) can be found in ESM1 of **manuscript I**). The first LC signal at 16.4 min has a charge envelope distribution between 1200 and 2250 m/z with its maximum at 1379.70 (z=+17) while the last LC signal at 20.5 min has a charge envelope distribution between 800 and 2250 m/z with its maximum at 938.71 (z=+25). After deconvolution of the individual signals the first signal in the EIE of each subunit has a mass that is 4 Da smaller than the expected fully reduced subunit mass. The second signal in the EIE of each subunit has a deconvoluted mass that is 2 Da smaller than the expected fully reduced subunit mass. Interestingly, for LC the signals at 18.0 min and 19.3 min have the same deconvoluted mass but they are very well separated in the CZE. The same result is obtained for the signals at 18.5 min and 19.1 min in the EIE of the Fd subunit. Only the small signals at 20.5 min (LC) and 20.0 min (Fd) have the expected fully reduced subunit mass. For Fc/2 no fully reduced species is detected.

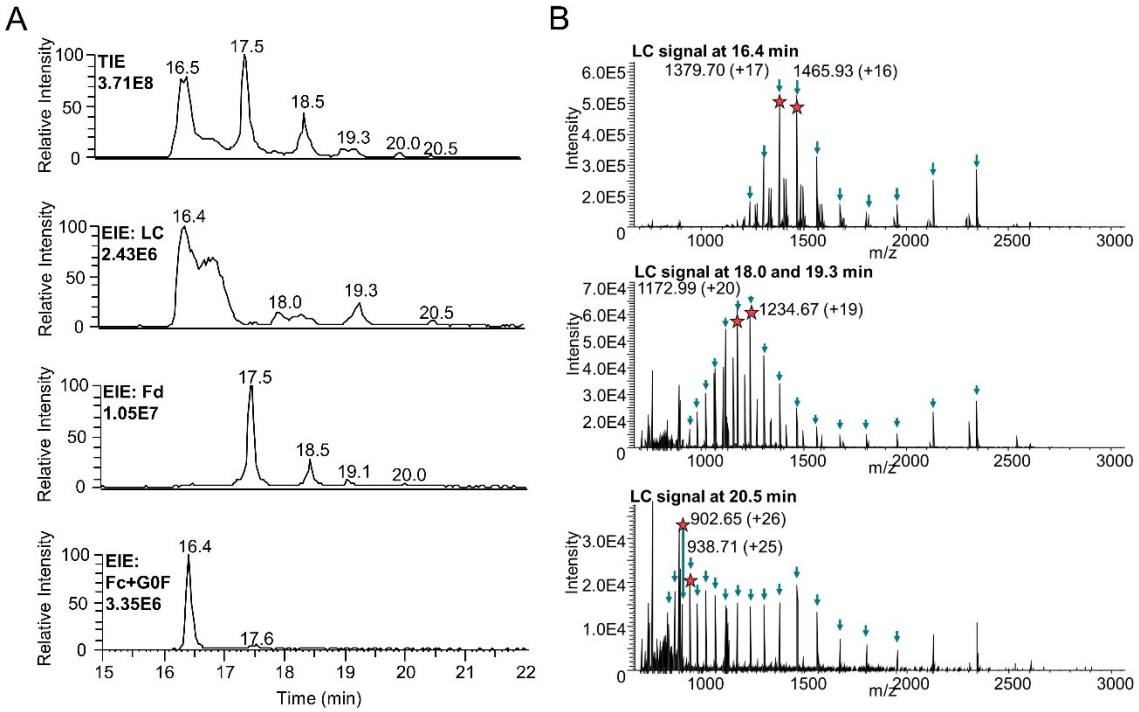

Figure 3.1: A: Separation of trastuzumab subunits using CZE-MS. EIEs for each subunit are generated based on the sum of the two most intense m/z values for each reduction state (total of 6 m/z values). B: The choice of m/z (red star) for subunit EIE generation in A is exemplarily shown for the LC subunit. Blue arrows highlight the charge envelope of the subunit moiety. Figure and figure caption adapted from Figure 1 and ESM1 of **manuscript I.**

Top-down fragmentation experiments were performed to further investigate the nature of the detected masses, in particular the two LC and Fd baseline-separated signals with the same deconvoluted mass. For this CID, HCD, ETD, and EThcD were tested and compared regarding their fragmentation coverage for each subunit and possible reduction state. The highest fragmentation coverage was achieved with EThcD fragmentation. A small compromise between fragmentation coverage and generic subunit application had to be made, as the highest fragmentation coverage was obtained with slightly different fragmentation energies for different subunits and reduction states. The final fragmentation parameters used for the analysis reveal that the two LC and Fd baseline-separated signals with the same deconvoluted mass are positional isomers (**manuscript I**). Figure 3.2 shows all fragmentation results grouped by subunit moiety (A: LC, B: Fd, and C: Fc/2). The first signal for each subunit moiety (blue lines in Figure 3.2) belongs to the completely oxidized subunit and fragmentation is limited due to both disulfide bridges being intact. The second and third signals in each EIE (signals are marked with grey arrows in yellow lines in Figure 3.2) contained a reduced and an oxidized disulfide bridge, respectively. For LC and Fd these two positional isomers are identified via the EThcD fragmentation with a very good fragmentation coverage. The Fc/2 subunit only shows one of these positional isomers since the disulfide bond in the C_H3 domain is the least susceptible one to break [97]. The last signal in each EIE (green line in Figure 3.2) contains two reduced disulfide bridges. Here, fragmentation coverage is limited since the signal intensities are relatively low. This sample preparation-induced increase in heterogeneity was not intended, nevertheless, it proves the selectivity of the CZE separation and the power in combination with MS/MS fragmentation and identification. This makes this method especially valuable for variant analysis.

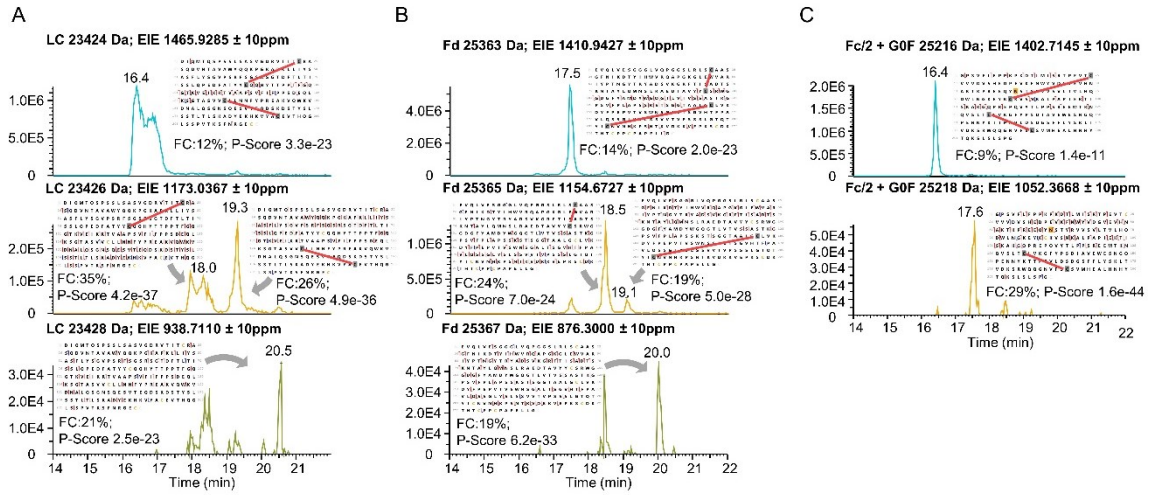

Figure 3.2: EIEs for the different reduction states for each trastuzumab subunit. The EIE is generated based on the most intense m/z for each reduction state of each subunit. Based on the MS/MS experiment fragmentation map, fragmentation coverage (FC) and P-Score are given for each reduction stage. Red lines indicate closed disulfide bridges. Figure and adapted figure caption of Figure 2 of **manuscript I.** Consult **manuscript I** for high resolution image.

3.1.2 CZE-TIMS orthogonality evaluation for mAb variant separation

Since the initial sample reduction is not sufficient to completely reduce the mAb subunits, creating a large induced heterogeneity with most likely superimposed variants, a further separation using ion mobility (IM) is considered. However, first, an evaluation of the CZE-IM orthogonality has to be performed as hardly any data on the combination of CZE and IM-MS exists and a different selectivity might not be obtained due to the same separation principle. TIMS TOF MS has so far not been studied in coupling with CZE. Unfortunately, the subunits are not suitable to evaluate this orthogonality properly. Instead in **manuscript II,** the CZE-TIMS orthogonality evaluation is performed using a commercially available tryptic digest of human proteins from HeLa cells. HeLa cells are a continuous cancer cell line named after Henrietta Lack [98]. In 1951, the tissue sample was given to George Gey who successfully cultivated the cells together with Margret Gey and Mary Kubicek [98]. Today HeLa cells are used in research for multiple purposes, which is why this cell line is very well characterized. To increase peak capacity and reduce overlapping signals a 1.5 m long CZE-capillary is used for the orthogonality evaluations. Using the parallel accumulation serial fragmentation (PASEF) algorithm the peptides are fragmented based on their mobility in the gas phase. Following the MS measurement peptides are identified by a Mascot search (detailed separation and data processing parameters can be found in **manuscript**

II) which allows a detailed evaluation of the peptides by size, amino acid composition, and charge state in the liquid and gas phase. The heat map of migration time (liquid phase mobility) and peptide mass shown in Figure 3.3A leads to the formation of distinct areas (curved patterns). These areas can be correlated to the charge state of the peptides in the liquid phase, which at the given pH of the BGE mostly correlate with the amount of basic amino acids in the peptide. In the gas phase, such a distinct separation based on the amount of basic amino acids is not achieved (compare Figure 3.3B). A small offset remains, which is most likely because a higher gas phase charge state leads to a larger CCS value due to the repulsive forces of the positive charges within one peptide. Nevertheless, the high orthogonality of CZE and IM is already indicated in Figure 3.3C (charge-normalized inverse mobility – migration time plot), where only the Mascot-identified peptides are visualized. A quite high orthogonality is obtained for CZE-IM-MS if all measured signals are examined as is done in Figure 3.3D. Since the Mascot search is performed for peptides with a charge state between +2 and +4, excluding all the other possible charge states, the final CZE-IM orthogonality of around 80% is calculated based on the area of all measured signals, as shown in Figure 3.3D.

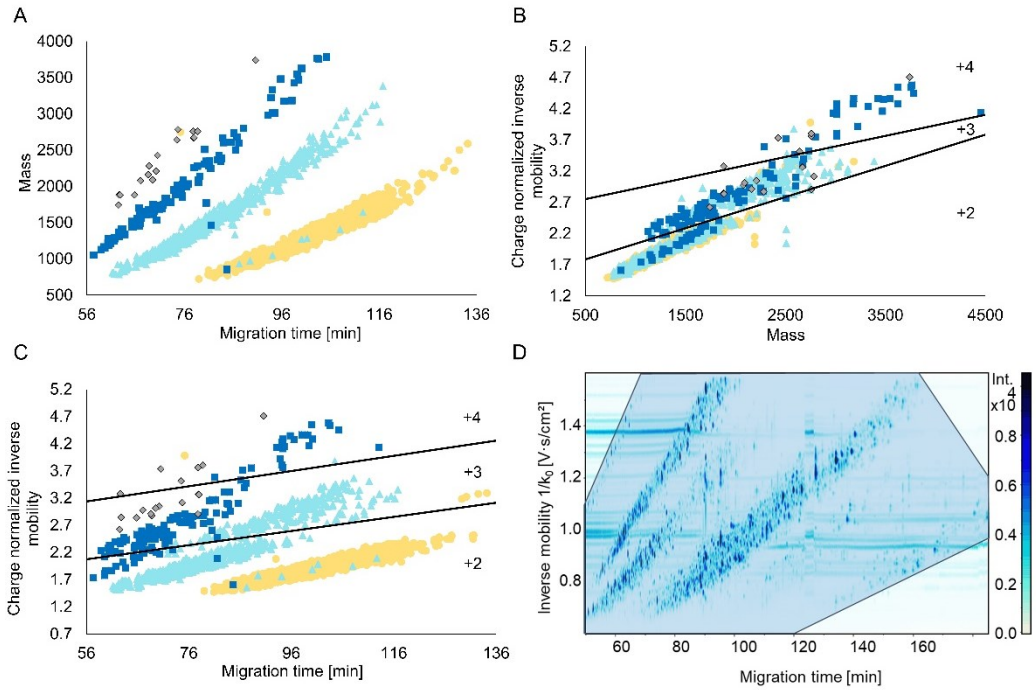

Figure 3.3: Evaluation of the Mascot search identified peptides. A: Migration time-mass plot; B: Mass-charge normalized inverse mobility plot; C: Migration time-charge normalized inverse mobility plot; D: Orthogonality of all signals from CZE-TIMS analysis. In each diagram, peptides are colored according to the number of basic amino acids in the peptide. Yellow circle: One, light blue triangle: Two, dark blue square: Three, grey diamond: Four basic amino acids. Numbers in B and C indicate the charge state of the peptide in the gas phase. Combined figure and figure caption from Figures 3,4 and 5 of **manuscript II**.

The promising results of the orthogonality assessment raise the hope that CZE-IM coupling will further separate the incompletely reduced subunits to obtain more information about the mAb variants even with incompletely reduced subunits being present. The exact method parameters are available in **manuscript I.** The different reduction states indeed show different mobilities in the gas phase. As shown exemplarily for the LC in Figure 3.4 (for Fd and Fc/2 compare Figure 4 in **manuscript I**) the non-reduced LC shows a higher mobility than the partly reduced LC, and the partly reduced LC shows a higher mobility than the fully reduced LC.

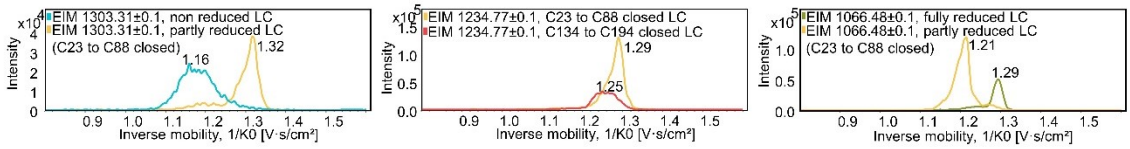

Figure 3.4: Inverse gas phase mobilities of differently reduced LC subunits. Since charge envelopes only overlap poorly, different m/z values were chosen for comparison of reduction states. Blue: non-reduced form; yellow: partly-reduced form (N-terminal disulfide closed); red: partly-reduced form (C-terminal disulfide closed); green: fully-reduced form. Adapted figure and adapted figure caption of Figure 4 of **manuscript I.**

This result is also obtained for the Fd subunit and can be explained by the different shapes of the subunits within the gas phase. The gas phase shape is influenced by the presence of oxidized and reduced disulfide bridges leading to the separation of these isomers. However, the gas phase mobilities only differ slightly and show a quite broad mobility distribution which is especially evident for the positional isomers. While the positional isomers are baseline separated by the CZE (compare Figure 3.2) the IM separation is significantly reduced. These broad gas-phase mobility signals would make positional isomers indistinguishable if they had not been previously separated by CZE. Even though the CZE is successfully coupled to the IM and CZE-IM has a high orthogonality it is concluded that possible variants will not be further separated using this sample and separation approach. After this evaluation in **manuscript I,** it became clear that proper sample reduction is needed to avoid non-reduced variants in the subunit analysis of mAbs. IM is a great tool to add another separation dimension which was proved by the tryptic HeLa digest however for this separation problem it was not as beneficial as the CZE separation.

3.1.3 Optimization of mAb reduction

The previous results of **manuscript I** show that no proper mAb variant evaluation can be achieved with incompletely reduced subunits. Even the combination of CZE and TIMS was not selective enough to further separate the variants of this highly complex and incompletely reduced mAb sample. In addition to that variant signal intensities are decreased since they are distributed between the different reduction states. So, sample reduction approaches are further examined (**manuscript I**). The water-based, initial reduction approach is applied in the literature but either the different reduction states were not separated [99, 100] or the mass shift was not conclusive [101, 102]. As it turns out a chaotropic salt is mandatory in the reduction step for proper sample reduction [103]. After testing different reduction temperatures and two chaotropic salts a reduction using DTT in the presence of 4 M urea at 37°C for 1 hour is proposed to generate fully reduced subunit moieties. Urea and guanidinium hydrochloride can both be used to generate completely reduced subunits. However, in the CZE-MS system using the low-EOF system (PEO-coated capillary and an acidic BGE), guanidinium hydrochloride migrates toward the MS and causes high background signals. In contrast, urea as a neutral component is not migrating in this system and is simply removed from the capillary after the separation is done. The optimized urea-based reduction approach is applied to the set of ten mAb samples (compare **manuscripts III)** and full reduction is achieved for eight mAb samples. Even though all mAbs are IgG1-type antibodies, the sample preparation is not complete for mAb4 and mAb5. These two mAbs still show highly intense signals for partly reduced and even unreduced subunit moieties (listed in the supplementary material of **manuscript III**). Why these two mAbs behaved differently can not be clarified conclusively. This deviation of mAb4 and mAb5 is certainly not related to the formulation buffer of the mAb, as mAb1-mAb5 are all formulated identically. Nevertheless, this shows the importance and separation efficiency of the CZE-MS system. Without the separation efficiency of CZE, this incomplete sample reduction might have been overseen so CZE-MS is a great tool to separate and identify sample preparation-induced variants. In combination with MS/MS, a detailed analysis can be performed enabling the detailed characterization of heterogeneities and mAb variants caused by sample preparation.

3.1.4 mAb variant evaluation

Since the CZE-MS/MS approach was advantageous to separate and determine the sample preparation induces positional isomeres of mAb subunits this approach was also used for mAb variant evaluation. As introduced in chapter 1.1.2 a multiplicity of variants can be present on one mAb. The subunit level is reducing that heterogeneity because not all variants are located at the same mAb subunit. Even though this makes an overall mAb variant evaluation impossible this allows detailed site-specific identification. Detailed information on the method and the data evaluation can be found in **manuscript III**. The overall variant evaluation results in 12-27 identified variants and 12-40 other possible variants depending on the mAb analyzed (compare Table 2 in **manuscript III**). These variants are identified by migration time shifts and mass differences compared to the unmodified subunits. Many mAb variants are related to the mAb glycosylation at the asparagine in the C_H2 domain of the mAb. Depending on the mAb up to 10 different glycoforms can be identified. The ten different glycoforms of mAb1 are exemplarily shown in Figure 3.5B and the three main glycoforms Fc/2+G0F, Fc/2+G1F, and Fc/2+G2F are identified for all mAbs. Figure 3.5A shows the separation of the ten identified glycoforms and the aglycosylated Fc/2 subunit of mAb1. The glycosylation is in most cases only changing the mass (+162 Da) and size of the antibody but not its charge. Although this purely size-based shift in migration time is small, these glycoforms are slightly separated from each other. Compared to that the absence of a glycan results in Fc/2 being the first subunit to migrate through the capillary. A large shift in migration time is also detected as soon as sialic acids are part of the glycan. The introduced negative charge from the sialic acid significantly reduces the mobility of the mAb which leads to roughly one minute longer migration times. The very well-separated subunit moieties allow the identification of minor glycosylation variants as well. As illustrated in Figure 3.5C mAb1 glyoforms with a relative abundance below 2% compared to Fc/2+G0F are detected.

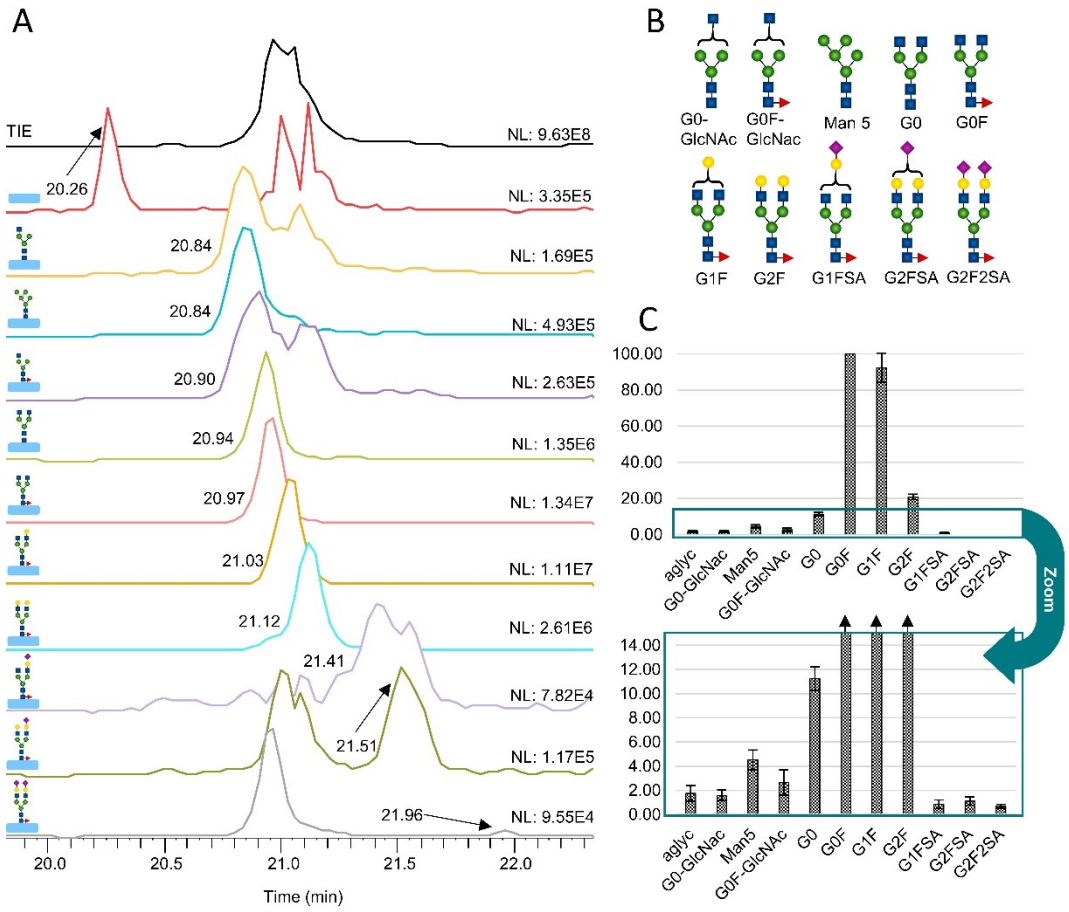

Figure 3.5: A: Separation of different glycosylation variants on Fc/2 of mAb1. Each EIE was generated based on 6 m/z values. Positional isomers are correctly annotated in B.; B) Most common glycan structures and possible isomeric structures. Blue square: N-Acetylglucosamine, green circle: mannose; yellow circle: galactose, pink diamond: sialic acid, red triangle: fucose; C) Glycan distribution of mAb1 relative to G0F (n=4). Separation conditions can be taken from **manuscript III.** Figure and adapted figure caption of Figure 2 of **manuscript III.**

Other quite abundant variants are lysine variants. mAb lysine variants carry an additional lysine at the C-terminus of the heavy chain so lysine is detected at the Fc/2 subunit using the approach from **manuscripts I and III.** Lysine increases the mass and the positive charge of the subunit by 128 Da and one unit respectively, which leads to faster migration times (compare Figure 3.6A). The lysine variants are baseline-separated from their Fc/2 variants without lysine. Because of this separation, the low-abundant Fc/2+G1F+Lys of mAb1 with a relative intensity of 0.59±0.11% compared to Fc/2+G1F can still be detected.

Apart from the glycosylation and the lysine variant other variants like glycation, oxidation, the loss of water or ammonia, and carbamylation can be detected. LC glycation results in a slightly higher migration time (compare Figure 3.6A and B) which follows the migration order of the system. The level of LC glycation is

relatively low compared to the LC subunit. For NIST and mAb2 shown in Figure 3.6, the relative intensity of LC glycation is around 4.5% (detailed values can be found in **manuscript III**). Fd glycation is only detected for mAb1 with a relative intensity of 3.4%. Fc/2 glycation is possible however it is challenging to distinguish between a glycated Fc/2+G0F and a Fc/2+G1F subunit. Subunit oxidation mostly happens at methionine. In Figure 3.6B the oxidation of mAb2 LC is shown which causes a minimal migration time shift towards higher values. In **manuscript III** mAb3 oxidation is discussed in detail since this mAb shows intense and multiple oxidation of the LC and Fd subunit. The loss of water or ammonium which causes a mass shift of either -18 Da or -17 Da respectively is also detected multiple times. As shown by the LC and Fd in Figure 3.6A this loss sometimes causes no migration time shift. However, in Figure 3.6B the loss of 17 Da causes a large migration time shift for the FdpyroQ subunit but only a small migration time shift for the LC subunit. The detected 43 Da mass difference, indicating carbamylation, is inconclusive because it could be caused by the 4 M urea concentration needed for sample reduction.

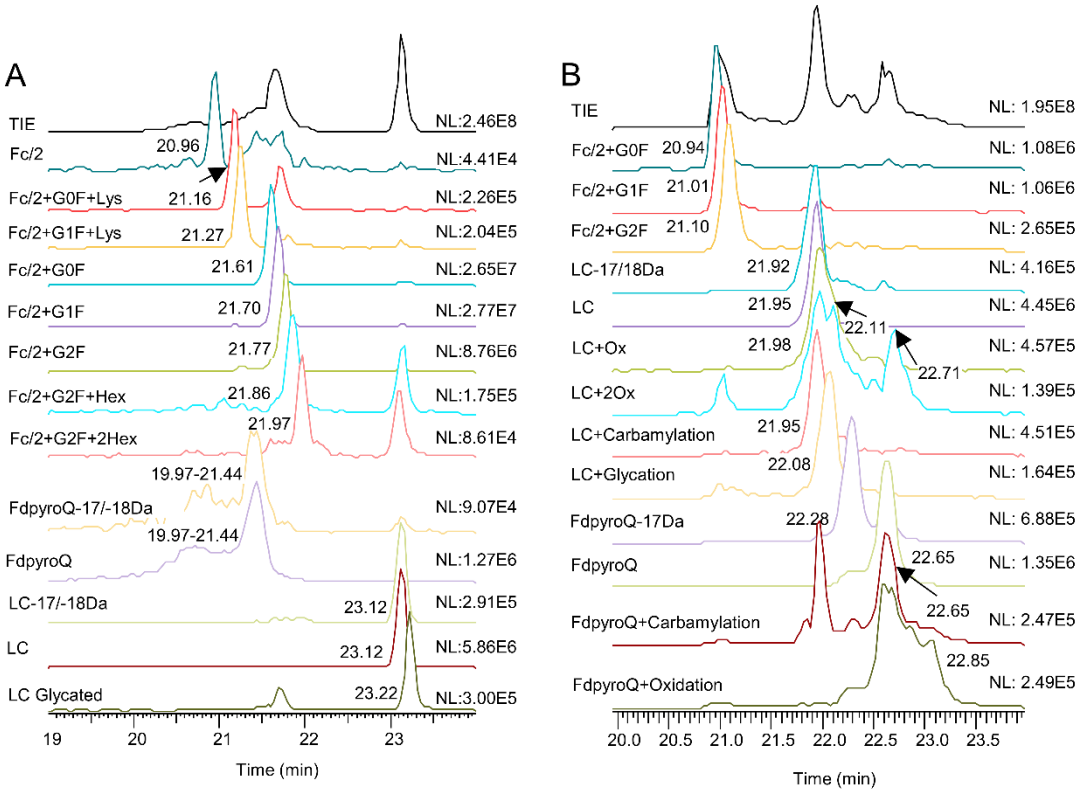

Figure 3.6 EIEs of identified variants of A: NIST mAb and B: mAb2. Only the three main glycosylation forms G0F, G1F, and G2F are shown. Separation conditions can be taken from **manuscript III.** Adapted figure and adapted figure caption of S5 and S11 of **manuscript III.**

So far modifications were identified by differences in deconvoluted mass (MS1 level) and migration time shifts compared to the unmodified subunits. For more detailed, positional information, the respective subunit moieties were fragmented by EThcD fragmentation as previously done for the positional isomers in **manuscript I.** The individual MS/MS spectra were deconvoluted and compared to the sequence of the mAb by using ProSight Lite (detailed parameters can be found in **manuscripts I and III**). Site specificity can be easily determined by the middle-down experiments for baseline-separated variants, such as the lysine variant, or for variants that cause a large mass difference compared to the main variant, such as glycosylation variants. However, the subunit approach using middle-down fragmentation has limitations. In general, several modification sites are present within a subunit, as the subunits are still quite large e.g. oxidation can happen at multiple amino acids like methionine, histidine, and tryptophan (compare discussion in **manuscript III**). Even though positional isomers can theoretically be separated as shown in **manuscript I** the fragmentation results for monooxidized positional isomers show simultaneous migration. The fragmentation is therefore inconclusive because fragments for all possible modification sites are detected. So here fragmentation can not determine an unequivocal site specificity. This once again highlights the importance of separation for mAb variant identification. If the separation approach is sufficient to separate positional isomers as shown for the disulfide bridges in **manuscript I,** site-specific information can be gained. If the separation is not sufficient fragmentation can not determine the variant position unequivocally. Generally, the subunit CZE-MS/MS approach is a fast analysis method for mAb variant analysis without risking artifact generation and still being able to determine site specificity whenever the mAb variants are separated.

3.2 UV-based CZE approaches for intact mAb charge variant analysis

Even though the developed CZE-MS approach on the subunit level is suitable for mAb variant separation, characterization, and identification some sample preparation is needed which could cause artifacts like the incompletely reduced subunits described in **manuscript I** and the detected carbamylation described in **manuscript III**. As previously mentioned intact mAb analysis approaches allow the determination of the overall mAb composition with minimal sample preparation and

a low risk of artifact formation. A very well-known CZE-UV system for mAb variant separation on an intact level was published a few years ago by He et al. [38]. The exceptionally good separation of basic and acidic mAb variants of this method is based on a quite complex BGE composition of 400 mM 6-aminocaproic acid (EACA), 0.05% hydroxypropyl methylcellulose, and 2 mM triethylenetetramine (TETA) at pH 5.7. These BGE components are necessary to suppress the EOF, prevent protein adsorption to the capillary wall, and improve peak shape and resolution [38]. Therefore, in **manuscript IV** for initial mAb variant evaluation, a slightly modified CZE-EACA-UV method regarding the flushing pressure due to the much longer capillary is used. Figure 3.7 shows the ten mAb samples measured with that CZE-EACA-UV system with clearly marked areas for acidic and basic variant migration behavior. Acidic variants migrate later compared to the main peak and basic variants migrate earlier than the main variant. Each mAb shows at least one acidic and one basic variant separated from the mAb main form and in many cases, more than one variant is detected. Most importantly the results of the ten mAb samples in Figure 3.7 show that the method is generic and can be widely applied (mAb pI range between 7.3 and 8.7) for selective and efficient mAb variant separation, even for highly heterogeneous mAbs like Cetuximab and pH stressed mAb1. Additionally, the method showed a high reproducibility and repeatability e.g. the migration time of the mAb1 main variant is 18.05 ± 0.11 min for 18 measurements.

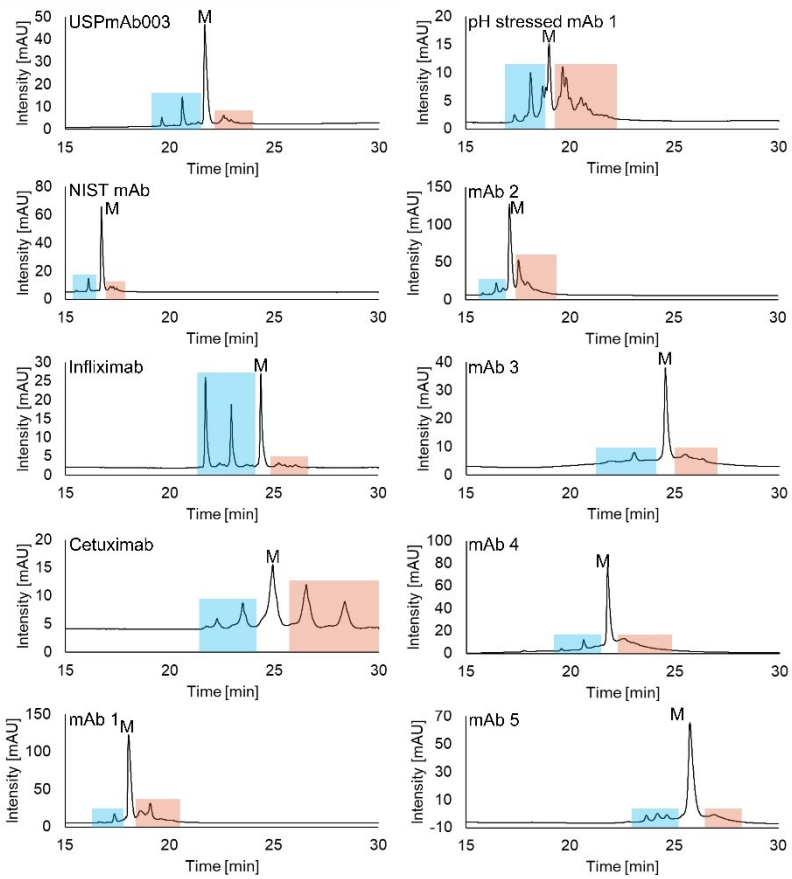

Figure 3.7:Separation of ten mAb samples using a slightly adapted method from He et al. [38]. 60 cm (50 µm ID / 365 µm OD) fused silica separation capillary, BGE: 400 mM EACA, 2 mM TETA, 0.05% hydroxypropyl cellulose pH 5.7. Spectra were acquired at 214 nm. M: Main variant, blue areas: basic variants, red areas: acidic variants.

However, over the years some inconsistencies were observed when the CZE-EACA-UV system was performed. A recent interlaboratory study concluded, that these inconsistencies can be attributed to non-intended changes in the method [104]. This led to the development of CZE-UV systems using other dynamic coating agents, additives, and polymeric compounds to find a combination with similar or even better mAb variant separation selectivity. For more information on possible substitutes compare the “CZE-UV and CZE-MS for mAb variant analysis” discussion in **manuscript IV**. Even though all CZE-UV methods mentioned in **manuscript IV** separate mAb variants to a certain degree, the high molar concentrations of additives and dynamic coating materials in the BGE prevent the MS coupling. Therefore, MS-compatible approaches are here tested using static capillary coatings (Polyvinyl alcohol (PVA) and PEO) in combination with acidic BGEs (formic acid (FA) or acetic acid (HAc)). However, as shown in Figure 3.8 (exemplarily shown for mAb1 and one of the tested separation options) none of

these approaches are suited to separate mAb variants as selectively as the CZE-EACA-UV system for mAb variant separation does.

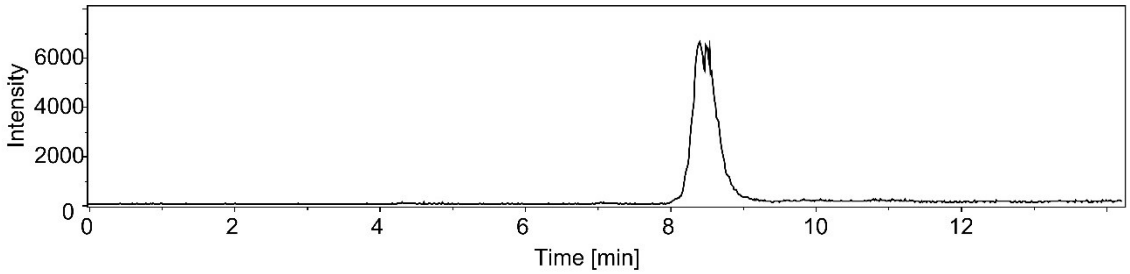

Figure 3.8: Separation of mAb1 variants using a 60 cm PEO-coated capillary. BGE: 2 M HAc, separation voltage 30 kV, injection: 50 mbar, 9 seconds (1% capillary volume), SL: IPA: H2O 1:1 + 0.5% FA.

This shows the importance of the capillary coating and BGE composition for mAb variant separation. Especially without a proper capillary coating mAb variant separation can not be done on an intact level. This coating was developed within another project [43] and will be briefly discussed in chapter 3.3.1.

3.3 CZE-MS, IEX-MS, and CIEF-MS of intact mAb variants

Until now MS analysis of mAb variants was performed at the mAb subunit level, since the neutral-coated capillary CZE-MS approaches at the intact level mentioned in chapter 3.2 have not provided the desired selectivity for mAb variant separation. In parallel to this thesis, new capillary coatings and separation systems were developed which provided the selectivity needed for mAb variant separation using CZE-MS under acidic conditions [43] and under near-native conditions [65]. The acidic system is used to compare the results with the IEX-MS and CIEF-MS methods developed in this work. The individual methods are described in chapter 3.3.1, chapter 3.3.2, and chapter 3.3.3 respectively.

3.3.1 CZE-MS for mAb variant analysis on an intact level

As previously mentioned in chapter 3.2 a proper capillary coating is key to mAb variant separation on the intact level. Since the CZE-EACA-UV-based separation approach is not MS compatible a SMIL-coated capillary operated under acidic conditions is used. This CZE-MS system published by Höchsmann et al. [43] prevents protein adsorption and creates an EOF within the capillary. This allows the separation of mAb variants without any MS-interfering components in the BGE and allows MS detection in a mass range of 2500-4000 m/z. This method is applied

here to all ten mAb samples without any method development. Figure 4 in **manuscript IV** illustrates the variant separation achieved for all ten mAb samples three of which are exemplarily shown in Figure 3.9. As visible from the base peak electrophreogram (BPE) in Figure 3.9 most mAbs in the sample set show at least one separated acidic variant that migrates earlier than the main peak and at least one basic variant that migrates later than the main peak. Only for highly heterogeneous samples (cetuximab and stressed mAb1), no variant separation is achieved. Several mAb variants can be detected using this CZE-MS method, a detailed list of which can be found in the supplementary information of **manuscript IV**. Generally, for all mAb samples, the glycosylation pattern including minor glycosylation species can be detected in the main peak as exemplarily shown for the three mAbs in Figure 3.9. The EIEs of the different glycosylation species reveal a small shift in migration time depending on the size of the glycans (compare Höchsmann et al. [43]). Although this purely size-based shift in migration time is small, these glycoforms are slightly separated from each other. The basic variants in Figure 3.9 of NIST mAb (B1 and B2) are lysine variants while the basic variants of mAb1 (B2) and mAb2 (B1) indicate a loss of water or ammonium. A shift towards higher migration times is also detected for monoglycosylated species (B1 of mAb1 and mAb2 and B2 of NIST mAb), aglycosylated species (B3 of mAb2), and presumably mAb fragments (compare 148770 Da signal of B2 of mAb2). A shift towards lower migration times is detected as soon as sialic acids are part of the glycan (A1 of mAb1). Additionally, all mAbs show an acidic species with a shift of around 2 Da after deconvolution. Even if this shift of 2 Da could be due to deamidation, it rather indicates an open disulfide bridge [43]. After a closer look at the mass spectrum and the charge envelope distribution, a shift was noticed compared to the main peak charge envelope distribution supporting the reduced disulfide bridge theory. This CZE-MS system is very valuable since such a good separation has not been achieved by any acidic separation system so far especially not by using a standard CZE system (a detailed comparison can be found in **manuscript IV**). A better separation is only possible under near-native conditions as recently shown by van der Zon et al. [65] and multiple chip-based methods [19, 105–110].

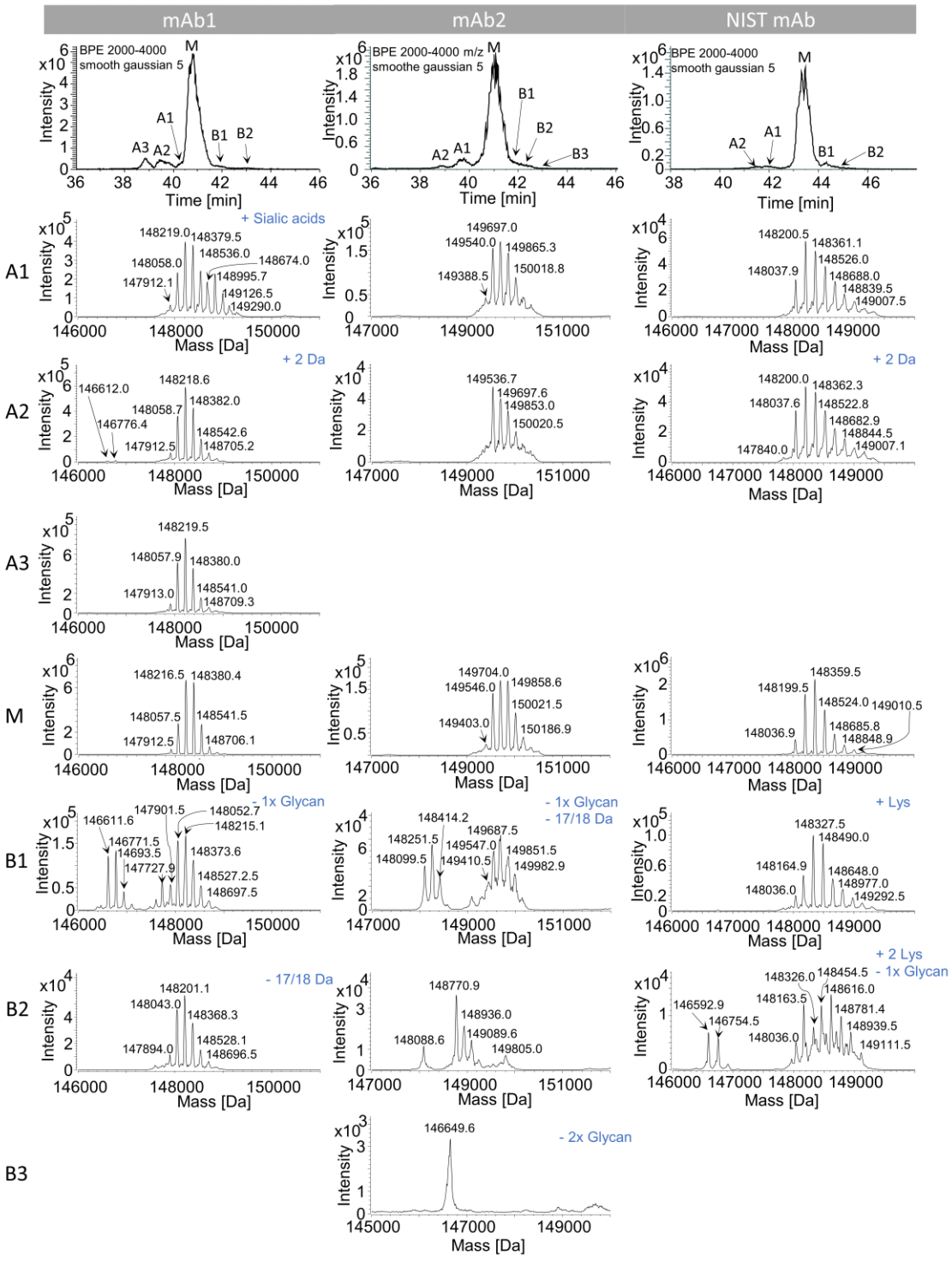

Figure 3.9:CZE-MS separation and identification of mAb1, mAb2, and NIST mAb all measured on the Orbitrap Fusion Lumos instrument. Top row: Base peak electropherograms (BPE) from 2000 to 4000 m/z (smoothed). Following rows: Deconvoluted spectra of separated variants. A: acidic variant, M: main variant, B: basic variant. Figure is generated analog to Figure 5 in **manuscript IV.**

3.3.2 IEX-MS for mAb variant analysis on an intact level

Apart from CZE charge variants can also be separated by IEX. For IEX and CIEF discussed in chapter 3.3.3 a TOF-MS (MaXis Bruker Daltonics) was used and not the Orbitrap Fusion Lumos. This change in MS is further discussed in chapter 3.3.4. As described in chapter 1.3.2 ion exchange is a great method for mAb variant separation and **manuscript IV** discusses the detailed method development and the parameters used for IEX-MS measurements. Briefly, the initial IEX-UV-based method with a flow rate of 0.3 mL/min and 160 mM ammonium acetate in eluent B was optimized regarding MS coupling by first reducing the ammonium acetate concentration to 100 mM. After that the flow rate was reduced to 0.1 mL/min and the gradient was adjusted for mAb variant separation. This separation system was coupled to the MS either directly (native conditions) or after post-column acetonitrile (ACN) and formic acid (FA) addition (acidic conditions). Post-column ACN and FA addition results in the detection of the mAb in an m/z range between 2000 and 4000 m/z. However, the post-column addition of ACN and FA heavily dilutes the sample and results in low signal intensities which makes direct and native detection more desirable. Native MS spectra are acquired between 4500 and 7000 m/z. For all ten mAb samples a separation of mAb variants is achieved even though the mAbs span a pI range from 7.3 to 8.7. Three mAbs are exemplarily shown in Figure 3.10 while the full mAb set is available in Figure 2 in **manuscript IV**. No mAb-specific method development is done and different resolutions (R) are obtained between the main form (M) and the lysine variant (B1) of USPmAb003, NISTmAb, and infliximab. For USPmAb003 (pI: 8.1) a resolution of R=0.85, for NIST mAb (pI: 8.6) a resolution of R=1.38, and for infliximab (pI: 7.3) a resolution of R= 2.66 is calculated. As discussed in **manuscript IV** this difference in resolution most likely correlates with the pH gradient of the method. A linear pH gradient is highly desired to achieve a reproducible and high-resolution separation. When an ammonium acetate-based buffer system is used the pH response as a function of the base content is not linear [49, 51]. This can result in different resolutions for different mAbs with different pI values. The antibody variant separation and identification are exemplarily shown in Figure 3.10 for mAb1, mAb2, and NISTmAb. A full list of all mAb variants determined for these three mAbs as well as all other mAbs of the sample set can be found in the supplementary information of

manuscript IV. The IEX-MS method can detect the general glycosylation pattern including minor glycosylation species in the main peak as shown for mAb1 and NISTmAb in Figure 3.10. For mAb1 the main peak also contains monoglycosylation, which is not separated since the charge is not changed by this variant. The basic variant that migrates later than the main form was identified for NIST mAb (B1) as a lysine variant. An unknown mass shift of -13 Da was detected for the basic variant of mAb1 (B2). Acidic species that migrate earlier than the main form with a small mass shift of +2 Da compared to the main form (A1 of mAb1) could theoretically be assigned to a deamidation however this is equivocal due to the poor spectral quality. Unambiguous assignment of deamidated species is always challenging and often not feasible due to the small mass shift that could not be resolved by the MS on an intact level even if the spectral quality is good [50, 51, 111–113]. A final answer if A1 of mAb1 is a deamidation can not be given. All other separated, but low-abundant species are challenging with this IEX-MS method. It was not possible to detect minor variants even though IEX-MS is generally able to detect variants like sialylated glycans [111], succinimide [113], and pyroGlu [51]. These variants are most likely present below the peaks that were detected via the online UV detection but could not be identified by MS due to the low spectral quality in combination with the native ionization and the generally low abundance. Nevertheless, IEX-MS is a promising technique for mAb variant separation and identification.

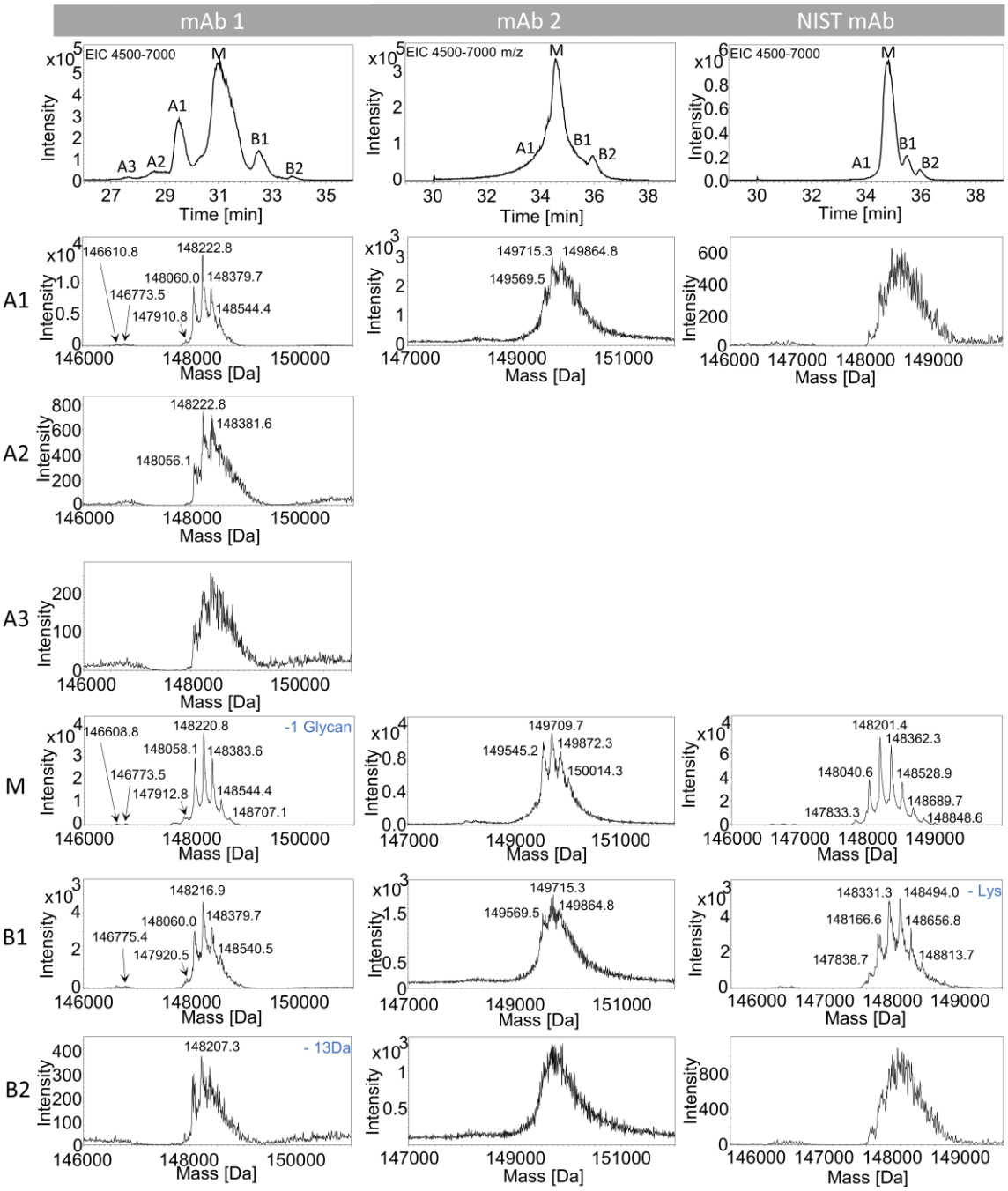

Figure 3.10: IEX-MS separation and identification of mAb1, mAb2, and NIST mAb all measured on the Bruker MaXis TOF instrument. Top row: Extracted ion chromatograms from 4500 to 7000 m/z. Following rows: Deconvoluted spectra of separated variants. A: acidic variant, M: main variant, B: basic variant. Figure is generated analog to Figure 5 in **manuscript IV.**

3.3.3 CIEF-MS method development for mAb variant analysis on an intact level

Apart from CZE and IEX charge variants can also be separated by CIEF. As described in chapter 1.3.3 CIEF and ICIEF separate mAbs variants based on their pI values. Coupling CIEF to MS is a relatively new development since CIEF-UV often contains MS-incompatible substances like methylcellulose or high molar concentrations of carrier ampholyte or urea [114–116]. These substances either can be removed by 2D approaches [117, 118] or the systems can be modified to be more MS compatible as shown in Table 2 in **manuscript IV**. The initial CIEF-MS approach was published by Naghdi et al. [58]. To reduce MS contamination and interfering substances as much as possible the amount of ampholyte and formamide in the master mix was reduced as described in **manuscript IV**. In ICIEF-UV systems no mobilization is necessary for detection. For MS coupling the focused mAbs have to be transported to the MS, which can be done by chemical or pressure-driven mobilization. Pressure-driven mobilization can significantly reduce the resolution compared to chemical mobilization [119], which makes chemical mobilization highly desirable for MS coupling. Chemical mobilization can be done with the nanoCEasy, which was previously shown by Naghdi et al. [58]. This setup was slightly modified by using a valve instead of a T-union. By using two syringes in syringe pumps and a valve shown in Figure 3.11, the flow of the catholyte and SL to the emitter can be regulated. During focusing the MS voltage is off to prevent MS contamination and the emitter is flushed with catholyte. After focusing the valve is switched and SL is flushed to the emitter. Now the MS spray voltage is turned on and the measurement can be done. This measuring setup was used for the results generated in **manuscript IV**.

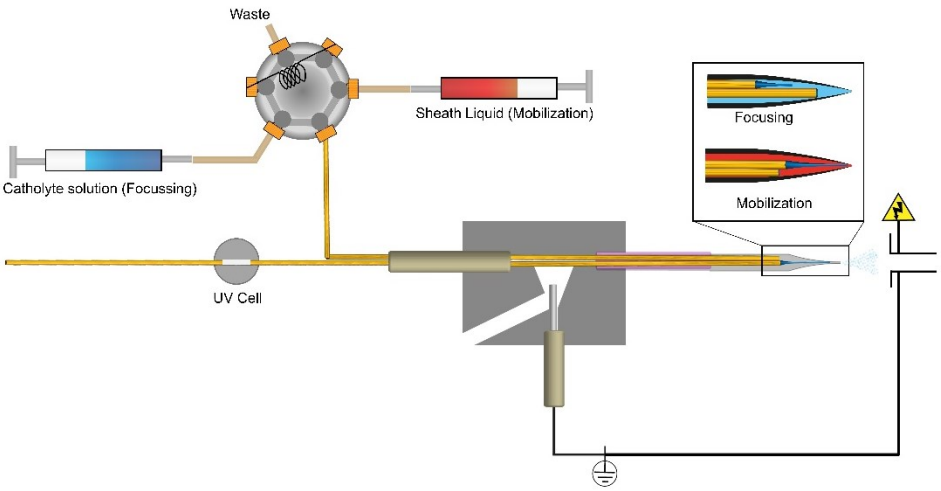

Figure 3.11: Schematic setup of CIEF-MS coupling using the nanoCEasy interface.

Variants are separated for all mAb samples according to the online UV detection (compare Figure 3 in **manuscript IV**) with basic variants migrating earlier than the main peak and acidic variants migrating later. However, only six mAbs can be detected in the MS. Infliximab, mAb3 (both pI 7.3), and USP mAb003 (pI: 8.1) are not identified in the MS (compare Figure 3 in **manuscript IV**) which indicates a solubility problem at the emitter tip when the nearly native mAb is transferred to the acidic sheath liquid. Since this behavior is not present for all mAb samples this seems to be a mAb-specific behavior. Even though this method needs further improvement some variants could already be detected. As shown in Figure 3.12 the major glycosylation pattern as well as some minor glycoforms can be detected. Similar to IEX the unseparated monoglycosylation for mAb1 and mAb2 can be detected in the main peaks. Basic variants and acidic variants for all mAbs show no mass difference compared to the main form. Nevertheless, the online UV detection shows the strength of CIEF for mAb variant separation which is why this technique is further developed in the following project.

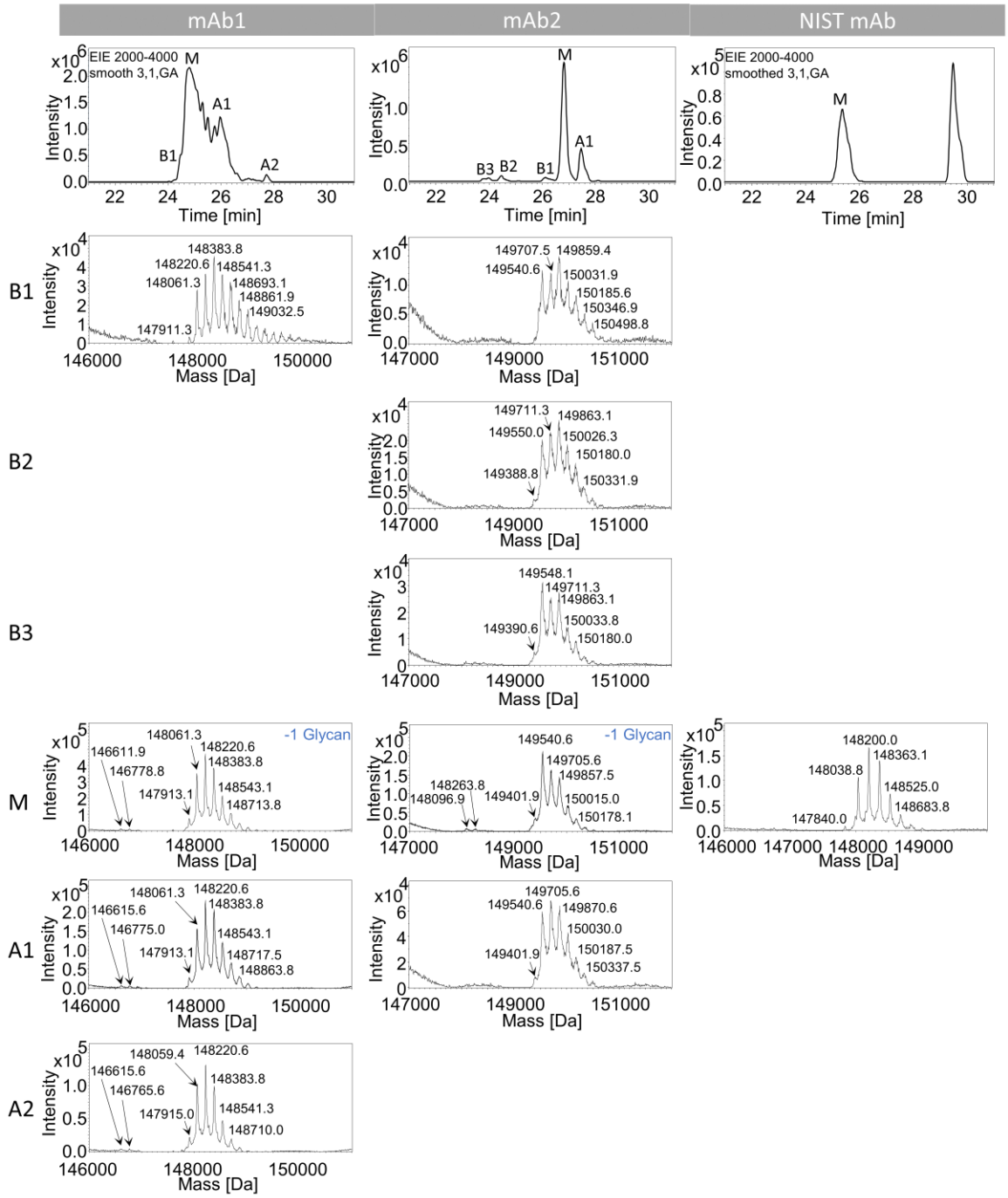

Figure 3.12: CIEF-MS separation and identification of mAb1, mAb2, and NIST mAb all measured on the Bruker MaXis TOF instrument. Top row: Extracted ion electropherograms from 2000 to 4000 m/z (smoothed). Following rows: Deconvoluted spectra of separated variants. A: acidic variant, M: main variant, B: basic variant. Figure is generated analog to Figure 5 in **manuscript IV.**

3.3.4 Comparison of variant analysis approaches

A detailed comparison and discussion of IEX, CIEF, and CZE on an intact and subunit level can be found in **manuscript IV**. A summary of the discussion done there shall be given here starting with the direct comparison of all three intact and MS-coupled methods. Generally, all tested intact methods determine the overall mAb variant composition and separate acidic, main, and basic mAb variants. MS-based mAb variant identification like the glycosylation profile including minor glycosylation species and monoglycosylation is possible with all intact methods. However, the variant assignment is highly method-dependent. IEX-separated variants suffer from low spectral quality when introduced into the MS and CIEF-mediated variant separation is slightly lost towards the MS. Even though CIEF-MS and IEX-MS generally seem to have a significantly lower spectra quality compared to the CZE-MS approach the different mass spectrometers used, lead to changing declustering abilities. In QTOF instruments increased skimmer and fragmentor voltage enhance salt and water declustering which improves sensitivity [120]. In Orbitrap instruments, a too-high trapping voltage leads to a decline in sensitivity [121]. These characteristics result in different sensitivity and thus, make a direct comparison complicated. The lysine variant of three mAbs can be used to compare the resolution of the techniques. The detailed values and a detailed discussion can be found in **manuscript IV** but the MS incompatible CZE-EACA-UV method provides the highest resolution followed by all MS compatible approaches. The different selectivity of the methods also becomes evident for monoglycosylation which is found in the main variant peak using IEX and CIEF and is separated from the main variant peak using the CZE. Table 4 in **manuscript IV** shows that almost every variant was at least once unequivocally identified for some mAb in the literature by one of these selective separation approaches.

As previously mentioned intact mAb analysis allows the determination of the overall mAb composition while keeping sample preparation and the risk of artifact formation to a minimum. Even though this information is partly lost at the subunit level the subunit approach enables a more detailed analysis (discussed in **manuscript III** and **manuscript IV**) regarding the location of the variant within the mAb. The subunit approach narrows down the modification site, enables MS/MS fragmentation, and therefore allows the detection of several variants all described

in **manuscript III**. Informational output is only narrowed down when positional isomers are not properly separated and several possible modification sites are available within the subunit. For this thesis, mAb subunits were only analyzed by CZE-MS since the chaotropic salt mandatory in the reduction process is interfering with the IEX, and CIEF is commonly used for the intact analysis of mAbs possibly because subunits cover a broad pI range.

Lastly, **manuscript IV** discusses instrumental parameters and sample-specific requirements. Both have an enormous impact on the selective and sensitive separation and identification of mAb variants. Sample-specific requirements are especially evident in the previously discussed solubility problem for some mAbs in CIEF (compare chapter 3.3.3). Instrumental parameters are most evident for the presented IEX method which suffers from the use of a standard LC sprayer and the high flow rate towards the MS. As evident from Table 1 in **manuscript IV** IEX-MS approaches tend to minimize the amount of eluent by using a post-column flow splitter, nanoflow-IEX columns, and special nanoflow and microspray ionization sources. Miniaturization and nanospray sources are also generally applied for CIEF-MS and CZE-MS methods as shown in Table 2 and Table 3 in **manuscript IV**. Short cartridges and nanospray sources are preferred in CIEF. Even though all approaches in Table 2 in **manuscript IV** provide quite high mass spectra quality the separation is always impaired by the mobilization step. Similar to CIEF, CZE benefits from chip applications. The fast and efficient separation of mAb variants can however be compromised when coupled to the MS. Sample dilution due to excessive SL consumption can significantly reduce the signal intensity [63] which is the main reason for coupling CZE rather with low-flow sheath liquid CZE-MS interfaces or sheathless CZE-MS interfaces [62].

In addition to the general considerations regarding informational output, these instrumental parameters can prevent selective MS detection and identification. All aspects discussed in **manuscript IV** prove that the method and instrumental setup for mAb variant analysis have to be chosen carefully.

Conclusion and Outlook

In conclusion, it can be said that each analytical approach, no matter if done on the intact or subunit mAbs level, separated by CZE, CIEF, or IEX, detected by UV or MS, has its benefits and drawbacks, and the method for variant separation and identification has to be chosen accordingly. While the intact approach allows the overall analysis of the mAb and its variants while keeping sample preparation and artifacts to a minimum, the subunit approach gives a more detailed mAb picture due to the reduction of the mAb complexity by generating subunit moieties and making them available for MS/MS experiments. Some methods are better platform methods (CZE and IEX to a certain extent) while others (CIEF) need further method development. CZE-MS separated and identified multiple variants and reduced variants on the intact and subunit levels. With only injecting ng of a sample, proteoforms with a relative intensity of 0.5% compared to the respective main form were determined. Incomplete sample reduction was initially introducing artificial heterogeneity to the sample using the CZE-MS subunit approach. Even though this was later solved by adding urea as a chaotropic salt to the sample reduction, this initial artificial heterogeneity was successfully separated and identified by CZE-MS (MS/MS). In general, fragmentation by EThcD proved to be a valuable tool for the site-specific characterization of mAb variants, achieving an overall fragmentation coverage of up to 30% depending on the subunit. The subunits were additionally separated by TIMS, which has so far not been done, and different subunits and reduction states could be separated in the gas phase. To evaluate the orthogonality of CZE and TIMS, which has so far not been done methodically, a complex peptide mixture (tryptic digest of HeLa proteins) was analyzed. The resulting very high orthogonality of around 80% is most likely related to solvation effects leading to different charges and sizes in the liquid phase compared to the gas phase. Antibody variant separation on the intact level by CZE-MS has so far mostly been done under native conditions. By using novel capillary coatings in combination with the sensitive nanoESI ionization, intact mAb variants could be separated using acidic separation conditions. IEX-MS and CIEF-MS could be used to separate and identify some minor mass changes of the antibody, but compared to CZE-MS on the intact and subunit level, the informational output was limited. All tested methods have different selectivities; nevertheless, the selective separation of mAb variants

with very high resolving powers could be achieved with all methods. A sample set of ten mAb samples was applied to all methods without any mAb-specific method optimization, which proves the generic application of these methods within the tested pI range.

All methods have considerable potential in the future for in-depth mAb variant characterization and identification. Capillary coatings can be further improved or modified to even better separate the mAb variants, with the additional option to separate under less acidic (“native”) conditions. CIEF chemical mobilization using the nanoCEasy interface already showed promising results but surely can benefit from improved handling and robustness. The already really good IEX separation can benefit from MS optimization by using e.g. a post-column flow splitter or a nanoESI interface. Generally, when analyzing mAb variants, a combination of different methods should always be considered. This combination of different approaches complements the mAb picture, which can not be gained by solely relying on one method. A combination of all these methods and the detailed characterization of the peptide level is highly beneficial when analyzing mAb variants to get the overall mAb composition. Nevertheless, each method alone can already give quite important information to characterize mAb variants.

References

[1] Walsh G, Walsh E. Biopharmaceutical benchmarks 2022. Nat Biotechnol. 2022; 40: 1722–60.

[2] Vidarsson G, Dekkers G, Rispens T. IgG subclasses and allotypes: from structure to effector functions. Front Immunol. 2014; 5: 520.

[3] Chiu ML, Goulet DR, Teplyakov A, Gilliland GL. Antibody Structure and Function: The Basis for Engineering Therapeutics. Antibodies (Basel). 2019; 8.

[4] Kumar R, Guttman A, Rathore AS. Applications of capillary electrophoresis for biopharmaceutical product characterization. Electrophoresis. 2022; 43: 143–66.

[5] Zheng JY, Janis LJ. Influence of pH, buffer species, and storage temperature on physicochemical stability of a humanized monoclonal antibody LA298. Int J Pharm. 2006; 308: 46–51.

[6] Li Y. A brief introduction of IgG-like bispecific antibody purification: Methods for removing product-related impurities. Protein Expr Purif. 2019; 155: 112–9.

[7] Beyer B, Schuster M, Jungbauer A, Lingg N. Microheterogeneity of Recombinant Antibodies: Analytics and Functional Impact. Biotechnol J. 2018; 13.

[8] Khawli LA, Goswami S, Hutchinson R, Kwong ZW, Yang J, Wang X, et al. Charge variants in IgG1: Isolation, characterization, in vitro binding properties and pharmacokinetics in rats. mAbs. 2010; 2: 613–24.

[9] Beck A, Liu H. Macro- and Micro-Heterogeneity of Natural and Recombinant IgG Antibodies. Antibodies (Basel). 2019; 8.

[10] Liu L. Antibody Glycosylation and Its Impact on the Pharmacokinetics and Pharmacodynamics of Monoclonal Antibodies and Fc-Fusion Proteins. Journal of Pharmaceutical Sciences. 2015; 104: 1866–84.

[11] Liu H, Bulseco G-G, Sun J. Effect of posttranslational modifications on the thermal stability of a recombinant monoclonal antibody. Immunol Lett. 2006; 106: 144–53.

[12] Mo J, Yan Q, So CK, Soden T, Lewis MJ, Hu P. Understanding the Impact of Methionine Oxidation on the Biological Functions of IgG1 Antibodies Using

Hydrogen/Deuterium Exchange Mass Spectrometry. Anal. Chem. 2016; 88: 9495–502.

[13] Liu D, Ren D, Huang H, Dankberg J, Rosenfeld R, Cocco MJ, et al. Structure and stability changes of human IgG1 Fc as a consequence of methionine oxidation. Biochemistry. 2008; 47: 5088–100.

[14] Lu X, Machiesky LA, Mel N de, Du Q, Xu W, Washabaugh M, et al. Characterization of IgG1 Fc Deamidation at Asparagine 325 and Its Impact on Antibody-dependent Cell-mediated Cytotoxicity and FcγRIIIa Binding. Sci Rep. 2020; 10: 383.

[15] Lacy ER, Baker M, Brigham-Burke M. Free sulfhydryl measurement as an indicator of antibody stability. Anal Biochem. 2008; 382.

[16] McAuley A, Jacob J, Kolvenbach CG, Westland K, Lee HJ, Brych SR, et al. Contributions of a disulfide bond to the structure, stability, and dimerization of human IgG1 antibody CH3 domain. Protein Sci. 2008; 17: 95–106.

[17] Faid V, Leblanc Y, Berger M, Seifert A, Bihoreau N, Chevreux G. C-terminal lysine clipping of IgG1: impact on binding to human FcγRIIIa and neonatal Fc receptors. European Journal of Pharmaceutical Sciences. 2021; 159: 105730.

[18] Lyubarskaya Y, Houde D, Woodard J, Murphy D, Mhatre R. Analysis of recombinant monoclonal antibody isoforms by electrospray ionization mass spectrometry as a strategy for streamlining characterization of recombinant monoclonal antibody charge heterogeneity. Anal Biochem. 2006; 348: 24–39.

[19] Füssl F, Trappe A, Carillo S, Jakes C, Bones J. Comparative Elucidation of Cetuximab Heterogeneity on the Intact Protein Level by Cation Exchange Chromatography and Capillary Electrophoresis Coupled to Mass Spectrometry. Anal Chem. 2020; 92: 5431–8.

[20] Giorgetti J, Lechner A, Del Nero E, Beck A, François Y-N, Leize-Wagner E. Intact monoclonal antibodies separation and analysis by sheathless capillary electrophoresis-mass spectrometry. Eur J Mass Spectrom (Chichester). 2019; 25: 324–32.

[21] Dai J, Lamp J, Xia Q, Zhang Y. Capillary Isoelectric Focusing-Mass Spectrometry Method for the Separation and Online Characterization of Intact Monoclonal Antibody Charge Variants. Anal Chem. 2018; 90: 2246–54.

[22] Kellie JF, Schneck NA, Causon JC, Baba T, Mehl JT, Pohl KI. Top-Down Characterization and Intact Mass Quantitation of a Monoclonal Antibody Drug

from Serum by Use of a Quadrupole TOF MS System Equipped with Electron-Activated Dissociation. J Am Soc Mass Spectrom. 2023; 34: 17–26.

[23] Mao Y, Valeja SG, Rouse JC, Hendrickson CL, Marshall AG. Top-down structural analysis of an intact monoclonal antibody by electron capture dissociation-Fourier transform ion cyclotron resonance-mass spectrometry. Anal Chem. 2013; 85: 4239–46.

[24] Srzentić K, Fornelli L, Tsybin YO, Loo JA, Seckler H, Agar JN, et al. Interlaboratory Study for Characterizing Monoclonal Antibodies by Top-Down and Middle-Down Mass Spectrometry. J Am Soc Mass Spectrom. 2020; 31: 1783–802.

[25] Dick LW, Mahon D, Qiu D, Cheng K-C. Peptide mapping of therapeutic monoclonal antibodies: improvements for increased speed and fewer artifacts. Journal of Chromatography B. 2009; 877: 230–6.

[26] Lippincott J, Apostol I. Carbamylation of cysteine: a potential artifact in peptide mapping of hemoglobins in the presence of urea. Anal Biochem. 1999; 267: 57–64.

[27] Gahoual R, Biacchi M, Chicher J, Kuhn L, Hammann P, Beck A, et al. Monoclonal antibodies biosimilarity assessment using transient isotachophoresis capillary zone electrophoresis-tandem mass spectrometry. mAbs. 2014; 6: 1464–73.

[28] Lew C, Gallegos-Perez J-L, Fonslow B, Lies M, Guttman A. Rapid level-3 characterization of therapeutic antibodies by capillary electrophoresis electrospray ionization mass spectrometry. J Chromatogr Sci. 2015; 53: 443–9.

[29] Cao M, Mel N de, Wang J, Parthemore C, Jiao Y, Chen W, et al. Characterization of N-Terminal Glutamate Cyclization in Monoclonal Antibody and Bispecific Antibody Using Charge Heterogeneity Assays and Hydrophobic Interaction Chromatography. Journal of Pharmaceutical Sciences. 2022; 111: 335–44.

[30] Belov AM, Zang L, Sebastiano R, Santos MR, Bush DR, Karger BL, et al. Complementary middle-down and intact monoclonal antibody proteoform characterization by capillary zone electrophoresis – mass spectrometry. Electrophoresis. 2018; 39: 2069–82.

[31] Leblanc Y, Faid V, Lauber MA, Wang Q, Bihoreau N, Chevreux G. A generic method for intact and subunit level characterization of mAb charge variants by native mass spectrometry. Journal of Chromatography B. 2019; 1133: 121814.

[32] Zhao Y, Sun L, Knierman MD, Dovichi NJ. Fast separation and analysis of reduced monoclonal antibodies with capillary zone electrophoresis coupled to mass spectrometry. Talanta. 2016; 148: 529–33.

[33] Verscheure L, Oosterlynck M, Cerdobbel A, Sandra P, Lynen F, Sandra K. Middle-up characterization of monoclonal antibodies by online reduction liquid chromatography-mass spectrometry. J Chromatogr A. 2021; 1637: 461808.

[34] An Y, Zhang Y, Mueller H-M, Shameem M, Chen X. A new tool for monoclonal antibody analysis: application of IdeS proteolysis in IgG domain-specific characterization. mAbs. 2014; 6: 879–93.

[35] Gstöttner C, Nicolardi S, Haberger M, Reusch D, Wuhrer M, Domínguez-Vega E. Intact and subunit-specific analysis of bispecific antibodies by sheathless CE-MS. Anal Chim Acta. 2020; 1134: 18–27.

[36] Seth Madren, Linda Yi. Microchip electrophoresis separation coupled to mass spectrometry (MCE–MS) for the rapid monitoring of multiple quality attributes of monoclonal antibodies. Electrophoresis. 2022; 43: 2453–65.

[37] Bouvarel T, Camperi J, Guillarme D. Multi-dimensional technology - Recent advances and applications for biotherapeutic characterization. J Sep Sci. 2024; 47: e2300928.

[38] He Y, Isele C, Hou W, Ruesch M. Rapid analysis of charge variants of monoclonal antibodies with capillary zone electrophoresis in dynamically coated fused-silica capillary. J Sep Sci. 2011; 34: 548–55.

[39] Henk H. Lauer, Gerard P. Rozing, editor. High Performance Capillary Electrophoresis: A Primer.

[40] Breadmore MC. Electrokinetic and hydrodynamic injection: making the right choice for capillary electrophoresis. Bioanalysis. 2009; 1: 889–94.

[41] Huhn C, Ramautar R, Wuhrer M, Somsen GW. Relevance and use of capillary coatings in capillary electrophoresis-mass spectrometry. Analytical and bioanalytical chemistry. 2010; 396: 297–314.

[42] Iki N, Yeung ES. Non-bonded poly(ethylene oxide) polymer-coated column for protein separation by capillary electrophoresis. Journal of Chromatography A. 1996; 731: 273–82.

[43] Höchsmann A, Dhellemmes L, Leclercq L, Cottet H, Neusüß C. Charge variant analysis of monoclonal antibodies by CZE-MS using a successive multiple ionic-polymer layer coating based on diethylaminoethyl-dextran. Electrophoresis. 2024.

[44] Leclercq L, Morvan M, Koch J, Neusüß C, Cottet H. Modulation of the electroosmotic mobility using polyelectrolyte multilayer coatings for protein analysis by capillary electrophoresis. Anal Chim Acta. 2019; 1057: 152–61.

[45] Liu AP, Yan Y, Wang S, Li N. Coupling Anion Exchange Chromatography with Native Mass Spectrometry for Charge Heterogeneity Characterization of Monoclonal Antibodies. Anal Chem. 2022; 94: 6355–62.

[46] Neill A, Nowak C, Patel R, Ponniah G, Gonzalez N, Miano D, et al. Characterization of Recombinant Monoclonal Antibody Charge Variants Using OFFGEL Fractionation, Weak Anion Exchange Chromatography, and Mass Spectrometry. Anal Chem. 2015; 87: 6204–11.

[47] Wallace RG, Rochfort KD. Ion-Exchange Chromatography: Basic Principles and Application. Protein Chromatography. 2023: 161–77.

[48] Goyon A, Excoffier M, Janin-Bussat M-C, Bobaly B, Fekete S, Guillarme D, et al. Determination of isoelectric points and relative charge variants of 23 therapeutic monoclonal antibodies. J Chromatogr B Analyt Technol Biomed Life Sci. 2017; 1065-1066: 119–28.

[49] Farsang E, Murisier A, Horváth K, Beck A, Kormány R, Guillarme D, et al. Tuning selectivity in cation-exchange chromatography applied for monoclonal antibody separations, part 1: Alternative mobile phases and fine tuning of the separation. J Pharm Biomed Anal. 2019; 168: 138–47.

[50] Füssl F, Millán-Martín S, Bones J, Carillo S. Cation exchange chromatography on a monodisperse 3 µm particle enables extensive analytical similarity assessment of biosimilars. J Pharm Biomed Anal. 2023; 234: 115534.

[51] Murisier A, Duivelshof BL, Fekete S, Bourquin J, Schmudlach A, Lauber MA, et al. Towards a simple on-line coupling of ion exchange chromatography and native mass spectrometry for the detailed

characterization of monoclonal antibodies. J Chromatogr A. 2021; 1655: 462499.

[52] Robert Weinberger. Practical Capillary Electrophoresis. Elsevier. 2000.

[53] Righetti PG. Isoelectric Focusing: Theory, Methodology and Application. Elsevier. 2000.

[54] Kurreck J, Engels JW, Lottspeich F, editors. Bioanalytik. 4. Auflage. Berlin, Heidelberg: Springer Spektrum; 2022.

[55] Bana A, Mehta P. Similarity assessment of charge variants for bevacizumab biosimilar formulations using imaged capillary isoelectric focusing. Journal of Liquid Chromatography & Related Technologies. 2021; 44: 801–8.

[56] Candreva J, Esterman AL, Ge D, Patel P, Flagg SC, Das TK, et al. Dual-detection approach for a charge variant analysis of monoclonal antibody combination products using imaged capillary isoelectric focusing. Electrophoresis. 2022; 43: 1701–9.

[57] He X, ElNaggar M, Ostrowski MA, Guttman A, Gentalen E, Sperry J. Evaluation of an icIEF-MS system for comparable charge variant analysis of biotherapeutics with rapid peak identification by mass spectrometry. Electrophoresis. 2022; 43: 1215–22.

[58] Naghdi E, Reinau ME, Krogh TN, Neusüß C. Chemical Mobilization-Based Capillary Isoelectric Focusing–Mass Spectrometry Using the nanoCEasy Interface for Pharmaceutical Protein Analysis. Anal. Chem. 2024; 96: 12827–37.

[59] Mack S, Arnold D, Bogdan G, Bousse L, Danan L, Dolnik V, et al. A novel microchip-based imaged CIEF-MS system for comprehensive characterization and identification of biopharmaceutical charge variants. Electrophoresis. 2019; 40: 3084–91.

[60] Bonvin G, Schappler J, Rudaz S. Capillary electrophoresis-electrospray ionization-mass spectrometry interfaces: fundamental concepts and technical developments. J Chromatogr A. 2012; 1267: 17–31.

[61] Gross JH, editor. Mass Spectrometry: A Textbook. 3rd ed. 2017. Cham: Springer International Publishing; Imprint: Springer; 2017.

[62] Naumann L, Schairer J, Höchsmann A, Naghdi E, Neusüß C. Capillary Electrophoresis–Mass Spectrometry Interfacing: Principles and Recent Developments. In: Ramautar R, Chen DDY, editors. Capillary

Electrophoresis-Mass Spectrometry for Proteomics and Metabolomics. Wiley; 2022. p. 1–33.

[63] Höcker O, Montealegre C, Neusüß C. Characterization of a nanoflow sheath liquid interface and comparison to a sheath liquid and a sheathless porous-tip interface for CE-ESI-MS in positive and negative ionization. Anal Bioanal Chem. 2018; 410: 5265–75.

[64] Schlecht J, Stolz A, Hofmann A, Gerstung L, Neusüß C. nanoCEasy: An Easy, Flexible, and Robust Nanoflow Sheath Liquid Capillary Electrophoresis-Mass Spectrometry Interface Based on 3D Printed Parts. Anal Chem. 2021; 93: 14593–8.

[65] van der Zon AA, Höchsmann A, Bos TS, Neusüß C, Somsen GW, Jooß K, et al. Characterization of monoclonal antibody charge variants under near-native separation conditions using nanoflow sheath liquid capillary electrophoresis-mass spectrometry. Anal Chim Acta. 2024; 1331: 343287.

[66] Höcker O, Bader T, Schmidt TC, Schulz W, Neusüß C. Enrichment-free analysis of anionic micropollutants in the sub-ppb range in drinking water by capillary electrophoresis-high resolution mass spectrometry. Analytical and bioanalytical chemistry. 2020; 412: 4857–65.

[67] Höcker O, Knierman M, Meixner J, Neusüß C. Two capillary approach for a multifunctional nanoflow sheath liquid interface for capillary electrophoresis-mass spectrometry. Electrophoresis. 2021; 42: 369–73.

[68] Höchsmann A, Schairer J, Schott O, Höneise R, Neusüß C. Flow Rate Determination of the Nanoflow Sheath Liquid CE-MS-Coupling Applying the nanoCEasy Interface. Electrophoresis. 2024.

[69] Fuerstenau SD, Benner WH. Molecular weight determination of megadalton DNA electrospray ions using charge detection time-of-flight mass spectrometry. Rapid Commun Mass Spectrom. 1995; 9: 1528–38.

[70] Fuerstenau SD, Benner WH, Thomas JJ, Brugidou C, Bothner B, Siuzdak G. Mass Spectrometry of an Intact Virus. Angewandte Chemie. 2001; 113: 559–62.

[71] Thermo Scientifi Orbitrap Fusion Lumos Tribrid Mass Spectrometer Specifications Sheet; 2017 [cited 11.11.24] Available from: URL: https://assets.thermofisher.com/TFS-Assets/CMD/Specification-Sheets/PS-64391-LC-MS-Orbitrap-Fusion-Lumos-Tribrid-PS64391-EN.pdf.

[72] Hecht ES, Scigelova M, Eliuk S, Makarov A. Fundamentals and Advances of Orbitrap Mass Spectrometry. In: Meyers RA, editor. Encyclopedia of analytical chemistry. Chichester, New York: Wiley; 2000. p. 1–40.

[73] Perry RH, Cooks RG, Noll RJ. Orbitrap mass spectrometry: instrumentation, ion motion and applications. Mass Spectrom Rev. 2008; 27: 661–99.

[74] Makarov A. Electrostatic axially harmonic orbital trapping: a high-performance technique of mass analysis. Anal Chem. 2000; 72: 1156–62.

[75] Scigelova M, Makarov A. Orbitrap mass analyzer--overview and applications in proteomics. Proteomics. 2006; 6 Suppl 2: 16–21.

[76] Shliaha PV, Gibb S, Gorshkov V, Jespersen MS, Andersen GR, Bailey D, et al. Maximizing Sequence Coverage in Top-Down Proteomics By Automated Multimodal Gas-Phase Protein Fragmentation. Anal. Chem. 2018; 90: 12519–26.

[77] Meier F, Beck S, Grassl N, Lubeck M, Park MA, Raether O, et al. Parallel Accumulation-Serial Fragmentation (PASEF): Multiplying Sequencing Speed and Sensitivity by Synchronized Scans in a Trapped Ion Mobility Device. J Proteome Res. 2015; 14: 5378–87.

[78] Michelmann K, Silveira JA, Ridgeway ME, Park MA. Fundamentals of Trapped Ion Mobility Spectrometry. J Am Soc Mass Spectrom. 2015; 26: 14–24.

[79] Hernandez DR, Debord JD, Ridgeway ME, Kaplan DA, Park MA, Fernandez-Lima F. Ion dynamics in a trapped ion mobility spectrometer. Analyst. 2014; 139: 1913–21.

[80] timsTOF SCP; 2024 [cited 2024 December 8] Available from: URL: https://www.bruker.com/en/products-and-solutions/mass-spectrometry/timstof/timstof-scp.html.

[81] Ogata K, Ishihama Y. Extending the Separation Space with Trapped Ion Mobility Spectrometry Improves the Accuracy of Isobaric Tag-Based Quantitation in Proteomic LC/MS/MS. Anal Chem. 2020; 92: 8037–40.

[82] Baglai A, Gargano AFG, Jordens J, Mengerink Y, Honing M, van der Wal S, et al. Comprehensive lipidomic analysis of human plasma using multidimensional liquid- and gas-phase separations: Two-dimensional liquid chromatography-mass spectrometry vs. liquid chromatography-trapped-ion-mobility-mass spectrometry. J Chromatogr A. 2017; 1530: 90–103.

[83] Jeanne Dit Fouque K, Ramirez CE, Lewis RL, Koelmel JP, Garrett TJ, Yost RA, et al. Effective Liquid Chromatography-Trapped Ion Mobility Spectrometry-Mass Spectrometry Separation of Isomeric Lipid Species. Anal. Chem. 2019; 91: 5021–7.

[84] DeLaney K, Jia D, Iyer L, Yu Z, Choi SB, Marvar PJ, et al. Microanalysis of Brain Angiotensin Peptides Using Ultrasensitive Capillary Electrophoresis Trapped Ion Mobility Mass Spectrometry. Anal Chem. 2022; 94: 9018–25.

[85] Drouin N, Mielcarek A, Wenz C, Rudaz S. Evaluation of ion mobility in capillary electrophoresis coupled to mass spectrometry for the identification in metabolomics. Electrophoresis. 2021; 42: 342–9.

[86] Glazyrin YE, Mironov GG, Kichkailo AS, Berezovski MV. Separation Abilities of Capillary Electrophoresis Coupled with Ion Mobility Mass Spectrometry for the Discrete Detection of Sequence Isomeric Peptides. Separations. 2022; 9: 106.

[87] Gou M-J, Kose MC, Crommen J, Nix C, Cobraiville G, Caers J, et al. Contribution of Capillary Zone Electrophoresis Hyphenated with Drift Tube Ion Mobility Mass Spectrometry as a Complementary Tool to Microfluidic Reversed Phase Liquid Chromatography for Antigen Discovery. Int J Mol Sci. 2022; 23.

[88] Hooijschuur K, Liu X, Grootendorst A, Pieterman I, Sastre Toraño J. In-line sample trap columns with diatomite for large-volume injection in CZE-IM-MS. Electrophoresis. 2023; 44: 395–402.

[89] Johnson KR, Greguš M, Ivanov AR. Coupling High-Field Asymmetric Ion Mobility Spectrometry with Capillary Electrophoresis-Electrospray Ionization-Tandem Mass Spectrometry Improves Protein Identifications in Bottom-Up Proteomic Analysis of Low Nanogram Samples. J Proteome Res. 2022; 21: 2453–61.

[90] Jooß K, Meckelmann SW, Klein J, Schmitz OJ, Neusüß C. Capillary zone electrophoresis coupled to drift tube ion mobility-mass spectrometry for the analysis of native and APTS-labeled N-glycans. Analytical and bioanalytical chemistry. 2019; 411: 6255–64.

[91] Li J, Purves RW, Richards JC. Coupling capillary electrophoresis and high-field asymmetric waveform ion mobility spectrometry mass spectrometry for the analysis of complex lipopolysaccharides. Anal. Chem. 2004; 76: 4676–83.

[92] Mast DH, Liao H-W, Romanova EV, Sweedler JV. Analysis of Peptide Stereochemistry in Single Cells by Capillary Electrophoresis-Trapped Ion Mobility Spectrometry Mass Spectrometry. Anal Chem. 2021; 93: 6205–13.

[93] Mironov GG, Clouthier CM, Akbar A, Keillor JW, Berezovski MV. Simultaneous analysis of enzyme structure and activity by kinetic capillary electrophoresis-MS. Nat Chem Biol. 2016; 12: 918–22.

[94] Shen B, Zhou F, Nemes P. Electrophoresis-Correlative Ion Mobility Deepens Single-cell Proteomics in Capillary Electrophoresis Mass Spectrometry. Mol Cell Proteomics. 2024: 100892.

[95] Xu T, Wang Q, Wang Q, Sun L. Coupling High-Field Asymmetric Waveform Ion Mobility Spectrometry with Capillary Zone Electrophoresis-Tandem Mass Spectrometry for Top-Down Proteomics. Anal. Chem. 2023; 95: 9497–504.

[96] Zhong X, Chen Z, Snovida S, Liu Y, Rogers JC, Li L. Capillary Electrophoresis-Electrospray Ionization-Mass Spectrometry for Quantitative Analysis of Glycans Labeled with Multiplex Carbonyl-Reactive Tandem Mass Tags. Anal Chem. 2015; 87: 6527–34.

[97] Liu H, Chumsae C, Gaza-Bulseco G, Hurkmans K, Radziejewski CH. Ranking the susceptibility of disulfide bonds in human IgG1 antibodies by reduction, differential alkylation, and LC-MS analysis. Anal Chem. 2010; 82: 5219–26.

[98] Masters JR. HeLa cells 50 years on: the good, the bad and the ugly. Nat Rev Cancer. 2002; 2: 315–9.

[99] Sokolowska I, Mo J, Dong J, Lewis MJ, Hu P. Subunit mass analysis for monitoring antibody oxidation. mAbs. 2017; 9: 498–505.

[100] Stoll DR, Harmes DC, Danforth J, Wagner E, Guillarme D, Fekete S, et al. Direct identification of rituximab main isoforms and subunit analysis by online selective comprehensive two-dimensional liquid chromatography-mass spectrometry. Anal Chem. 2015; 87: 8307–15.

[101] Duivelshof BL, Beck A, Guillarme D, D'Atri V. Bispecific antibody characterization by a combination of intact and site-specific/chain-specific LC/MS techniques. Talanta. 2022; 236: 122836.

[102] Giorgetti J, Beck A, Leize-Wagner E, François Y-N. Combination of intact, middle-up and bottom-up levels to characterize 7 therapeutic monoclonal

antibodies by capillary electrophoresis - Mass spectrometry. J Pharm Biomed Anal. 2020; 182: 113107.

[103] Scheffer K, Damoc E. Antibody subunit analysis workflow on a quadrupole-Orbitrap mass spectrometer: from optimized sample preparation to data analysis. 2018.

[104] Wiesner R, Zagst H, Lan W, Bigelow S, Holper P, Hübner G, et al. An interlaboratory capillary zone electrophoresis-UV study of various monoclonal antibodies, instruments, and ε-aminocaproic acid lots. Electrophoresis. 2023.

[105] Cageling R, Carillo S, Boumeester AJ, Lubbers-Geuijen K, Bones J, Jooß K, et al. Microfluidic capillary electrophoresis - mass spectrometry for rapid charge-variant and glycoform assessment of monoclonal antibody biosimilar candidates. J Pharm Biomed Anal. 2024; 248: 116301.

[106] Cao L, Fabry D, Lan K. Rapid and comprehensive monoclonal antibody Characterization using microfluidic CE-MS. J Pharm Biomed Anal. 2021; 204: 114251.

[107] Carillo S, Jakes C, Bones J. In-depth analysis of monoclonal antibodies using microfluidic capillary electrophoresis and native mass spectrometry. J Pharm Biomed Anal. 2020; 185: 113218.

[108] Füssl F, Carillo S, Millán-Martín S, Jakes C, Bora K, Liberatori S, et al. Exploring proteoforms of the IgG2 monoclonal antibody panitumumab using microchip capillary electrophoresis-mass spectrometry. J Pharm Biomed Anal. 2023; 234: 115494.

[109] Sun Q, Wang L, Li N, Shi L. Characterization and monitoring of charge variants of a recombinant monoclonal antibody using microfluidic capillary electrophoresis-mass spectrometry. Anal Biochem. 2021; 625: 114214.

[110] Wu Z, Wang H, Wu J, Huang Y, Zhao X, Nguyen JB, et al. High-sensitivity and high-resolution therapeutic antibody charge variant and impurity characterization by microfluidic native capillary electrophoresis-mass spectrometry. J Pharm Biomed Anal. 2023; 223: 115147.

[111] Di Marco F, Berger T, Esser-Skala W, Rapp E, Regl C, Huber CG. Simultaneous Monitoring of Monoclonal Antibody Variants by Strong Cation-Exchange Chromatography Hyphenated to Mass Spectrometry to Assess Quality Attributes of Rituximab-Based Biotherapeutics. Int J Mol Sci. 2021; 22.

[112] Dai J, Ji C. In-depth size and charge variants characterization of monoclonal antibody with native mass spectrometry. Anal Chim Acta. 2023; 1265: 341360.

[113] Sankaran PK, Kabadi PG, Honnappa CG, Subbarao M, Pai HV, Adhikary L, et al. Identification and quantification of product-related quality attributes in bio-therapeutic monoclonal antibody via a simple, and robust cation-exchange HPLC method compatible with direct online detection of UV and native ESI-QTOF-MS analysis. Journal of Chromatography B. 2018; 1102-1103: 83–95.

[114] Cao J, Sun W, Gong F, Liu W. Charge profiling and stability testing of biosimilar by capillary isoelectric focusing. Electrophoresis. 2014; 35: 1461–8.

[115] Haley Sutton, Feng Hong, Xuemei Han, Navin Rauniyar. Analysis of therapeutic monoclonal antibodies by imaged capillary isoelectric focusing (icIEF). Anal. Methods. 2024; 16: 5450–8.

[116] Kahle J, Zagst H, Wiesner R, Wätzig H. Comparative charge-based separation study with various capillary electrophoresis (CE) modes and cation exchange chromatography (CEX) for the analysis of monoclonal antibodies. J Pharm Biomed Anal. 2019; 174: 460–70.

[117] Montealegre C, Neusüß C. Coupling imaged capillary isoelectric focusing with mass spectrometry using a nanoliter valve. Electrophoresis. 2018; 39: 1151–4.

[118] Hühner J, Jooß K, Neusüß C. Interference-free mass spectrometric detection of capillary isoelectric focused proteins, including charge variants of a model monoclonal antibody. Electrophoresis. 2017; 38: 914–21.

[119] Mack S, Cruzado-Park I, Chapman J, Ratnayake C, Vigh G. A systematic study in CIEF: defining and optimizing experimental parameters critical to method reproducibility and robustness. Electrophoresis. 2009; 30: 4049–58.

[120] Schwenzer A-K, Kruse L, Jooß K, Neusüß C. Capillary electrophoresis-mass spectrometry for protein analyses under native conditions: Current progress and perspectives. Proteomics. 2024; 24: e2300135.

[121] Jooß K, McGee JP, Melani RD, Kelleher NL. Standard procedures for native CZE-MS of proteins and protein complexes up to 800 kDa. Electrophoresis. 2021.

List of Figures

Appendix

Manuscript I

CE-MS/MS and CE-timsTOF to separate and characterize intramolecular disulfide bridges of monoclonal antibody subunits and their application for the assessment of subunit reduction protocols

Jasmin Schairer, Jennifer Römer, Dietmar Lang, Christian Neusüß

Analytical and Bioanalytical Chemistry. 2024; 416: 1599–612 DOI: 10.1007/s00216-024-05161-8

Analytical and Bioanalytical Chemistry (2024) 416:1599–1612
https://doi.org/10.1007/s00216-024-05161-8

RESEARCH PAPER

CE-MS/MS and CE-timsTOF to separate and characterize intramolecular disulfide bridges of monoclonal antibody subunits and their application for the assessment of subunit reduction protocols

Jasmin Schairer[1,2] · Jennifer Römer[3] · Dietmar Lang[3] · Christian Neusüß[1]

Received: 8 December 2023 / Revised: 15 January 2024 / Accepted: 17 January 2024 / Published online: 1 February 2024

Abstract
Characterization at the subunit level enables detailed mass spectrometric characterization of posttranslational modifications (PTMs) of monoclonal antibodies (mAbs). The implemented reduction often leaves the intramolecular disulfide bridges intact. Here, we present a capillary electrophoretic (CE) method based on a neutral-coated capillary for the separation of immunoglobulin G-degrading enzyme of *Streptococcus pyogenes* (IdeS) digested and reduced mAb subunits followed by mass spectrometry (MS), MS/MS identification, and trapped ion mobility mass spectrometry (timsTOF). Our CE approach enables the separation of (i) different subunit moieties, (ii) various reduction states, and (iii) positional isomers of these partly reduced subunit moieties. The location of the remaining disulfide bridges can be determined by middle-down electron transfer higher energy collisional dissociation (EThcD) experiments. All these CE-separated variants show differences in ion mobility in the timsTOF measurements. Applying the presented CE-MS/MS method, reduction parameters such as the use of chaotropic salts were studied. For the investigated antibodies, urea improved the subunit reduction significantly, whereas guanidine hydrochloride (GuHCl) leads to multiple signals of the same subunit in the CE separation. The presented CE-MS method is a powerful tool for the disulfide-variant characterization of mAbs on the subunit level. It enables understanding disulfide bridge reduction processes in antibodies and potentially other proteins.

Keywords mAb subunits · Disulfides · Reduction · Capillary electrophoresis · Middle down · Ion mobility

Abbreviations

BGE	Background electrolyte
CE	Capillary electrophoresis
CID	Collision-induced dissociation
C_H1	Constant heavy chain domain 1
C_L	Constant light chain domain
CQA	Critical quality attributes
DTT	Dithiothreitol
EIEs	Extracted ion electropherograms
EIMs	Extracted ion mobilograms
ETD	Electron transfer dissociation
EThcD	Electron transfer higher energy collisional dissociation
FA	Formic acid
FAIMS	Field asymmetric waveform ion mobility spectrometry
$F(ab)_2$	Antigen-binding fragment
Fc/2	C-Terminal half of heavy chain
Fd	N-Terminal half of heavy chain
GuHCl	Guanidine hydrochloride
HC	Heavy chain
HCD	Higher energy collisional dissociation
HCl	Hydrochloric acid
HF	Hydrofluoric acid
HILIC	Hydrophilic interaction liquid chromatography
HPLC	High-performance liquid chromatography
ID	Inner diameter
IdeS	Immunoglobulin G-degrading enzyme of Streptococcus pyogenes
IgG1	Immunoglobulin G1
IM-MS	Ion mobility mass spectrometry
IPA	Isopropanol

✉ Christian Neusüß
christian.neuseuss@hs-aalen.de

[1] Faculty of Chemistry, Aalen University, Aalen, Germany

[2] Faculty of Science, University of Tübingen, Tübingen, Germany

[3] Rentschler Biopharma SE, Laupheim, Germany

LC	Light chain
mAbs	Monoclonal antibodies
MOPS	3-(*N*-Morpholino)propane sulfonic acid
MS	Mass spectrometry
NaOH	Sodium hydroxide
OD	Outer diameter
PEO	Polyethylene oxide
PTM	Posttranslational modification
RP	Reversed-phase chromatography
RT	Room temperature
SL	Sheath liquid
TCEP	Tris(2-carboxyethyl)phosphine
TIE	Total ion electropherogram
TIMS	Trapped ion mobility mass spectrometry
V_H	Variable heavy chain domain
V_L	Variable light chain domain

Introduction

Monoclonal antibodies (mAbs) are important biotherapeutics applied for the treatment of many human diseases, with anticancer therapy being one of the main fields [1]. The characterization of mAbs is important because changes in the structure or posttranslational modifications (PTMs) can happen due to production or storage [2]. These critical quality attributes (CQA), such as the glycosylation pattern, deamidation, disulfide bridges, C-terminal lysin clipping, pyroglutamate, or oxidation, can change the mAbs stability, efficacy, structure, and functionality [3–8]. Proper disulfide bridge formation is vital for the antibodies' structure [9], stability [9, 10], and functionality [8].

Depending on the desired information, mAbs can be analyzed at an intact, reduced, subunit, or peptide level [11]. On the peptide level, the CQAs can be analyzed in great detail, and small changes can be detected [12, 13] even though sample preparation is quite elaborate and artifacts might occur. The approach with the least sample preparation is the analysis on an intact level. However, small changes are difficult to characterize by mass spectrometry (MS) [11, 14]. As a compromise between the intact and peptide level, mAbs can be reduced or enzymatically cut to their subunit moieties. The subunit term is not specified, so several approaches exist to obtain subunits. If the mAb is reduced, heavy chain (HC, 50 kDa) and light chain (LC, 25 kDa) subunits can be analyzed [15, 16]. Enzymes that cleaves the mAb underneath the hinge region [17] produce the C-terminal half of heavy chain (Fc/2; 25 kDa) and the antigen-binding fragment ($F(ab)_2$; 100 kDa) subunits [16, 18, 19]. If these moieties are reduced, the N-terminal half of the heavy chain (Fd), LC, and Fc/2 are received, each with a molecular weight of ~ 25 kDa [11, 16, 20]. To obtain the 25 kDa subunits, different approaches can be done. The initial digestion using the immunoglobulin G-degrading enzyme of *Streptococcus pyogenes* (IdeS) is well established (standard procedure uses 1 U enzyme/1 µg antibody followed by incubation for 30 min at 37 °C). However, the following reduction to obtain the 25 kDa subunits can be performed quite differently. Dithiothreitol (DTT) [16, 20–29] or tris(2-carboxyethyl)phosphine (TCEP) [11, 20, 23, 25, 30–34] are used as reduction chemicals, and the reduction is then carried out for 5–60 min at room temperature (RT) [11, 25, 30–33], 37 °C [21, 23, 26, 28, 29], 45 °C [27], 55–60 °C [16, 20, 22, 25, 34], or 70 °C [24]. The reduction can be performed in guanidine hydrochloride (GuHCl) [16, 20, 22, 23, 25, 31, 33, 34], urea [24, 32], ammonium formate [28], or without chaotropic salt [11, 21, 25–27, 29, 30]. The reduction can be followed by further steps like acidification using trifluoroacetic acid [31, 33], formic acid (FA) [32], or hydrochloric acid (HCl) [29] or rebuffering and desalting [11, 20, 23, 34]. It is also known that removing the reducing agent after reduction leads to scrambled disulfide bridge detection [30].

The main advantage of all these sample preparation steps is the ability to make the 25 kDa subunits accessible for middle-down MS/MS fragmentation experiments [25, 30, 31]. In contrast, fragmentation of the intact antibody requires dedicated equipment and delivers moderate fragmentation coverages [35, 36]. Various PTMs, like changes in the general glycosylation pattern, can be analyzed at the subunit level, as well as deamidation, C-terminal lysine clipping, pyroglutamate formation, disulfide bridges, and oxidation [5, 37]. Still, small mass differences require separated proteoforms. This especially applies to disulfide bridge analysis on the subunit level [20, 27].

For the separation of mAb proteoforms on the subunit level, different high-performance liquid chromatography (HPLC) approaches like hydrophilic interaction liquid chromatography (HILIC) or reversed-phase chromatography (RP) are used. In HILIC approaches, the works focus on glycosylation analysis due to the changes in hydrophilicity of the Fc/2 subunit depending on the sugar attached [27, 38, 39]. RP approaches focus on general mass analysis of subunits [27, 32, 34], glycosylation analysis [28, 31, 32, 34], and methionine oxidation analysis [22, 29]. The separation and analysis of charge variants like lysin clipping or sialylation is mostly done using 2D approaches. In the first dimension, charge variants are separated using ion exchange chromatography or HILIC, followed by an RP separation for desalting or reduction in the second dimension [21, 40–42]. Nevertheless, 2D setups are complex and need a high instrumental effort. Since charge variants change an antibody's size and charge, they are prone to capillary electrophoresis (CE) separation. Minimal size and charge shifts can be analyzed [19, 30]. Disulfides that

change the subunit size without changing its charge were separated by CE on a cationic capillary coating followed by MS characterization [30]. However, the location of the disulfide remained unknown.

Compared to CE, ion mobility mass spectrometers (IM-MS) also separate molecules based on their size-to-charge but in the gas phase [43]. IM-MS is, therefore, highly interesting to analyze protein folding and conformation [44]. It was already shown that LC and HC could be separated in a field asymmetric waveform ion mobility spectrometry (FAIMS) device without a chromatographic pre-separation [45]. Conformational variants of antibodies were analyzed using IM-MS [46, 47], as well as peptides with different disulfide bridge conformations [48]. To the best of our knowledge, ion mobility was not used to study the 25 kD subunits of mAbs.

Here, we present CE-MS/MS and CE-trapped ion mobility mass spectrometry (timsTOF) MS methods to separate and analyze the intramolecular disulfides on the mAbs subunit level using a neutral-coated capillary. Coupling the CE to the MS was straightforward using the nanoCEasy interface [49]. For complete sample reduction, different approaches were tested, as well as the applicability of the reduction towards other immunoglobulin G1 (IgG1) mAbs.

Materials and methods

Chemicals and materials

Trastuzumab (N1050H05; 21 mg/mL) was purchased from Evidentic GmbH (Berlin, Germany); mAb1 (21.7 mg/mL), mAb2 (18.5 mg/mL), and mAb3 (18.3 mg/mL) were kindly provided by Rentschler Biopharma SE (Laupheim, Germany). USP mAb003 (Cat. No. 1445595, LOT: F12980, 10 mg/mL), 3-(N-morpholino) propanesulfonic acid (MOPS)-buffer, 1,4-dithiothreitol (DTT), and hydrochloric acid (37%) were purchased from Sigma (Steinheim, Germany). IdeS protease was purchased from GENOVIS (FabRICATOR, 5000 units, Lund, Sweden). Urea (Ultrapure) and guanidine hydrochloride (99.5%) were purchased from Thermo Fisher Scientific (Dreieich, Germany). Isopropanol (IPA, LC–MS grade) and formic acid (FA, ≥ 98%) were purchased from Carl Roth GmbH & Co. KG (Karlsruhe, Germany). Sodium hydroxide (NaOH) and hydrofluoric acid (40%(v/v), HF) were purchased from Merck (Darmstadt, Germany). Polyethylene oxide (PEO, Mw: 1.000.000) was purchased from Alfa Aesar (Kandel, Germany).

Ultrapure water (18 MΩ*cm at 25 °C, SG Ultra Clear UV from Siemens Water Technologies, USA) was used for all solutions.

Sample preparation

All mAbs were digested following the FabRICATOR digestion protocol from GENOVIS. Five thousand units of FabRICATOR were reconstituted in water at a concentration of 67 U/µL. 9.5 µL of trastuzumab (21 mg/mL) were digested in 87.5 µL100 mM MOPS buffer at pH 7.2 using 3 µL of IdeS, resulting in a final mAb concentration of 2 mg/mL. The sample was incubated for 30 min at 37 °C and 500 rpm.

After digestion, 9 µL digest was reduced using 6 µL 0.5 M DTT (freshly prepared) and 15 µL of reduction medium (8 M urea/16 M urea/8 M GuHCl/water). The final solution contains 0.6 mg/mL of mAb, 100 mM DTT, and 4 M/8 M reduction medium. The reduction was incubated for 60 min at 37 °C and 500 rpm. The samples were then transferred to a glass inlet for CE vials and frozen at − 20 °C until measurement.

CE analysis

The experiments were conducted on an Agilent 7100 CE instrument (Agilent Technologies GmbH, Waldbronn, Germany). Fused silica capillaries (separation capillary: 50 µm inner diameter (ID), 365 µm outer diameter (OD), and sheath liquid (SL) capillary: 100 µm ID, 240 µm OD) were purchased from Polymicro Technologies (Phoenix, AZ, USA).

An etched 60 cm length and 50 µm ID PEO-coated capillary was used for all experiments to avoid protein adsorption. For capillary etching, the polyimide of the separation capillary was removed at one end. The remaining glass was closed with hot glue and etched with HF (40% (v/v)) for 1 h to a thickness of < 150 µm [49]. The PEO coating procedure was adapted from Iki and Yeung [50]. For the PEO stock solution, 100 mg PEO was dissolved in 45 mL of water by heating the solution to 95 °C. 450 µL of the stock solution was then acidified using 50 µL 0.1 M HCl. The capillary was prepared with 1 M NaOH, water, and 1 M HCl for 5 min, respectively, followed by the PEO coating solution for 10 min, water, and background electrolyte (BGE) for 5 min, respectively. The solutions were flushed using the CE and an external pressure of 3 bar. The capillary coating was done each day to guarantee proper capillary coating.

The BGE consisted of 10% IPA in water containing 1 M FA. Sample injection was done hydrodynamically using 50 mbar pressure for 10 s. A 20 kV voltage was applied for the separation. The capillary was flushed for 3 min with BGE between the runs.

nanoCEasy interface

For all CE-MS and CE-MS/MS experiments, the homebuilt nanoCEasy interface [49] was used. Emitters were obtained from BioMedical Instruments (Zoellnitz, Germany). The

setup was controlled using a digital microscope (Dino-Lite, Almere, The Netherlands). The tip of the emitter had an opening of 30 µm and a tip length of 4 mm and was placed 3 mm in front of the MS orifice. In the separation mode, the separation capillary was placed 3 mm behind the emitter tip.

MS and MS/MS and timsTOF analysis

To determine the m/z values for further fragmentation experiments of the subunits, MS experiments were performed using the Orbitrap Fusion Lumos Tribrid MS (Thermo Fisher Scientific, San Jose, CA, USA). IPA: Water (50:50) + 0.5% FA was used in all experiments as SL.

The MS was operated in positive ionization mode with a spray voltage of 2000 V, sweep gas of 3 Arb, and 300 °C ion transfer tube temperature. Data acquisition was done from 700 to 3000 m/z with an Orbitrap resolution of 120.000.

For MS/MS experiments, the Orbitrap was used at a resolution of 7500 in the MS1 scan. For MS2, the scan range was 150–2000 m/z with an Orbitrap resolution of 120,000. Electron transfer higher energy collisional dissociation (EThcD) was used to fragment the precursor ions. Electron transfer dissociation (ETD) reaction time was 12 ms (ETD reaction target of 6E5 in 200 ms), followed by 12% normalized higher energy collisional dissociation (HCD) collision energy.

A timsTOF SCP (Bruker Daltonics GmbH & Co.KG, Bremen, Germany) was used for IM-MS experiments. The instrument was operated in positive ionization mode with a capillary voltage of 1800 V, a dry gas flow of 3.0 L/min, and a dry temperature of 200 °C. The mobility (1/k0) was measured between 0.8 V*s/cm^2 and 1.60 V*s/cm^2 with a ramp time of 100 ms and an accumulation time of 20 ms.

Data analysis

Orbitrap data were evaluated using Freestyle 1.5. To generate the extracted ion electropherograms (EIEs) of the subunits, the most intense charge states of each reduction state were summed up. The EIEs for the different reduction states were generated based on the most intense m/z of the charge envelope. Deconvolution of the Orbitrap MS data was done in Freestyle 1.5 using Xtract, setting the charge range from 5 to 50 and the minimum number of detected charges to 3. The MS/MS data was also deconvoluted using Xtract. The deconvoluted fragments were analyzed using ProSight Lite v1.4 (Northwestern University, Evanston, IL, USA) with a fragment tolerance of 10 ppm.

The timsTOF data were evaluated using DataAnalyst 5.3. For deconvolution, MaxEnt was used. Deconvolution was performed between 20,000 Da and 30,000 Da with a resolving power of 30,000 and normal resolution. Extracted ion mobilograms (EIMs) were generated for m/z values specifically.

The liquid phase charge of the subunits was determined using the Prot pi Protein Tool (https://www.protpi.ch/Calculator/ProteinTool) using the respective pH of the BGE and the sequence of the subunit.

Results

CE-MS

Subunits can be generated using various reduction approaches. Initially, we digested trastuzumab with IdeS enzyme and further reduced the moieties without any chaotropic salt in water using DTT for 60 min at 37 °C. Three signals were expected based on the assumption that trastuzumab is digested and fully reduced to the three subunit moieties Fc/2 (G0F as the main glycoform is exemplarily used for the Fc/2 part of trastuzumab throughout the paper; 25,220 Da), Fd (25,367 Da), and LC (23,428 Da). However, several signals were observed in the total ion electropherogram (TIE), as shown in Fig. 1a. MS spectra can be found in Online Resource ESM 1.

The EIEs of the three moieties showed the separation of the subunits (Fig. 1a). LC and Fc/2 migrated simultaneously (16.4 min) but can be distinguished by their mass and m/z charge envelope, while Fd is well separated (17.5 min). For each subunit moiety, several signals appeared in their respective EIEs. For the LC masses of 23,424.72 Da, 23,426.60 Da, and 23,428.57 Da are obtained after deconvolution, with the latter being close to the theoretical fully reduced mass of 23,428.52 Da. The − 2 Da/ − 4 Da mass shift compared to the fully reduced mass can be expected to be due to an incomplete sample reduction. The same mass shifts were detected for Fd. For Fc/2, no fully reduced form was detected (see Fig. 1b). Another point to mention is that the mass shift of − 2 Da appeared two times in the EIE of the LC and Fd (18.0 min and 19.3 min for LC and 18.5 min and 19.1 min for Fd). To get a better understanding, especially of the − 2 Da shifted signals, MS/MS experiments were needed.

CE-MS/MS

MS/MS experiments were performed to confirm the ability of CE to characterize the different reduction states and to locate the oxidized and reduced disulfide bridges in the subunit moieties. Different fragmentation approaches were tested (collision-induced dissociation (CID), higher energy collisional dissociation (HCD), electron transfer dissociation (ETD), and electron transfer higher energy collisional dissociation (EThcD)), where EThcD yielded the best fragmentation coverage of the molecule (see ESM 2). Figure 2 shows the fragmentation results for each subunit and reduction state.

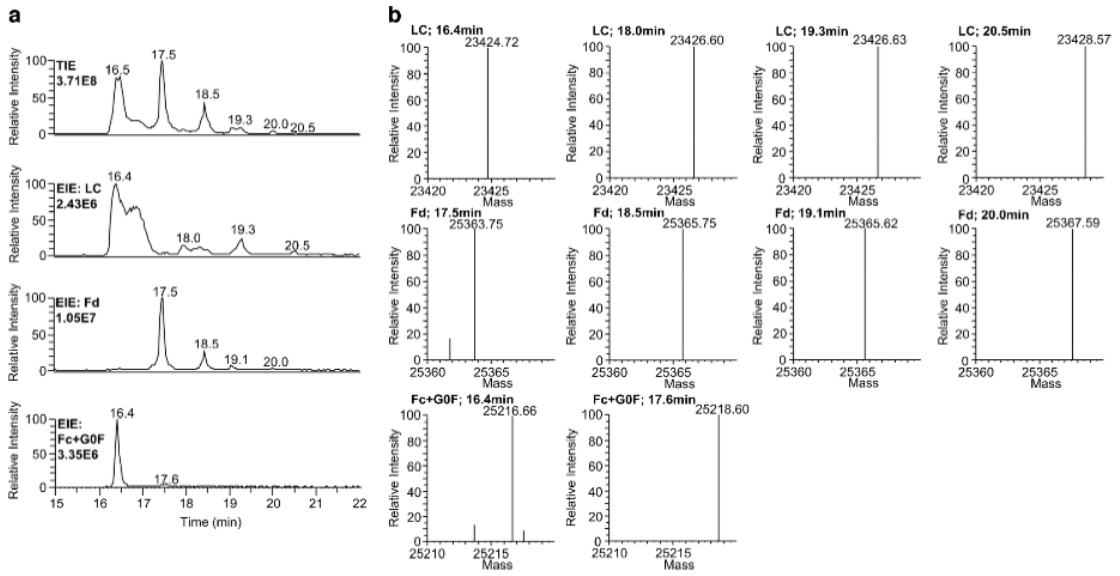

Fig. 1 **a** Separation of trastuzumab subunits using the CE-MS system without fragmentation. EIEs are generated based on the sum of the two most intense m/z for each reduction state. Mass spectra of each subunit and reduction state are shown in Online Resource ESM 1. **b** Charge deconvoluted monoisotopic masses detected for each subunit and time point

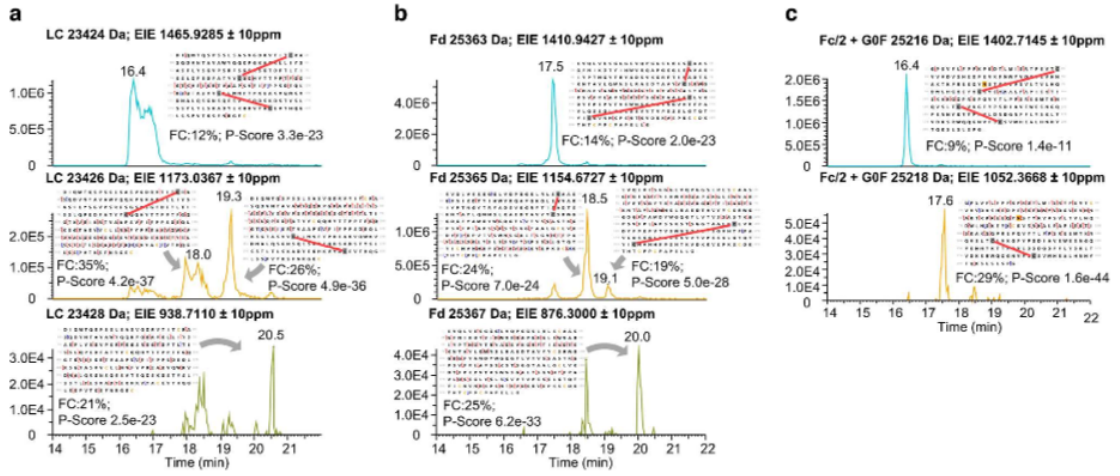

Fig. 2 EIEs for the different reduction states for each subunit of trastuzumab **a** LC; **b** Fd, and **c** Fc/2. The EIE is generated based on the most intense m/z for each reduction state of each subunit. Based on the MS/MS experiment, fragmentation map, fragmentation coverage (FC), and P-score are given for each reduction stage. Red lines indicate closed disulfide bridges. m/z values chosen for EIE generation are marked in Online Resource ESM 1

The first signal in the EIE of the LC (Fig. 2a) at 16.4 min showed a mass shift of − 4 Da, indicating no disulfide bridge reduction. The fragmentation result confirmed that the disulfide bridges in the variable light chain domain (V_L; C23 to C88) and the constant light chain domain (C_L; C134 to C194) remained intact. Fragments, one at the N terminus (*z* ion 212) and one at the C terminus (*c* ion 210), contributed to the fact that both disulfide bridges are closed.

Fragments present between C88 and C134 indicated that no scrambling is present. The two peaks in the EIE, with a − 2 Da shift (18.0 min and 19.3 min), could be assigned to isomeric subunits with different disulfide bridge positions. For the signal at 18 min, the disulfide bridge in the C_L domain (C134 to C194) is open, showing a fragmentation coverage of 35%; for the signal at 19.3 min, the disulfide bridge in the V_L domain (C23 to C88) is open revealing a fragmentation coverage of 26%. This statement is confirmed by several fragments that can only appear if the respective disulfide bridge is open. No scrambled disulfide bridges were detected. However, low amounts of scrambled disulfide bridges would not be detected if they co-migrate with these two partly reduced LCs. The apparent double peaks in the EIE of LC are most likely related to ion suppression due to the co-migrating Fc/2 subunit at 16.4 min and the co-migrating Fd subunit at 18.5 min. The last signal in the EIE of the LC at 20.5 min indicated a full reduction based on mass. The MS/MS approach confirms this due to the detection of fragments that are only possible when both disulfides are open. The fragmentation coverage of 21% is low because the intensity of this reduction state is low using the sample preparation approach with no chaotropic salt. Higher fragmentation coverages with the same analysis were achieved in another sample preparation approach, which will be discussed later (see chapter sample preparation–reduction efficiency).

The same results described for the LC were achieved for Fd (Fig. 2b). Fd carries two disulfide bridges, one in the variable heavy chain domain (V_H) between C22 and C96 and the other in the constant heavy chain domain 1 (C_H1) between C147 and C203. As shown for the LC, the non-reduced, the two partly reduced, and the fully reduced species were separated with CE and identified using MS/MS experiments.

For Fc/2 (Fig. 2c), no completely reduced subunit moiety was detected, and only one signal appeared for partly reduced species, which could be attributed to the Fc/2 subunit with a reduced disulfide bridge in the C_H2-domain between C25 and C85 (C264 and C324 in HC).

All detected masses of the different reduction states are summarized in Table 1.

CE-timsTOF MS

In another experiment, we evaluated whether the disulfides and positional isomers can be distinguished by gas phase IM-MS. The same CE system was used and coupled via the nanoCEasy interface to a timsTOF SCP. Exemplary charge envelopes plotted against the inverse mobility for the four LC forms are shown in Fig. 3.

The co-migrating subunit moieties described previously are visible for the different time points (Fig. 3a and b). A similar separation compared to the CE-MS/MS setup in Fig. 1 was observed, with a slight shift in migration time for all subunits. The different charge envelopes (marked by ovals) for the different reduction states are clearly visible. The non-reduced LC charge envelope (Fig. 3a) showed higher m/z values compared to the partly reduced (Fig. 3b and c) and the fully reduced (Fig. 3d) species. Within one charge envelope, higher m/z values correspond to a lower gas phase mobility. Different mobilities for the different reduction states are obtained. Non-reduced species show a higher mobility than partly and fully reduced species if the same charge state is compared. EIMs were generated for selected charge states for a more detailed analysis of the different reduction states. Since the m/z charge envelopes of non-reduced and fully reduced species barely overlap, different m/z values were chosen to generate EIMs (Fig. 4).

For all subunits, the gas phase mobility could be determined even if the charge state used for comparison was present in low intensities like one of the partly reduced Fd subunits or the fully reduced Fd subunit. For non-reduced and partly reduced LC, 1303.31 ($z = +18$) was chosen to generate the EIM (Fig. 4a). The non-reduced LC showed a higher mobility than the partly-reduced LC. The EIM of 1066.48 ($z = 22$) (Fig. 4c) showed that the fully reduced LC has a smaller mobility compared to the partly-reduced species. For Fd, a similar result was obtained as for the LC. The non-reduced Fd has a higher mobility than the partly reduced Fd (Fig. 4d), and even though the fully reduced species is only present in low intensities, it showed a slightly lower mobility than the partly reduced species (Fig. 4f). For Fc/2 (Fig. 4g), only fully and partly reduced species can be compared, but the same result was observed. The non-reduced Fc/2 showed a higher mobility than the partly reduced Fc/2.

The two positional isomers of LC and Fd were hardly separated in the gas phase. For the partly reduced LC (Fig. 4b), there is only a small difference in the gas phase mobility between the two isomeric species. If the disulfide bridge between C23 and C88 is closed, the molecule has a lower mobility than the LC, where the disulfide between C134 and C194 is closed. The same result was obtained for the Fd (Fig. 4e). If the disulfide bridge between C22 and C96 is closed, the molecule has a lower mobility than the Fd, where the disulfide between C147 and C203 is closed.

Sample preparation–reduction efficiency

Based on the ability to characterize the reduction state of subunits in detail by applying the CE-MS/MS method developed, we tested different approaches to optimize subunit reduction. The CE-MS data of various sample preparation protocols are shown in Fig. 5. All reduction approaches were tested using the same mAb and the same enzymatic digest protocol.

Table 1 All mAb subunits identified including positional isomers, their migration time, disulfide bond location, and theoretical and measured mass. Trastuzumab above the bold line was reduced in water, while trastuzumab and other mAbs below bold line were reduced in 4 M Urea. x*: no MS/MS data

mAb	subunit	Reduction state	Position of S–S bridge determined by MS/MS	Migration time [min]	Measured mass [monoisotopic]	Theoretical mass [monoisotopic]	Delta [ppm]
Trastuzumab	LC	2 S–S bridges	C23-C88 C134-C194	16.4	23,424.72	23,424.49	10
	LC	1 S–S bridge	C23-C88	18.0	23,426.60	23,426.51	4
	LC	1 S–S bridge	C134-C194	19.3	23,426.63	23,426.51	5
	LC	no S–S bridge	-	20.5	23,428.57	23,428.52	2
	Fd	2 S–S bridges	C22-C96 C147-C203	17.5	25,363.75	25,363.49	10
	Fd	1 S–S bridge	C22-C96	18.5	25,365.75	25,365.50	10
	Fd	1 S–S bridge	C147-C203	19.1	25,365.62	25,365.50	5
	Fd	no S–S bridge	-	20.0	25,367.59	25,367.52	3
	Fc/2	2 S–S bridges	C25-C85 C131-C189	16.4	25,216.66	25,216.43	9
	Fc/2	1 S–S bridge	C131-C189	17.6	25,218.60	25,218.44	6
Trastuzumab	LC	no S–S bridge	-	21.8	23,428.72	23,428.52	9
	Fd	no S–S bridge	-	23.3	25,367.73	25,367.52	8
	Fc/2	no S–S bridge	-	23.9	25,220.69	25,220.46	9
mAb1	LC	2 S–S bridges	x*	19.3	23,432.49	23,432.40	4
	LC	1 S–S bridge	C23-C88	21.1	23,434.49	23,434.42	3
	LC	no S–S bridge	-	23.0	23,436.53	23,436.43	4
	Fd	2 S–S bridges	x*	20.1	25,925.74	25,925.63	4
	Fd	1 S–S bridge	x*	21.2	25,927.70	25,927.64	2
	Fd	no S–S bridge	-	22.6	25,929.80	25,929.66	5
	Fc/2	2 S–S bridges	x*	18.8	25,216.47	25,216.43	2
	Fc/2	1 S–S bridge	C131-C189	20.0	25,218.59	25,218.45	6
	Fc/2	no S–S bridge	-	21.0	25,220.55	25,220.46	4
mAb2	LC	2 S–S bridges	C23-C93 C139-C199	20.6	23,887.84	23,887.77	3
	LC	1 S–S bridge	C23-C93	21.8	23,889.85	23,889.79	3
	LC	1 S–S bridge	C139-C199	22.3	23,889.91	23,889.79	5
	LC	no S–S bridge	-	23.5	23,891.89	23,891.80	4
	Fd	2 S–S bridges	x*	20.4	25,550.61	25,550.49	5
	Fd	1 S–S bridge	C148–C204	21.2	25,552.58	25,552.51	3
	Fd	1 S–S bridge	C22-C96	21.5	25,552.58	25,552.51	3
	Fd	no S–S bridge	-	22.0	25,554.61	25,554.52	4
	Fc/2	1 S–S bridge	C132-C190	20.5	25,257.61	25,257.51	4
	Fc/2	no S–S bridge	-	21.5	25,259.59	25,259.53	2
mAb3	LC	no S–S bridge	-	21.4	25,188.56	25,188.49	3
	Fd	no S–S bridge	-	22.9	25,631.63	25,631.53	4
	Fc/2	no S–S bridge	-	23.7	23,424.49	23,424.39	4
USP mAb003	LC	no S–S bridge	-	22.2	25,220.58	25,220.46	5
	Fd	no S–S bridge	-	24.0	25,250.64	25,250.47	7
	Fc/2	no S–S bridge	-	26.7	22,387.07	22,386.89	8

In the first experiment, the reduction temperature was increased from 37 to 55 °C. As shown in Fig. 5a (see Online Resource ESM 3 for deconvoluted spectra), this did not increase the amount of fully reduced species. The TIE showed a similar peak pattern, and the signal intensity is decreased. The presence of primarily unreduced subunits was confirmed using MS/MS experiments (data not shown). Since this approach did not suffice proper reduction, a

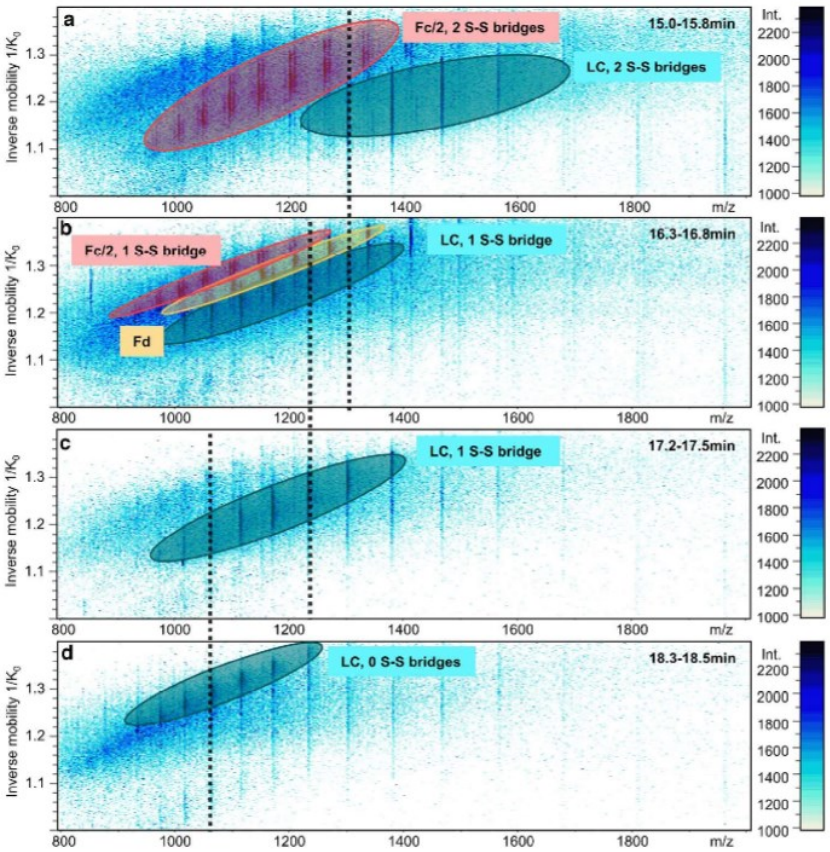

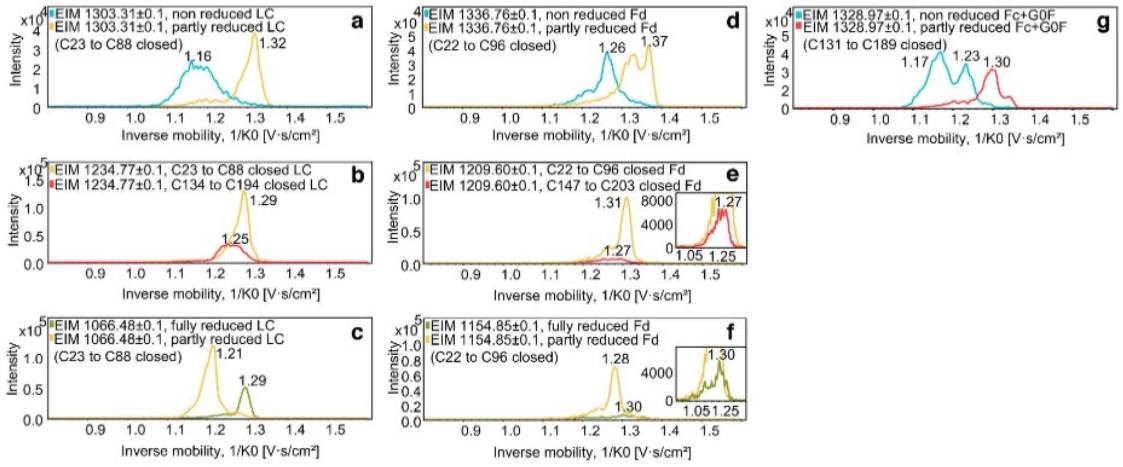

Fig. 3 m/z-gas phase mobility heatmaps of the four migration time windows where the LC subunit of trastuzumab was detected. **a** Non-reduced LC and co-migrating non-reduced Fc/2; **b** partly-reduced LC (C134 to C194 open) with co-migrating partly-reduced Fc/2 and partly reduced Fd; **c** partly reduced LC (C23 to C88 open); **d** fully reduced LC. The black dotted lines indicate the m/z values used for the EIM generation of the various LC-subunits in Fig. 4**a**-**c**)

Fig. 4 Gas phase separation of different subunits and positional isomers of LC, Fd and Fc/2. Since charge envelopes only overlap poorly, different m/z values (see Fig. 3) were chosen for comparison. Blue: non-reduced form; yellow: partly reduced form (N-terminal disulfide closed); red: partly reduced form (C-terminal disulfide closed); green: fully reduced form

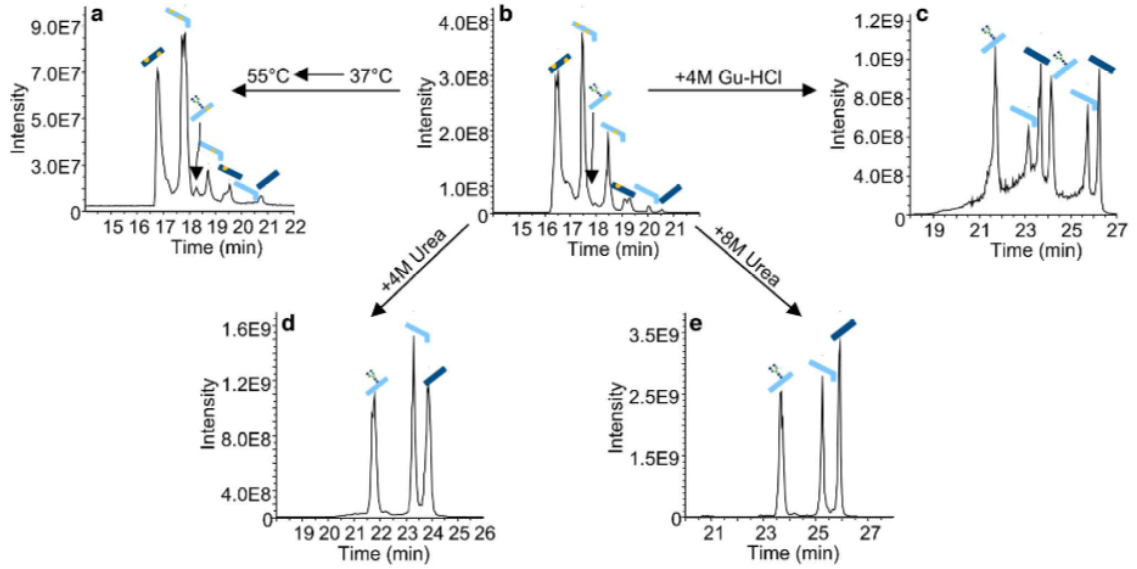

Fig. 5 TIE of the five tested sample reduction approaches. **a** Reduction in water, 55 °C; **b** reduction in water, 37 °C; **c** reduction in 4 M GuHCl, 37 °C; **d** reduction in 4 M urea, 37 °C; **e** reduction in 8 M urea, 37 °C. The most intense subunit is illustrated with the respective symbol. Overlapping subunits are not annotated. For detailed information, see deconvoluted mass spectra in Online Resource ESM 5 (reduction in 4 M GuHCl), Online Resource ESM 3 (reduction in water 37/55 °C), and Online Resource ESM 6 (reduction in 4 M/8 M urea)

chaotropic salt was used in the reduction step, and the temperature was decreased back to 37 °C. Using 4 M GuHCl at 37 °C for 60 min, a complete reduction of all the subunit moieties (Fig. 5c) was observed and confirmed by MS/MS experiments (Online Resource ESM 4). No masses for partly reduced or non-reduced species were detected. The drawback is that the fully reduced masses for Fc/2, Fd, and LC appear at least twice in the TIE. After a Fd or LC signal, there is no return to the baseline. LC and Fd signals were present over the complete separation (Online Resource ESM 5). Therefore, another chaotropic salt (urea) was tested for complete sample reduction. Compared to the other approaches, adding 4 M urea resulted in the three expected signals in the TIE (Fig. 5d/Online Resource ESM 6). Each signal represented one subunit moiety. The subunits are fully reduced, and no partly or non-reduced species were detected even when looking specifically for these m/z values. Fragmentation coverages of 31% for Fc/2 + G0F, 34% for Fd, and 37% for LC were achieved using the EThcD fragmentation (data not shown). The migration times for the fully reduced species in the 4 M urea reduction approach are higher compared to the sample reduction in water. This correlates with an unstable but reproducible CE current that drops to 18 µA after 0.5 min and recovers to 27 µA over 15 min compared to a 27 µA stable current when no chaotropic salt was used. The migration times are even higher when 8 M urea (Fig. 5e) is used, increasing the overall analysis time. There, the current drops to 15 µA and rises back to 27 µA over 30 min. Since the sample reduction is already complete using 4 M urea, this amount of salt was used for further measurements.

Other mAbs

After the reduction approach was optimized for trastuzumab, four mAbs (IgG1 candidates: mAb1, mAb2, mAb3, and USP mAb003) were measured with the same approach. The aim was to evaluate the general applicability of the sample preparation for other mAbs to separate and identify the states of various disulfide bridges by the presented CE-MS/MS approach (Table 1).

mAb3 (Fig. 6a) and USP mAb003 (Fig. 6b) showed complete sample reduction using the optimized reduction approach containing 4 M urea. Three main signals appeared in the TIE and can be assigned by mass to the fully reduced species. Fragmentation experiments confirmed the full sample reduction. For each subunit, m/z values for fragmentation were adapted, but further fragmentation parameters were not adjusted. Sequence coverages for USP subunits of 28% (Fd) and 30% (Fc/2 + G0F, LC) and for mAb3 subunits of 14% (Fc/2 + G0F), 24% (Fd), and 30% (LC) were achieved.

mAb1 is not fully reduced using the optimized reduction approach (Fig. 6c). Small amounts of non-reduced and

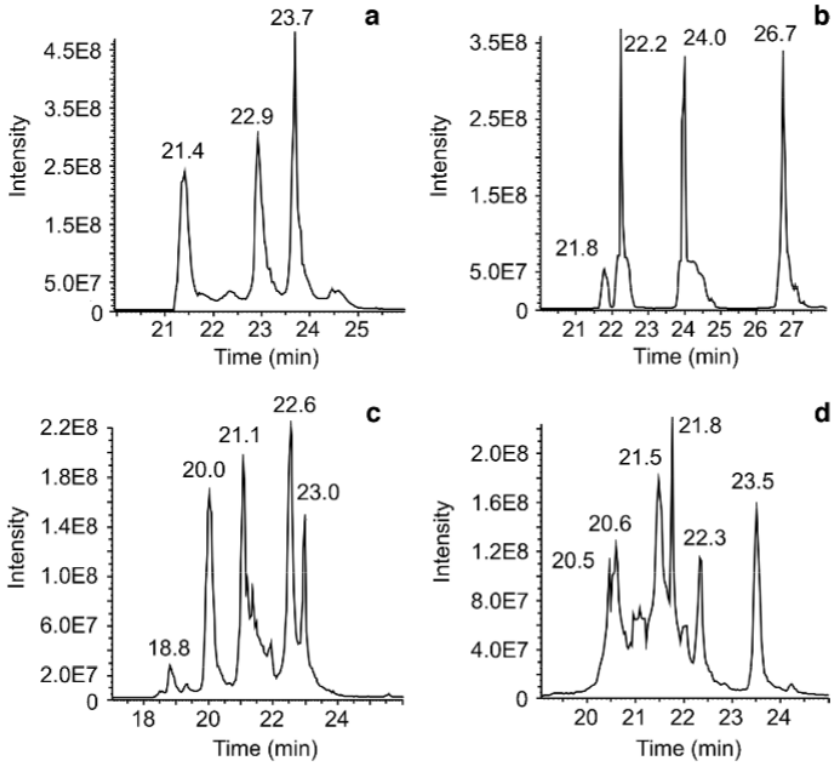

Fig. 6 CE-MS of different mAb subunits. Identification of different disulfide bridges was done by MS/MS. **a** TIE of mAb3; **b** TIE of USP mAb003; **c** TIE of mAb1; **d** TIE of mAb2

partly reduced species remain. The CE separates the different reduction states, and MS/MS spectra were acquired for all forms with sufficient intensities. Separating and locating the disulfide bridge for partly reduced LC and Fc/2 was possible. The partly reduced Fd was separated but identified via mass only since signal intensity was quite low. The signals of mAb1 that could be fragmented showed fragmentation coverages of 24% (Fc/2 + G0F; fully reduced), 23% (Fc/2 + G0F; partly reduced C131-C189), 35% (Fd, fully reduced), 24% (LC, fully reduced), and 32% (LC partly reduced C23-C88). Non-reduced species were not fragmented since they were only present in small amounts.

mAb2 (Fig. 6d) showed incomplete sample reduction as well. Here, the positional isomers of mAb2 showed sufficient intensities for meaningful fragmentation. The subunits that were fragmented showed fragmentation coverages of 22% (LC; partly reduced C23–C93), 13% (LC; partly reduced C139–C199), 24% (LC; fully reduced), 9% (Fc/2 + G0F; partly reduced C132–C190), 15% (Fc/2 + G0F; fully reduced), 6% (Fd; partly reduced C148–C204), 8% (Fd; partly reduced C22–C96), and 15% (Fd; fully reduced). The non-reduced species were either not present anymore (Fc/2), in low intensity (Fd), or not fragmented (LC).

Discussion

The analysis of mAb subunits allows intramolecular disulfide characterization compared to the intact antibody analysis. We present a CE-MS system that allows the separation of the different mAb subunit moieties, as well as different reduction states of the subunit moieties (non-reduced, partly reduced, and fully reduced subunits) due to their − 4 Da, − 2 Da, and 0 Da mass shift compared to the theoretically fully reduced mass, respectively (compare Fig. 1). Sample reduction in water was executed in several publications [11, 21, 25–27, 29, 30]; however, incomplete reduction can be overseen due to insufficient separation of these proteoforms differing by only two to four Dalton. This mass shift was only seen when the reduction agent was removed prior to analysis [11, 30], when a 2D approach was applied [21], or when TCEP was used for reduction [25]. The mass shift was attributed to intact intramolecular disulfide bridges; however, no further analysis on the location of the disulfide bridge in the molecule was done. In the case of the partly-reduced subunits, our CE method can separate the disulfide bridge positional isomers. However, a CE-MS method does not determine the location of the disulfide bridge in the molecule, and

there are four possibilities where the disulfide bridge could be located for each subunit. In the LC, the native disulfide bridges are between C23–C88 and C134–C194, in the Fd between C22–C96 and C147–C203, and in the Fc/2 between C25–C85 and C131–C189 (C264–C324 and C370–C428 in the HC nomenclature). If these disulfide bridges were not reduced in the first place, they should still be in their original conformation. If the bridges were reduced and oxidized again, the disulfides could be scrambled. The location of the disulfide bridges was determined for each subunit and reduction state using a CE-MS/MS approach. The positional isomers separated by CE could be identified using EThcD fragmentation with an Orbitrap mass spectrometer. In all cases where the intensities were high enough for adequate fragmentation, we could determine the exact location of the disulfide bridge in the molecule (compare Fig. 2). In these measurements, it became clear that the original disulfides were conserved and no scrambled disulfides were detected. This could have two possible explanations. First, the intramolecular disulfides of a subunit moiety show a similar tendency to be reduced [51]. If that's the case, the light chain disulfide bridge between C23 and C88 can be reduced as easily as the disulfide bridge between C134 and C194, leading to the appearance of these two positional isomers in the sample. Second, even if both disulfide bridges are reduced, the reduced SH groups could remain in close proximity due to the lack of chaotropic salt and could rebuild their original disulfide bridge. These explanations can be applied to LC and Fd subunits, respectively. The only exception was the Fc/2 subunit, where only one positional isomer was detected. The disulfide bridge in the C_H3-domain between C131 and C189 (C370 and C428 in HC) remained intact because it is the least susceptible disulfide to break [30, 51]. Therefore, if a disulfide bridge in the Fc/2 subunit is reduced, the C_H2-domain bridge is more likely to be reduced, which was confirmed by the MS/MS approach. That also explains why the Fc/2 was not detected in a fully reduced form. After evaluating the different reduction states, it also became clear that non-reduced species showed poor fragmentation coverage because the intact disulfides prevented fragmentation [25]. To the best of our knowledge, the only reference that described disulfide bridge-based separation of digested and reduced mAb subunits is from Scheffler and Damoc (Application Note 72,854) using reversed-phase HPLC [25]. The different reduction states (fully, partly, non-reduced) were separated on a MabPac RP column, with subsequent identification of the positional isomers of the LC. Our approach demonstrates baseline separation of the positional isomers of all subunits and unequivocal attribution to the respective disulfide isomer using EThcD. Additionally, our approach showed a better fragmentation coverage of the subunits (Fig. 2) compared to the HCD approach of the Application Note.

In addition to the MS/MS approach, the subunits were also measured using the timsTOF SCP. CE separates molecules based on their mobility in the liquid phase. The coupling to the timsTOF adds another separation dimension. In the TIMS, the ions are transported by a carrier gas according to their collisional cross section (CCS) and an electrical field traps the molecules based on their charge. The IM-MS analysis of a peptide mix of positional disulfide isomers was previously done by Delvaux et al. [48]. While the positional isomers could be separated using CE, the drift tube IM-MS was not able to baseline separate the peptides when a mixture was analyzed. Our subunit measurements achieved a similar result. While the CE already baseline-separated the positional isomers, they were not baseline-separated in the gas phase (compare Figs. 3 and 4). However, differences in gas phase mobility can be detected depending on the reduction state. Non-reduced species showed a larger mobility than fully reduced species, which can be explained by the different shapes of the molecules due to different protein folding when disulfide bridges are oxidized or reduced. Positional isomers could be distinguished, however, requiring prior separation since gas phase mobilities differ only slightly. These experiments show the strength of the mobility separation in the liquid and gas phase. In both techniques, subunits of different reduction states can be separated. However, the positional isomers were baseline-separated using CE, while the signals for the gas phase were not baseline-separated and quite broad. Especially without separating the two positional isomers in the liquid phase, they could probably not be distinguished in the TIMS. This shows the higher resolution of the CE compared to the ion mobility separation.

For a detailed analysis of the subunit moieties, a complete reduction is beneficial to prevent sample preparation-induced heterogeneity and signal overlap, as has been the case so far. Initially, we reduced the digested mAbs in water at 37 °C for 60 min. The sample preparation in water is described in the literature a few times [11, 21, 25–27, 29]. However, a pure water-based reduction was unsuitable for complete sample reduction. The tested sample preparation approaches differed depending on the reduction conditions (compare Fig. 5). The initial increase in reduction temperature, as assumed by some studies [25, 27] does not support mAb reduction in our case. A possible explanation is that the disulfide bridges in the subunit moieties are embedded between β-sheets, hindering the DTT reduction process if no denaturing reagent is present [8, 52]. A complete trastuzumab reduction was only achieved when a chaotropic salt was used in the reduction step. GuHCl has previously been used to support the reduction of IdeS digested mAb subunits [16, 20, 22, 23, 25, 31, 33, 34]. However, in some cases, an

incomplete sample reduction was still observed when samples were desalted prior to the measurement [20, 23] or the reduction was done at RT in combination with 4 M GuHCl [25]. That's why, in our approach, the salt was left in the sample after reduction, and the reduction was carried out at 37 °C for 60 min. Even though this approach fully reduced subunits, two significant drawbacks for CE-MS may arise. First, GuHCl is positively charged in that BGE, leading to its migration towards the MS using the applied system. It causes a high background signal and contamination of the MS; however, the CE effluent can be guided to the waste due to movable CE and SL capillaries in our nanoCEasy interface [53]. In that way, the early migrated GuHCl was cut out, and the subunits reaching the MS later were analyzed without a GuHCl background signal. Second, the fully reduced subunit moieties appeared multiple times in the electropherogram. Even though it is unclear what kind of separation is observed (isomeric compounds or artifacts), GuHCl seems improper for sample reduction in the applied CE-MS system. However, that approach may work with another CE or HPLC separation system since fully reduced subunits are obtained. Another chaotropic salt is urea, which can be used for IdeS digested mAb subunit reduction [1, 24, 32]. Compared to the GuHCl approach, no salt migrates towards the MS because urea is an uncharged molecule. Therefore, the separation capillary could be positioned at the emitter tip at the beginning of the run, and no salt contaminated the MS when the nanoCEasy interface is put into conditioning mode. The light migration time shift of the urea-based approach compared to the water-based approach can be explained by the fact that urea reproducibly influences the electric conductivity of the sample zone, as observed by a drop in electric current at the beginning of the measurement. Using 4 M urea, sample reduction was complete.

Three of the five mAbs showed complete disulfide bridge reduction using the proposed sample preparation, and two mAbs showed a mixture of partly reduced and non-reduced species. One of these (mAb2) did not show the IdeS consensus sequence (CPAPELLG/GPSVF) but had two amino acids changed (CPAPELAG/APSVF). Therefore, IdeS was not cleaving the mAb at the intended location. The glycine (G) that should remain at the C-terminus of the Fd was located at the N-terminus of the Fc/2, instead. If this was considered, evaluation of subunit disulfide bridges could analogously be done to the other mAbs. The reason for the different behavior of the various IgG1 molecules could be an object to further future investigations.

In conclusion, the presented CE-MS/MS approach can be used as a fast analysis method to distinguish between complete and incomplete sample reduction. The separation and subsequent characterization/identification of the subunit variants differing in the number and position of disulfide bridges can be performed for all subunit moieties and for all tested mAbs. Ion mobility adds another separation dimension and also distinguishes different reduction states of the subunits. Complete sample reduction can be obtained using 4 M-8 M urea, whereas guanidinium hydrochloride leads to multiple signals for the same subunit of unclear origin. The here presented CE-MS approach is a valuable tool for disulfide-bridge variant characterization of mAbs on the subunit level and potentially also for other proteins.

Supplementary Information The online version contains supplementary material available at https://doi.org/10.1007/s00216-024-05161-8.

Acknowledgements The authors thank Rentschler Biopharma SE for financial support and for providing samples.

Funding Open Access funding enabled and organized by Projekt DEAL.

Data availability The data that support the findings of this study are available from the corresponding author [CN], upon reasonable request.

Declarations

Conflict of interest The authors declare no competing interests.

References

1. Dadouch M, Ladner Y, Perrin C. Analysis of monoclonal antibodies by capillary electrophoresis: sample preparation, separation, and detection. Separations. 2021. https://doi.org/10.3390/separations8010004.
2. Kahle J, Zagst H, Wiesner R, Wätzig H. Comparative charge-based separation study with various capillary electrophoresis (CE) modes and cation exchange chromatography (CEX) for the analysis of monoclonal antibodies. J Pharm Biomed Anal. 2019. https://doi.org/10.1016/j.jpba.2019.05.058.
3. Pacis E, Yu M, Autsen J, Bayer R, Li F. Effects of cell culture conditions on antibody N-linked glycosylation–what affects high mannose 5 glycoform. Biotechnol Bioeng. 2011. https://doi.org/10.1002/bit.23200.
4. Beck A, Wagner-Rousset E, Ayoub D, van Dorsselaer A, Sanglier-Cianférani S. Characterization of therapeutic antibodies and related products. Anal Chem. 2013. https://doi.org/10.1021/ac3032355.
5. Beck A, Liu H. Macro- and micro-heterogeneity of natural and recombinant IgG antibodies. Antibodies (Basel). 2019. https://doi.org/10.3390/antib8010018.

6. Jefferis R. Glycosylation as a strategy to improve antibody-based therapeutics. Nat Rev Drug Discov. 2009. https://doi.org/10.1038/nrd2804.
7. Khawli LA, Goswami S, Hutchinson R, Kwong ZW, Yang J, Wang X, Yao Z, Sreedhara A, Cano T, Tesar D, Nijem I, Allison DE, Wong PY, Kao Y-H, Quan C, Joshi A, Harris RJ, Motchnik P. Charge variants in IgG1: isolation, characterization, in vitro binding properties and pharmacokinetics in rats. mAbs. 2010. https://doi.org/10.4161/mabs.2.6.13333.
8. Moritz B, Stracke JO. Assessment of disulfide and hinge modifications in monoclonal antibodies. Electrophoresis. 2017; https://doi.org/10.1002/elps.201600425.
9. Traxlmayr MW, Hasenhindl C, Hackl M, Stadlmayr G, Rybka JD, Borth N, Grillari J, Rüker F, Obinger C. Construction of a stability landscape of the CH3 domain of human IgG1 by combining directed evolution with high throughput sequencing. J Mol Biol. 2012. https://doi.org/10.1016/j.jmb.2012.07.017.
10. Lacy ER, Baker M, Brigham-Burke M. Free sulfhydryl measurement as an indicator of antibody stability. Anal Biochem. 2008. https://doi.org/10.1016/j.ab.2008.07.016.
11. Giorgetti J, Beck A, Leize-Wagner E, François Y-N. Combination of intact, middle-up and bottom-up levels to characterize 7 therapeutic monoclonal antibodies by capillary electrophoresis - mass spectrometry. 2020. J Pharm Biomed Anal. https://doi.org/10.1016/j.jpba.2020.113107.
12. Gahoual R, Beck A, François Y-N, Leize-Wagner E. Independent highly sensitive characterization of asparagine deamidation and aspartic acid isomerization by sheathless CZE-ESI-MS/MS. J Mass Spectrom. 2016. https://doi.org/10.1002/jms.3735.
13. Lew C, Gallegos-Perez J-L, Fonslow B, Lies M, Guttman A. Rapid level-3 characterization of therapeutic antibodies by capillary electrophoresis electrospray ionization mass spectrometry. J Chromatogr Sci. 2015. https://doi.org/10.1093/chromsci/bmu229.
14. Giorgetti J, Lechner A, Del Nero E, Beck A, François Y-N, Leize-Wagner E. Intact monoclonal antibodies separation and analysis by sheathless capillary electrophoresis-mass spectrometry. 2019. Eur J Mass Spectrom (Chichester). https://doi.org/10.1177/1469066718807798.
15. Zhao Y, Sun L, Knierman MD, Dovichi NJ. Fast separation and analysis of reduced monoclonal antibodies with capillary zone electrophoresis coupled to mass spectrometry. Talanta. 2016. https://doi.org/10.1016/j.talanta.2015.11.020.
16. Han M, Rock BM, Pearson JT, Rock DA. Intact mass analysis of monoclonal antibodies by capillary electrophoresis-mass spectrometry. 2016. J Chromatogr B Analyt Technol Biomed Life Sci. https://doi.org/10.1016/j.jchromb.2015.12.045.
17. von Pawel-Rammingen U, Johansson BP, Björck L. IdeS, a novel streptococcal cysteine proteinase with unique specificity for immunoglobulin G. EMBO J. 2002. https://doi.org/10.1093/emboj/21.7.1607.
18. Dadouch M, Ladner Y, Bich C, Larroque M, Larroque C, Morel J, Bonnet P-A, Perrin C. An in-line enzymatic microreactor for the middle-up analysis of monoclonal antibodies by capillary electrophoresis. Analyst. 2020. https://doi.org/10.1039/c9an01906e.
19. Haselberg R, de Vijlder T, Heukers R, Smit MJ, Romijn EP, Somsen GW, Domínguez-Vega E. Heterogeneity assessment of antibody-derived therapeutics at the intact and middle-up level by low-flow sheathless capillary electrophoresis-mass spectrometry. 2018. Anal Chim Acta. https://doi.org/10.1016/j.aca.2018.08.024.
20. Gstöttner C, Nicolardi S, Haberger M, Reusch D, Wuhrer M, Domínguez-Vega E. Intact and subunit-specific analysis of bispecific antibodies by sheathless CE-MS. 2020. Anal Chim Acta. https://doi.org/10.1016/j.aca.2020.07.069.
21. Stoll DR, Harmes DC, Danforth J, Wagner E, Guillarme D, Fekete S, Beck A. Direct identification of rituximab main isoforms and subunit analysis by online selective comprehensive two-dimensional liquid chromatography-mass spectrometry. Anal Chem. 2015. https://doi.org/10.1021/acs.analchem.5b01578.
22 An Y, Zhang Y, Mueller H-M, Shameem M, Chen X. A new tool for monoclonal antibody analysis: application of IdeS proteolysis in IgG domain-specific characterization. mAbs. 2014. https://doi.org/10.4161/mabs.28762.
23. Resemann A, Jabs W, Wiechmann A, Wagner E, Colas O, Evers W, Belau E, Vorwerg L, Evans C, Beck A, Suckau D. Full validation of therapeutic antibody sequences by middle-up mass measurements and middle-down protein sequencing. mAbs. 2016. https://doi.org/10.1080/19420862.2015.1128607.
24. Römer J, Stolz A, Kiessig S, Moritz B, Neusüß C. Online top-down mass spectrometric identification of CE(SDS)-separated antibody fragments by two-dimensional capillary electrophoresis. J Pharm Biomed Anal. 2021. https://doi.org/10.1016/j.jpba.2021.114089.
25. Scheffer K, Damoc E. Antibody subunit analysis workflow on a quadrupole-Orbitrap mass spectrometer: from optimized sample preparation to data analysis; 2018. https://assets.thermofisher.com/TFS-Assets/CMD/Application-Notes/an-72854-lc-ms-antibody-subunit-analysisan72854-en.pdf.
26. Sun Q, Wang L, Li N, Shi L. Characterization and monitoring of charge variants of a recombinant monoclonal antibody using microfluidic capillary electrophoresis-mass spectrometry. Anal Biochem. 2021. https://doi.org/10.1016/j.ab.2021.114214.
27. Duivelshof BL, Beck A, Guillarme D, D'Atri V. Bispecific antibody characterization by a combination of intact and site-specific/chain-specific LC/MS techniques. 2022. Talanta. https://doi.org/10.1016/j.talanta.2021.122836.
28. Liu T, Guo H, Zhu L, Zheng Y, Xu J, Guo Q, Zhang D, Qian W, Dai J, Guo Y, Hou S, Wang H. Fast characterization of Fc-containing proteins by middle-down mass spectrometry following IdeS digestion. Chromatographia. 2016. https://doi.org/10.1007/s10337-016-3173-2.
29 Sokolowska I, Mo J, Dong J, Lewis MJ, Hu P. Subunit mass analysis for monitoring antibody oxidation. mAbs. 2017. https://doi.org/10.1080/19420862.2017.1279773.
30. Belov AM, Zang L, Sebastiano R, Santos MR, Bush DR, Karger BL, Ivanov AR. Complementary middle-down and intact monoclonal antibody proteoform characterization by capillary zone electrophoresis – mass spectrometry. 2018. Electrophoresis. https://doi.org/10.1002/elps.201800067.
31. Ayoub D, Jabs W, Resemann A, Evers W, Evans C, Main L, Baessmann C, Wagner-Rousset E, Suckau D, Beck A. Correct primary structure assessment and extensive glyco-profiling of cetuximab by a combination of intact, middle-up, middle-down and bottom-up ESI and MALDI mass spectrometry techniques. 2013. mAbs. https://doi.org/10.4161/mabs.25423.
32. Cotham VC, Brodbelt JS. Characterization of therapeutic monoclonal antibodies at the subunit-level using middle-down 193 nm ultraviolet photodissociation. Anal Chem. 2016. https://doi.org/10.1021/acs.analchem.6b00302.
33. Fornelli L, Ayoub D, Aizikov K, Beck A, Tsybin YO. Middle-down analysis of monoclonal antibodies with electron transfer dissociation orbitrap Fourier transform mass spectrometry. Anal Chem. 2014. https://doi.org/10.1021/ac4036857.
34. Zhu W, Li M, Zhang J. Integrating intact mass analysis and middle-down mass spectrometry approaches to effectively characterize trastuzumab and adalimumab structural heterogeneity. 2021. J Proteome Res. https://doi.org/10.1021/acs.jproteome.0c00373.
35. Lodge JM, Schauer KL, Brademan DR, Riley NM, Shishkova E, Westphall MS, Coon JJ. Top-down characterization of an intact monoclonal antibody using activated ion electron transfer dissociation. 2020. Anal Chem. https://doi.org/10.1021/acs.analchem.0c00705.

36. Shaw JB, Liu W, Vasil Ev YV, Bracken CC, Malhan N, Guthals A, Beckman JS, Voinov VG. Direct determination of antibody chain pairing by top-down and middle-down mass spectrometry using electron capture dissociation and ultraviolet photodissociation. Anal Chem. 2020. https://doi.org/10.1021/acs.analchem.9b03129.
37. Guo J, Tu H, Atouf F. Measurement of macro- and micro-heterogeneity of glycosylation in biopharmaceuticals: a pharmacopeia perspective. Futur Drug Disc. 2020. https://doi.org/10.4155/fdd-2020-0021.
38. Duivelshof BL, Deslignière E, Hernandez-Alba O, Ehkirch A, Toftevall H, Sjögren J, Cianferani S, Beck A, Guillarme D, D'Atri V. Glycan-mediated technology for obtaining homogeneous site-specific conjugated antibody-drug conjugates: synthesis and analytical characterization by using complementary middle-up LC/HRMS analysis. Anal Chem. 2020. https://doi.org/10.1021/acs.analchem.0c00282.
39. Bobály B, D'Atri V, Beck A, Guillarme D, Fekete S. Analysis of recombinant monoclonal antibodies in hydrophilic interaction chromatography: a generic method development approach. J Pharm Biomed Anal. 2017. https://doi.org/10.1016/j.jpba.2017.06.016.
40. Verscheure L, Cerdobbel A, Sandra P, Lynen F, Sandra K. Monoclonal antibody charge variant characterization by fully automated four-dimensional liquid chromatography-mass spectrometry. J Chromatogr A. 2021. https://doi.org/10.1016/j.chroma.2021.462409.
41. Stoll DR, Harmes DC, Staples GO, Potter OG, Dammann CT, Guillarme D, Beck A. Development of comprehensive online two-dimensional liquid chromatography/mass spectrometry using hydrophilic interaction and reversed-phase separations for rapid and deep profiling of therapeutic antibodies. Anal Chem. 2018. https://doi.org/10.1021/acs.analchem.8b00776.
42 Sorensen M, Harmes DC, Stoll DR, Staples GO, Fekete S, Guillarme D, Beck A. Comparison of originator and biosimilar therapeutic monoclonal antibodies using comprehensive two-dimensional liquid chromatography coupled with time-of-flight mass spectrometry. mAbs. 2016. https://doi.org/10.1080/19420862.2016.1203497.
43. Michelmann K, Silveira JA, Ridgeway ME, Park MA. Fundamentals of trapped ion mobility spectrometry. J Am Soc Mass Spectrom. 2015. https://doi.org/10.1007/s13361-014-0999-4.
44. Christofi E, Barran P. Ion mobility mass spectrometry (IM-MS) for structural biology: insights gained by measuring mass, charge, and collision cross section. Chem Rev. 2023. https://doi.org/10.1021/acs.chemrev.2c00600.
45 Melani RD, Srzentić K, Gerbasi VR, McGee JP, Huguet R, Fornelli L, Kelleher NL. Direct measurement of light and heavy antibody chains using ion mobility and middle-down mass spectrometry. mAbs. 2019. https://doi.org/10.1080/19420862.2019.1668226.
46. Bagal D, Valliere-Douglass JF, Balland A, Schnier PD. Resolving disulfide structural isoforms of IgG2 monoclonal antibodies by ion mobility mass spectrometry. Anal Chem. 2010. https://doi.org/10.1021/ac1013139.
47. Deslignière E, Ollivier S, Ehkirch A, Martelet A, Ropartz D, Lechat N, Hernandez-Alba O, Menet J-M, Clavier S, Rogniaux H, Genet B, Cianférani S. Combination of IM-based approaches to unravel the coexistence of two conformers on a therapeutic multispecific mAb. Anal Chem. 2022. https://doi.org/10.1021/acs.analchem.2c00928.
48. Delvaux C, Massonnet P, Kune C, Haler JRN, Upert G, Mourier G, Gilles N, Quinton L, de Pauw E, Far J. Combination of capillary zone electrophoresis-mass spectrometry, ion mobility-mass spectrometry, and theoretical calculations for cysteine connectivity identification in peptides bearing two intramolecular disulfide bonds. Anal Chem. 2020. https://doi.org/10.1021/acs.analchem.9b03206.
49. Schlecht J, Stolz A, Hofmann A, Gerstung L, Neusüß C. nanoCEasy: An easy, flexible, and robust nanoflow sheath liquid capillary electrophoresis-mass spectrometry interface based on 3D printed parts. Anal Chem. 2021. https://doi.org/10.1021/acs.analchem.1c03213.
50. Iki N, Yeung ES. Non-bonded poly(ethylene oxide) polymer-coated column for protein separation by capillary electrophoresis. J Chromatogr A. 1996. https://doi.org/10.1016/0021-9673(95)01158-7.
51. Liu H, Chumsae C, Gaza-Bulseco G, Hurkmans K, Radziejewski CH. Ranking the susceptibility of disulfide bonds in human IgG1 antibodies by reduction, differential alkylation, and LC-MS analysis. Anal Chem. 2010. https://doi.org/10.1021/ac100575n.
52. Padlan EA. Anatomy of the antibody molecule. Mol Immunol. 1994. https://doi.org/10.1016/0161-5890(94)90001-9.
53. Höcker O, Knierman M, Meixner J, Neusüß C. Two capillary approach for a multifunctional nanoflow sheath liquid interface for capillary electrophoresis-mass spectrometry. Electrophoresis. 2021. https://doi.org/10.1002/elps.202000169.

Manuscript II

Ion mobility in gas and liquid phases: How much orthogonality is obtained in capillary electrophoresis-ion mobility-mass spectrometry?

Jasmin Schairer, Florian Plathe, Sonja Hudelmaier, Eckhard Belau, Stuart Pengelley, Lena Kruse, Christian Neusüß

Electrophoresis 2024; 45: 735-742. DOI: 10.1002/elps.202300210

Received: 21 September 2023 | Revised: 16 November 2023 | Accepted: 30 November 2023

DOI: 10.1002/elps.202300210

ELECTROPHORESIS

RESEARCH ARTICLE

Ion mobility in gas and liquid phases: How much orthogonality is obtained in capillary electrophoresis–ion mobility–mass spectrometry?

Jasmin Schairer[1,2] | **Florian Plathe**[1] | **Sonja Hudelmaier**[1] | **Eckhard Belau**[3] | **Stuart Pengelley**[3] | **Lena Kruse**[1] | **Christian Neusüß**[1]

[1]Faculty of Chemistry, Aalen University, Aalen, Germany

[2]Faculty of Science, University of Tübingen, Tübingen, Germany

[3]Bruker Daltonics GmbH & Co.KG, Bremen, Germany

Correspondence
Christian Neusüß, Faculty of Chemistry, Aalen University, Beethovenstraße 1, 73430 Aalen, Germany.
Email: christian.neusuess@hs-aalen.de

Color online: See the article online to view Figures 1–5 in color.

Abstract

Ion mobility–mass spectrometry (IM–MS) is an ever-evolving tool to separate ions in the gas phase according to electrophoretic mobility with subsequent mass determination. CE is rarely coupled to IM–MS, possibly due to similar separation mechanisms based on electrophoretic mobility. Here, we investigate the orthogonality of CE and ion mobility (IM) by analyzing a complex peptide mixture (tryptic digest of HeLa proteins) with trapped ion mobility mass spectrometry (TIMS–MS). Using the nanoCEasy interface, excellent sensitivity was achieved by identifying thousands of peptides and achieving a peak capacity of 7500 (CE: 203–323 in a 150 cm long capillary, IM: 27–31). Plotting CE versus mass and CE versus (inverse) mobility, a clear grouping in curved striped patterns is observed according to the charge-to-size and mass-to-charge ratios. The peptide charge in the acidic background electrolyte can be estimated from the number of basic amino acids, with a few exceptions where neighboring effects reduce the positive charge. A surprisingly high orthogonality of CE and IM is observed, which is obviously caused by solvation effects leading to different charges and sizes in the liquid phase compared to the gas phase. A high orthogonality of CE and ion mobility is expected to be observed for other peptide samples as well as other substance classes, making CE–IM–MS a promising tool for various applications.

KEYWORDS

capillary electrophoresis, peak capacity, trapped ion mobility mass spectrometry, tryptic HeLa digest

1 | INTRODUCTION

Ion mobility–mass spectrometry (IM–MS) has gained much attention over the last two decades due to the commercialization of various ion mobility (IM) techniques, including drift tube IM (DTIM, Agilent Technologies),

Abbreviations: CCS, collisional cross-section; DTIM, drift tube ion mobility; FAIMS, field asymmetric ion mobility spectrometry; IM, ion mobility; IM-MS, ion mobility–mass spectrometry; PASEF, parallel accumulation serial fragmentation; TIMS, trapped ion mobility spectrometry; TWIM, traveling wave IM; UPW, ultrapure water.

traveling wave IM (TWIM, Waters), field asymmetric IM spectrometry (FAIMS, Thermo Fisher Scientific), differential mobility spectrometry (DMS, Sciex) and trapped IM spectrometry (TIMS, Bruker). These devices are already used for the in-depth characterization of complex proteins and samples [1–4] and isomeric or isobaric structures [5, 6]. TIMS is a technique where ions are pushed forward by a gas flow proportional to their collisional cross-section (CCS) and trapped by an electrical field based on the molecule's charge. The ions are released by manipulating the electrical field. Parallel accumulation serial fragmentation (PASEF) allows the fragmentation of molecules based on their mobility in the gas phase, enabling very fast and sensitive MS/MS acquisition in TIMS–QTOF MS instruments [7].

CE is a powerful technique to efficiently separate ions due to minor differences in their electrophoretic mobility (charge-to-size ratio) in the liquid phase. Thus, CE–MS is used in many fields including the analysis of complex mixtures of proteins or metabolites [8–11]. New developments in interfacing technology [12–17] compensate for the limiting sample introduction volumes regarding achievable concentration sensitivities, enabling the analysis of metabolites and peptides down to sub-ppb levels [18]. CE–MS is applied for the analysis of peptides due to its different selectivity compared to LC–MS [8, 19, 20]. HeLa digest is often used as a model for proteomics samples to evaluate separation and MS/MS performance both in LC–MS [4] and CE–MS [21–23].

In contrast to CE–MS, only a few studies have been published on the coupling of CE with IM–MS. In one of the first studies, Jooß et al. analyzed protein-derived glycans, showing the benefit of combining both technologies [24], similar to a work on labeled glycans [25]. The sensitivity of glycan analysis was increased by developing an in-line SPE for the CE–DTIM–MS set-up by Hooijschuur et al. [26]. CE–TIMS–MS has been applied to analyze targeted peptides from low volume samples: Mast et al. showed the separation of diastereomeric neuropeptides in single cells [27], while Delaney et al. analyzed nine targeted angiotensin peptides in mouse tissue samples [28]. CE–FAIMS–MS has been used to perform top-down proteomics experiments [29] as well as for the characterization of complex bacterial lipopolysaccharides [30]. CE–TWIM–MS has been used for the detection of protein conformational isomers, including affinity experiments, to describe their enzymatic activity and their inhibition [31]. Drouin et al. investigated CE–IM–MS for metabolite profiling, showing the benefit for the identification of isobaric analytes, primarily in the neutral (nonseparated) zone [32]. In most of these applications, IM assists in the separation of a few analytes not separated by CE or by MS. Gou et al., investigated the application of CE—DTIM–MS for proteome samples in comparison to LC–MS [33]. Beside a substantial orthogonality of CE and LC, they also found orthogonality for CE and DTIM. There is hardly any study discussing the orthogonality of CE and IM in detail, which seems to be of great interest, especially since both techniques rely on electrophoretic mobility, leading to potentially small differences in selectivity.

Here, we present CE–TIMS–MS measurements of tryptic HeLa-digest for the discussion of orthogonality in CE–IM–MS. Various capillary lengths were evaluated regarding peak capacity. To obtain a high number of MS/MS experiments, a 1.5-m long capillary was finally applied. Resulting data are discussed regarding peptide charge in liquid and gas phases, respectively, as well as the resulting orthogonality of CE and IM.

2 | MATERIALS AND METHODS

2.1 | Sample preparation and CE separation

Lyophilized Pierce™ HeLa Protein Digest Standard (Thermo Fischer Scientific, Dreieich, Germany) was diluted to a final concentration of 1 µg/µL protein using a mixture of isopropanol (IPA, LC–MS grade, Carl Roth GmbH+Co.KG, Karlsruhe, Germany) and 0.1 M formic acid (FA, ≥98%; Carl Roth GmbH+Co.KG) in water (ultrapure [UPW], 18 MΩ*cm at 25°C, SG Ultra Clear UV from Siemens Water Technologies, USA) in the ratio of 1:99 (v/v). CE was performed on an Agilent 7100 CE instrument (Agilent Technologies GmbH, Waldbronn, Germany). Fused silica capillaries (separation capillary: 50 µm id, 365 µm od, and SL capillary: 100 µm id, 240 µm od) were purchased from Polymicro Technologies (Phoenix, AZ, USA). PEO-coated capillaries of various lengths were applied, with a length of 1.5 m for the final experiments. To penetrate the glass emitter (30 µm tip opening), the separation capillary was etched at one end to a wall thickness of less than 150 µm using hydrofluoric acid (40%(v/v), Merck, Darmstadt, Germany) prior to the coating procedure [12]. The PEO stock solution was prepared by dissolving 100 mg PEO (*Mw*: 1.000.000; Alfa Aesar, Kandel, Germany) in 45 mL UPW. The solution was heated to 95°C. A total of 450 µL of that stock solution was acidified using 50 µL 0.1 M hydrochloric acid (conc. HCl: 37%, Sigma, Steinheim Germany). The coating was applied to the capillary using the CE and an external pressure of 4 bar in the following steps: 1 M sodium hydroxide (NaOH, Merck), UPW, and 1 M HCl for 5 min each, followed by the PEO coating solution for 10 min, UPW, and BGE for 5 min. The BGE consisted of 10% IPA in water containing 1 M FA. A large sample plug (200 ng of protein; 6.81% capillary volume) was injected in a dynamic

pH-junction/transient ITP mode. For that, a plug of 1 M ammonia (conc. NH_3: 30%; Carl Roth GmbH+Co.KG) was injected hydrodynamically (100 mbar, 20 s, equimolar to acid amount) before the sample plug. Sample injection was done using the CE flush option (950 mbar) for 21 s. A total of 30 kV was applied for the separation and was executed for 200 min without additional pressure. An additional pressure of 100 mbar was applied after that time point. The capillary was flushed for 5 min with BGE between the runs.

2.2 | CE–MS

The CE was coupled to the timsTOF Pro2 using the nanoCEasy interface [12, 34]. The timsTOF was operated in positive ionization mode using captive spray source settings of 1700 V electrospray voltage, 150°C dry gas temperature, and 3 L/min dry gas flow. The mobility of the ions was measured between 0.6 and 1.6 V*s/cm^2 with a ramp time of 100 ms. One MS acquisition was combined with 10 TIMS cycles for MS/MS experiments using the PASEF algorithm for fragmentation experiments, resulting in an overall duty cycle of 1.1 s. Using the polygonic function in the IM—MS–heatmap singly charged signals were excluded from MS/MS experiments. The mgf file for the Mascot database search was generated based on a threshold intensity (TIC AllMSn) of 25,000 counts, and 10,000 compounds were set as the maximum number. Fragment spectra of the same precursor were combined in a retention time window of 0.5 min with a precursor m/z window of 0.1. Data files were processed using a Mascot search using the SwissProt database and a Homo sapiens (human) taxonomy filter. Only peptides with a charge between +2 and +4 were evaluated. The results were exported to CSV files without showing duplicate peptides. Data were further assessed using Data Analysis 5.3 and Excel 2019. The charge of the peptides at a specific pH was gained using ProtpI.

3 | RESULTS AND DISCUSSION

CE–timsTOF coupling was straightforward using the nanoCEasy interface. The schematic setup is shown in Figure 1. A total of 200 ng of tryptic HeLa digest was injected using stacking experiments. The measurement could be done without further sample preparation in an acidic BGE (1 M FAin 10% IPA). A positive voltage was applied to the CE inlet so that positively charged proteins migrated toward the MS. MS/MS experiments were done using the PASEF algorithm. The overall separation time strongly depended on the capillary length used.

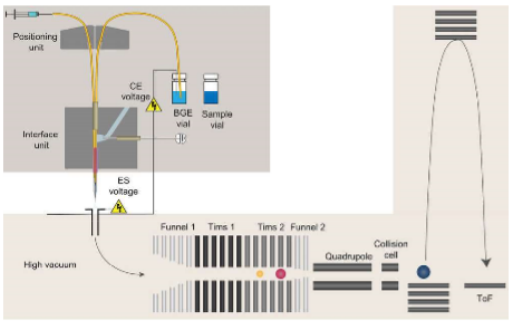

FIGURE 1 Schematic CE-nanoCEasy-timsTOF setup.

Different capillary lengths were tested to increase the peak capacity. To calculate the peak capacity of a CE separation, the start and end times of the separation were estimated. Nine peaks were chosen (three at the beginning, middle, and end of the separation window) to determine the average full width at half maximum. Calculating the mean width at 13.4% peak height (4σ), a peak capacity for the CE separation was determined. The same approach was done for the gas phase IM for the same set of peptides. The total peak capacity is the product of both individual peak capacities. For a 0.6-m and a 1-m long capillary, an average peak capacities of 1700 (n = 2) and 2700 (n = 2) were achieved, respectively. By increasing the capillary length to 1.5 m, the peak capacity increased to a mean value of 7500 (6223–9497, n = 3). As expected, the peak capacity strongly depends on the capillary length. which is obviously caused by the separation window increase. The results for the individual measurements are shown in Supporting Information S1.

Due to the strongly increased peak capacity in CE, a 1.5-m long capillary was used for the following measurements. Applying 30 kV, the peptides migrated in a time window of > 100 min, as illustrated in Figure 2A, showing the base peak electropherogram of one representative measurement.

The heatmap of migration time and m/z values (Figure 2B) showed a separation of the peptides leading to distinct, slightly curved distributions due to the distinct charges in the acidic liquid phase (see discussion below). CE separates based on the size and charge of the molecule. A large molecule with many charges can, therefore, have the same mobility in the liquid phase as a small molecule with few charges. At the same time, peptides with similar mass and charge can have different mobilities in the liquid phase due to different hydrodynamic radii. The CE has a higher separation efficiency than the IM separation in the gas phase (Figure 2B,C). Plotting the inverse mobility against the CE migration time (Figure 2D), a distinct,

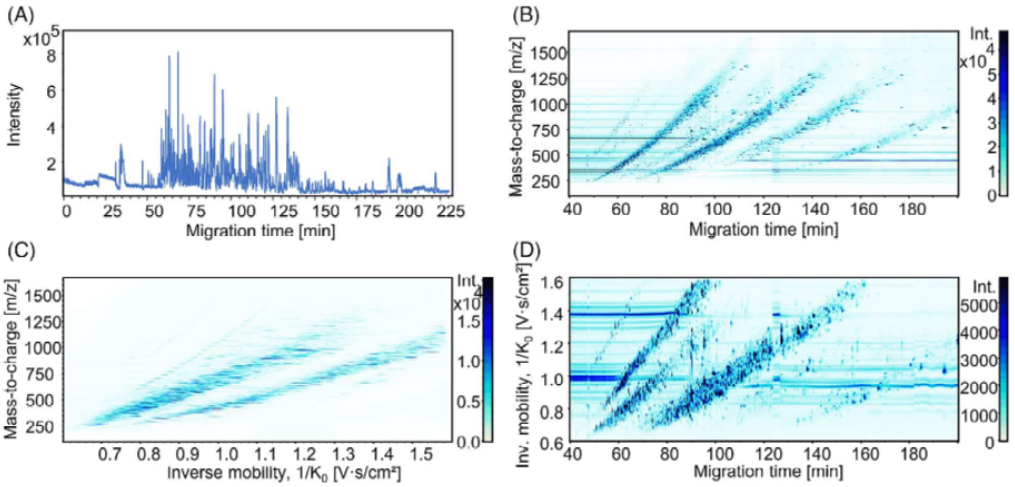

FIGURE 2 Separating tryptic HeLa digest using 1.5-m long PEO coated capillary. (A) Base peak electropherogram (BPE; 350–2200 *m/z*). (B) Heatmap of migration time and *m/z* value. (C) Heatmap of gas phase mobility and *m/z* value. (D) Combined heatmap of liquid and gas phase mobility.

slightly curved distribution is observed again. Furthermore, a large area of the heatmap is covered with data points of peptides, demonstrating already the different selectivity of CE and IM, leading to a high orthogonality.

To understand the separation profiles in more detail, the peptides of CE–MS/MS experiments were identified based on the fragment spectra using a Mascot database search. Only the most intense MS/MS spectra were used to obtain unequivocal peptide sequence information. Based on the obtained peptide sequence, the amount of basic and acidic amino acids in the peptide, their charge in the liquid phase, and pI were derived. By calculating the peptide charge in solution at the pH of the BGE (pH = 1.9 for the aqueous part), it was revealed that their charge almost solely depends on the number of basic amino acids. It was almost independent of the amount of acidic amino acids present in the molecule. A peptide with one basic and one acidic amino acid had almost the same charge as a peptide with one basic and eight acidic amino acids (differences in charge < 0.07; see discussion below). Thus, the charge of the peptide in the acidic solution equals to the number of basic amino acids + 1 (*N*-terminus). Figure 3A shows the migration time– *m/z*– heatmap of the identified peptides colored by the number of basic amino acids in the peptide. The distinct, slightly curved distributions are related to the different amounts of basic amino acids and therefore different charge states in the liquid phase. However, multiple stripes with the same number of basic amino acids exist and are partially overlapping with stripes containing other numbers of basic amino acids. For example, peptides with two or three basic amino acids overlap between 56 and 76 min. The reason for the existence of several stripes is that the peptides have a distinct charge state in the liquid phase, but exist in several charge states in the gas phase. Thus, a charge deconvolution of the m/z data was performed. The resulting CE–mass–heatmap reveals single stripes for each charge state in solution (Figure 3B).

Peptides containing one basic amino acid (all tryptic peptides should have at least one basic amino acid at the *C*-terminus) are doubly charged in solution and have a smaller mobility in the liquid phase (higher migration time) than those carrying two or even three basic amino acids. Each curved distribution contains peptides with the same charge in solution, and larger masses migrate slower than smaller ones. Such a picture was already described by Faserl et al., where LC fractions were analyzed by CE using sequential sample injection, and the peptides overlapping could be traced back to their LC fractions depending on their net charge and mass [35].

A few peptides seem not to fit into this scheme. A closer examination of the stray peptides revealed that those peptides that are migrating in CE at a lower charge state than expected either contain a basic amino acid on the *N*-terminus or two basic amino acids in close proximity (see b, c, and e-l in Supporting Informaion S2). This is obviously due to an overestimation of the charge using the simple approximation without taking neighboring effects into account. Furthermore, the few peptides that are migrating in CE at a higher charge state than expected, are most likely wrong sequence attributions since these peptides appear

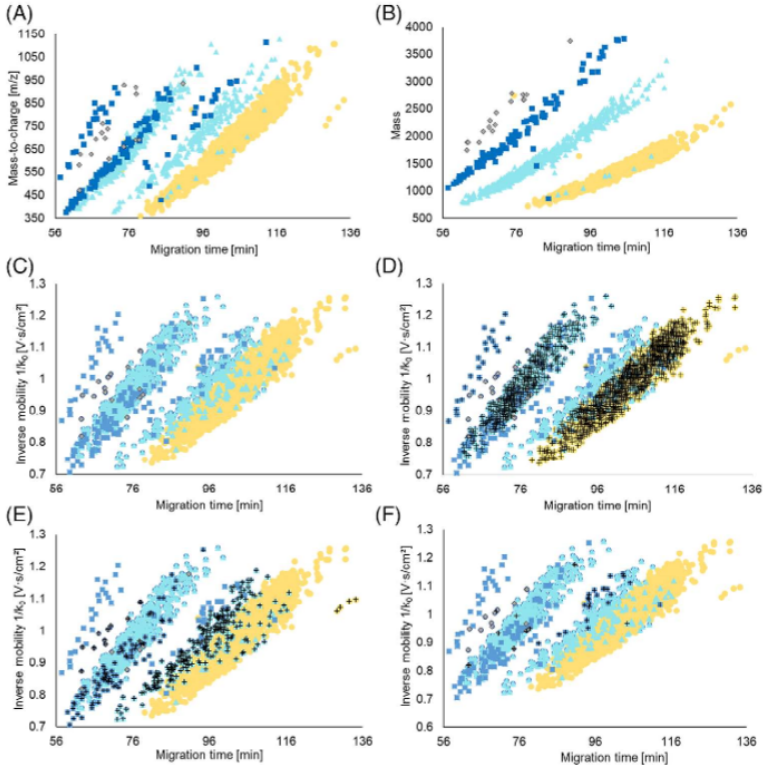

FIGURE 3 Evaluation of the identified peptides. (A) Migration time–m/z–heatmap (analog to Figure 1B). (B) Heatmap after deconvolution, migration time-mass plot. (C) Migration time–mobility heatmap (analog to Figure 1D. (D) Migration time–mobility heatmap with gas phase charge state +2 (cross). (E) Migration time–mobility heatmap with gas phase charge state +3 (cross). (F) Migration time–mobility heatmap with gas phase charge state +4 (cross). In all diagrams, peptides are colored according to the amount of basic amino acids in the peptide. Yellow circle: One, light blue triangle: Two, dark blue square: Three, grey diamond: Four basic amino acids.

only in single measurements with a rather low Mascot score (see a and d) in Supporting Information S2. No correlation between peptide size, general amino acid sequence, or character of amino acids was identified as the reason for the misbehaving peptides.

Similar to the migration time–m/z–heatmap, a striped pattern is observed when the inverse mobility is plotted against the migration time (Figure 3C). Peptides with the same mobility in the liquid phase show different mobilities in the gas phase and vice versa. To better understand stripes where peptides with different basic amino acids are mixed, the gas phase charge state was evaluated. In Figure 3D, it is visible that peptides containing one, two, or even three basic amino acids carry two positive charges in the gas phase (MS). Peptides with three charges in the MS have either two, three, or four basic amino acids (Figure 3E), and peptides with four charges in the MS have three or four basic amino acids (Figure 3F). Within an area where peptides with different basic amino acids are mixed, their charge in the gas phase differs.

Since charge deconvolution of the mass led to a better understanding of the behavior of the peptides in the liquid phase, the same was executed for the gas phase mobility as well. The $1/k_0$ value was first converted into the K_0 value, divided by the gas phase charge, and then reconverted into a charge-normalized $1/k_0$ value. These values were plotted against the migration time to get a "charge normalized" 2D mobility plot. As shown in Figure 4A, the peptides group again in stripes according to their number of basic amino acids.

However, compared to the charge-deconvoluted mass result in Figure 2B, where all peptides of the same charge form distinct sections, the charge-normalized inverse mobility still shows small gaps separating the peptides by their gas phase charge state. This indicates that a charge normalization for the mobility can be done, but a

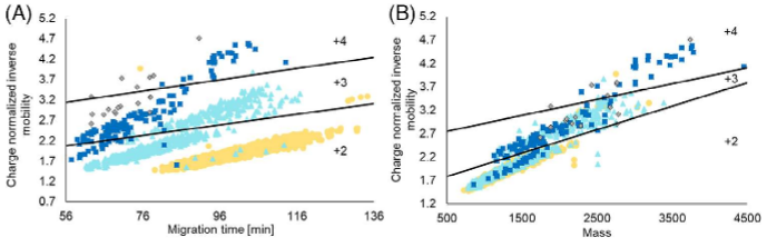

FIGURE 4 Evaluation of the mascot search identified peptides. (A) Migration time–charge normalized inverse mobility plot. (B) Mass-charge normalized inverse mobility plot. In each diagram, peptides are colored according to the number of basic amino acids in the peptide. Yellow circle: One, light blue triangle: Two, dark blue square: Three, grey diamond: Four basic amino acids. Numbers indicate the charge state in the gas phase.

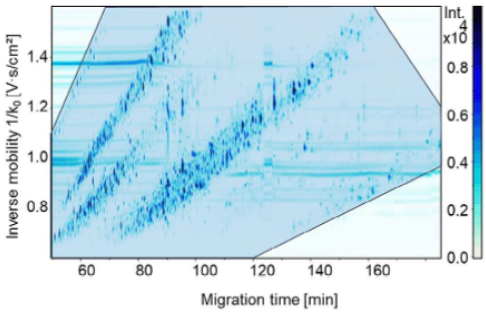

FIGURE 5 Orthogonality of CE–TIMS analysis. Data are identical to Figure 2D with the relevant migration time range and lines indicating the edge of the region where peptides are found.

small offset remains. This is most likely because higher gas phase charge states lead to larger CCS values (larger $1/k_0$ value) due to the repulsing forces of the charges within one molecule in the gas phase. The high area coverage in the charge normalized inverse mobility—migration time—heatmap (Figure 4A) is retained to a large degree, indicating a high orthogonality of CE and IM even when the gas phase charge state is subtracted. This area is much larger than a similar mass-charge normalized $1/k_0$-plot (Figure 4B).

To obtain a full picture of the orthogonality of CE and IM, the original heatmap of inverse mobility versus migration time (Figure 2D) is considered since the data of Figures 3 and 4 do not contain all peptides (e.g., singly charged peptides were excluded from MS/MS experiments).

The orthogonality of the 2D separation was estimated based on the area covered by signals in the range used for peak capacity calculation (Figure 5). Assuming that the quadratic area represents 100% orthogonality we achieved an orthogonality of around 80%. This is only an estimation (see Gilar et al. [36] for more detailed discussion), however, it clearly shows that CE–MS can significantly benefit from the additional IM dimension. The orthogonality is higher than the one from IM–MS data and rather in the order of a well performed 2D-separation by LCxLC [37].

A more detailed calculation would reduce the orthogonality value to some extent since the empty room between the distinct, slightly curved distributions are considered. However, the information (about the charge state in solution) obtained from these stripes (see discussion above) is valuable. A spreading of the signal could be obtained by increasing the pH. This can be seen in the data of Gou et al. [33]., where a BGE of 2.5% acetic acid (pH of 2.6) was used, making it difficult to observe such a pattern. Indeed, when calculating the expected charge in solution for pH = 2.6, deviations of 0.34 from the nominal charge states derived from the basic amino acids alone are calculated when acidic amino acids are present in the respective peptide. For the BGE at pH = 1.9 (aqueous part of the here applied BGE), this deviation is less than 0.07 (see Supporting Information S3). Although the striped patterns merge into each other at higher BGE pH values, we still expect in this case a high orthogonality of CE and IM due to solvation effects in CE.

4 | CONCLUDING REMARKS

Coupling the CE using the nanoCEasy interface to the timsTOF enabled the sensitive characterization of complex tryptic peptide mixtures derived from a complete proteome. The tryptic HeLa digest could be injected in relatively large volumes (6.81% of capillary) without losing separation performance. A total peak capacity of up to 9500 demonstrates the analytical performance gain for complex samples by adding a factor of around 30 in peak capacity by the TIMS even when fast IM-gradient is used—in conjunction with the ability to generate MS/MS spectra at

almost 100 Hz without compromising sensitivity. The peak capacity of the CE reaches a value of 323 for these complex peptide samples.

The acidic BGE leads to well-distinct curved patterns in the migration time–m/z profile. Similarly, curved patterns of identical charge in solution and gas phases are obtained in the migration time-inverse mobility heatmap. A charge normalization based on the gas phase charge obtained from the MS reduces the number of stripes to one for each charge state in solution with a slight gap resulting from the initial gas phase charge. This agrees with the expectation that a higher charge in the gas phase leads to larger molecules due to repulsion forces. Even after charge normalization, a high orthogonality for CE and gas-phase IM is observed. Although the underlying separation principle is the same, the solvation leads to differences not only in charge but also in size, resulting in a significantly different selectivity of CE and IM. The high orthogonality obtained here for peptides is expected to be observed also for other analytes, making CE–IM–MS a promising tool for various applications, especially when applying the ultrafast and sensitive MS/MS performance of the TIMS system.

ACKNOWLEDGMENTS

Thanks to Bruker Daltonics GmbH & Co.KG, especially Christian Albers, Jörg Sauer, and Stefan Slamnoiu for providing the opportunity to couple the CE to the timsTOF.

We thank Lukas Naumann for the support during initial measurements.

Open access funding enabled and organized by Projekt DEAL.

CONFLICT OF INTEREST STATEMENT

The authors have declared no conflict of interest.

DATA AVAILABILITY STATEMENT

The data that support the findings of this study are available from the corresponding author upon reasonable request.

ORCID

Jasmin Schairer https://orcid.org/0009-0007-3526-1998
Christian Neusüß https://orcid.org/0000-0003-2404-4924

REFERENCES

1. Gerbasi VR, Melani RD, Abbatiello SE, Belford MW, Huguet R, McGee JP, et al. Deeper protein identification using field asymmetric ion mobility spectrometry in top-down proteomics. Anal Chem. 2021;93:6323–28.
2. Guergues J, Wohlfahrt J, Stevens SM. Enhancement of proteome coverage by ion mobility fractionation coupled to PASEF on a TIMS-QTOF instrument. J Proteome Res. 2022;21:2036–44.
3. Orsburn BC, Yuan Y, Bumpus NN. Single cell proteomics using a trapped ion mobility time-of-flight mass spectrometer provides insight into the post-translational modification landscape of individual human cells. Nat Commun. 2022;13:7246.
4. Ogata K, Ishihama Y. Extending the separation space with trapped ion mobility spectrometry improves the accuracy of isobaric tag-based quantitation in proteomic LC/MS/MS. Anal Chem. 2020;92:8037–40.
5. Hadavi D, Borzova M, Porta Siegel T, Honing M. Uncovering the behaviour of ions in the gas-phase to predict the ion mobility separation of isomeric steroid compounds. Anal Chim Acta. 2022;1200:339617.
6. Wei J, Tang Y, Ridgeway ME, Park MA, Costello CE, Lin C. Accurate identification of isomeric glycans by trapped ion mobility spectrometry-electronic excitation dissociation tandem mass spectrometry. Anal Chem. 2020;92:13211–20.
7. Meier F, Beck S, Grassl N, Lubeck M, Park MA, Raether O, et al. Parallel accumulation-serial fragmentation (PASEF): Multiplying sequencing speed and sensitivity by synchronized scans in a trapped ion mobility device. J Proteome Res. 2015;14:5378–5387.
8. Chen D, McCool EN, Yang Z, Shen X, Lubeckyj RA, Xu T, et al. Recent advances (2019–2021) of capillary electrophoresis-mass spectrometry for multilevel proteomics. Mass Spectrom Rev. 2023;42:617–42.
9. Štěpánová S, Kašička V. Recent developments and applications of capillary and microchip electrophoresis in proteomics and peptidomics (mid-2018–2022). J Sep Sci. 2023;46:e2300043.
10. Zhang W, Ramautar R. CE-MS for metabolomics: Developments and applications in the period 2018–2020. Electrophoresis. 2021;42:381–401.
11. Zhang W, Ramautar R. Utility and Advances of Capillary Electrophoresis–Mass Spectrometry for Metabolomics. In: Ramautar R, Chen DDY, editors. Capillary electrophoresis mass spectrometry for proteomics and metabolomics. Weinheim:Wiley-VCH;2022. p. 147–77.
12. Schlecht J, Stolz A, Hofmann A, Gerstung L, Neusüß C. nanoCEasy: An easy, flexible, and robust nanoflow sheath liquid capillary electrophoresis-mass spectrometry interface based on 3D printed parts. Anal Chem. 2021;93:14593–98.
13. Lindenburg PW, Haselberg R, Rozing G, Ramautar R. Developments in interfacing designs for CE–MS: Towards enabling tools for proteomics and metabolomics. Chromatographia. 2015;78:367–77.
14. Týčová A, Ledvina V, Klepárník K. Recent advances in CE-MS coupling: Instrumentation, methodology, and applications. Electrophoresis. 2017;38:115–34.
15. Sauer F, Sydow C, Trapp O. A robust sheath-flow CE-MS interface for hyphenation with Orbitrap MS. Electrophoresis. 2020;41:1280–86.
16. Höcker O, Montealegre C, Neusüß C. Characterization of a nanoflow sheath liquid interface and comparison to a sheath liquid and a sheathless porous-tip interface for CE-ESI-MS in positive and negative ionization. Anal Bioanal Chem. 2018;410:5265–75.
17. Naumann L, Schairer J, Höchsmann A, Naghdi E, Neusüß C. Capillary Electrophoresis–Mass Spectrometry Interfacing: Principles and Recent Developments. In: Ramautar R, Chen DDY, editors. Capillary electrophoresis mass spectrometry for

proteomics and metabolomics. Weinheim: Wiley-VCH;2022. p. 1–33.
18. Höcker O, Bader T, Schmidt TC, Schulz W, Neusüß C. Enrichment-free analysis of anionic micropollutants in the sub-ppb range in drinking water by capillary electrophoresis-high resolution mass spectrometry. Anal Bioanal Chem. 2020;412:4857–65.
19. Kuzyk VO, Somsen GW, Haselberg R. CE-MS for proteomics and intact protein analysis. Adv Exp Med Biol. 2021;1336: 51–86.
20. Štěpánová S, Kašička V. CE–MS Approaches for Peptidomics. In: Ramautar R, Chen DDY, editors. Capillary electrophoresis mass spectrometry for proteomics and metabolomics. Weinheim: Wiley-VCH;2022. p. 235–59.
21. Johnson KR, Greguš M, Ivanov AR. Coupling high-field asymmetric ion mobility spectrometry with capillary electrophoresis-electrospray ionization-tandem mass spectrometry improves protein identifications in bottom-up proteomic analysis of low nanogram samples. J Proteome Res. 2022;21: 2453–2461.
22. Johnson KR, Greguš M, Kostas JC, Ivanov AR. Capillary electrophoresis coupled to electrospray ionization tandem mass spectrometry for ultra-sensitive proteomic analysis of limited samples. Anal Chem. 2022;94:704–13.
23. Sun L, Hebert AS, Yan X, Zhao Y, Westphall MS, Rush MJP, et al. Over 10,000 peptide identifications from the HeLa proteome by using single-shot capillary zone electrophoresis combined with tandem mass spectrometry. Angew Chem Int Ed Engl. 2014;53:13931–33.
24. Jooß K, Meckelmann SW, Klein J, Schmitz OJ, Neusüß C. Capillary zone electrophoresis coupled to drift tube ion mobility-mass spectrometry for the analysis of native and APTS-labeled N-glycans. Anal Bioanal Chem. 2019;411:6255–64.
25. Zhong X, Chen Z, Snovida S, Liu Y, Rogers JC, Li L. Capillary electrophoresis-electrospray ionization-mass spectrometry for quantitative analysis of glycans labeled with multiplex carbonyl-reactive tandem mass tags. Anal Chem. 2015;87: 6527–6534.
26. Hooijschuur K, Liu X, Grootendorst A, Pieterman I, Sastre Toraño J. In-line sample trap columns with diatomite for large-volume injection in CZE-IM-MS. Electrophoresis. 2023;44:395–402.
27. Mast DH, Liao H-W, Romanova EV, Sweedler JV. Analysis of peptide stereochemistry in single cells by capillary electrophoresis-trapped ion mobility spectrometry mass spectrometry. Anal Chem. 2021;93:6205–13.
28. DeLaney K, Jia D, Iyer L, Yu Z, Choi SB, Marvar PJ, et al. Micro-analysis of brain angiotensin peptides using ultrasensitive capillary electrophoresis trapped ion mobility mass spectrometry. Anal Chem. 2022;94:9018–25.
29. Xu T, Wang Q, Wang Q, Sun L. Coupling high-field asymmetric waveform ion mobility spectrometry with capillary zone electrophoresis-tandem mass spectrometry for top-down proteomics. Anal Chem. 2023;95:9497–504.
30. Li J, Purves RW, Richards JC. Coupling capillary electrophoresis and high-field asymmetric waveform ion mobility spectrometry mass spectrometry for the analysis of complex lipopolysaccharides. Anal Chem. 2004;76:4676–83.
31. Mironov GG, Clouthier CM, Akbar A, Keillor JW, Berezovski MV. Simultaneous analysis of enzyme structure and activity by kinetic capillary electrophoresis–MS. Nat Chem Biol. 2016;12:918–22.
32. Drouin N, Mielcarek A, Wenz C, Rudaz S. Evaluation of ion mobility in capillary electrophoresis coupled to mass spectrometry for the identification in metabolomics. Electrophoresis. 2021;42:342–49.
33. Gou M-J, Kose MC, Crommen J, Nix C, Cobraiville G, Caers J, et al. Contribution of capillary zone electrophoresis hyphenated with drift tube ion mobility mass spectrometry as a complementary tool to microfluidic reversed phase liquid chromatography for antigen discovery. Int J Mol Sci. 2022;23: 13350.
34. Höcker O, Knierman M, Meixner J, Neusüß C. Two capillary approach for a multifunctional nanoflow sheath liquid interface for capillary electrophoresis-mass spectrometry. Electrophoresis. 2021;42:369–73.
35. Faserl K, Sarg B, Sola L, Lindner HH. Enhancing proteomic throughput in capillary electrophoresis-mass spectrometry by sequential sample injection. Proteomics. 2017;17:1700310. https://doi.org/10.1002/pmic.201700310
36. Gilar M, Fridrich J, Schure MR, Jaworski A. Comparison of orthogonality estimation methods for the two-dimensional separations of peptides. Anal Chem. 2012;84:8722–32.
37. Gilar M, Olivova P, Daly AE, Gebler JC. Orthogonality of separation in two-dimensional liquid chromatography. Anal Chem. 2005;77:6426–34.

SUPPORTING INFORMATION

Additional supporting information can be found online in the Supporting Information section at the end of this article.

How to cite this article: Schairer J, Plathe F, Hudelmaier S, Belau E, Pengelley S, Kruse L, et al. Ion mobility in gas and liquid phases: How much orthogonality is obtained in capillary electrophoresis–ion mobility–mass spectrometry? Electrophoresis. 2024;45:735–42. https://doi.org/10.1002/elps.202300210

Manuscript III

CE-MS and CE-MS/MS for the multiattribute analysis of monoclonal antibody variants at the subunit level

Jasmin Schairer, Jennifer Römer, Christian Neusüß

Journal of pharmaceutical and biomedical analysis. 2025; 252: 116495. DOI: 10.1016/j.jpba.2024.116495

Journal of Pharmaceutical and Biomedical Analysis 252 (2025) 116495

Contents lists available at ScienceDirect

Journal of Pharmaceutical and Biomedical Analysis

journal homepage: www.journals.elsevier.com/journal-of-pharmaceutical-and-biomedical-analysis

CE-MS and CE-MS/MS for the multiattribute analysis of monoclonal antibody variants at the subunit level

Jasmin Schairer [a,b,1], Jennifer Römer [c,2], Christian Neusüß [a,3,*]

[a] Faculty of Chemistry, Aalen University, Beethovenstraße 1, Aalen 73430, Germany
[b] Faculty of Science, University of Tübingen, Auf der Morgenstelle 8, Tübingen 72076, Germany
[c] Rentschler Biopharma SE, Erwin-Rentschler-Straße 21, Laupheim 88471, Germany

ARTICLE INFO

Keywords:
monoclonal antibodies
subunit variant analysis
capillary electrophoresis mass spectrometry
middle-down

ABSTRACT

The analysis of product-related substances and impurities is a critical step in the biopharmaceutical quality control of multiattribute monoclonal antibodies (mAbs), as posttranslational modifications or other variants can influence the product's biological activity. Many approaches are available for variant analysis; however, they are either variant-specific, mAb-specific, time-consuming, or require expensive equipment. Here, we present a generic capillary electrophoretic method based on a neutral-coated capillary which was coupled to mass spectrometry (MS) via the nanoCEasy interface for mAb variant analysis at the subunit level (enzymatically digested and reduced mAb). The method enabled the separation of several (i) size variants (e.g. glycosylation variants) and (ii) charge variants (e.g. c-terminal lysin clipping) as well as (iii) multiple other proteoforms (e.g. additional glycation) and (iv) incompletely reduced subunits. Separated variants were confirmed by MS/MS fragmentation even for small mass deviations like deamidation or open disulfide bridges. The system, initially developed for one mAb, was tested with nine other IgG1s to show the general applicability of the system. The presented multi-attribute method enables fast and detailed characterization of mAb variants with little sample preparation and relatively simple separation equipment enabling the separation of a large set of mAb variants.

1. Introduction

Approximately 50 % of the biopharmaceuticals approved in the last decade were monoclonal antibodies (mAb) [1]. Patients depend on stable, safe, and effective medications that require critical product validation. Critical quality attributes are tested and analyzed to ensure that product variations and impurities are within a predefined range to guarantee product quality and safety. Even with a highly controlled production process, monoclonal antibodies can have a multiplicity of macro and microheterogeneities [2]. These heterogeneities arise from the cell culture in which the mAbs are produced, the chosen process parameters, the cleanup procedure, or the storage conditions. These mAb variants, such as C-terminal lysine variants, oxidation, deamidation, and glycosylation change the mAb in size and charge [2]. These variants can be analyzed on an intact, subunit, or peptide level using reversed-phase liquid chromatography (RPLC), hydrophilic interaction liquid chromatography (HILIC), ion exchange chromatography (IEX), capillary electrophoresis (CE) or capillary isoelectric focusing (CIEF) coupled to UV and mass spectrometry (MS).

The mass spectrometric analysis of mAb variants on an intact level is fast and relatively easy. Using RPLC, which is generally used for desalting, the overall proteoform population on the mAb and the

Abbreviations: BGE, Background electrolyte; CE, Capillary electrophoresis; CIEF, Capillary isoelectric focusing; DTT, Dithiothreitol; EIE, Extracted ion electropherogram; EThcD, Electron transfer higher energy collisional dissociation; FA, Formic acid; Fc/2, C-terminal half of heavy chain; Fd, N-terminal half of heavy chain; HC, Heavy chain; HILIC, Hydrophilic interaction liquid chromatography; ID, Inner diameter; IEX, Ion exchange chromatography; IPA, Isopropanol; LC, Light chain; MAb, Monoclonal antibody; MOPS, 3-N-morpholino propanesulfonic acid; MS, Mass spectrometry; OD, Outer diameter,PEO, Polyethylene oxid pI, Isoelectric point; RPLC, Reversed-phase liquid chromatography; SL, Sheath liquid; TIE, Total ion electropherogram.

* Correspondence to: Department of Chemistry, Aalen University, Beethovenstrasse 1, Aalen73430 Germany
E-mail address: christian.neusuess@hs-aalen.de (C. Neusüß).
[1] 0009-0007-3526-1998
[2] 0000-0001-6841-0389
[3] 0000-0003-2404-4924

https://doi.org/10.1016/j.jpba.2024.116495
Received 12 August 2024; Received in revised form 21 September 2024; Accepted 30 September 2024
Available online 1 October 2024

glycosylation pattern can be detected. Both information is lost as soon as the mAb or the glycans are enzymatically digested. RPLC-MS is also capable of detecting variants with high mass differences and many samples can be measured (high-throughput) [3]. With CE-MS, the glycosylation patterns that are not separated with RPLC can be marginally separated and mono- and aglycosylated mAbs can be analyzed [4]. With CIEF-MS C-terminal lysine variants can be separated and identified [5] and a well-optimized IEX-MS method can provide additional information on acidic and basic species with smaller mass differences compared to the main form [6,7]. Although the intact approach is great for high-throughput analysis, it is not accessible for fragmentation experiments. Additionally, modifications with small mass differences are only detected with well-optimized separation, which, in the case of IEX-MS cannot be universally applied to all mAbs because of their different isoelectric points (pI).

The mass spectrometric analysis of mAb variants on the peptide level (peptide mapping) enables fragmentation experiments and a detailed analysis of the location of the variant. Variants with low mass differences like deamidations can be very well characterized even though the analysis is significantly more time-consuming. Sample preparation takes several hours to days depending on the approach, followed by relatively long separation methods using RPLC [8,9]. Apart from these prolonged analysis times, the peptide mapping approach faces the problem of artifacts and induced variants like deamidation or carbamylation when high temperatures, high pH, or urea is used [8,10,11]. In addition, the presence of several modifications can not be determined on the peptide level.

As a compromise between both approaches, mAbs can be analyzed in a reduced (heavy chain (HC) and light chain (LC)) or enzymatically digested and reduced (LC, N-terminal half of heavy chain (Fd), and C-terminal half of heavy chain (Fc/2)) subunit state. The interpretation of the MS spectra gets easier compared to the intact level since e.g. only one glycan is bound to the HC or Fc/2 subunit. Furthermore, the subunit moieties are accessible for MS/MS experiments, so the location of the variant can be determined. The subunit approach also enables a better separation compared to the intact level and is less prone to artifacts compared to peptide mapping. Prior to MS characterization, subunits can be separated by RPLC, HILIC, CE, IEX, or CIEF. RPLC is mostly used to separate specific variants like oxidation [12,13], glycosylation [14], or disulfides [15,16]. RPLC is also used for sequence coverage optimization [17]. Since each modification requires another column, this approach is not suitable for multiattribute analysis. HILIC is used for glycosylation analysis [6,18] but other proteoforms will not be very well separated. IEX is useful for charge variant separation of enzymatically digested mAb [19] however reduced subunit samples containing salts and the different pI of the subunits can cause troubles when applied to the IEX. CIEF was used for the analysis of cetuximab subunits [20] although, CIEF is more commonly used for intact analysis. Compared to all these approaches CE is expected to be the only multiattribute separation method at the subunit level that allows the separation of different samples and variants without large method adjustments (as needed in RPLC or IEX) and can be relatively easily coupled to MS without contaminating the MS with salts or ampholytes (as in IEX or CIEF). Several CE-based studies analyzed mAb on different subunit levels for glycosylation, deamidation, oxidation, pyroglutamate, and C-terminal lysine clipping [4,21–26]. However, these methods either did not systematically study several mAbs or variants [4,21,23,25], were not directly coupled to the MS [21], were only used as a supplement to intact or peptide level analysis [4,22–25], were facing incomplete sample reduction due to desalting prior to the analysis [22], or require dedicated equipment [26].

Here, we present a generic method to separate and analyze subunits (enzymatically digested and reduced) of mAbs using an online CE-MS (MS/MS) system. The systematic variant evaluation was performed for all subunits of nine different mAbs and one stressed mAb using MS/MS to identify and determine the location of the modification. We also briefly evaluated incomplete sample reduction and determined the overall number of possible proteoforms based on the deconvoluted masses, demonstrating the high potential of the method.

2. Materials and methods

2.1. Chemicals and materials

Infliximab (10 mg/mL, charge: 8KMKA90603) and cetuximab (5 mg/mL, charge: 248033), were purchased from Evidentic GmbH (Berlin, Germany). Protein A purified research antibodies mAb1 (20 mg/mL), mAb2 (16.8 mg/mL), mAb3 (18.3 mg/mL) mAb4 (21.7 mg/mL), and mAb5 (18.5 mg/mL) were kindly provided by Rentschler Biopharma SE (Laupheim, Germany). NIST mAb (10 mg/mL, Reference Material 8671, lot: 14HB-D-002) was purchased from the National Institute of Standard and Technology (NIST, Gaithersburg, MD, USA). USP mAb003 (Cat. No. 1445595, LOT: F12980, 10 mg/mL), 3-(N-morpholino) propanesulfonic acid (MOPS)-buffer, 1,4-dithiothreitol (DTT), and hydrochloric acid (37 %) were purchased from Sigma (Steinheim, Germany). Isopropanol (IPA, LC-MS grade), ammonia solution (p.a., 30 %), and formic acid (FA, ≥98 %) were purchased from Carl Roth GmbH & Co. KG (Karlsruhe, Germany). Urea (Ultrapure) and guanidine hydrochloride (99.5 %) were purchased from ThermoFisher Scientific (Dreieich, Germany). Sodium hydroxide (NaOH) and hydrofluoric acid (40 %(v/v), HF) were purchased from Merck (Darmstadt, Germany). Polyethylene oxide (PEO, Mw: 1.000.000) was purchased from Alfa Aesar (Kandel, Germany). IdeS protease was purchased from GENOVIS (FabRICATOR, 5000 units, Lund, Sweden). Ultrapure water was used for all solutions (SG Ultra Clear UV from Siemens Water Technologies, USA).

2.2. Sample Preparation

pH stress was achieved by pipetting 0.5 µL concentrated ammonia solution to 10 µL undiluted mAb. The sample was then left in the dark for 7 days at room temperature. Afterwards, the samples were directly used for further sample preparation.

All mAbs were digested following the FabRICATOR digestion protocol of GENOVIS. 200 µg mAb was digested in MOPS buffer at pH 7.2 using 200 U of IdeS. The samples were incubated for 30 min at 37°C and 500 rpm.

After digestion, a part of the samples were reduced with DTT in the presence of urea leading to a final mAb concentration of 0.6 mg/mL. The reduction was incubated for 60 min at 37°C and 500 rpm. Samples were frozen at −20°C until measurement. Detailed sample preparation parameters were published elsewhere [27].

2.3. CE analysis

The experiments were conducted on an Agilent 7100 CE instrument (Agilent Technologies GmbH, Waldbronn, Germany). Fused silica capillaries (separation capillary: 50 µm inner diameter (ID), 365 µm outer diameter (OD), and sheath liquid (SL) capillary: 100 µm ID, 240 µm OD) were purchased from Polymicro Technologies (Phoenix, AZ, USA).

An etched 60 cm length and 50 µm ID polyethylenoxid (PEO) coated capillary was used for all experiments to avoid protein adsorption. Capillary etching and PEO coating were performed as described in detail elsewhere [27]. Briefly, for capillary etching, the polyimide was removed from the capillary end and then dipped into hydrofluoric acid for 60 min. The capillary was prepared with 1 M NaOH, water, and 1 M HCl for 5 min, respectively, followed by the PEO coating solution for 10 min, water, and background electrolyte (BGE) for 5 min, respectively. The PEO coating solution was prepared by first preparing a PEO stock solution where 100 mg PEO was dissolved in 45 mL of water. 450 µL of the stock solution was then acidified using 50 µL 0.1 M HCl. The capillary coating was applied each day to guarantee a proper capillary

coating.

The BGE consisted of 10 % IPA in water containing 1 M FA. Sample injection was carried out hydrodynamically using 50 mbar pressure for 10 s. A 20 kV voltage was applied for the separation. The capillary was flushed for 3 min with BGE between the runs.

2.4. nanoCEasy interface

For all CE-MS and CE-MS/MS experiments, the nanoCEasy interface was used [28]. The emitters were obtained from BioMedical Instruments (Zoellnitz, Germany). The interface was supervised using a digital microscope (Dino-Lite, Almere, The Netherlands). The emitter had a 30 μm tip opening and a tip length of 4 mm and was placed 3 mm in front of the MS orifice. In the separation mode, the separation capillary was placed 3 mm behind the emitter tip.

2.5. MS and MS/MS analysis

MS experiments were performed using the Orbitrap Fusion Lumos Tribrid MS (Thermo Fisher Scientific, SanJose, CA, USA). IPA: Water (50:50) + 0.5 % FA was used in all experiments as SL. Positive ionization mode, a spray voltage of 2000 V, sweep gas of 3 Arb, and 300°C ion transfer tube temperature were used. Data were acquired from 700 to 3000 *m/z* with an Orbitrap resolution of 120,000.

For MS/MS experiments, the Orbitrap resolution was set to 7500 in the MS1 scan and the scan range was set from 700 to 3000 *m/z*. For MS2, the scan range was set to from 150 – 2000 *m/z* with an Orbitrap resolution of 120,000. Electron transfer higher energy collisional dissociation (EThcD) was used to fragment the precursor ions. Electron transfer dissociation (ETD) reaction time was 12 ms (ETD reaction target of 6E5 in 200 ms), followed by 12 % normalized higher energy collisional dissociation (HCD) collision energy.

2.6. Data analysis

Orbitrap data was evaluated using Freestyle 1.8. The extracted ion electropherograms (EIEs) for the different charge variants were generated based on the six most intense *m/z* of the charge envelope and smoothed using Freestyle Gaussian 5 smoothing. The deconvolution of Orbitrap MS data was done using the Xtract algorithm, setting the charge range from 5 to 50 and the minimum number of detected charges to 5. At first, selected proteoforms were searched for. The identified proteoforms had (i) at least five charge states (already determined in the Freestyle deconvolution algorithm) (ii) a mass accuracy of below 15 ppm, (iii) a charge envelop distribution in successive order, and (iv) a migration behavior that fitted the estimated proteoform. Further, unassigned proteoforms had to undergo the same criteria. However, since criteria (ii) and (iv) could not be applied the signal intensity had to exceed 30,000 counts. All unassigned masses below this threshold were excluded from the final list.

The MS/MS data were deconvoluted using Xtract, however, the minimum number of detected charges was decreased to 1. The deconvoluted fragments were analyzed using ProSight Lite v1.4 (Northwestern University, Evanston, IL, USA) with a fragment tolerance of 10 ppm.

3. Results and discussion

3.1. Subunit moiety separation

The analysis of antibody subunits is straightforward, requires a limited amount of sample preparation, and therefore reduces the overall analysis time. Separation parameters like BGE composition and separation voltage were tested. On the neutrally coated capillary a BGE containing 5 % acetic acid was not separating the three subunit moieties and the Fc/2 signals were less intense compared to the LC and Fd signals. 0.2 M formic acid (FA) as BGE improved the separation but the Fc/2 subunit signal remained quite low intense compared to the other two subunit moieties. The BGE containing 10 % IPA and 1 M FA provided peaks with similar intensities for each subunit moiety. 10 kV and 20 kV separation voltages were tested. Since 10 kV was only prolonging the separation time without showing additional signals in the MS, 20 kV was used for further experiments (data not shown). Sample preparation was also optimized and was described elsewhere [27]. Briefly, the sample preparation was improved by using 4 M urea to enhance sample reduction using DTT. Without this chaotropic salt sample reduction was insufficient and almost no reduction was achieved. The digested and reduced antibodies were directly analyzed without the removal of enzyme or urea prior to the measurement. As shown by the total ion electropherograms (TIEs) in Fig. 1, the separation is done in under 30 min and the three subunits can be separated in most cases.

Fc/2 is in all cases migrating first, followed by Fd and LC. mAb2 is the only mAb where the LC migrates faster than the Fd. For NIST, Fc/2 and Fd were not separated from each other and for cetuximab, no Fd peak was detected even with a prolonged analysis time to rule out a slower migration behavior. Cetuximab was the only antibody in the set that contained Fd glycosylation, which could explain why this is the only mAb where Fd was not detected. The complex glycosylation heterogeneity influences the signal intensity. We saw a quite noisy, low intense signal at the end of the LC subunit peak that could not be deconvoluted using the Xtract algorithm. That could possibly be the Fd exhibiting a large microheterogeneity due to additional glycosylation, potentially suppressed due to the LC subunit. mAb1 and pH-stressed mAb1 differ in migration time due to ammonia in the sample used for pH stressing. Some mAbs such as infliximab, mAb2, mAb4, and mAb5 show additional intense signals, which will be discussed in detail later.

3.2. Glycosylation/aglycosylation/sialic acid

Most IgG1 mAbs are glycosylated in the CH2 domain of the mAb which is highly responsible for the structure, stability, and functionality of mAbs [29]. The N-glycosylation core consists of a five-hexose structure followed by several hexose moieties (see Fig. 2B).

The separation of the different glycoforms of the Fc/2 as well as the aglycosylated Fc/2 using the method described above is shown in Fig. 2A. Aglycosylated Fc/2 is migrating at 20.26 min and can be separated from the Fc/2 variants carrying different glycosylation around 21 min. Fc/2 variants with larger glycans migrate slower (Fc/2+G2F, 21.12 min) compared to Fc/2 variants carrying smaller glycans (e.g. Fc/2+G0F, 20.97 min). Fc/2 with sialylated glycans (sialic acid, SA, adds an additional charge to the molecule; the lowest three EIE of Fig. 2A) are baseline separated from Fc/2 with non-sialylated glycans. The migration order of the different Fc/2 proteoforms is conclusive with the applied neutrally coated PEO capillary where no EOF is present and molecules are separated based only on their mobility. The appearance of a second, baseline-separated signal in the extracted ion electropherogram (EIE) of aglycosylated Fc/2, Fc/2+G2FSA, and Fc/2+G2F2SA is a result of the chosen *m/z* values for EIE generation and the underlying isotopic pattern of different proteoforms. E.g. *m/z* 902.3866 (z=29) used in the EIE generation for Fc/2+G2F2SA is out of the 5 ppm range of 902.2836 (z=28) used for Fc+G0F. However, the isotopic distribution of 902.2836 (z=28) shows an *m/z* at 902.3890 which is covered by the 5 ppm range of Fc/2+G2F2SA. This does not disturb the analysis here, because these two peaks can be assigned to their correct proteoform by migration time, mass, and fragmentation results. The double peaks for Fc/2+G0-GlcNAc, Fc/2+G0F-GlcNAc, and Fc/2+G1FSA could theoretically be positional isomers as indicated in Fig. 2B. However, such a separation is not expected and no further experiments were done to confirm or deny this theory.

The ratio of the detected glycan species relative to the most intense glycoform was also evaluated based on the EIE. The Fc/2+G0F intensity was set to 100 % for each of the four runs (n=4) and the relative amount

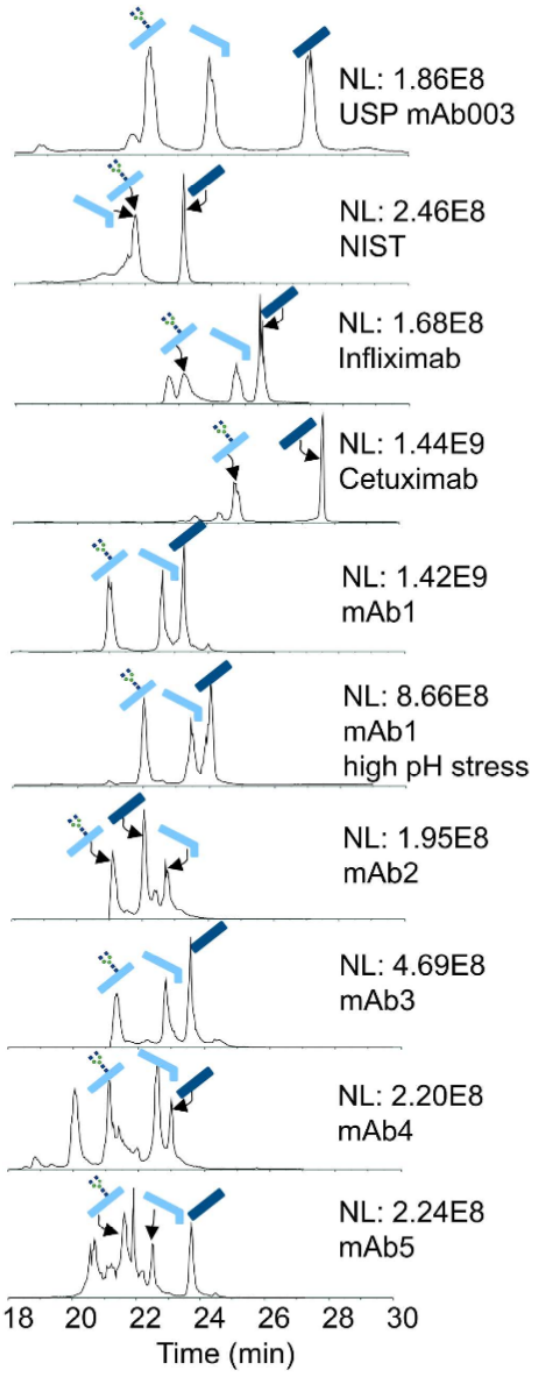

Fig. 1. TIEs of the different mAb subunits separated with the proposed CE system. BGE: 10 % IPA in water containing 1 M FA, 20 kV, 1 % capillary volume injected, SL: IPA: H_2O 1:1 + 0.5 % FA.

of each glycoform was calculated. The results in Fig. 2C show that most species have an intensity below 6 % compared to the G0F glycoform and very low abundant species such as Fc/2+G2F2SA with a relative intensity of 0.67 % can still be detected. This demonstrates that the proposed method is capable of describing the glycosylation pattern of mAbs in great detail.

As shown here for mAb1 the same separation of different glycoforms was achieved for all mAbs measured. Only NIST mAb was challenging since Fc/2 and Fd proteoforms migrated similarly potentially causing ion suppression, especially to the low abundant glycosylation species. The detected masses as well as the EIEs for the detected glycans of each mAb can be found in Supplementary Information S2-S12.

3.3. Additional glycation

In addition to the glycosylation discussed above, there are further possibilities for sugar moieties to be attached to the molecule. This mAb modification with single hexose moieties happens non-enzymatically at lysine residues due to the sugars used in cell culture media. [30] This glycation was found on the LC of NIST mAb, USP mAb003, pH-stressed mAb1, and mAb2. LC glycation causes an increase in migration time of 0.06 min up to 0.25 min depending on the mAb that was analyzed. The glycation on the lysine reduces the positive charge of the molecule by one unit and creates an acidic variant which results in a longer migration time using the above presented method. LC glycation was detected at relatively low levels of 4.9 % ± 0.4 % for NIST, 3.7 % ± 0.4 % for USPmAb003, 2.6 % ± 0.2 % for pH stressed mAb1, and 4.6 % ± 1.1 % for mAb2 (n=3 for all mAbs). Although fragmentation experiments were conducted, it was unclear where the glycation was located. This has two possible explanations. First, the signals are quite low and provide only a few fragment ions and second, there are several possible lysine moieties to which the hexose could be attached. A recent interlaboratory study was analyzing NIST regarding variants including glycation using reduced mAb [31]. There, glycation in the LC was detected on various lysine residues in low abundances (smaller 0.82 % per Lys using peptide mapping). Taking this into account, the glycation peak detected with our method probably contains all of these proteoforms, which makes the identification using MS/MS complicated. No Fd glycation on NIST was detected with our approach even though it was reported in several publications [26,31]. As already mentioned a proper separation of the proteoforms is crucial for their detection, especially if the proteoform is low-abundant. It is most likely that for NIST the Fd glycation was not detected because Fd and Fc/2 are not separated. This hypothesis is supported by the fact that Fd glycation was detected for mAb1. There, glycation was detected with a migration time shift of 0.06 min at a level of 3.4 % ± 0.2 % compared to the non-glycated Fd. Apart from mAb1, no Fd glycation was detected in any other mAb.

A glycation on the Fc/2 subunit is difficult to analyze because it can easily be mistaken for another glycoform, especially without proper separation. E.g. Fc/2+G0F +Hex has the same mass as the Fc/2+G1F. The glycated proteoform must be separated from this glycosylated form for identification. mAb1 was the only mAb with a possible glycation on the Fc/2. After EIE generation a low-intensity partly separated peak at 21.31 min for Fc/2+G0F (20.97 min) and 21.41 min for Fc/2+G1F (21.03 min) was determined. These minor peaks could be possible glycated species of the respective Fc/2 glycoforms. However, this is only an assumption based on the fact that none of the other mAbs showed a minor peak next to the main glycoform. The detected masses as well as the EIEs for the detected glycation of each mAb can be found in supplementary material S2-S11.

3.4. Lysine variants

Lysine variants are another modification that is present in many mAbs. The different variants of lysine occur due to posttranslational C-terminal processing with carboxypeptidases resulting in clipping of the

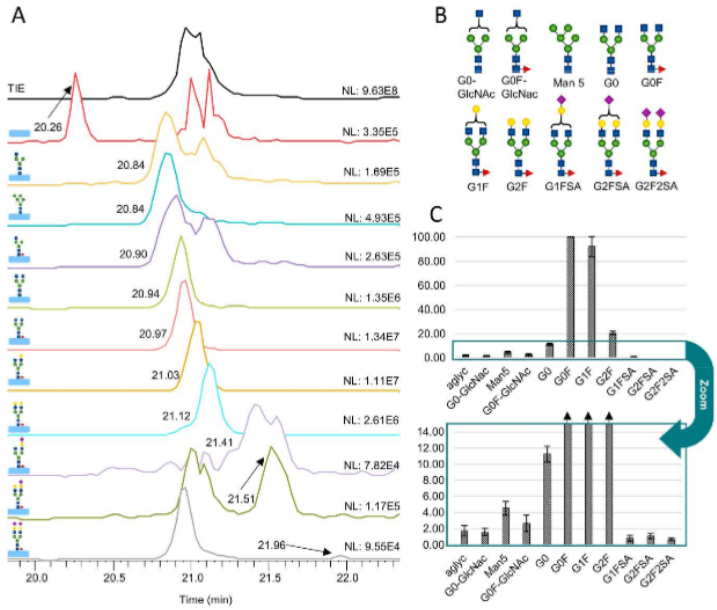

Fig. 2. A) Separation of different glycosylation variants on Fc/2 of mAb1. Separation conditions as in Fig. 1. Each EIE was generated based on 6 *m/z* values. Positional isomers are correctly annotated in B.; B) Most common glycan structures and possible isomeric structures. blue square: N-Acetylglucosamine, green circle: mannose; yellow circle: galactose, pink diamond: sialic acid, red triangle: fucose; C) Glycan distribution of mAb1 relative to G0F (n=4).

lysine [32]. Lysine variants were detected in various amounts in mAb1, pH-stressed mAb1, USPmAb003, NIST, infliximab, and cetuximab. Especially infliximab showed extensive lysine variants. The TIE in Fig. 3A shows two separated Fc/2 signals with similar intensity, one for Fc/2 still carrying a lysine and one where the lysine is clipped. The respective variants are baseline-separated. E.g. Fc/2+G0F+Lys migrates at 22.64 min whereas Fc/2+G0F migrates at 23.09 min. This difference in migration time can also be determined for the G1F and G2F

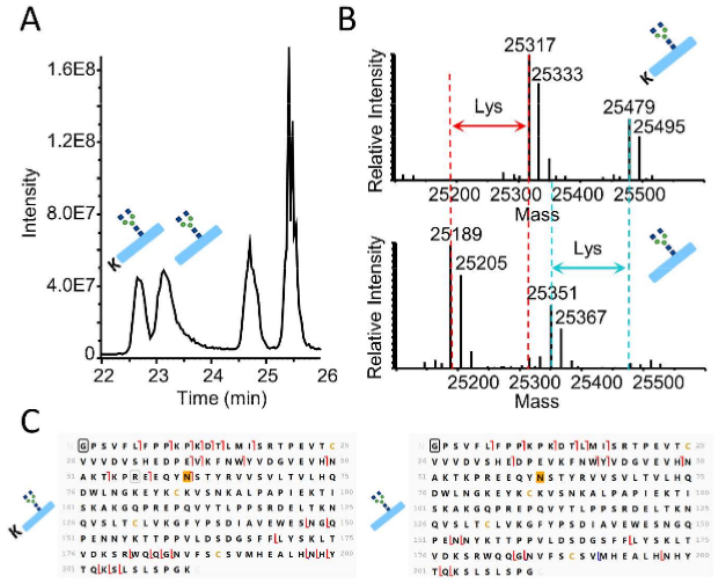

Fig. 3. A) TIE of infliximab with two Fc/2 signals. First signal: +Lys; Second signal: -Lys. Separation conditions as in Fig. 1; B) Deconvoluted mass spectrum of both signals. Upper spectrum for Fc/2 with the lysine still attached. Lower spectrum for Fc/2 without the lysine. Lysine distances between different glycan species are indicated with arrows. Red: Fc/2+G0F, blue: Fc/2+G1F; C) MS/MS results of Fc+G0F+Lys (left) and Fc+G0F(right).

proteoforms of Fc/2 and their respective lysine variants. The migration order of the different Fc/2 proteoforms is conclusive with the applied neutrally coated PEO coating. The additional C-terminal lysine adds a positive charge, resulting in a faster migration time. The deconvoluted mass spectra in Fig. 3B clearly show the 128 Da mass shift for the two main glycosylation forms of Fc/2. The MS/MS data in Fig. 3C confirm the lysine variant with the respective y and z ions.

The ratio of Fc/2 with lysine compared to Fc/2 without lysine was calculated for each glycoform. Therefore, the intensities for Fc/2 without lysine were set to 100 % for each glycoform and each of the three runs, and the relative amount of each lysine variant was calculated based on the EIE. Compared to Fc/2+G0F without lysine, the lysine variant of the Fc/2+G0F has a relative intensity of 92.06 ± 15.83 %. The lysine variant of Fc/2+G1F has a relative intensity of 100.44 ± 17.78 % compared to Fc/2+G1F without lysine, and the lysine variant of Fc/2+G2F has a relative intensity of 108.23 ± 9.07 % compared to Fc/2+G2F without lysine. These values indicate that Fc/2+G2F seems to be a bit more prominent in the lysine form than in the form without lysine. At the same time, the G0F glycoform seems to be a bit less abundant in the lysine proteoform compared to the proteoform without lysine. The Fc/2+G1F glycoform has a similar intensity for both proteoforms.

As shown here for infliximab, the same separation of different glycoforms and lysine variants was achieved for all mAbs with single lysine clipping. While for infliximab, lysine variants were easily detected, other mAbs such as mAb1 only have minor lysine variants. Still, Fc/2+G1F+Lys with a relative intensity of 0.59 ± 0.11 % (n=3) compared to Fc/2+G1F was detected for mAb1. The detected masses and the EIEs for the detected glycans and lysine variants of each mAb can be found in supplementary material S2-S12.

3.5. Oxidation

Another mAb variant is the oxidized form. Methionine is the most prominent amino acid for oxidation, but other amino acids such as histidine and tryptophan can also be oxidized [33]. Oxidation was detected in eight of the ten mAbs using the method mentioned above, except for USPmAb003 and cetuximab. In all cases, it was either LC or Fd oxidation that was identified. Fc/2 oxidation remained unclear because Fc/2+G0F in its oxidized form has the same mass as an Fc/2+G1 and an Fc/2+G1F in its oxidized form has the same mass as an Fc/2+G2. Sample preparation-induced oxidation was ruled out since all samples were prepared on the same day and frozen until measurement. In most cases, only a single oxidation on a single subunit moiety was detected. As shown in Fig. 4 the most oxidized species were detected on mAb3. LC and Fd were both oxidized three times, and a slight shift in migration time of around 0.1 min per oxidation was detected.

The Fd of mAb3 contains three methionine moieties, M18, M34, and M85 so single, double, and triple oxidized species are possible. MS/MS experiments were performed for the single-oxidized Fd, however the exact location of the oxidation site in the molecule remains unknown. This can be explained by the fact that no separation of the positional isomers is obtained leading to mixed MS/MS spectra. Thus, the exact location of the oxidation remains unknown even though the proteoform is quite abundant with a relative abundance of 34.45 ± 5.50 %. Compared to that, the double and triple oxidation is less abundant as can be taken from Table 1. The sequence of the LC of mAb3 only contains one methionine moiety at M55. This location for single oxidized LC could be confirmed by MS/MS experiments due to the high abundance of this proteoform (Table 1). Since double and triple oxidation is also present based on the shift in migration time and mass, other amino acids than methionine are most likely oxidized. Additionally, the EIE for double and triple-oxidized LC showed a second, intense signal at 24.45 min and 24.55 min respectively. After a detailed examination of the data (charge envelope distribution, signal intensity, and deconvoluted mass), there is no indication of a misinterpretation of these signals

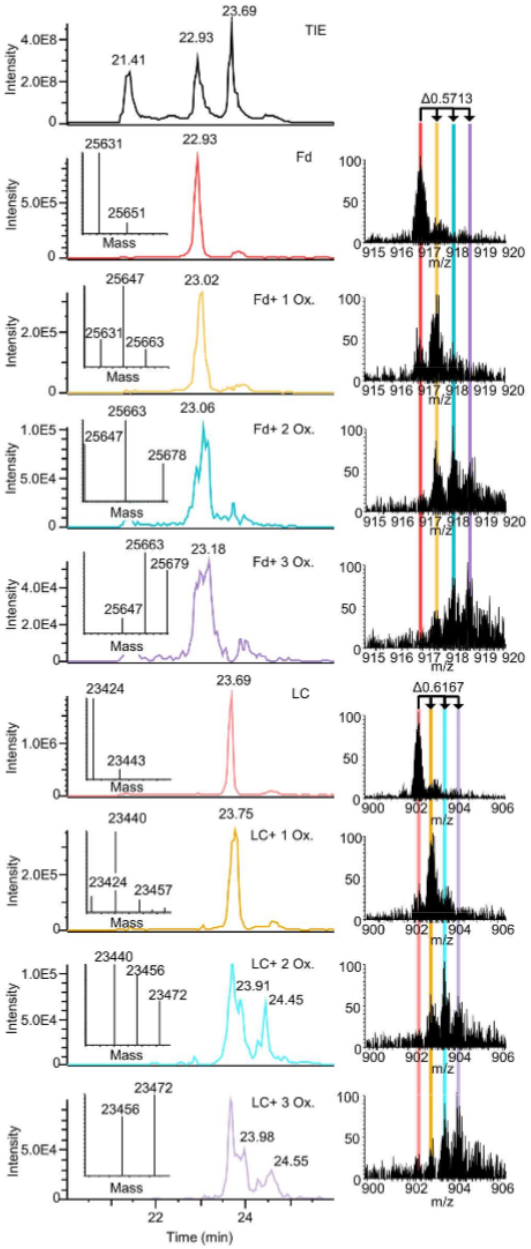

Fig. 4. EIEs, deconvoluted mass spectra (left), and MS spectra (right) of different oxidation species for Fd and LC of mAb3. Deconvoluted MS spectra show the 16 Da mass difference between the oxidation species. MS spectra at peak maximum of Fd (z=28) and LC (z=26) Separation conditions as in Fig. 1.

caused by another variant or isotopic distribution. Nevertheless, the interpretation of these second doubly and triply oxidized species peaks remains open.

Similar to mAb3, different oxidized species are separated for eight mAbs. The detected masses and the EIEs for the detected oxidation of

Table 1
Relative amount of oxidation variants relative to its respective subunit main form (n=3).

Subunit	Relative amount [%]	Standard deviation [%]
LC		
LC + 1 Oxidation	16.62	6.16
LC + 2 Oxidation (23.91 min)	4.13	1.65
LC + 3 Oxidation (23.98 min)	1.86	1.40
LC + 2 Oxidation (24.45 min)	3.64	1.26
LC + 3 Oxidation (24.55 min)	1.41	0.12
Fd		
Fd + 1 Oxidation	34.45	5.50
Fd + 2 Oxidation	8.98	4.21
Fd + 3 Oxidation	4.91	2.75

each mAb can be found in supplementary material S2-S11.

3.6. PyroGlu and succinimide

Mass differences of −17 Da or −18 Da are often detected. At least one subunit of each mAb provided such a mass shift. In most cases, this detected proteoform is not separated from its main form. E.g. in supplementary material S3 the mass shift was detected for LC and Fd of mAb1 but the migration times of these proteoforms did not differ.

Besides these unseparated variants, there are other variants where the migration time is slower indicating an acidic variant in the applied CE system. Based on the sequence Fd of mAb2 has a monoisotopic mass of 26041 Da which was not detected. Instead, a mass of 26024 Da (22.65 min) was deconvoluted and assigned to the pyroGlu variant of the Fd via MS/MS experiments. mAb2 contains a Q at the N-terminus of Fd and the detected −17 Da loss in mass is due to the loss of the N-terminal amine in the form of ammonia. An acidic migration time shift of Fd pyroGlu compared to Fd can not be described due to the absence of the Fd subunit. In contrast, mAb5 showed a separation of Fd and Fd pyroGlu migrating at 21.55 min and 22.03 min respectively (see supplementary material S8). Here the acidic Fd pyroGlu from Q is indeed migrating around 0.5 min later compared to the Fd subunit.

Shifts in migration time towards faster values and therefore basic variants were detected several times. Especially mAb2 showed these shifts (see Fig. 5).

The LC of mAb2 has a sequence-based theoretical mass of 23,548 Da.

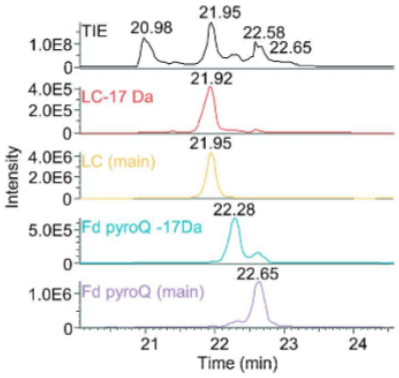

Fig. 5. Exemplary migration behavior of LC and Fd subunits of mAb2 with a 17 Da lower mass compared to the subunit main form. EIEs are generated based on 6 *m/z* values. Separation conditions as in Fig. 1.

This mass was detected at a migration time of 21.95 min. A −17 Da shift in mass (23,531 Da) was detected as a basic variant at 21.92 min, however, this does not fit the pyroGlu formation from E. An N-terminal glutamic acid (E) can transform to pyroglutamic acid, resulting in a water loss and therefore a mass shift of −18 Da [34,35]. Since we can not distinguish the −17 Da and −18 Da mass shift from each other due to the isotopic distribution of the subunits pyroGlu from E and succinimide are both possible modifications. Another basic peak with a −17 Da mass shift was detected on the Fd. From the Fd pyroGlu (26,024 Da) peak at 22.65 min a baseline-separated, basic peak at 22.31 min with an intense, deconvoluted mass of 26,007 Da was detected. This variant is 17 Da lighter and, based on fragmentation results, it seems that succinimide formation on one of the several asparagines in the sequence (based on IMGT unique numbering for C-DOMAIN namely numbers 48, 64, 82, 85, and 92) might have occurred (see supplementary material S13 for detailed information on fragmentation). However, we cannot determine where the modification is located. The detected masses as well as the EIEs of each mAb can be found in supplementary material S2-S12.

3.7. Carbamylation

In peptide mapping approaches, carbamylation is a problem whenever urea is used and has already been discussed in several publications [8,10,11]. Carbamylation results in a loss of positive charges and therefore an acidic variant due to the reaction of cyanate with amines [11]. Carbamylation is identified in the MS by a 43 Da mass shift. Carbamylation has been reported to become a major issue when high urea concentrations are used and the reaction takes place at high temperatures for an extended period of time [10]. To avoid carbamylation in our experiments as much as possible, the reduction was carried out only at 37°C for 1 h. The samples were immediately frozen afterward. Nevertheless, carbamylation was detected based on the deconvoluted mass even though no shift in migration time was detected. mAb1, mAb2, and mAb3 showed masses that were assigned to carbamylation of the LC. It could not be experimentally proved whether this carbamylation is due to the use of urea because urea-free sample preparation is required. As was previously shown in another publication without urea, sample preparation was highly inefficient, and guanidinium hydrochloride, as an alternate chaotropic salt, migrated in the CE system, making the evaluation challenging [27]. Removing any chaotropic salt (urea or guanidinium hydrochloride) would remove the reducing agent DTT potentially leading to disulfide scrambling as shown by Belov et al. [4]

3.8. LC deamidation on high-pH stressed mAb1

Deamidation is one of the most challenging modifications in MS with a mass change of 1 Da. Especially on the intact level, this mass difference can be easily overseen if there is no separation before the MS analysis. The subunit approach in combination with middle-down fragmentation aimed to separate and analyze these deamidated forms. To induce deamidation, mAb1 was pH-stressed for 7 days. After this time, a mass difference on the LC (23,429 Da compared to 23,428 Da) was deconvoluted indicating deamidation. Since EIE generation is impossible for the individual variants, the fragmentation results for each MS/MS experiment in the time window of interest were evaluated and compared to the MS/MS results of non-stressed mAb1. A deamidation close to the N-terminus was more likely based on the fragmentation results. For example, the MS/MS result at 24.12 min provides 10 fragments (b and c ions) for a deamidation closer to the N-terminus (probably at N30) while a deamidation close to the C-terminus (N158 or N210) only provides 3 fragments (y and z ions). With this deamidation location, further evaluation was executed as shown in Fig. 6 (a middled EThcD MS/MS spectrum can be found in supplementary information S14).

The direct comparison of stressed and non-stressed mAb1 in Fig. 6A and Fig. 6B shows that more ions are detected for deamidated LC in the

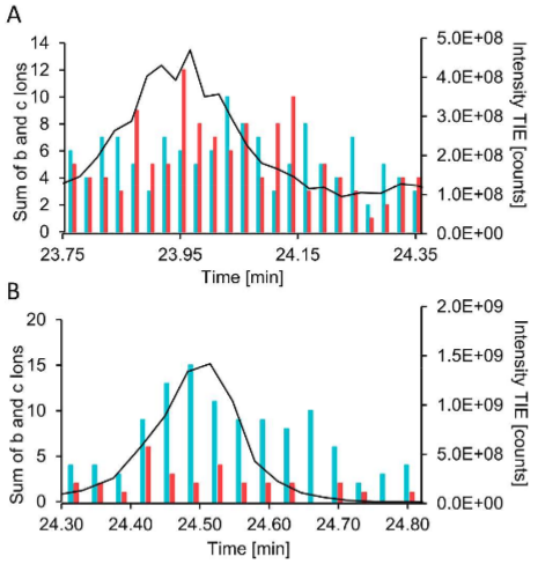

Fig. 6. A) TIE (black line) of LC of high pH stressed mAb1. Columns represent amount of b and c ions indicating LC (blue) or N-terminal deamidation of LC (red) B) Same picture generated for non-stressed mAb1.

stressed sample compared to the non-stressed sample. At certain time points in the stressed sample (Fig. 6A), more fragmentation ions are attributed to the deamidated LC than to the non-modified LC. In comparison to the non-stressed mAb (Fig. 6B) where the LC is the dominant proteoform this result for the stressed mAb strongly suggests deamidation (any single deamidated LC would statistically lead to the same number of fragment ions attributed to deamidated and non-deamidated LC). The whole peak is expected to be a mixture of positional isomers of singly deamidated LC, which contains 20 possible deamidation sites. The shift in migration time towards lower values compared to the unstressed sample is due to the alkaline stress conditions. Nevertheless, middle-down fragmentation might be an alternative tool for the detection of deamidated LC, though further experiments are required here.

3.9. Miscleavages of IdeS and partial reduction

mAb5 showed many signals in the TIE (compare Fig. 1) and the masses for Fc/2 and Fd were not detected at first. Fc/2+G0F showed an increase in mass of 57 Da while Fd showed a loss in mass of 74 Da. The reason for this remained unknown until the consensus sequence was inspected more closely. All mAbs in this study showed the IdeS consensus sequence of CPAPELLG/GPSV. mAb5 had a slightly changed consensus sequence (CPAPELAGAPSV). The two altered amino acids lead to a shifted cleavage site by one amino acid. The G that should remain at the C-terminus of the Fd subunit was located at the N-terminus of the Fc/2 subunit. This explained the 57 Da increase in the Fc/2 subunit. The loss of 74 Da on the Fd is the sum of the missing G at the C-terminus and a pyroGlu formation on the N-terminus. This hypothesis was then confirmed with fragmentation experiments.

mAb4 and mAb5 showed a high amount of still unreduced and partly reduced species. Subunit reduction has already been discussed elsewhere [27]. It remains unknown why large amounts of unreduced species are present even though all mAbs are IgG1. Nevertheless, these species can be separated using this CE method and are identified using MS and MS/MS.

3.10. Other intense but unassigned proteoforms

So far, specific charge variants have been searched and analyzed (compare supplementary information S1). However, independent of the strict criteria mentioned in the method section, several deconvoluted masses that were not assigned to a variant remain. Between 12 (Infliximab) and 40 (mAb1), deconvoluted masses for each mAb remain unassigned to a proteoform (compare Table 2).

These possible proteoforms show a signal intensity above 30,000 counts and have a minimum of 5 charge states in consecutive order. E.g. a very prominent but unassigned mass is 26,043 Da on mAb2 migrating with the Fd pyroGlu. The Fd pyroGlu has a mass of 26,023 Da creating an unexplainable mass shift of +20 Da. Additionally, there were increases in mass that were detected for some subunit moieties but could not be assigned to any proteoform of the respective subunit. There are further deconvoluted masses that passed the evaluation criteria but could not be assigned to any subunit moiety. These masses could be possible fragments of the subunit moieties like losses of amino acids or the sum of several proteoforms on one subunit that were not included in the evaluation process. Overall, Table 2 shows that many variants were detected for the different mAbs with relatively little effort. Since the evaluation of these data was done manually with individually summed time slices, the actual number can be even higher.

4. Conclusion

In conclusion, the presented CE-MS/MS method can be used as a fast analysis method to determine mAb variants. The separation of the subunit moieties was possible for all mAbs tested except NIST and cetuximab. Variants such as C-terminal lysine, glycosylation, glycation, pyroGlu, or oxidation can be separated or partly separated from their main form. Even if the deamidation was not separated from the main form the MS/MS experiments indicated the presence of this variant in the sample. Additionally, the method was able to determine incomplete sample reduction as well as enzymatic miscleavage due to a changed sequence of the mAb in the IdeS cleavage site. With only injecting ng of sample we were able to determine proteoforms with a relative intensity below 0.5 % compared to their respective main variant. In contrast to peptide level approaches, our CE-MS subunit method enables the characterization of proteoforms with several differently exhibited modifications as shown here in several examples.

Overall, the presented setup proves that no extensive equipment or software is needed for variant analysis and that the analysis can be done without much sample preparation. This generic multiattribute method is applicable for several mAbs without individual adjustments for each mAb. In the case of a more detailed MS/MS analysis, fragmentation parameters can of course be adjusted for each mAb and subunit

Table 2
Overview of identified and other possible proteoforms of each mAb.

mAb	Identified proteoform	Other possible proteoform
mAb1	27	40
mAb1 high pH stress	26	25
mAb2	14	14
mAb3	18	22
mAb4	26 (including incomplete reduction)	20
mAb5	25 (including incomplete reduction)	18
USP mAb003	15	20
NIST	16	16
Infliximab (Evidentic)	12	12
Cetuximab (Evidentic)	15 (including incomplete reduction)	28

individually. However, the general settings used here can already be used to locate the variant of the proteoform.

Funding sources

Publication funded by Aalen University of Applied Sciences

CRediT authorship contribution statement

Jasmin Schairer: Writing – original draft, Methodology, Investigation, Data curation, Conceptualization, Formal analysis, Visualization. **Jennifer Römer:** Writing – review & editing, Supervision, Project administration, Resources. **Christian Neusüß:** Writing – review & editing, Supervision, Project administration.

Declaration of Competing Interest

The authors declare that they have no known competing financial interests or personal relationships that could have appeared to influence the work reported in this paper.

Data Availability

The data that support the findings of this study are available from the corresponding author, [CN], upon reasonable request.

Acknowledgments

The authors thank Rentschler Biopharma SE for financial support and for providing samples.

Appendix A. Supporting information

Supplementary data associated with this article can be found in the online version at doi:10.1016/j.jpba.2024.116495.

References

[1] G. Walsh, E. Walsh, Biopharmaceutical benchmarks 2022, Nat. Biotechnol. 40 (2022) 1722–1760, https://doi.org/10.1038/s41587-022-01582-x.

[2] A. Beck, H. Liu, Macro- and micro-heterogeneity of natural and recombinant IgG antibodies, Antibodies 8 (2019), https://doi.org/10.3390/antib8010018.

[3] L. Naumann, P. Schlossbauer, F. Klingler, F. Hesse, K. Otte, C. Neusüß, High-throughput glycosylation analysis of intact monoclonal antibodies by mass spectrometry coupled with capillary electrophoresis and liquid chromatography, J. Sep Sci. 45 (2022) 2034–2044, https://doi.org/10.1002/jssc.202100865.

[4] A.M. Belov, L. Zang, R. Sebastiano, M.R. Santos, D.R. Bush, B.L. Karger, et al., Complementary middle-down and intact monoclonal antibody proteoform characterization by capillary zone electrophoresis – mass spectrometry, Electrophoresis 39 (2018) 2069–2082, https://doi.org/10.1002/elps.201800067.

[5] L. Wang, D.D.Y. Chen, Analysis of four therapeutic monoclonal antibodies by online capillary isoelectric focusing directly coupled to quadrupole time-of-flight mass spectrometry, Electrophoresis 40 (2019) 2899–2907, https://doi.org/10.1002/elps.201900195.

[6] B.L. Duivelshof, A. Beck, D. Guillarme, V. D'Atri, Bispecific antibody characterization by a combination of intact and site-specific/chain-specific LC/MS techniques, Talanta 236 (2022) 122836, https://doi.org/10.1016/j.talanta.2021.122836.

[7] F. Ma, F. Raoufi, Bailly MA, L. Fayadat-Dilman, D. Tomazela, Hyphenation of strong cation exchange chromatography to native mass spectrometry for high throughput online characterization of charge heterogeneity of therapeutic monoclonal antibodies, mAbs 12 (2020) 1763762, https://doi.org/10.1080/19420862.2020.1763762.

[8] L.W. Dick, D. Mahon, D. Qiu, K.-C. Cheng, Peptide mapping of therapeutic monoclonal antibodies: improvements for increased speed and fewer artifacts, J. Chromatogr. B 877 (2009) 230–236, https://doi.org/10.1016/j.jchromb.2008.12.009.

[9] T. Mouchahoir, J.E. Schiel, Development of an LC-MS/MS peptide mapping protocol for the NISTmAb, Anal. Bioanal. Chem. 410 (2018) 2111–2126, https://doi.org/10.1007/s00216-018-0848-6.

[10] L. Kollipara, R.P. Zahedi, Protein carbamylation: in vivo modification or in vitro artefact? Proteomics 13 (2013) 941–944, https://doi.org/10.1002/pmic.201200452.

[11] J. Lippincott, I. Apostol, Carbamylation of cysteine: a potential artifact in peptide mapping of hemoglobins in the presence of urea, Anal. Biochem 267 (1999) 57–64, https://doi.org/10.1006/abio.1998.2970.

[12] Y. An, Y. Zhang, H.-M. Mueller, M. Shameem, X. Chen, A new tool for monoclonal antibody analysis: application of IdeS proteolysis in IgG domain-specific characterization, mAbs 6 (2014) 879–893, https://doi.org/10.4161/mabs.28762.

[13] C. Regl, T. Wohlschlager, J. Holzmann, C.G. Huber, A generic HPLC method for absolute quantification of oxidation in monoclonal antibodies and Fc-fusion proteins using UV and MS detection, Anal. Chem. 89 (2017) 8391–8398, https://doi.org/10.1021/acs.analchem.7b01755.

[14] T. Liu, H. Guo, L. Zhu, Y. Zheng, J. Xu, Q. Guo, et al., Fast characterization of Fc-containing proteins by middle-down mass spectrometry following IdeS digestion, Chromatographia 79 (2016) 1491–1505, https://doi.org/10.1007/s10337-016-3173-2.

[15] V. Faid, Y. Leblanc, N. Bihoreau, G. Chevreux, Middle-up analysis of monoclonal antibodies after combined IgdE and IdeS hinge proteolysis: Investigation of free sulfhydryls, J. Pharm. Biomed. Anal. 149 (2018) 541–546, https://doi.org/10.1016/j.jpba.2017.11.046.

[16] G. Mazzoccanti, G. Pierri, A. Ciogli, O.H. Ismail, F. Giorgi, R. de Santis, et al., Stepwise "bridge-to-bridge" reduction of monoclonal antibodies and light chain detection: Case studies of tenatumomab and trastuzumab, Sep. Sci. 1 (2018) 261–269, https://doi.org/10.1002/sscp.201800002.

[17] M. Cejkov, T. Greer, R.O.'B. Johnson, X. Zheng, N. Li, Electron Transfer dissociation parameter optimization using design of experiments increases sequence coverage of monoclonal antibodies, J. Am. Soc. Mass Spectrom. 32 (2021) 762–771, https://doi.org/10.1021/jasms.0c00458.

[18] V. D'Atri, S. Fekete, A. Beck, M. Lauber, D. Guillarme, Hydrophilic interaction chromatography hyphenated with mass spectrometry: a powerful analytical tool for the comparison of originator and biosimilar therapeutic monoclonal antibodies at the middle-up level of analysis, Anal. Chem. 89 (2017) 2086–2092, https://doi.org/10.1021/acs.analchem.6b04726.

[19] Y. Leblanc, V. Faid, M.A. Lauber, Q. Wang, N. Bihoreau, G. Chevreux, A generic method for intact and subunit level characterization of mAb charge variants by native mass spectrometry, J. Chromatogr. B 1133 (2019) 121814, https://doi.org/10.1016/j.jchromb.2019.121814.

[20] J. Dai, Y. Zhang, A middle-up approach with online capillary isoelectric focusing/mass spectrometry for in-depth characterization of cetuximab charge heterogeneity, Anal. Chem. 90 (2018) 14527–14534, https://doi.org/10.1021/acs.analchem.8b04396.

[21] Y.-N. François, M. Biacchi, N. Said, C. Renard, A. Beck, R. Gahoual, et al., Characterization of cetuximab Fc/2 dimers by off-line CZE-MS, Anal. Chim. Acta 908 (2016) 168–176, https://doi.org/10.1016/j.aca.2015.12.033.

[22] J. Giorgetti, A. Beck, E. Leize-Wagner, Y.-N. François, Combination of intact, middle-up and bottom-up levels to characterize 7 therapeutic monoclonal antibodies by capillary electrophoresis - Mass spectrometry, J. Pharm. Biomed. Anal. 182 (2020) 113107, https://doi.org/10.1016/j.jpba.2020.113107.

[23] C. Gstöttner, S. Nicolardi, M. Haberger, D. Reusch, M. Wuhrer, E. Domínguez-Vega, Intact and subunit-specific analysis of bispecific antibodies by sheathless CE-MS, Anal. Chim. Acta 1134 (2020) 18–27, https://doi.org/10.1016/j.aca.2020.07.069.

[24] Haselberg, R. Vijlder, T. de, R. Heukers, M.J. Smit, E.P. Romijn, G.W. Somsen, et al., Heterogeneity assessment of antibody-derived therapeutics at the intact and middle-up level by low-flow sheathless capillary electrophoresis-mass spectrometry, Anal. Chim. Acta 1044 (2018) 181–190, https://doi.org/10.1016/j.aca.2018.08.024.

[25] M. Li, X. Zhao, D. Shen, G. Wu, W. Wang, C. Yu, et al., Identification of a monoclonal antibody clipping variant by cross-validation using capillary electrophoresis – sodium dodecyl sulfate, capillary zone electrophoresis – mass spectrometry and capillary isoelectric focusing – mass spectrometry, J. Chromatogr. A 1684 (2022) 463560, https://doi.org/10.1016/j.chroma.2022.463560.

[26] Seth Madren, Linda Yi, Microchip electrophoresis separation coupled to mass spectrometry (MCE–MS) for the rapid monitoring of multiple quality attributes of monoclonal antibodies, Electrophoresis 43 (2022) 2453–2465, https://doi.org/10.1002/elps.202200129.

[27] J. Schairer, J. Römer, D. Lang, C. Neusüß, CE-MS/MS and CE-timsTOF to separate and characterize intramolecular disulfide bridges of monoclonal antibody subunits and their application for the assessment of subunit reduction protocols, Anal. Bioanal. Chem. 416 (2024) 1599–1612, https://doi.org/10.1007/s00216-024-05161-8.

[28] J. Schlecht, A. Stolz, A. Hofmann, L. Gerstung, C. Neusüß, nanoCEasy: an easy, flexible, and robust nanoflow sheath liquid capillary electrophoresis-mass spectrometry interface Based on 3D printed parts, Anal. Chem. 93 (2021) 14593–14598, https://doi.org/10.1021/acs.analchem.1c03213.

[29] L. Liu, Antibody glycosylation and its impact on the pharmacokinetics and pharmacodynamics of monoclonal antibodies and Fc-fusion proteins, J. Pharm. Sci. 104 (2015) 1866–1884, https://doi.org/10.1002/jps.24444.

[30] W. Li, J.L. Kerwin, J. Schiel, T. Formolo, D. Davis, A. Mahan, et al., Structural Elucidation of Post-Translational Modifications in Monoclonal Antibodies, in: J. E. Schiel, D.L. Davis, O. Borisov (Eds.), State-of-the-art and emerging technologies for therapeutic monoclonal antibody characterization, American Chemical Society, Washington DC, 2014, pp. 119–183.

[31] K. Srzentić, L. Fornelli, Y.O. Tsybin, J.A. Loo, H. Seckler, J.N. Agar, et al., Interlaboratory study for characterizing monoclonal antibodies by top-down and middle-down mass spectrometry, J. Am. Soc. Mass Spectrom. 31 (2020) 1783–1802, https://doi.org/10.1021/jasms.0c00036.

[32] L.W. Dick, D. Qiu, D. Mahon, M. Adamo, K.-C. Cheng, C-terminal lysine variants in fully human monoclonal antibodies: investigation of test methods and possible causes, Biotechnol. Bioeng. 100 (2008) 1132–1143, https://doi.org/10.1002/bit.21855.
[33] Y. Li, A. Polozova, F. Gruia, J. Feng, Characterization of the degradation products of a color-changed monoclonal antibody: tryptophan-derived chromophores, Anal. Chem. 86 (2014) 6850–6857, https://doi.org/10.1021/ac404218t.
[34] D. Chelius, K. Jing, A. Lueras, D.S. Rehder, T.M. Dillon, A. Vizel, et al., Formation of pyroglutamic acid from N-terminal glutamic acid in immunoglobulin gamma antibodies, Anal. Chem. 78 (2006) 2370–2376, https://doi.org/10.1021/ac051827k.
[35] Z. Liu, J. Valente, S. Lin, N. Chennamsetty, D. Qiu, M. Bolgar, Cyclization of N-terminal glutamic acid to pyro-glutamic acid impacts monoclonal antibody charge heterogeneity despite its appearance as a neutral transformation, J. Pharm. Sci. 108 (2019) 3194–3200, https://doi.org/10.1016/j.xphs.2019.05.023.

Manuscript IV

Ion-exchange chromatography, capillary isoelectric focusing, and capillary zone electrophoresis coupled to mass spectrometry for charge variant analysis of monoclonal antibodies

Jasmin Schairer, Alisa Höchsmann, Benedikt Bauer, Volker Höfer, Jennifer Römer, Christian Neusüß

mAbs. 2025; 17: 2537116. DOI: 10.1080/19420862.2025.2537116

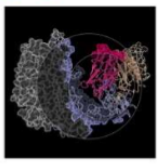

mAbs

ISSN: 1942-0862 (Print) 1942-0870 (Online) Journal homepage: www.tandfonline.com/journals/kmab20

Ion-exchange chromatography, capillary isoelectric focusing, and capillary zone electrophoresis coupled to mass spectrometry for charge variant analysis of monoclonal antibodies

Jasmin Schairer, Alisa Höchsmann, Benedikt Bauer, Volker Höfer, Jennifer Römer & Christian Neusüß

To cite this article: Jasmin Schairer, Alisa Höchsmann, Benedikt Bauer, Volker Höfer, Jennifer Römer & Christian Neusüß (2025) Ion-exchange chromatography, capillary isoelectric focusing, and capillary zone electrophoresis coupled to mass spectrometry for charge variant analysis of monoclonal antibodies, mAbs, 17:1, 2537116, DOI: 10.1080/19420862.2025.2537116

To link to this article: https://doi.org/10.1080/19420862.2025.2537116

MABS
2025, VOL. 17, NO. 1, 2537116
https://doi.org/10.1080/19420862.2025.2537116

Taylor & Francis
Taylor & Francis Group

REPORT

OPEN ACCESS Check for updates

Ion-exchange chromatography, capillary isoelectric focusing, and capillary zone electrophoresis coupled to mass spectrometry for charge variant analysis of monoclonal antibodies

Jasmin Schairer[a,b], Alisa Höchsmann[a,b], Benedikt Bauer[a], Volker Höfer[a], Jennifer Römer[c], and Christian Neusüß[a]

[a]Faculty of Chemistry, Aalen University, Aalen, Germany; [b]Faculty of Science, University of Tübingen, Tübingen, Germany; [c]Rentschler Biopharma SE, Laupheim, Germany

ABSTRACT

Monoclonal antibody (mAb) charge variant analysis, which ensures the quality of biopharmaceuticals, is primarily performed by either cation exchange chromatography (CEX), capillary isoelectric focusing (CIEF), or capillary zone electrophoresis (CZE). Though selectivity is different for all methods, mAb proteoforms can be quantified on the intact level with a low risk of artifacts. Identification and characterization can be performed by mass spectrometry (MS), but coupling is hampered by the use of non-volatile constituents. Here, we present comparative data and a thorough review of CEX-MS, CIEF-MS, and CZE-MS for the analysis of charge variants on the intact level. The separation of the proteoforms is confirmed by online UV detection with subsequent online MS coupling. Each method was tested for generic use by measuring 10 mAbs with an isoelectric point (pI) of 7.3 to 8.7 without individually adjusting the method parameters for each mAb. The methods and the identified proteoforms are compared among each other as well as to a previously published CZE-MS method on the subunit level. The lysine variant was used to compare the resolution of the different separation methods and showed a high resolving power for all separation methods tested. The different method selectivities were revealed by the monoglycosylation, which was found in the peak of the main variant with CEX and CIEF, while it was separated from the main peak with CZE. In combination with a comprehensive literature review, our results provide a complete overview of the current state of the methods with information on the advantages and limitations of each methodology.

ARTICLE HISTORY
Received 22 May 2025
Revised 12 July 2025
Accepted 16 July 2025

KEYWORDS
Charge heterogeneity; direct MS coupling; generic methods; intact mab analysis; subunit mab analysis

Introduction

Monoclonal antibody (mAb) variants are critical quality attributes that must be analyzed to ensure the stability and safety of biopharmaceuticals. Given the increasing number of mAbs that are approved as therapeutics each year,[1] methods have been developed to address the challenges of mAb variant characterization. Antibody variants are post-translational modifications that are introduced during the production, purification, or storage of the mAb. These modifications often change the mass, the charge, and the isoelectric point (pI) of the mAb, which makes them accessible to analytical techniques that use these characteristics for separation, such as cation exchange chromatography (CEX), capillary zone electrophoresis (CZE), or capillary isoelectric focusing (CIEF). Currently, mAb variant identification is commonly done using mass spectrometry (MS). MS allows the identification of variants by detecting mass differences between modified and unmodified species. For large mass differences and highly abundant proteoforms (like the main mAb glycosylation forms,[2] MS can distinguish these species without any proteoform preseparation. Low abundant proteoforms and/or proteoforms with small mass differences, however, are more challenging to characterize using MS. As large molecules (~150 kDa), mAbs have broad isotopic distributions (with a full peak width at half maximum of around 24 Da), which requires separation for detection of proteoforms with a smaller mass difference.

CONTACT Christian Neusüß christian.neusuess@hs-aalen.de Faculty of Chemistry, Aalen University, Beethovenstraße 1, Aalen 73430, Germany

Supplemental data for this article can be accessed online at https://doi.org/10.1080/19420862.2025.2537116

MAbs and mAb variants are positively charged at a pH below their pI value, which makes them accessible for CEX separation. The analysis can also be performed using anion exchange chromatography, but CEX is commonly used due to the more efficient ionization in subsequent electrospray ionization (ESI) in positive mode and the generally basic pI value for most mAbs. CEX-UV separation systems often use MS-incompatible salts or buffers (e.g., sodium hydrochloride or 2-(N-morpholino) ethane sulfonic acid (MES)).[3,4] For MS coupling, ammonium acetate, and ammonium formate-based eluents, which provide good variant separation and identification of mAb variants, are typically used.[5–7] CEX-UV and CEX-MS methods have a limited generic application due to the different pIs of different mAbs in combination with the pH and ionic strength of the buffer system. Thus, individual method optimizations for each mAb can improve the separation significantly.[8] An ideally linear or at least precisely controlled pH gradient is highly desired to achieve reproducible and high-resolution separations. This can be easily achieved by involatile buffer components,[9–11] but, for MS-compatible ammonium acetate, the pH response as a function of the base content is not linear[3,12] and column-dependent.[12] A method well suited for the separation of mAb variants of one mAb might therefore not be suitable/ideal for another mAb with a different pI value. CEX-MS can be performed with standard LC-MS equipment, but the nanoESI conditions and harsh transfer parameters in MS are required to decluster the ammonia adducts and a high m/z range is needed due to native-like ESI conditions.

The different pI values of mAb variants enable separation by CIEF. CIEF, in particular imaged CIEF (iCIEF), is increasingly used for charge variant analysis of mAbs for quality control and batch release.[13–15] If not specifically stated otherwise, CIEF covers CIEF and iCIEF and both techniques are very well established using UV detection. However, generic CIEF-UV methods contain MS-incompatible substances such as ampholytes, methylcellulose, urea, or sodium hydroxide, which is why CIEF has rarely been coupled with MS until recently.[16–18] CIEF-MS coupling is only possible if MS interfering components are removed or substituted to the greatest possible extent and when focusing and ionization can still be done with the capillary outlet installed in the MS interface.[19,20] Designated commercially available CIEF-MS systems for fast, reliable, and robust mAb variant analysis have been introduced recently.[21,22] Nevertheless, the separation from focusing is generally reduced or even lost by the necessary mobilization process to transport the focused proteoforms to the MS.[19,23] Even chip-based systems, which have short separation canals, suffer from peak broadening during mobilization[22,24]

CZE separates mAb variants based on their charge and size in the liquid phase. This principle has been applied to separate mAb variants, typically with a CZE-UV-based system using 6-aminocaproic acid (EACA), triethylenetetramine (TETA), and hydroxypropyl cellulose (HPC) as first published by He et al.[25] This generic and widespread method was evaluated in an intercompany study using 23 mAb samples with a pI between 7.4 and 9.5.[26] However, as previously mentioned for CEX and CIEF, many CZE-UV methods, including the EACA-UV method, cannot be coupled to MS due to incompatible substances like dynamic coating agents or polymers.[27–29] MS-compatible CZE methods either use native (ammonium acetate-based) or denatured (acetic or formic acid-based) separation systems.[30,31] Commercially available native microchip-based systems provide very good mAb variant separation using native-like separation conditions,[28,32,33] but these systems can suffer from reduced signal intensities and often lack flexibility, similar to CEX-MS methods.

In many studies and applications, one single technology is used. Thus, their performance with respect to resolution, sensitivity, instrumental aspects, and handling issues is difficult to evaluate. In this study, we present data and review the literature for CEX-MS, CIEF-MS, and CZE-MS methods for mAb variant separation on the intact level to evaluate their analytical performance along with practical concerns. Ten mAb samples covering a pI range from 7.3 to 8.7 were analyzed regarding acidic (A) and basic (B) proteoforms by CEX-MS, CIEF-MS, and CZE-MS with one generic method for each technique. Additionally, variant separation was online UV monitored, which proved to be a valuable tool for further method evaluation. The results for each method are discussed individually, compared to the other techniques, and put into perspective with results from the literature. The results from the intact analysis were also compared to a CZE-MS method on the subunit level.[34,35]

Results

Intact mAb variant analysis was executed with all three separation techniques, CEX-MS, CIEF-MS, and CZE-MS, as mentioned in the method section. All mentioned proteoforms in this section are shown in the supplementary Table S2-S4 sorted by method and mAb.

CEX-UV-MS for mAb variant analysis

The initial eluents for the CEX-UV-based separation, 50 mM ammonium acetate + 2% acetonitrile (ACN) pH 5.0 as eluent A and 160 mM ammonium acetate + 2% ACN pH 8.5 as eluent B, are based on the report by Murisier et al.[12] Here, a linear gradient from 10% [B] to 80% [B] over 13 min with a flow rate of 0.3 mL/min and a detection wavelength of 280 nm was utilized. As shown by the blue line in supplementary Figure S1, a slight separation of acidic and basic species was achieved for mAb1, but an improvement of the separation of acidic and basic variants from the main form was attempted. Therefore, eluent B starting conditions were successively increased (compare supplementary Figure S1), which resulted in resolved acidic and basic variants, but also massive peak broadening if values above 55% B were used as a starting condition. For MS coupling, the amount of ammonium acetate in eluent B was decreased to 100 mM, resulting in later elution and a decreased separation efficiency (compare Figure 1a). The method length was therefore increased to 40 min after reducing the flow rate to 0.1 mL/min, and the gradient was adapted to the prolonged analysis time rising linearly after a 2 min hold at 55% [B] to 85% [B] over 25 min. The final gradient resulted in baseline-separated acidic and basic peaks, respectively, as shown in Figure 1b.

After UV-based gradient optimization, we coupled the method to the MS (including online UV detection) and measured all 10 mAb samples (2 mg/mL). The online UV chromatograms, the extracted ion chromatograms (EICs, m/z: 4500–6500), and the deconvoluted masses of the main peak are shown in Figure 2. All mAbs show retention on the column and therefore variant separation no matter their respective pI values. All mAbs contain basic proteoforms, which elute later than the main peak, and acidic proteoforms, which elute earlier than the main peak. Even for highly retained mAbs like NIST mAb and mAb2 (pI 8.6 and 8.7, respectively) acidic and basic variants are separated. The method is expected to be generic for the tested pI range (pI: 7.3–8.7). Comparing the resolution (R) for mAbs with at least one lysine variant, we calculated values between the main variant (M) and the basic variant (B1) of $R = 0.85$ for USPmAb003, $R = 1.38$ for NIST mAb, and $R = 2.66$ for infliximab. The separation is maintained toward the MS, which is evident when comparing the UV and MS data in Figure 2, with average extracted ion electropherogram (EIE) signal intensities in the 5E5 range. mAbs with high heterogeneities (cetuximab and pH-stressed mAb1) are challenging since signal intensities are decreased by the heterogeneity when the

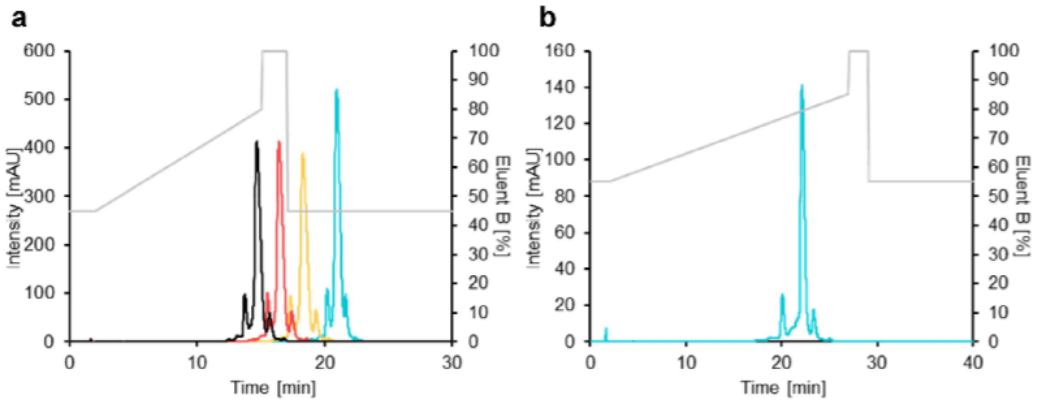

Figure 1. Method development (combined salt and pH gradient) using 55%B starting conditions for charge variant separation of mAb1. a: reduction of ammonium acetate in eluent B from 160 mM to 100 mM. Black: 160 mM, red: 140 mM, orange: 120 mM, blue: 100 mM, the gradient is shown as a gray line. b: mAb1 variant separation using a final gradient (gray line) with 100 mM ammonium acetate in eluent B, a flow rate of 0.1 mL/min, and an adapted gradient for a 40-minute run time.

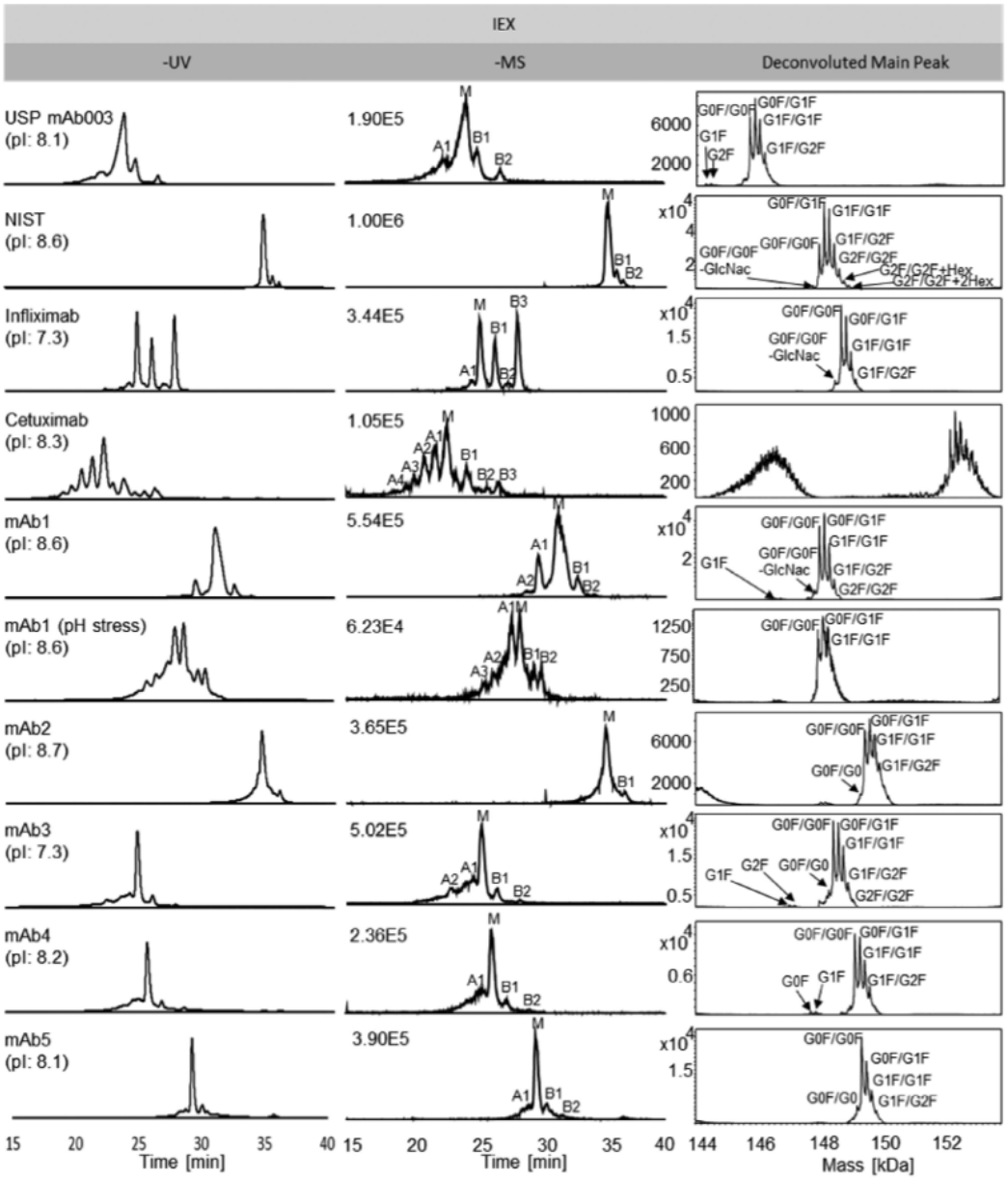

Figure 2. CEX-UV-MS separation and identification of 10 mAb samples all measured on the Bruker MaXis TOF instrument. Left column: online UV traces (214 nm); middle column: extracted ion chromatograms (EICs, 4500–6500 m/z); right column: deconvoluted mass spectrum of the main form. A: acidic variant, M: main variant, B: basic variant.

same concentration of mAb is used for all mAb samples. The generally low spectral quality is also a challenge for all detected acidic or basic species, especially if they are of low abundance. A +2 Da mass shift was detected only for mAb1, with its prominent acidic variant (A1). For all other, low abundant acidic peaks, no statistically significant mass shift was observed. Nevertheless, the method can be used to gain mAb information. After the deconvolution of the main peak (compare right column in Figure 2), the glycosylation pattern was analyzed and intense glycoforms (G0F/G0F, G0F/G1F, G1F/G1F) were annotated for all mAbs. There is a slight separation depending on size between the different glycosylation patterns and mAbs with smaller glycans elute slightly later than mAbs with larger glycans (compare supplementary Figure S2). In addition to that, for some mAbs, even minor glycoforms like G0F/G0F-GlcNAc, G0F/G0, or G2F/G2F +Hex (possible glycation of NISTmAb) were detected (compare right column in Figure 2).

Monoglycosylated antibodies were also detected in the main form peak for USPmAb003, mAb1, mAb3, and mAb4. Basic proteoforms like the lysine variants could be deconvoluted and assigned for USPmAb003 (B1, B2), NISTmAb (B1, B2), and infliximab (B1, B3).

CIEF-UV-MS for mAb variant analysis

The initial CIEF conditions were taken from Naghdi et al..[20] The master mix for mAb A (pI:8.66) variant separation was composed of 1.25% of Pharmalyte pH 8 – 10.5, 0.62% of Pharmalyte pH 3 – 10, 0.3% of Pharmalyte pH 5 – 8 (total ampholyte concentration of 2.17%), 2.5 mM arginine, 0.5 mM IDA, 30% formamide and 0.5 mg/mL mAb A. CIEF was hyphenated to the MS with the new chemical mobilization methodology for charge variants separation of mAb A, demonstrating the feasibility of the CIEF–ESI-MS.[20] We briefly tested in a UV-based setup whether mAb1 (pI: 8.6) can be separated with the same CIEF system and if reduced concentrations of ampholyte and formamide in the master mix affect mAb1 variant separation. First, the ampholyte concentration in the master mix was reduced from 2.1% to 1%, which resulted in reduced analysis time without losing the separation of the mAb variants significantly (compare supplementary Figure S3A). Following this, the amount of formamide was successively reduced in 5% steps from 30% to 15% without losing the separation of the mAb variants (compare supplementary Figure S3B). Arginine, IDA, and the final sample concentration remained unchanged and used as mentioned by Naghdi et al.[20] at concentrations of 2.5 mM, 0.5 mM, and 0.5 mg/mL respectively. Ampholyte and formamide were used at concentrations of 1% ampholyte and 15% formamide as mentioned above.

This system was coupled to the MS with the nanoCEasy interface, which allowed chemical mobilization within the interface by exchanging the sheath liquid from basic conditions during focusing to acidic conditions for chemical mobilization along with acidic ESI conditions. The system was equipped with an external UV detector to obtain online UV data during mobilization before entering the MS. The method used for mAb1 variant separation was applied to all nine mAb samples (except for stressed mAb1). The online UV results, the MS spectra (m/z: 4500–6500), and the deconvoluted masses for the main peak are shown in Figure 3. For all mAbs, a separation of several acidic and basic variants in the online UV detection (see CIEF-UV column in Figure 3) is obtained, independently from their respective pI values (pI: 7.3–8.7). All mAbs contain basic proteoforms that migrate earlier than the main peak and acidic proteoforms that migrate later than the main peak. For the tested pI range, the method can be seen as generic and MS signal intensities are on average in the 1E6 range (see CIEF-MS column in Figure 3). The resolution (R) for mAbs with at least one lysine variant was calculated based on the UV signal and values between the main variant (M) and the basic variant (B1) of $R = 1.50$ for USPmAb003, $R = 1.27$ for NIST mAb, and $R = 1.68$ for infliximab were obtained. However, while online UV can detect all mAbs, MS detection seems to be highly antibody-dependent. USPmAb003 (pI 8.1), infliximab (pI 7.3), and mAb3 (pI 7.3) were not detected via MS, possibly due to solubility issues. The other mAbs can be detected via MS, but in most cases, separation is lost. The overall glycosylation pattern of G0F/G0F, G0F/G1F, G1F/G1F, G1F/G2F, and G2F/G2F could be detected in the main peak for all mAbs (compare right column in Figure 3). In addition, some minor glycosylation species like G0F/G0, G0F/G0F-GlcNac, and G2F/G2F+Hex (possible glycation of NIST) could be detected for several mAbs, as well as monoglycosylated species of G0F and G1F for mAb1, mAb2, and mAb4. For cetuximab, glycosylation seems to increase for the acidic species (compare supplementary Figure S4). All mAbs show some acidic and basic variants in the UV detector that could not be identified by MS. This indicates that further improvement is needed until the CIEF-MS system is robust regarding handling and can be used universally for a more detailed mAb variant analysis.

CZE-UV and CZE-MS for mAb variant analysis

All 10 mAb samples were analyzed with the CZE-UV method from He et al.[25] that was slightly modified regarding the flushing pressure due to the much longer capillary used in our setup. As shown by the CZE-UV results (Figure 4, left column), all mAbs were analyzed successfully and showed different amounts of variant separation in the 30-minute separation window. All mAbs contain basic proteoforms that migrate earlier and acidic proteoforms that migrate later than the main peak. Some mAbs like infliximab, cetuximab, and stressed mAb1 show very prominent and intense variants while other mAbs like mAb3–5 only

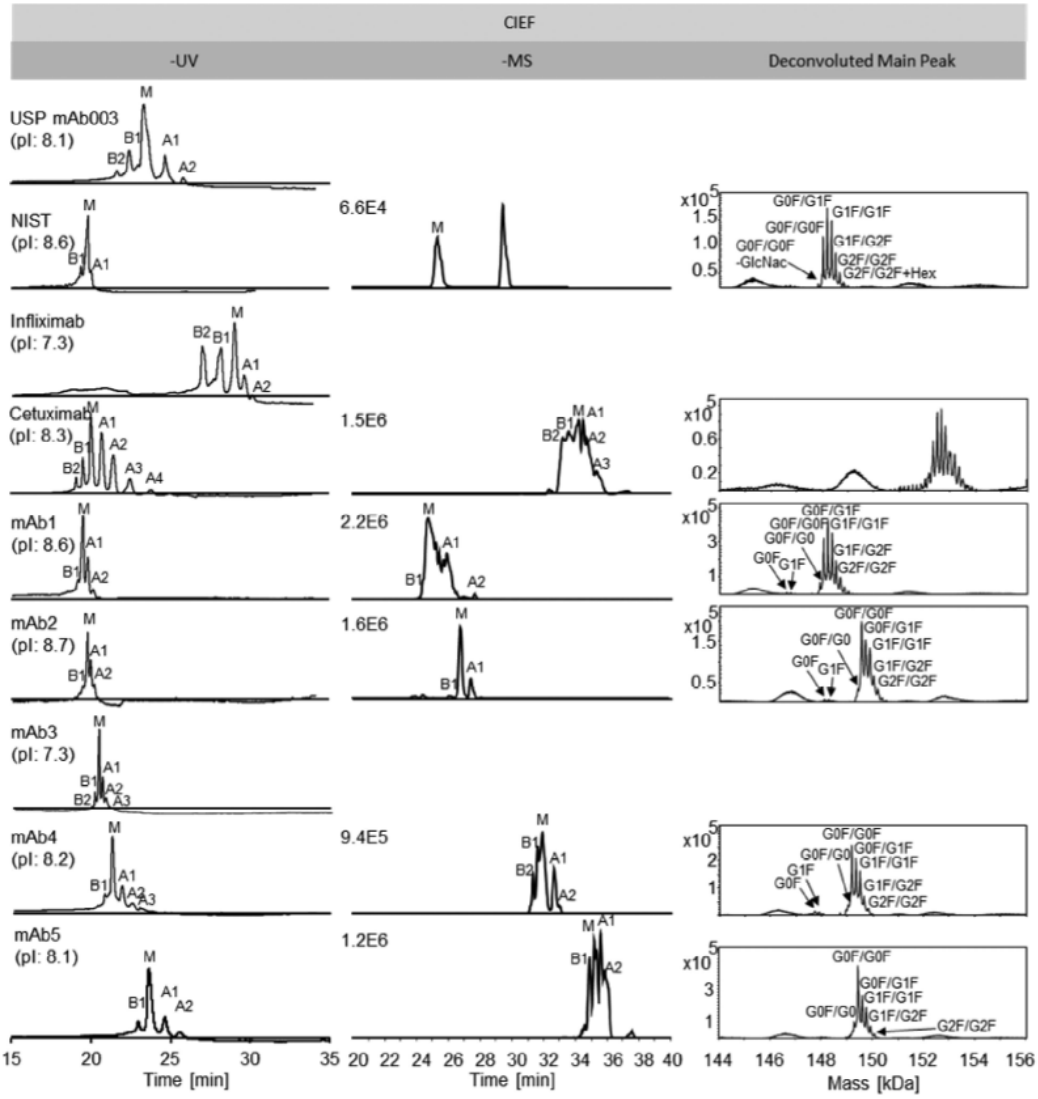

Figure 3. CIEF-UV-MS separation and identification of nine mAb samples all measured on the Bruker MaXis TOF instrument. Left column: online UV traces (280 nm); middle column: extracted ion electropherograms (EIEs, 2000–4000 m/z, smoothed: gaussian 5); right column: deconvoluted mass spectrum of the main form. A: acidic variant, M: main variant, B: basic variant.

show some minor variants. The resolution (R) for mAbs with at least one lysine variant was calculated and values between the main variant (M) and the basic variant (B1) of $R = 5.10$ for USPmAb003, $R = 3.92$ for NIST mAb, and $R = 8.30$ for infliximab were obtained. A slightly longer analysis time might be used for cetuximab, as the separation seems not to be completed after 30 minutes in a 60 cm capillary. The CZE-UV method shows a very good reproducibility regarding mAb1 main variant migration time (18.05 ± 0.11 min, $n = 18$) and is generic regarding variant separation over the tested pI range (pI: 7.3–8.7). However, the background electrolyte (BGE) of the CZE-UV method is not MS-compatible.

CZE-MS method development and optimization were published by Höchsmann et al.[30] and their final method was used here to analyze all 10 mAb samples. The method contains a BGE of 4 M aqueous acetic acid (HAc) and a cationic 5-layer DEAED-PSS successive multiple ionic-polymer layers (SMIL)-coated capillary to generate a reversed electroosmotic flow (EOF) of median velocity. The base peak electropherograms (BPEs, m/z: 2000–4000, smoothed Gaussian 5), and the deconvoluted result of the main peak are shown in Figure 4. As shown by the CZE-MS results in Figure 4, separation of acidic and

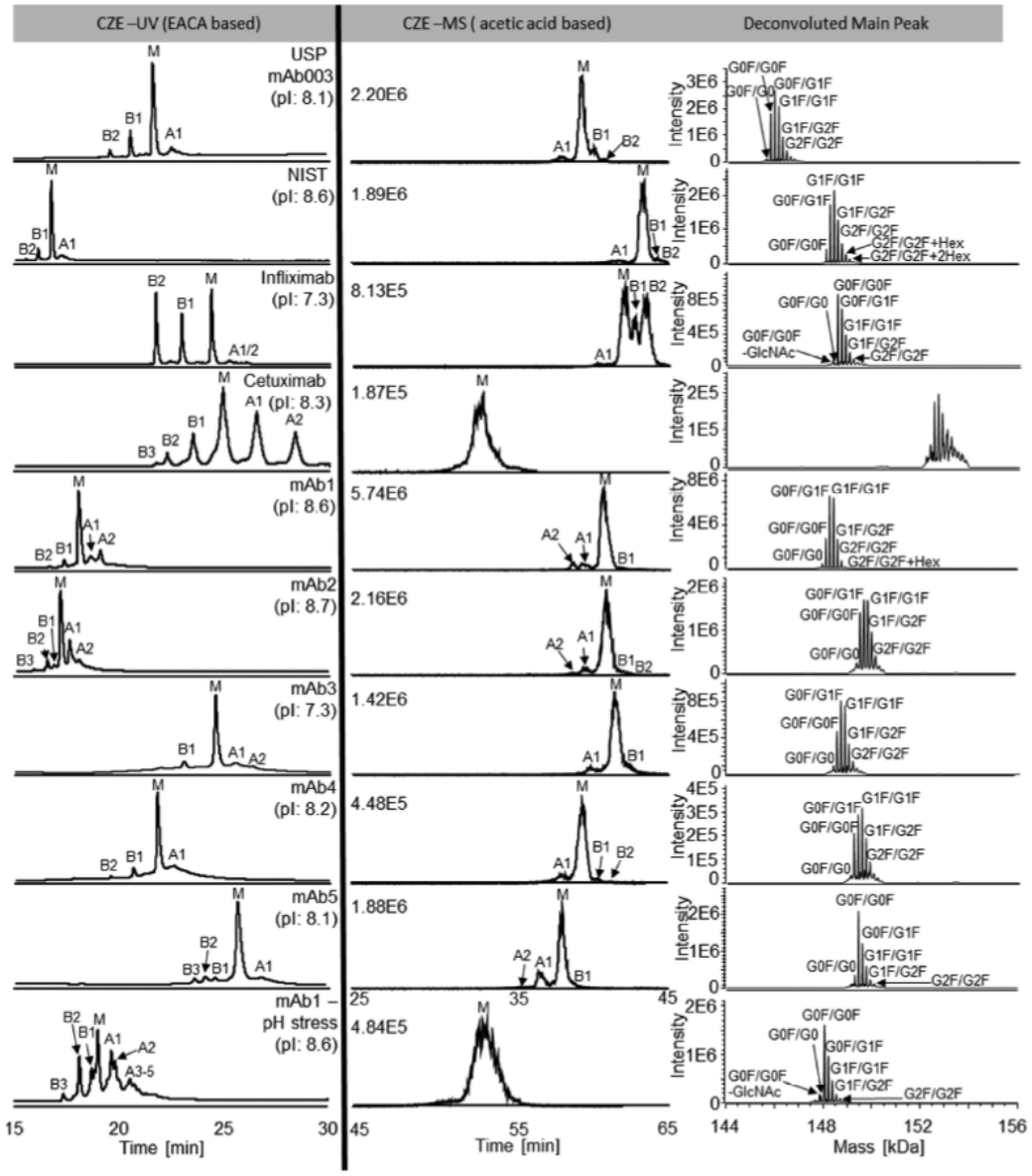

Figure 4. CZE-UV and CZE-MS separation and identification of 10 mAb samples. MS data were acquired using the Orbitrap fusion Lumos. Left column: CZE-UV traces (214 nm); middle column: base peak electropherograms (BPEs, m/z: 2000–4000, smoothed gaussian 5); right column: deconvoluted mass spectrum of the main form. A: acidic variant, M: main variant, B: basic variant.

basic variants can be achieved for eight of the 10 mAb samples with an average signal intensity in the 1E6 range. Compared to the CZE-UV method, in this CZE-MS method, the migration order is reversed, e.g., basic proteoforms are detected later and acidic proteoforms are detected earlier than the main peak. For cetuximab and pH-stressed mAb1, no variant separation is observed due to the increased heterogeneity from the complex glycosylation of cetuximab and the presumably increased amount of deamidation in the high pH-stressed mAb1 sample. Deamidation for pH-stressed mAb1 is assumed since the deconvoluted mass is 2–4 Da larger over the complete signal compared to the main peak of the non-stressed mAb sample (data not shown). Nevertheless, the CZE-MS system still is generic regarding variant separation over the tested pI range (pI: 7.3–8.7) if mAb heterogeneity is not too complex.

The main form of each mAb contains the different glycosylation species (compare the right column in Figure 4). For all eight mAbs, the main glycosylation species G0F/G0F, G0F/G1F, G1F/G1F (or G0F/G2F), G1F/G2F, and G2F/G2F were identified and detailed masses can be found in supplementary table S2-S4. In addition, some mAbs showed minor glycosylation species like G0F/G0, G0F/G0F-GlcNac, and G2F/G2F +Hex (or + 2Hex, possible glycation of NIST mAb and mAb1) that were also detected. The EIEs of the different glycosylation species revealed a small shift in migration time depending on the size of the glycans (data not shown, compare Höchsmann et al..[30] For USPmAb003 (B1 and B2), NIST mAb (B1 and B2), mAb3 (B1), and infliximab (B1 and B2), the later migrating, basic proteoforms were identified as lysine variants (1x and 2x lysine remaining at the mAb; detailed masses can be found in supplementary table S2-S4). The resolution (R) for these mAbs with at least one lysine variant was calculated and values between the main variant (M) and the basic variant (B1) of $R = 1.66$ for USPmAb003, $R = 1.52$ for NIST mAb, and $R = 0.94$ for infliximab were obtained. For mAb1 (B2) and mAb2 (B1), the basic proteoform could be a loss of water or ammonia (detailed masses can be found in supplementary table S2-S4). Additionally, the basic variants of USPmAb003 (B1), NIST mAb (B2), mAb1 (B1), mAb2 (B1), mAb3 (B1), mAb4 (B1), and mAb5 (B1) contain monoglycosylated mAb species. Aglycosylation was determined for mAb2 (B2) and mAb4 (B2). Other later migrating species are presumably mAb fragments (e.g., mAb with loss of a light chain) since they show the characteristic 162 Da pattern specific for glycosylation. These fragments (detailed masses can be found in the supplementary table S2-S4) were detected for USPmAb003 (123 kDa and 101 kDa), mAb2 (148 kDa, 126 kDa, and 103 kDa), mAb3 (125 kDa), mAb4 (126 kDa), and mAb5 (125 kDa).

For USPmAb003 (A1) and mAb1 (A1), earlier migrating, acidic species are mAb proteoforms that carry glycans with sialic acids (detailed masses can be found in the supplementary table S2-S4). Additionally, all eight mAbs showed acidic species with a slight shift toward lower m/z values in the charge envelope distribution compared to the main peak. This shift in m/z value in combination with a deconvoluted mass shift of around 2 Da indicates mAb variants with an open disulfide bridge.

CZE-MS for mAb variant analysis on the subunit level

In addition to all intact approaches, the mAbs were analyzed via CZE-MS (MS/MS) on the subunit level as described elsewhere.[35] For the 10 different mAb samples, different proteoforms like oxidation, glycation, lysin variants, sialic acids, pyroGlu, water or ammonium losses, and aglycosylation were separated and identified (compare supplementary Figure S8). Some of them were not determined on the intact level. Further information regarding the subunit approach and a detailed list of the identified variants of each antibody can be found in our previous publication and supporting information.[35]

Discussion

CEX-UV and CEX-UV-MS for mAb variant analysis

Many systematic studies involving UV detection of CEX-separated mAb variants are available. Generally, three approaches are used to elute proteins from the CEX column: 1) increasing the pH, which reduces the charge of the protein,[11,36,37] 2) adding salts that displace the proteins from the column[4,8,38–40] or 3) a combination of both approaches.[10,12] The individual methods were compared in several studies and both showed good separation of mAb variants.[3,41,42] The composition and pH of the eluents, rather than the method, seem to be more important for proper variant separation. Farsang et al.[3] compared different salt and pH gradients with the result that a pure pH gradient with ammonium acetate resulted in no separation of charge variants while a pH gradient containing MES showed separated mAb variants. Still, gradients are only partly transferable and cannot be applied automatically to other mAbs with the same separation power. Goyon et al. showed that the separation power can be optimized for infliximab when adapting the gradient compared to a generic method.[8] Zhang et al.[10] proposed what is probably the most generic CEX-UV method, in which a salt-mediated pH gradient provided mAb variant separation over a tested pI range from 6.2 to 9.4. All in all, CEX-UV methods generally separate mAb variants very efficiently, but they are mostly composed of buffers that contain MES-buffer,[4,8,38,41–43] sodium hydrochloride,[10,39,40,42] or Tris-buffer,[11,37] which are not compatible to online ESI-MS. Potentially information can be extracted from these separation

systems by collecting fractions and determining the mAb variants of each fraction by an MS-compatible method[44–49] or by using 2D and 4D setups.[50,51] However, this requires extra-analysis time, as well as the risk of inducing variants during sample handling. Automatic, multidimensional methods where CEX is used in the first dimension can reduce the risk of artificial variants, but the methods are still time-consuming, and multidimensional systems are elaborative and hardly used for routine analysis applications.[50–52] The development of MS-compatible separation systems is therefore of utmost importance.

Online CEX-MS studies are listed in Table 1. MS-coupled CEX separation methods mainly work with ammonium acetate or ammonium formate-based eluents, which are either used as pure pH gradients with weak cation exchangers[5,6,48] or as a combination of salt and pH gradient with strong cation exchangers.[7,12,64,66,68,69,71] Another common eluent system uses bicarbonate and acetic acid as eluent A and ammonium hydroxide as eluent B with strong cation exchangers.[21,42,59,63] CEX-MS methods have limited generic application due to the different pIs of mAbs in combination with the pH and ionic strength of the buffer system. As can be seen from Table 1, around half of the methods were developed specifically for just one mAb, or in the case of several mAbs, the gradient was adapted according to the respective mAb. A linear pH gradient profile is highly desired to achieve a generic method for mAbs of varying pI values and can be generated using a set of involatile buffer components.[9–11] Using ammonium acetate, the pH response as a function of the base content is nonlinear[3,12] and column dependent.[12]

A buffer system consisting of 50 mM ammonium acetate with 2% of ACN at pH 5.0 (eluent A), and 160 mM ammonium acetate with 2% of ACN at pH 8.5 (eluent B) provides a good compromise between pH range, stability, and MS compatibility.[12] However, we witnessed quite high ion suppression effects when using these concentrations coupled to the MS. After method optimization, we coupled the CEX to the MS and analyzed the separated signals. Overall, we were able to detect several proteoforms, including the glycosylation pattern, monoglycosylation, and lysine variants when applicable. This corresponds to data from other studies since these variants are frequently detected with CEX-MS.[7,12,59,63] The difference in main and lysine variant resolution (ranging from $R = 0.8$ to $R = 2.6$) for the different mAbs most likely correlates with the previously mentioned challenge for linear pH gradients in ammonium acetate buffer systems. We were not able to detect minor mass proteoforms like sialylated glycoforms, succinimide, and pyroGlu modifications even though CEX-MS is generally able to detect sialylated glycans,[63] succinimide,[6] and pyroGlu[12] proteoforms for other mAbs with possibly higher abundances. Our experiments, especially for cetuximab and stressed mAb1, show that the increase in heterogeneity, caused by a second glycosylation site or the induced deamidations, significantly reduces the spectral quality. The low spectral quality in combination with the native ionization and the generally low abundance of some proteoforms limited the resulting information, which can be overcome by applying nanoESI as discussed in more detail below.

Limitations regarding the information from the MS are particularly related to acidic variants containing deamidated proteoforms. A common conclusion in the literature is that the unambiguous assignment of deamidated species is not feasible due to the small mass shift of 1 Da, which is mostly not distinguishable by the MS on an intact level.[6,12,42,63,66] Instead, often fractions of the CEX separation are collected and then additionally analyzed by peptide mapping approaches[48,54,56,69,71] or on a subunit level.[6,71]

CIEF-UV and CIEF-UV-MS for mAb variant analysis

Two general detection approaches are used when mAb variants are analyzed by CIEF. The whole capillary can be monitored (imaged, iCIEF) or the focused analytes can be mobilized toward the detector (CIEF). If not specifically stated otherwise, our discussion of CIEF covers CIEF and iCIEF. Depending on whether the mobilization is done pressure-driven or chemically, the separation previously established during the focusing step can decrease. In particular, pressure-driven mobilization can significantly reduce the peak resolution compared to a chemical mobilization,[87] which is why chemical mobilization is standard in CIEF-UV.[17,18,39,87–89] In the case of the iCIEF methods, the focused variants do not have to be mobilized toward the UV detector, which eliminates losses based on mobilization. However, this benefit of iCIEF does not play any role when coupled with MS since mobilization is required for MS characterization. Apart from mobilization, the separation is influenced by various chemicals used to optimize the CIEF process, as shown by Cao et al.[17] and Lin et al..[18] Both studies showed that especially the urea, methylcellulose, carrier ampholyte, and arginine concentrations have a significant effect on the mAb variant separation and have

Table 1. Direct and online CEX-MS methods for intact mAb analysis (excludes ADCs, fraction collection, or multidimensional methods). mAbs 1–5 included in this table do not correlate with mAbs 1–5 mentioned in the results section.

Sample(s)	Column	Eluent A	Eluent B	Gradient	Interface	MS	Aim of analysis	Ref.
mAb1, 2, and 3	ProSwiftTM SCX-1S **AND** ProSwiftTM WCX-1S (4.6 mm × 50 mm)	5 mM AMH buffer containing 20% (v/v) methanol at pH 9.5	5 mM AMH buffer containing 20% (v/v) methanol at pH 10.5	A linear gradient of eluent A to eluent B in 20 min. The flow rate was 1 mL/min.	Agilent G1385A microflow nebulizer	TOF	Resolve charge variants of mAbs with the aid of CEX monolithic columns	Talebi et al.[53]
Trastuzumab	ProPac WCX-10 column (2.0 mm × 250 mm, 5 µm particle size)	50 mM ammonium acetate pH 6.6	50 mM ammonium acetate, pH 10.1	20 min gradient of 1–8% B and flow rate of 0.3 mL/min	Not specified	Orbitrap	Native intact mass and charge variant analysis	Bailey et al.[5]
Trastuzumab Adalimumab Infliximab Bevacizumab Cetuximab	MAbPac SCX-10 RS (2.1 mm × 50 mm, 5 µm particle size)	25 mM ammonium bicarbonate and 30 mM acetic acid (pH 5.3)	10 mM ammonium hydroxide in 2 mM acetic acid (pH 10.18)	mAb dependent compare Table 1 in publication	Heated electrospray ionization-II (HESI-II) Ion Max ion source	Orbitrap	Low ionic strength pH gradient elution for characterization of mAb charge variants	Füssl et al.[54]
mAb	ProPac™ WCX-10 (4 mm × 250 mm, 10 µm particle size)	20 mM ammonium formate pH 6.5	20 mM ammonium formate pH 8.6	0% B for equilibration; change in the composition of B to 17% for 0.00–10 min, 38% B for 10.00–20.00 min, then linear increase to 100% B for 20.00–50.00 min and 50.00–57.00 min, and re-equilibration by 0% B for 57.00–58.00 and 58.00–65.00 min in the end. Used a constant flow rate of 0.8 mL/min	Not specified	TOF	Analysis and characterization of mAb charge variant heterogeneities	Sankaran et al.[6]
deglycosylated NISTmAb and mAb1–5	YMC-BioPro SP-F (100 mm × 4.6 mm, 5 µm particle size)	20 mM ammonium acetate, pH 5.6	140 mM ammonium acetate, 10 mM ammonium bicarbonate, pH 7.4	100% mobile phase A for 2 min; linear increase to 100% mobile phase B in 16 min, hold at 100% mobile phase B for 4 min, and then return to 100% mobile phase A to recondition the column for 7 min. Used a flow rate of 0.4 mL/min.	Nanospray Flex Ion Source	Orbitrap	In-depth charge heterogeneity characterization of therapeutic mAbs	Yan et al.[55]
Trastuzumab Adalimumab Infliximab Bevacizumab Cetuximab NIST mAb Rituximab	MAbPac™ SCX-10 RS column (2.1 mm × 50 mm, 5 µm particle size)	25 mM ammonium bicarbonate and 30 mM acetic acid in water (pH 5.3)	10 mM ammonium hydroxide in water (pH 10.9)	mAb dependent compare Table 1 in publication	Heated electrospray ionization-II (HESI-II) Ion Max ion source	Orbitrap	Charge variant analysis of mAbs (Adalimumab in detail)	Füssl et al.[56]
Trastuzumab Infliximab NIST mAb Rituximab	BioResolve SCX mAb, (2.1 mm × 50 mm, 3 µm particle size)	50 mM ammonium acetate, pH 5.0, 2% acetonitrile	160 mM ammonium acetate, pH 8.5, 2% acetonitrile	Start at 40% Eluent B for 1 min, linear gradient to 98% Eluent B (1-21 min), hold for 1 min, return to start conditions (1 min), and re-equilibration for 7 min. Used a flow rate of 0.1 mL/min.	Not specified	TOF	The broad applicability of the method on the BioAccord LC-MS System	Ippoliti et al.[57]

(*Continued*)

Table 1. (Continued).

Sample(s)	Column	Eluent A	Eluent B	Gradient	Interface	MS	Aim of analysis	Ref.
NISTmAb and mAb1, 2, and 3	Bioresolve SCX mAb (2.1 mm × 100 mm, 3 µm particle size)	20 mM ammonium acetate pH 5.6	200 mM ammonium acetate pH 7.0	Isocratic elution at 22% B for 2 min, linear gradient from 22% to 100% B in 16 min, column wash for 9 min at 100% B, and equilibrated during 17 min at 22% B. A flow rate of 0.4 mL/min	Not specified	TOF	A cation exchanger was evaluated for the charge variant analysis of mAbs in direct coupling with native MS	Leblanc et al.[7]
Bispecific mAbs Misspaired mAbs	ProPac WCX-10 column (4 mm ×250 mm, 10 µm particle size)	50 mM ammonium acetate, pH 7	50 mM ammonium acetate plus 0.8% ammonium hydroxide, pH 10	1%-8% solvent B over 40 min. Step-change to 100% B for 5 min. Step-changed to 1% B for 10 min. Used a flow rate of 300 mL/min	Not specified	Orbitrap	Optimized native charge variant mass spectrometry application for bispecific and mispaired IgG separation	Phung et al.[58]
Cetuximab	Not specified	6.25 mM ammonium bicarbonate and 7.5 mM acetic acid in water (pH 5.40)	5 mM ammonium hydroxide in water (pH 9.85)	A linear gradient of 20 – 100% buffer B in 15 min followed by 3 min of column flushing at 100% buffer B, 3 min equilibration to 0% buffer B, and 12 min equilibration to the starting conditions of 20% buffer B. Flow rate not specified.	Not specified	Orbitrap	In-depth analysis in terms of charge variant and glycoform heterogeneity using two orthogonal approaches (CEX and CZE)	Füssl et al.[59]
Trastuzumab (stressed) Infliximab NIST mAb mAb1–4	MABPac SCX-10 RS (2.1 mm × 50 mm column, 5 µm particle size)	20 mM ammonium acetate (pH 5.5)	140 mM ammonium acetate, 10 mM ammonium bicarbonate, pH 7.4	100% A or 60% A for 2 min, followed by a linear curve to 100% B in 12 min. The gradient stayed at 100% B for 3 min for column flushing and returned to the initial gradient. It was then re-equilibrated for 6 min. Three different flow rates (0.1 mL/min, 0.2 mL/min, 0.4 mL/min)	Not specified	Orbitrap	pH and salt gradients were used for the universal separation of mAbs (wide range of pI values)	Ma et al.[60]
Roledumab	MAbPac SCX-10 column (4 mm ×150 mm)	50 mM ammonium formate buffered with formic acid at pH 3.9	500 mM ammonium acetate at pH 7.4	After an isocratic elution at 15% of B for 5 min, a linear gradient was applied from 15% to 31% in 40 min thus to 85% of B in 30 min. The column was then washed for 5 min at 90% of B and further equilibrated for 15 min at 15% of B. Using a flow rate of 0.4 mL/min	Not specified	TOF	Identification of the charge variants of purified mAb dimers.	Rouby et al.[61]
mAb	ProPac WCX-10 column (2.0 mm × 250 mm, 5 µm particle size)	Ammonium acetate, pH 5.0	Ammonium acetate, pH 9.5	100% A for 1 min followed by an increase to 16% B in 2 min. Increase to 18% B linearly in 40 min. Further, increase to 100% B in 2 min and hold for 4 min. Return to 100% A in 2 min and hold at 100% phase A for 10 min. Three different flow rates (0.1 mL/min, 0.2 mL/min, 0.4 mL/min)	Not specified	Orbitrap	Addition of top-down to CEX-MS to achieve site-specific structural information of charge modifications	Shi et al.[62]
MabThera® Reditux™	MAbPac SCX-10 RS (2.1 mm × 50 mm column, 5 µm particle size)	25 mM ammonium bicarbonate and 30 mM acetic acid in water (pH 5.3)	10 mM ammonium hydroxide in water (pH 10.8)	75% to 99% mobile-phase B in 15 min followed by a flushing step with 99% B for 5 min an equilibration step with 10% B for 10 min and 75% B for 25 min. Using a flowrate of 400 µL min – 1	Not specified	Orbitrap	Separation of charge variants of MabThera® and Reditux™ under native conditions using volatile salts	Di Marco et al.[63]

(*Continued*)

Table 1. (Continued).

Sample(s)	Column	Eluent A	Eluent B	Gradient	Interface	MS	Aim of analysis	Ref.
TCB Mab	ProPac WCX-10 HPLC column (4 mm × 250 mm, 10 µm particle size)	50 mM ammonium acetate, pH 6.0	50 mM ammonium acetate, pH 10.7	1% to 8% solvent B in 25 min, from 8% to 18% solvent B in 15 min, and from 18% to 100% solvent B in 2 min washing step from 100% to 1% solvent B in 2 min and an equilibration step with 1% solvent B for 6 min. Using a flow rate of 300 µL/min	Nanospray Flex ion source	Orbitrap	Characterization of the TCB Mab charge variants including native CEC-UV/MS method development	Haberger et al.[48]
NIST mAb, Adalimumab, Dalotuzumab, Elotuzumab, Infliximab Trastuzumab	BioResolve SCX mAb (2.1 mm × 50 mm, 3 µm particle size) **AND** MabPac SCX-10 RS (2.1 mm × 50 mm, 5 µm particle size)	50 mM ammonium acetate with 2% acetonitrile, pH 5.0	160 mM ammonium acetate with 2% acetonitrile, pH 8.5	mAb dependent: compare method section in the publication	Not specified	TOF	CEX-MS method development for the analytical characterization of various biopharmaceutical products	Murisier et al.[12]
Emicizumab	BioResolve SCX mAb (2.1 mm × 50 mm, 3 µm particle size)	50 mM ammonium acetate in 2% acetonitrile (pH 5.0)	160 mM ammonium acetate in 2% acetonitrile (pH 8.5)	Isocratic step at 50%B for 1 min followed by 50%–98%B in 16.5 min. 98%B was kept for 1.5 min followed by a column re-equilibration step at 50%B for 7 min. The flow rate was 0.1 mL/min.	Not specified	TOF	Comprehensive characterization of emicizumab by using orthogonal chromatographic methods coupled to MS	Duivelshof et al.[64]
NIST mAb IgG1, 2, 3, 4, 5, 6	YMC-BioPro QA-F SAX column (4.6 mm × 100 mm, 5 µm particle size) **AND** YMC BioPro SP-F SCX column (4.6 mm × 100 mm, 5 µm particle size)	10 mM ammonium acetate, pH 6.7/20 mM ammonium acetate, pH 5.6	300 mM ammonium acetate, pH 6.8/150 mM ammonium acetate, pH 6.8	100% mobile phase A for 2 min followed by a linear increase to 100% mobile phase B over 16 min. The gradient was then held at 100% mobile phase B for 4 min before returning to 100% mobile phase A. Using a flow rate of 0.4 mL/min.	Nanoelectrospray ionization (NSI) using a Microfabricated Monolithic Multinozzle emitter	Orbitrap	Development and optimization of a native AEX-MS method for charge variant analysis of mAbs.	Liu et al.[65]
Bevacizumab NISTmAb	BioResolve SCX mAb (2.1 mm × 100 mm, 3 µm particle size)	50 mM ammonium acetate with 20% acetonitrile, pH 5.5	150 mM ammonium acetate with 20% acetonitrile, pH 8.5.	Linear gradient: 45%–68% B in 25 min for bevacizumab and 40%–98% B in 20 min for NISTmAb. The gradient flow rate was 0.1 mL/min.	Jet stream electrospray ionization ion source	TOF	In-depth analysis of unstressed therapeutic mAbs and detailed protein heterogeneity	Dai et al.[66]
Adalimumab and biosimilars	ProPac 3 R SCX (2.1 mm × 50 mm, 3 µm particle size)	25 mM ammonium bicarbonate and 30 mM acetic acid water, pH 5.3	10 mM ammonium hydroxide in water pH 10.9	A linear gradient from 20–60% B in 20 min. The gradient time was followed by a 5 min column regeneration at 100% B and 10 min re-equilibration. The flow rate was 0.2 mL/min.	Not specified	Orbitrap	Characterization of a monodisperse SCX column format for monoclonal antibody charge variant separation	Füssl et al.[42]
Eculizumab Trastuzumab Pembrolizumab	BioResolve SCX column (2.1 mm × 100 mm, 3 µm particle size)	50 mM ammonium acetate at pH 5.0	160 mM ammonium acetate at pH 8.6	For intact trastuzumab, a linear gradient from 50% to 70% B in 10 min the mixture of mAbs was separated by first maintaining 0% B for 1 min followed by a linear gradient from 30% to 70% B in 9 min. The flow rate was 0.1 mL/min.	Z-Spray source	TOF	Online CEX–CIU method for the in-depth characterization of different mAb populations in their native state	van Schaick et al.[67]

(*Continued*)

Table 1. (Continued).

Sample(s)	Column	Eluent A	Eluent B	Gradient	Interface	MS	Aim of analysis	Ref.
mAb1	MabPac SCX-10, (2 mm × 250 mm, 10 µm particle size)	20 mM ammonium acetate, pH 5.6	150 mM ammonium acetate pH 6.8	According to a paper "similar to" Ma et al.[60] and Yan et al.[55] mentioned in this table here	Heated electrospray ionization source.	Orbitrap	Evaluation of succinimide formation in the CDR of mAb1	VanAernum et al.[68]
Infliximab Pembrolizumab Adalimumab Bevacizumab Daratumumab Atezolizumab Denosumab Guselkumab Rituximab	SCX: Not further specified	25 mM ammonium bicarbonate, pH 5.3	10 mM ammonia, pH 10.9	mAb dependent compares Table 2 in publication. The flowing rate was set at 0.3 mL/min	Ion Max ESI ion source, and a 34-gauge needle	Orbitrap	Comparison of CIEF and SCX regarding protein charge variant separation resolution, sensitivity, carryover effects, accuracy, and throughput	Wu et al.[21]
Bispecific mAb	bio pro-SPF-IEX (100 mm × 4.6 mm, 5 µm particle size)	50 mM ammonium acetate, pH 5.5	150 mM ammonium acetate, pH 10.2	100% A for 3 min, a 2% B/min gradient applied for 35 min, then washed with 100% buffer B for 5 min and equilibrated with 100% A for 5 min. Using a flow rate of 0.5 mL/min.	Not specified	Orbitrap	Characterization of the charge heterogeneity associated with bispecific antigen-binding proteins	Shah et al.[69]
Pembrolizumab Cetuximab Trastuzumab	Self-packed SCX columns (150 mm × 75 or 100 µm I. D.)	50 mM ammonium acetate, pH 5.0	250 mM ammonium acetate, pH 8.5	100% MPA went to 100% MPB in 22.5 min with directly coupled nanoflow (250 or 500 nL min − 1)	Nanospray-flex-series ion-source platform	Orbitrap	Development of an online nanoflow strong cation exchange chromatography with native MS detection for mAb separation	Zhai et al.[70]

Abbreviations: **AMH**: Ammonium hydroxide; **CDR**: Complementarity-determining regions, **CEC-UV-MS**: Cation-exchange chromatography native electrospray mass spectrometry, **CIEF**: Capillary isoelectric focusing, **CIU**: Collision-induced unfolding, **CZE**: Capillary zone electrophoresis, **HESI**: Heated electrospray ionization, **IEX**: Ion exchange chromatography, **SAX**: Strong anion exchanger, **MPA/MPB**: Mobile phase A or B; **SCX**: Strong cation exchanger, **WCX**: Weak cation exchanger.

to be carefully adjusted. Methylcellulose enhances the viscosity, which facilitates better separation and serves as a neutral hydrodynamic coating that reduces protein wall interactions.[16,17] Urea is used as a solubilizer to prevent protein aggregation,[16–18,89–91] and arginine functions as a spacer to prevent the loss of carrier ampholytes, pI markers, or analytes.[16–18,90] The carrier ampholytes establish the pH gradient during focusing and therefore have a major contribution to mAb variant resolution.[16] However methylcellulose[16,17,39,87,88] or molar concentrations of urea in the master mix[16–18,39,87,89,91] are not MS compatible and the use of sodium hydroxide as catholyte[16–18,39,89] eliminates any protein signal when coupled to MS.

The process of focusing and mobilization is also a challenge when CIEF is coupled to MS since the capillary is no longer positioned in an outlet vial and cannot be exchanged in case of chemical mobilization. These were the main reasons why CIEF was not directly coupled to MS for years and, for example, 2D separations were developed.[92,93] Indirect coupling to MS via a valve was shown by Montealgre et al. and Hühner et al.[94,95] to remove MS-incompatible substances before the MS. In 2018 Dai et al. coupled CIEF directly to MS for the detection and characterization of mAb variants[19] by applying a nanoSL interface (EMASS-II) that allowed focusing with an ammonium hydroxide plug (partial filling approach) in the capillary while the capillary end was installed in the interface with acidic SL. MS-interfering components were eliminated as much as possible by using a neutral-coated capillary, reducing the ampholytes concentration, and substituting urea with glycerol. Substituting MS incompatible components is the main task when CIEF is to be coupled to MS as shown in Table 2. Methylcellulose in the master mix can be avoided using capillaries with covalently bound methylcellulose[75,76] or by using other covalently bound capillary coatings like polyvinyl alcohol (PVA),[20,82,83] linear polyacrylamide (LPA),[84,96] dimethylpolysiloxane,[72] acrylamide,[21,74,85,86,97–99] PS1 or PS2,[19,77,100,101] or other hydrophilic coatings.[24,73,81] Urea can be substituted by glycerol[19,82–84,96,101] or formamide[20,73,74,86,97,99] and the basic sodium hydroxide catholyte can be exchanged for ammonium hydroxide,[19,20,82,83,101] ammonium bicarbonate,[84,96] ammonium acetate,[81] or diethylamine.[22,24,73,78,79] Several kits and systems, such as the CR3520 CIEF-MS reagent kit (CPM Scientific Corp),[77,100] CEInfinite (Advanced Electrophoresis Solutions Ltd),[21,74–76,80,85,86,97–99] the Intabio ZT system (SCIEX)[22,78,79] or the recently launched BioSummit™ CVA CIEF-MS system (CMP Scientific Corp), are commercially available. Despite the substitution of all MS-interfering compounds, CIEF generic mAb application can be limited due to the different pIs of different mAbs in combination with the used ampholytes as shown in Table 2. Some systems apply a narrow pH range that is optimized for mAbs with their pI in that specific range. In cases where several mAbs are analyzed ampholytes with a broader pH range are generally chosen to provide a more generic method.

In our CIEF-MS method, we reduced the amount of formamide and ampholyte in the master mix used by Naghdi et al.[20] to 15% and 1%, respectively, which reduces the amount of interfering ions and MS contamination. However, the CIEF-MS system is highly mAb-dependent. While a very nice separation and identification of mAbA was published by Naghdi et al.,[20] our experiments showed significant differences depending on the mAb samples. Infliximab, USPmAb003, and mAb3 could be detected via the online UV detector, but were never detected by the MS. This indicates a solubility problem at the emitter tip when nearly neutral mAbs are transferred to the acidic and isopropanol-containing sheath liquid. The reduced separation performance for CIEF-MS in comparison to the online UV signal is described in many publications and was also noted in our experiments even though chemical mobilization was used. This will be subject to further investigations in the future since CIEF-MS is a promising tool for mAb variant identification.

The strength of (i) CIEF-MS charge variant analysis is evident by several publications where the general glycosylation pattern,[19,21,22,24,73,74,79,80,82–84,96,99] the presence of sialic acids,[73,84] additional glycation,[21,73,74,79,84,86,99] incompletely clipped lysine variants,[19–22,24,73,74,77,79,82–84,86,96,99] N-terminal pyroGlu formation,[19,22,84,96] succinimide formation,[24,80] oxidation,[21] or deamidation[19–22,24,74,77,79,80,82–84,86,99] is analyzed. As for CEX-MS, deamidations are often supplemented with a peptide mapping approach to support the results gained by intact CIEF-MS. Nevertheless, this variety of variants for multiple mAbs shows the high potential of CIEF-MS coupling.

Table 2. Direct, online (i)CIEF-MS methods for intact mAb analysis (excluding ADCs). mAbs 1–5 included in this table do not correlate with mAbs 1–5 discussed in the results section.

Sample(s)	Ampholytes (final concentration)	Capillary coating	Catholyte / Anolyte	Focusing / Mobilization	Interface / Sheath liquid	MS	Aim of analysis	Ref.
NIST mAb	Pharmalyte pH 3 – 10, (5%)	DB-1	5% ammonia in 0.1% methylcellulose / 200 mM phosphoric acid (pH 1.38) in 0.1% methylcellulose	30 kV (15 min) / 0.5 psi (30 kV)	T-Junction Sheath-Flow Interface connected to nonorthogonal OptiFlow MS interface **OR** Open Port Interface connected to an OptiFlow Turbo V ion source / 50% methanol + 1% acetic acid pH 2.88 **OR** 50% acetonitrile + 2% formic acid pH 2.18	TOF	Introduction of a new interface for CZE-MS coupling (OPI) and compare its performance to that of a standard CE-MS interface (SFI) for capillary isoelectric focusing.	Beloborodov et al.[72]
Infliximab Trastuzumab Bevacizumab Cetuximab	Pharmalyte pH 3 – 10 (1.5%)	PS1	0.2 N ammonia with 15% glycerol / 1% formic acid with 15% glycerol	250 V/cm / 250 V/cm +10 mbar	EMASS-II ion source / 20% acetic acid with 25% acetonitrile	TOF	Development of CIEF-MS (TOF-MS detection and characterization) method for mAb charge variants correlating with iCIEF-UV profiles	Dai et al.[19]
mAb1, 2, 3, 4	Pharmalyte pH 3–10 (4.0%)	Not specified (hydrophilic coated)	1% diethylamine (pH 13) / 1% formic acid (pH 2.3)	1500 V (1 min) + 3000 V (1 min) + 4500 V (4.5 min) / 3000 V offset	Microfluidic chip-based iCIEF-MS / 25% acetic acid with 25% acetonitrile (pH 1.8)	Orbitrap	Charge variant analysis of mAbs using an iCIEF-MS setup	He et al.[73]
NISTmAb USP-mAb002 Bispecific mAb (BsAb)	**NISTmAb**: UR AESlyte™ 8.5–10 (2%) **USP-mAb002**: UH AESlyte™ 7–9 (2%) **BsAb**: HR AESlyte™ 8–10.5 (2%)	acrylamide derivate		1000 V (1 min) + 2000 V (1 min) + 3000 V (10 min) / 3000 V + mobilization solution (50 nL/min, 0.1% formic acid)	Ion Max ESI Ion Source with a 34-gauge needle **OR** Easy-Spray Ion Source / 50% acetonitrile and 0.5% (v/v) formic acid	Orbitrap	iCIEF-MS system with a nano-ESI interface to reduce flow rates, improve the ionization efficiency, lower analyte dispersion, and reduce the sample dilution.	Kwok et al.[74]
NISTmAb Bevacizumab Bispecific mAb (BsAb)	**NISTmAb**: Pharmalyte 3–10 (1%) + Pharmalyte 8–10.5 (3%) **Bevacizumab**: Pharmalyte 3–10 (4%) **BsAb**: HR AESlyte 9–12 (4%)	bi-layer polymerization, MC-coated capillary		1000 V (1 min) + 2000 V (1 min) + 3000 V (10 min) / 3000 V (15 min) + mobilization solution (50 **OR** 100 nL/min, 0.1% formic acid)	Ion Max ESI Ion Source with a 34-gauge needle / 50% acetonitrile and 1.0% (v/v) formic acid	Orbitrap	Development of an iCIEF method using an MC-coated capillary cartridge, to avoid the need for MC in the analysis.	Kwok et al.[75]

(*Continued*)

Table 2. (Continued).

Sample(s)	Ampholytes (final concentration)	Capillary coating	Catholyte / Anolyte	Focusing / Mobilization	Interface / Sheath liquid	MS	Aim of analysis	Ref.
mAb-M-AT	Pharmalyte 3–10 (3.5%) + Pharmalyte 8–10.5 (0.5%)	MC-coated capillary and micro-tee integrated AD-coated cartridges		1500 V (1 min) + 3000 V (7 min) / 3000 V (15 min) + mobilization solution (50 nL/min, 0.1% formic acid)	Ion Max ESI Ion Source with a 34-gauge needle / 50% acetonitrile and 0.1% (v/v) formic acid	Orbitrap	Using mAb-M-AT for charge variant characterization on an integrated iCIEF platform	Kwok et al.[76]
Bevacizumab	Pharmalyte 3–10 + Pharmalyte 8–10.5 (CR3520 cIEF-MS)	PS1	Buffer B / Buffer A	18 kV / 7 mbar (18 kV)	EMASS-II ion source / Not specified (acidic SL)	TOF	Identification of a bevacizumab clipping variant through several CE-MS technologies	Li et al.[77]
Trastuzumab biosimilar	Pharmalyte 5–8 (1%) + Pharmalyte 8–10.5 (3%)	Not specified (hydrophilic coated)	1% diethylamine / 1% formic acid	1500 V (1 min) + 3000 V (2 min) + 4500 V (4 min) / 2300 V offset	NanoElectrospray capillary cap set / 1% formic acid, 50% acetonitrile, and 49% water.	TOF	Development and application of a microchip-based iCIEF-MS system for CQA analysis	Mack et al.[24]
NISTmAb	Pharmalyte 3–10 (1%) Pharmalyte 8–10.5 (2.5%)	Not specified (hydrophilic coated)	0.25% diethylamine / 1% formic acid	1500 V (1 min) + 3000 V (1 min) + 4500 V (5 min) / 5500 V (10 min)	OptiFlow interface / 25% acetic acid, 25% acetonitrile, and 50% water.	TOF	The chip-based platform shows high resolution, high throughput, and high reproducibility regarding mAb charge variants	Madda et al.[78]
Deglycosylated NIST mAb	Pharmalyte 3–10 (1%) Pharmalyte 8–10.5 (2.5%)	Not specified	0.25% diethylamine / 1% formic acid	1500 V (1 min) + 3000 V (1 min) + 4500 V (5 min) / 5500 V (10 min)	OptiFlow interface / 25% acetic acid, 25% acetonitrile, and 50% water.	TOF	The Intabio ZT system enables a workflow to separate charge variants by iCIEF	Madda et al.[79]
mAb A	Pharmalyte 8 – 10.5 (1.25%) + Pharmalyte 3–10 (0.62%) + Pharmalyte 5 – 8 (0.3%)	PVA	0.2% ammonia in isopropanol/water (50/50) / 1% formic acid	290 V/cm (25 min / 500 V/cm (25 min	nanoCEasy interface / 0.20% formic acid in Isopropanol/water (50/50)	TOF	Chemical mobilization CIEF–MS method using the nanoCEasy interface and its application for different sample sets	Naghdi et al.[20]
Bispecific mAb	Pharmalyte 3–10 (1%) Pharmalyte 8–10.5 (2.5%)	Not specified	1% v/v diethylamine (pH 12.5) in water / 1% v/v formic acid (pH 2.2)	1500 V (1 min) + 3000 V (1 min) + 4500 V (4.5 min) / 5500 V (6.5 min)	Not specified / 25% acetic acid and 25% acetonitrile in water.	TOF	Demonstration that the microfluidic chip-based integrated iCIEF-MS technology is a new approach to CQA and charge variant analysis	Ostrowski et al.[22]

(*Continued*)

Table 2. (Continued).

Sample(s)	Ampholytes (final concentration)	Capillary coating	Catholyte / Anolyte	Focusing / Mobilization	Interface / Sheath liquid	MS	Aim of analysis	Ref.
Trastuzumab	2%–4% (v/v) ampholytes (Pharmalyte 3–10 and Pharmalyte 8–10.5, 1:3).	acrylamide derivative **OR** fluorocarbon	100 mM sodium hydroxide / 80 mM phosphoric acid	1500 V (1 min) + 3000 V (10 min) / 3000 V + mobilization solution (30 or 50 nL/min)	nanoCEasy / 50% isopropanol + 0.5% formic acid	TOF/Orbitrap	Online coupling of an iCIEF to mass spectrometry via the nanoCEasy interface for online identification of charge variants	Schlecht et al.[80]
SigmaMAb NIST mAb	Pharmalyte 3–10 (0.25%)	LCP **OR** LPA	50 mM ammonium acetate (pH 9.0) / 25 mM ammonium acetate (pH 6.8)	30 kV (5–20 min) / 50 mbar (30 kV)	EMASS-II ion source / 10 mM ammonium acetate (pH 6.8)	TOF	Novel native capillary isoelectric focusing (cIEF)-assisted CZE-MS	Shen et al.[81]
Infliximab	Carrier ampholytes 3–10	PVA	1.0% (w/v) ammonia in 39% water and 60% methanol / 1.0% (v/v) acetic acid	30 kV (30 min) / 34 mbar (30 kV)	Flow-through microvial interface / 2.0% formic acid in 80% methanol	Orbitrap	The progress of cIEF –MS analysis by the flow-through microvial interface is shown.	Wang et al.[82]
mAb Infliximab Adalimumab NIST	Fluka carrier ampholyte pH 3–10 (1.0%)	PVA	1.0% w/v ammonia in water (pH 11.51) containing 20% glycerol / 1.0% v/v acetic acid (0.175 M, pH 2.75) containing 20% v/v glycerol	30 kV (25 min) / 0.5 psi (25.5 kV)	Flow-through microvial interface / 1.0% formic acid and 80% methanol	TOF	Showing feasibility of online cIEF – MS method for charge and structural heterogeneity of mAbs using fully automated analyses and a sandwich on-capillary configuration	Wang et al.[83]
Infliximab Pembrolizumab Adalimumab Bevacizumab Daratumumab Atezolizumab Denosumab Guselkumab Rituximab	Compare Table 1 in Paper	acrylamide derivative	Not specified	1000 V (1 min) + 2000 V (1 min) + 3000 V (10 min) / 80 nL/min with water containing 0.1% formic acid, 15 min (3000 V)	Ion Max ESI Ion Source with a 34-gauge needle / water/acetonitrile 1:1, containing 1% formic acid	Orbitrap	Comparison of CIEF and SCX regarding protein charge variant separation resolution, sensitivity, carryover effects, molecular weight accuracy, and throughput	Wu et al.[21]
NIST mAb Trastuzumab Cetuximab mAb1	2.0% ampholyte mixtures (pH range of 3–10, 5–8, and 8–10.5, ratio 1: 2: 4)	LPA	10 mM ammonium bicarbonate, 15% glycerol, pH 10 / 0.1% formic acid and 15% glycerol, pH 2.7	20 kV (20 min) / 10 mbar (20 kV)	EMASS-II ion source / 25% acetonitrile and 20% acetic acid	TOF	Improve automated cIEF-MS method for characterization of intact charge variants of mAbs with high resolution and reproducibility.	Xu et al.[84]

(*Continued*)

Table 2. (Continued).

Sample(s)	Ampholytes (final concentration)	Capillary coating	Catholyte / Anolyte	Focusing / Mobilization	Interface / Sheath liquid	MS	Aim of analysis	Ref.
Pembrolizumab	2% HR AESlyte 6–8	acrylamide derivative	Not specified	1500 V (1 min) + 3000 V (10 min) / 40 nL/min with water containing 10 mM acetic acid (3000 V)	Ion Max ESI Ion Source with a 34-gauge needle / water/acetonitrile 1:1, containing 0.1% formic acid	Orbitrap	Development of an iCIEF-MS strategy for rapid iCIEF separation and reliable HRMS identification of protein charge variants	Zhang et al.[85]
NIST mAb Bevacizumab Pembrolizumab	**NIST mAb**: 0.5% HR AESlytes 3–10 + 1.5% HR AESlytes 8–10.5% **Bevacizumab**: 2% HR AESlyte 3–10 **Pembrolizumab**: 2% HR AESlyte 6–8	acrylamide derivative	Not specified	1000 V (1 min) + 2000 V (1 min) + 3000 V (10 min) / 50 nL/min with water containing 0.1% formic acid, 15 min (3000 V) **Slightly adapted depending on mAb**	Ion Max ESI Ion Source with a 34-gauge needle / water: acetonitrile = 1: 1, v/v, containing 0.1% **OR** 0.5% formic acid	Orbitrap	Development of an iCIEF-MS strategy for rapid iCIEF separation and reliable HRMS identification of protein charge variants	Zhang et al.[86]

Abbreviations: **CQA**: Critical quality attribute, **CZE**: Capillary zone electrophoresis, **ESI**: Electrospray ionization, **HRMS**: High-resolution MS, **LCP**: Linear carbohydrate polymer, **LPA**: Linear polyacrylamide, **MC**: Methyl cellulose, **PVA**: Polyvinyl alcohol, **TOF**: Time of flight, **SCX**: Strong cation exchange chromatography.

CZE-UV and CZE-MS for mAb variant analysis

The most commonly applied CZE-UV method, which consists of a fused silica capillary and a BGE containing EACA, TETA, and HPC, was developed by He et al..[25] As demonstrated by our results, this generic method shows very good separation of acidic and basic charge variants for all 10 mAb samples in this study. This method is also commonly used for UV-based charge variant separation.[26,28,29,89,102–106] A recent interlaboratory study was conducted because users experienced issues regarding reproducibility.[29] The EACA lot did not cause inconsistent results, which were instead attributed to unintended changes in the method.[29] Alternative dynamic coating agents, additives, and polymeric compounds are tested for similar or better charge variant separation.[27,89,107–112] BGEs contain, for example, Bis-Tris,[27,107] MES,[27] 3-morpholinopropane-1-sulfonic acid,[27] or ammonium or sodium acetate[108–110,112] in addition to EACA or as a substitute. HPC and TETA are substituted or supplemented by polyethylene oxide,[27,107,112] polysorbate 20,[111] Tween 20,[89] or spermine.[27] However, these methods cannot be coupled directly to the MS. 2D CZE systems are applied to remove the MS incompatible substances,[113–115] but the analysis time is prolonged and coupling two CZE systems is so far not suitable for routine analysis. This shows the need for CZE systems that provide proper mAb variant separation and can be directly coupled to the MS.

To couple CZE to MS, all interfering components like coating materials or polymeric compounds must be removed from the BGE, as shown in Table 3. Capillaries are covalently coated with either neutral-coating agents like linear polyacrylamide,[81,116,117,127] HP(M)C,[31,139] PVA,[2,134] or other neutral agents,[32,33,59,77,118–120,125,126,128,129,131,133,135,136] or they are cationic coated with M7C4I,[116] polyethyleneimine,[121–124] or other cationic polymers in a multilayer approach.[30,130] Antibody variants can be separated in an acidic BGE or a less acidic BGE typically based on ammonium acetate. The latter is here called "native," though it is not clear whether the acidic BGE is really denaturing and the better separation observed in ammonium acetate-based BGEs is due to native conditions or the fact that the mAb and the variants are less positively charged, resulting in a better separation as shown by Shi et al..[112] The system developed by Höchsmann et al. allows MS detection in a mass range of 2500–4000 m/z and a detailed analysis as shown by the evaluation of USPmAb003 variants using 10 kV separation voltage.[30] The method was applied to the 10 mAb samples and is universally applicable if the heterogeneity of the mAb is not too complex (cetuximab or pH-stressed mAb1). However, the variant separation we achieved can most likely be increased if the separation voltage is decreased from −20 kV to −10 kV or even smaller values as shown by Höchsmann et al..[30] Applying a voltage of −20 kV for the separation allowed the analysis to be done in 45 min and the separation of proteoforms like the mAb glycosylation including sialic acid proteoforms, monoglycosylation, aglycosylation, lysine variants, water or ammonia losses, reduced disulfides, and the presumed deamidation of pH stressed mAb1. Such a good separation has not been achieved by any acidic separation system so far. Redman et al. showed good separation of lysine variants of infliximab using BGE of 10% isopropanol/0.2% HAc (pH 3.17).[131] Giorgetti et al. also show some separation of variants using a 3% HAc BGE, but the deconvoluted masses for acidic, main, and basic proteoforms were similar and the author thus concluded that no specific proteoforms can be assigned.[121,122] In other cases, denatured systems only provide one signal without any separation of charge variants[2,127] or only a slight separation of the glycosylation species.[116] This makes the separation system applied here[30] very valuable in the field of denatured mAb variant analysis. A better separation is only possible at higher pH (native separation conditions, as listed also in Table 3). These CZE-MS systems provide very good charge variant separation and identification as recently shown by van der Zon et al.[31] and multiple chip-based methods.[32,33,59,118,119,133,135] However, native systems require an MS instrument that covers a high mass range (4500–7500 m/z depending on the mAb) and provides proper declustering.

Comparison of CEX, CIEF, and CZE on an intact and subunit level

To compare all tested methods, the variant separation and the deconvoluted mass spectra of mAb1 as obtained by CEX-MS, CIEF-MS, and CZE-MS are shown in Figure 5 (Supplementary Figure S5 – S7 show similar data for infliximab, NIST mAb, and mAb2, respectively). The acidic and basic variant assignment was highly method-dependent. In particular, the CEX-separated variants suffered from low spectral quality when introduced into the MS. This is due to the native ionization and still relatively high ammonium acetate

Table 3. Direct, online CZE-MS methods for intact mAb analysis (including MCE-MS methods but not CE-MALDI or the analysis of ADCs). mAbs 1–5 included in this table do not correlate with mAbs 1–5 discussed in the results section.

Sample(s)	Capillary coating	Background electrolyte	Sheath liquid	Interface	MS	Aim of analysis	Ref.
mAb	M7C4I	10% isopropanol, 0.2% formic acid	–	CESI (sheathless)	Orbitrap	Analysis of mAb on intact, native, and subunit levels for detailed variant analysis	Belov et al.[116]
mAb	Polyacrylamide	40 mM ammonium acetate, pH 7.5		CESI (sheathless)	Orbitrap	Analysis of mAb on intact, native, and subunit levels for detailed variant analysis	Belov et al.[116]
Trastuzumab	Polyacrylamide	20 mM ammonium acetate, pH 8.0	–	CESI (sheathless)	Orbitrap	Demonstration that native CZE-MS can serve as an orthogonal and complementary technique to conventional native MS methodologies	Belov et al.[117]
mAb and biosimilars	ZipChip HRN chip	Native Antibody BGE (908 Devices) + 4% DMSO	–	ZipChip Ti interface	Orbitrap	Investigation if MCE-MS is suitable as a tool for rapidly assessing monoclonal cell line candidates	Cageling et al.[33]
IgG4 mAb IgG1 mAb	ZipChip HRN chip	Native Antibody BGE (908 Devices)	–	ZipChip interface	Orbitrap	mAbs were analyzed by peptide mapping and native intact methods using a single microfluidic CZE-MS system	Cao et al.[118]
Rituximab, Bevacizumab Trastuzumab	ZipChip HRN chip	Native Antibody BGE (908 Devices) + 4% DMSO	–	ZipChip interface	Orbitrap	Confident identification of mAb variants	Carillo et al.[119]
NIST mAb	ZipChip HR chip	0.2% acetic acid and 10% 2-propanol (pH 3.17)	–	ZipChipTM CE interface	Orbitrap	Intact mAb characterization, and quantitative results on protein variants	Chen et al.[120]
Panitumumab	ZipChip HRN chip	Native Antibody BGE (908 Devices) + 4% DMSO	–	ZipChip interface	Orbitrap	The heterogeneity of panitumumab was investigated using SEC-MS and microchip CZE-MS.	Füssl et al.[32]
Cetuximab	ZipChip HRN chip	Native Antibody BGE (908 Devices)	–	ZipChip interface	Orbitrap	In-depth analysis in terms of charge variant and glycoform heterogeneity using two orthogonal approaches (CEX and CZE)	Füssl et al.[59]
Adalimumab Natalizumab Nivolumab Palivizumab Infliximab Rituximab Trastuzumab	PEI	3% acetic acid	–	Nano-ESI source (sheathless)	TimsTOF Pro (tims was switched off)	Development of a multi-level combined approach for complete structural characterization of mAbs based on a CE-ESI-MS coupling.	Giorgetti et al.[121]
Trastuzumab Rituximab Palivizumab	PEI	3% acetic acid	–	sheathless interface	TOF	Development of a CZE-ESI-MS method for the analysis of three well-known approved mAbs at the intact level	Giorgetti et al.[122]
bispecific mAbs	PEI	3% acetic acid	–	CESI 8000 (sheathless)	TOF	Analysis of the intact BsAbs for monitoring incomplete assemblies and free chains.	Gstöttner et al.[123]
bispecific mAbs	PEI	10% acetic acid (pH 2.1)	–	CESI 8000 (sheathless)	TOF	Potential evaluation of sheathless CE-MS to monitor exchange efficiency and stability of BsAbs.	Gstöttner et al.[124]
mAb-A	Neutrally coated OptiMS capillary	50 mM ammonium acetate pH 6.8 containing the FcgRIIIa V158 or F158 at a concentration of 0.25 mM.	–	CESI 8000 (sheathless)	Orbitrap	ACE-MS is a powerful platform for glycoform-resolved interaction studies between IgGs and different FcgRs.	Gstöttner et al.[125]
forced oxidation mAbs	OptiMS neutrally coated capillaries	50 mM Ammonium acetate solution was adjusted to pH 6.0	–	CESI 8000 (sheathless)	Orbitrap	Developed an approach based on mobility-shift ACE–MS	Gstöttner et al.[126]
Deglycosylated IgG1	LPA	30% acetic acid	0.5% formic acid, 50% methanol	EMASS-II interface	TOF	Proof of concept that the CZE-TOF platform can be used to measure the intact mass and fragments of mAbs	Han et al.[127]
Trastuzumab Infliximab Ustekinumab	Neutrally coated OptiMS capillary	10% acetic acid	–	CESI 8000 (sheathless)	TOF	Exploration of the capabilities of low-flow sheathless CZE-MS using acidic BGEs for antibodies	Haselberg et al.[128]

(*Continued*)

Table 3. (Continued).

Sample(s)	Capillary coating	Background electrolyte	Sheath liquid	Interface	MS	Aim of analysis	Ref.
USPmAb003 Infliximab Adalimumab Trastuzumab NISTmAb	SMIL	4 M acetic acid	Isopropanol: water (50:50) + 0.5% FA	nanoCEasy	Orbitrap	Develop a generic CZE-MS method for charge variant analysis and increase separation under acidic conditions using a new cationic capillary coating	Höchsmann et al.[30]
NIST mAb	Neutrally coated OptiMS capillary	40 mM ammonium acetate	–	Nanospray Flex™ ion source (sheathless)	Orbitrap	Establishing and discussing standard procedures for nCZE-TDMS using sheathless ionization	Jooß et al.[129]
Infliximab	Triple layer cationic coating based on PB-DS-PB	40 mM ammonium acetate pH 6.0	Water-isopropanol-acetic acid 50:50:0.1	Coaxial SL electrospray interface	TOF	Investigated online CZE-native MS with an SL interface to analyze stressed and unstressed mAb	Le-Minh et al.[130]
Bevacizumab	PS2	CZE sample buffer (P/N SB1121)	Not specified (acidic SL)	EMASS-II ion source	TOF	Identification of a bevacizumab clipping variant through several CE-MS technologies	Li et al.[77]
mAb1–3	PVA	2 M acetic acid	Isopropanol, water, and formic acid (50/49.9/0.1, v/v/v)	nanoCEsay / triple-tube SL interface	Orbitrap / TOF	Presentation of an optimized workflow for high throughput glycosylation analysis (RPLC-MS) Evaluation of separation techniques, RPLC and CZE, and data processing approaches	Naumann et al.[2]
Infliximab, mAb A and B	NHS-PEG_{450}	10% 2-propanol/0.2% acetic acid (pH 3.17)	–	Laboratory setup	TOF	New capillary coating and interface for mAb variant separation	Redman et al.[131]
SigmaMAb NIST mAb	LCP **OR** LPA	25 mM ammonium acetate (pH 6.8)	10 mM ammonium acetate (pH 6.8)	EMASS-II ion source	TOF	Novel native capillary isoelectric focusing (cIEF)-assisted CZE-MS	Shen et al.[81]
Sigma mAb NIST mAb Herceptin	Interlaboratory study: different systems and approaches were used. Compare Table S8					Highlights the current state of TD/MD MS to address biotechnology medicinal products and their limitations	Srzentić[132]
mAb	ZipChip HRN chip	Native Antibody BGE (908 Devices) + 4.0% DMSO, pH ~ 5.5	–	ZipChip interface	Orbitrap	CE-MS was used to identify mAb charge variants. CE-MS was compared to a CEX-UV separation	Sun et al.[133]
Innovator and biosimilar rituximab	PVA	2% acetic acid	0.5% acetic acid in 50% methanol	Not specified	TOF	CZE was used for monitoring the charge variants of innovator and biosimilar rituximab	Elektroforéza[134]
Pembrolizumab, Rituximab, Cetuximab, Pembrolizumab, NISTmAb	HPMC	50 mM acetic acid adjusted to pH 5.0	0.5% formic acid in 50/50 iso-propanol/water	nanoCEasy	Orbitrap	Closing the gap between a flexible CZE method that enables mAb variant quantification at pH 5–6 via UV and offering MS coupling for identification	van der Zon et al.[31]
deglycosylated NIST mAb	ZipChip HRN chip	Native Antibody BGE (908 Devices) + 3.8% DMSO, pH ~ 5.5	–	ZipChip interface	Orbitrap	Evaluation of a highly sensitive, high-resolution microfluidic nCE-MS method for antibody charge variant and impurity analysis	Wu et al.[135]
NIST mAb, mAb1 bispecific mAb1	ZipChip HRN chip	Native Antibody BGE (908 Devices) + 3.8% DMSO, pH ~ 5.5	–	ZipChip interface	Orbitrap	Applied ZipChip nCE-MS to investigate therapeutic antibodies under various stress conditions	Wu et al.[136]
mAb1, 2, 3	LPA	5% acetic acid	2% formic acid and 10% methanol	EMASS-II interface	TOF	Good performance of CZE-MS techniques for separating mAbs, half-assembled mAbs as well as free LC fragments	Xu et al.[137]
IgG1, IgG2	PVA	50 mM acetic acid	0.5% acetic acid in 50% methanol	Orthogonal triple tube sheath liquid interface (G1607B)	TOF	Analysis of two mAbs on an intact and reduced level.	Suresh Babu and Gudihal[138]

Abbreviations: **ACE**: Affinity capillary electrophoresis, **BGE**: Background electrolyte, **CESI**: Commercial sheathless interface, **DMSO**: Dimethyl sulfoxide, **ESI**: Electrospray ionization, **HPMC**: Hydroxypropyl methylcellulose, **HRN**: High resolution native, **LCP**: Linear carbohydrate polymer, **LPA**: Linear polyacrylamide, **MCE**: Microfluidic capillary electrophoresis, **PEI**: Polyethylenimine, **PVA**: Polyvinyl alcohol, **SEC**: Size exclusion electrophoresis, **SL**: sheath liquid, **SMIL**: Successive multiple ionic-polymer layers, **TOF**: Time of flight.

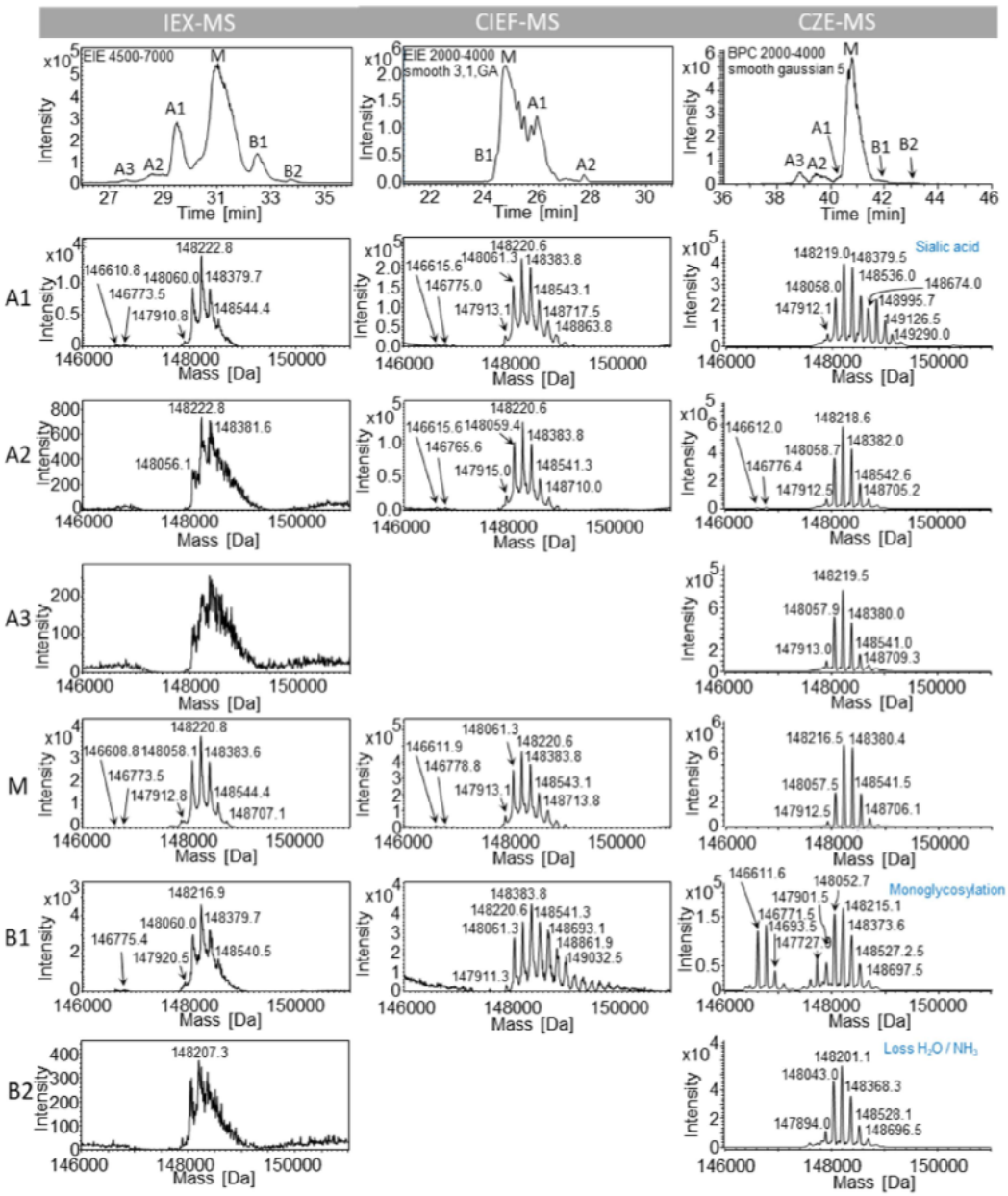

Figure 5. Comparison of CEX-MS, CIEF-MS, and CZE-MS separation and identification of mAb1 variants. For CZE-MS, data were acquired using the Orbitrap fusion Lumos while CEX-MS and CIEF-MS, data were acquired using the MaXis instrument.

amounts that are necessary for variant separation. As a result, our CEX-MS method is only applicable to abundant variants or variants that change the mAb mass to a greater extent. Our CIEF-MS method provides relatively good spectral quality (compare CIEF-MS in Figure 5), even though some mAbs cannot be detected using MS. With our CZE-MS method, low abundant mass and charge variants were detected (compare B2 in the CZE-MS column in Figure 5). Even though our CIEF and CEX spectral quality may seem significantly lower compared to the CZE-MS experiments, it needs to be kept in mind that different mass spectrometers, as well as different methods using the same mass spectrometer, might lead to changing declustering abilities and, thus, different sensitivity. Schwenzer et al. provide a more detailed discussion on this subject.[140]

All separation techniques used for intact mAb analysis selectively separate acidic and basic mAb variants. The lysine variant of three mAbs was used to compare the resolution of the different separation techniques. The resolution calculated between the main variant and the lysine variant of infliximab, USP mAb003, and NIST mAb can be found in supplementary Table S1. The MS incompatible CZE-EACA-UV method provided the highest resolution for all mAbs. Upon the MS-coupled methods, CEX separated the main and the lysine variant of infliximab best, followed by CIEF and CZE. However, for USP mAb003 and NIST mAb, CZE-MS showed the best resolution, possibly influenced by the mass spectra quality of these low-intensity lysine variants. The different selectivity is also evident for monoglycosylation, which is found in the main variant peak using CEX and CIEF and is separated from the main variant peak using the CZE. This CZE size-based selectivity enabled a more detailed analysis of the mAb monoglycosylation and the detection of low-abundant monoglycosylated and aglycosylated species. Additionally, the different selectivity is evident for highly heterogeneous mAbs like cetuximab, where variants were separated by CIEF-UV and CEX-UV but not by CZE-MS (compare cetuximab in Figures 2, 3 , and 4). As shown in Table 4, many variants (marked green) can be unequivocally identified due to these selective separation approaches.

In the literature, a broad mAb variety was analyzed with different methods. Almost every variant was selectively separated and identified for at least one mAb. This study only analyzed a selection of 10 mAbs, but still many variants were selectively separated and identified. Selective separation is the first part of successful mAb variant identification. Sensitive MS detection is a crucial part of the analysis of mAb variants as well. The orange-marked proteoforms in Table 4 were not separated by the respective separation technique and were only identified by sensitive MS detection. Further confirmation by applying a middle-down or peptide mapping method was sometimes needed (*marked proteoforms in Table 4).

All the methods described in this work have an analysis time of around 60 min to provide selective mAb variant separation. In the literature, a similar duration of the methods is described for CEX-MS,[6] CZE-MS,[31] and CIEF-MS[19] to achieve the best possible separation. The method duration can be shortened to some minutes for all techniques,[24,54,121] which proves that measuring time is not the most relevant criterion for the choice of the separation technique of mAb variants on the intact level.

After the mAb variants were analyzed on the intact level, the results can be compared to data obtained on the subunit level. The intact separation and identification of mAb variants is suitable to determine the overall mAb composition. This information is partly lost using the subunit approach if the variants are not on the same subunit moiety. The subunit approach, however, enables a more detailed analysis of the location of the variant within the mAb [141]. Detailed information about the mAb variant is obtained because small mass changes can be better detected on the subunit level compared to the intact level due to a

Table 4. Overview of charge variants analyzed with the different methods for different antibodies. Compared to our approach, for literature assignment other mAbs and stressed mAbs were taken into consideration as well as native CZE-MS approaches. Exemplary literature is given as a reference. Green: separated and identified by MS, orange: only MS detected w/o separation, red: not detected/no information available.

	IEX-MS (intact)		CIEF-MS (intact)		CZE-MS (intact)		CZE-MS (subunit)	
Modification	This study	Lit.	This study	Lit.	This study	Lit.	This study	Lit.
Glycosylation		55				117		108
Glycosylation sialic acids		59		97		31		125
Monoglycosylation		54				117		141
Aglycosylation						117		141
Lysine variants		54	#	19		31		141
Water/ammonium loss		55		19		31		134
Oxidation		68				31		128
Glycation		58		88		131		117
Deamidation	*	54*		19*	*	132*		141
Disulfide modifications								117

*typically further analysis is needed for unequivocal determination; # only separated and not MS detected.

narrower isotopic pattern and possible isotopic resolution using modern time of flight (TOF) and Orbitrap MS instrumentation. Additionally, the modification site can be narrowed down to the subunit moiety and even localized by MS/MS experiments.

With our CZE-MS subunit method (IdeS digested and reduced subunits) sialic acids, glycoforms, glycation, lysine variants, multiple oxidations, water and ammonia losses, and incomplete sample reduction, as well as enzymatic misscleavage, were determined.[34,35] Mono- and aglycosylation of the mAb could be determined based on the detection of aglycosylated Fc/2 fragments. MS/MS experiments were of utmost importance for the determination of the deamidation of pH-stressed mAb1 and the determination of sample preparation-induced modifications. The information gained by fragmentation was only limited when positional isomers were not properly separated and several possible modification sites were available within the subunit. Charge variant analysis of digested and reduced subunits (Fd, light chain, Fc/2) may not be performed selectively with just any separation technique due to, for example, a large change in pI of one or two of the subunits compared to the intact mAb. Subunit analysis on the CEX is mostly done with IdeS enzymatically digested mAbs,[7,55,60,71,142] which leaves a large 100 kDa $F(ab')_2$ fragment. Digested and reduced subunits are not analyzed since the chaotropic salt mandatory in the reduction process interferes with the column and removal of the chaotropic salt might cause disulfide scrambling if the disulfides are not alkylated.

CIEF was used for subunit analysis of cetuximab,[101] but apart from that, CIEF is commonly used for the intact analysis of mAbs. This may be attributed to the fact that different subunit moieties exhibit different pI values. To analyze a wide pI range, a wide pH range is needed during focusing, which potentially reduces the separation performance of charge variants and hamper the generic application of CIEF for different mAbs. CZE is the only method that can be performed independent of differences in pI of the subunits (by use of a sufficiently acidic BGE) or the chaotropic salt needed for reduction, though different resolution of charge variants is still obtained.

Finally, besides all the previously discussed parameters, instrumental parameters and sample-specific requirements have an enormous impact on the selective and sensitive separation and identification of mAb variants. This is especially evident in our CIEF-UV-MS method and CEX-UV-MS method. For both methods, the online UV detection hints at a selective separation of mAb variants, but MS detection and identification of these variants could not be fully achieved because of the previously discussed solubility problem in CIEF and the native ionization in CEX. Our CEX method most likely suffers from the application of a standard LC sprayer in combination with the high flow rate toward the MS. The literature applications shown in Table 1 either attempt to minimize the amount of eluent by using a post-column flow splitter[55,143] or nanoflow-CEX[70] to reduce the amount of salt in the eluents,[21,42,48] or to enhance the ionization efficiency by using special nanoflow and microspray ionization sources.[21,48,53,55,65] Our CIEF most likely suffers from handling and robustness issues in combination with mAb-specific requirements because the CIEF-nanoCEasy-MS was previously successfully applied for the analysis of mAb A variants.[20] For the literature applications shown in Table 2, either a small cartridge[21,74,80,86] or chip[24,73] was used or standard CIEF was coupled to the MS by a nanospray source.[19,20,72,83] All these approaches provide quite high mass spectra quality, even though separation is always impaired in the mobilization step.[19,23] Similar to CIEF, CZE may also benefit from microchip applications,[119,120,133] which provide a fast and efficient separation of mAb variants.[116,121,122] When a standard CZE system is coupled to the MS, the interface is a critical part as shown by Höcker et al..[144] Sample dilution due to excessive SL consumption can significantly reduce the signal intensity.

All aspects mentioned here prove that the method and instrumental setup for mAb variant analysis must be chosen carefully. With the increase in heterogeneity due to new mAb products like antibody-drug-conjugates (ADCs) and bispecific antibodies, the requirements for selective and sensitive variant characterization increase. Compared to mAbs, ADCs are composed of antibodies, linkers and payloads, which substantially increase heterogeneity.[98,145] Depending on the type and linkage of the conjugate, the methods presented here can be applied to separate ADCs, as shown for CEX-MS and icIEF-MS.[98]

In conclusion, no matter if executed on the intact or subunit level, all tested methods have their advantages and disadvantages, but, nevertheless, all of them are valuable for mAb variant characterization.

Some methods are better platform methods (CZE and CEX to a certain extent) while others (CIEF) need further method development especially when considered generic methods. A combination of several methods should always be considered when analyzing mAb variants to get the overall mAb composition.

Materials and methods

Materials

Infliximab (10 mg/mL, charge: 8KMKA90603) and cetuximab (5 mg/mL, charge: 248033), were purchased from Evidentic GmbH (Berlin, Germany). NIST mAb (10 mg/mL, Reference Material 8671, lot: 14HB-D-002) was purchased from the National Institute of Standards and Technology (NIST, Gaithersburg, MD, USA). Protein A purified research antibodies mAb1 (20 mg/mL), mAb2 (16.8 mg/mL), mAb3 (18.3 mg/mL) mAb4 (21.7 mg/mL), and mAb5 (18.5 mg/mL) were kindly provided by Rentschler Biopharma SE (Laupheim, Germany). USP mAb003 (Cat. No. 1445595, LOT: F12980, 10 mg/mL), iminodiacetic acid (IDA), capillary coating material poly(sodium styrene sulfonate) (PSS, polyanion, Mw 70,000 g/mol), 4-(2 hydroxyethyl)-1-piperazineethanesulfonic acid (HEPES), hydroxypropyl cellulose (HPC, Mw: 100.000), triethylenetetramine (TETA, ≥ 97%), sodium hydroxide, 3-(N-morpholino) propane sulfonic acid (MOPS)-buffer, 1,4-dithiothreitol (DTT), and L-arginine were purchased from Sigma-Aldrich (Steinheim, Germany). Hydrofluoric acid (40%(v/v), HF) and hydrochloric acid (1 M, HCl) were purchased from Merck (Darmstadt, Germany). Isopropanol (IPA, LC-MS grade), ammonia solution (ROTIPURAN p. a., 30%), ammonium acetate (LC-MS grade, ≥98%), ACN (ROTISOLV ≥ 99.95%), acetic acid (HAc, ROTIPURAN 100%), and formic acid (FA, ≥98%) were purchased from Carl Roth GmbH & Co. KG (Karlsruhe, Germany). Urea (Ultrapure) was purchased from ThermoFisher Scientific (Dreieich, Germany). Formamide, polyethylene oxide (PEO, Mw:1.000.000), and 6-aminocaproic acid (EACA, ≥99%) were purchased from Alfa Aesar (Kandel, Germany). Pharmalyte pH 3–10, Pharmalyte pH 8–10.5, and Pharmalyte pH 5–8 were obtained from GE Healthcare Bio-Sciences AB (Waukesha, WI, USA). Capillary coating material diethyl aminoethyl-dextran (DEAED, Mw = 500,000 g/mol, Batch 21,046) was from TdBLabs (Uppsala, Sweden). IdeS protease was purchased from GENOVIS (FabRICATOR, 5000 units, Lund, Sweden).

If not otherwise stated samples and chemicals were diluted and dissolved with ultrapure water (UPW) provided by an Ultra Clear TWF UV water system from Siemens (Munich, Germany).

Sample preparation

mAb1 was pH stressed by pipetting 0.5 µL concentrated ammonia solution to 10 µL undiluted mAb1. After 7 days in the dark at room temperature, the sample was directly used for further sample preparation. For intact (native) analysis with CEX, antibodies were diluted with UPW to a final concentration of 2 mg/mL and stored at −20°C until measurement. For CIEF, mAbs were first diluted to a concentration of 1 mg/mL with UPW. Then, each mAb was mixed 1:1 with CIEF master mix, resulting in a final concentration of 0.5 mg/mL mAb in 15% formamide, 1% ampholyte-mix (1:4:2 of Pharmalyte pH 5–8, Pharmalyte pH 8–10.5 and Pharmalyte pH 3–10), 2.5 mM arginine and 0.5 mM IDA. For intact CZE-UV analysis, mAbs were diluted to 1 mg/mL with UPW and for CZE-MS mAbs were diluted to 1 mg/mL in 4 M HAc (also serves as BGE). For subunit analysis, mAbs were first digested using the FabRICATOR digestion protocol of GENOVIS. Two hundred microgram mAb were digested using 200 U of IdeS in 100 mM MOPS buffer at pH 7.2 for 30 min at 37°C and 500 rpm. Following this, mAbs were further reduced in 4 M urea using DTT for 60 min at 37°C and 500 rpm. Detailed sample preparation parameters can be found elsewhere.[34]

Separation approaches

All CIEF and CZE experiments were conducted on an Agilent 7100 CE instrument (Agilent Technologies GmbH, Waldbronn, Germany). If not otherwise stated fused silica capillaries (separation capillary: 50 µm ID, 365 µm; sheath liquid capillary: OD 100 µm ID, 240 µm OD) were purchased from Polymicro Technologies (Phoenix, AZ, USA). CIEF-MS and CZE-MS using the nanoCEasy interface require the

etching of the separation capillary at one end as described in detail elsewhere.[34] Briefly, for capillary etching, the polyimide was removed from the capillary end and then dipped into concentrated HF for 60 min. Detailed information on the nanoCEasy interface can be found in the work of Schlecht et al.[146]

Ion exchange chromatography of intact mAbs

All samples were analyzed on an UltiMate™3000 HPLC system from Dionex (Germering, Germany), equipped with a variable wavelength detector VWD-3400 and directly coupled to the MS. The column used for all separations was a Proteomix® SCX-NP3 (2.1 mm × 100 mm) from Sepax Technologies (Delaware, USA). A 100 µL/min flow rate was applied, and the column temperature was held at 40°C. The injection volume was 12.5 µL, resulting in 25 µg of antibody on the column. The mAb variants were separated with a combined salt and pH gradient. Mobile phase A consists of 50 mM ammonium acetate + 2% ACN, at pH 5.0 (adjusted with acetic acid), and mobile phase B consists of 100 mM ammonium acetate + 2% ACN, at pH 8.5 (adjusted with ammonia solution). Subsequently, the eluents were degassed using an ultrasonic bath. The gradient started at 55% [B] for 2 min and was raised over 25 min to 85% [B]. The amount of [B] was quickly increased to 100% [B] over 0.1 min and held for 2 min. Afterward, the column was brought back to starting conditions over 0.1 min and re-equilibrated for 11 min. The total run time was 40 min. Online UV detection was performed at 280 nm.

Capillary isoelectric focusing of intact mAbs

PVA-coated separation capillaries (50 µm ID, 365 µm OD, 60 cm total length, 49 cm effective length) were kindly provided by Agilent Technologies (Waldbronn, Germany). Before each analysis, the PVA capillary was flushed (950 mbar) with UPW, 4 M urea, and UPW for 5 min each. The sample was injected for 120 seconds at 950 mbar to guarantee complete capillary filling. The ends of the capillary were then dipped in anolyte (1% FA, CZE inlet side) and catholyte (0.2% ammonium hydroxide; CZE outlet side), and a focusing voltage of 20 kV was applied for 20 min. After focusing, the voltage was turned off to switch to 0.5% FA for mobilization. Mobilization was done at 20 kV until the mAb was detected with the internal UV detector of the CZE instrument at 280 nm.

Capillary zone electrophoresis UV-system of intact mAbs

The separation system for UV detection was adapted from He et al..[25] A 60 cm (effective length: 52 cm) fused silica capillary (50 µm ID/365 µm OD) was used for the separation. A mixture of 400 mM EACA, 0.05% m/v HPC, 2 mM TETA, at pH 5.7 was used as BGE, and samples were diluted to 1 mg/mL in UPW. The capillary was flushed (950 mbar) previous to the first separation with 0.1 M HCl for 5 min and BGE for 10 min, followed by the application of 30 kV for 10 min. Samples were injected at 50 mbar for 8 seconds. The separation voltage was 30 kV and separated variants were detected at 214 nm with the internal UV detector of the CZE instrument. Between runs, the capillary was flushed (950 mbar) with 1 M HCl for 1 min followed by BGE for 3 min.

Capillary zone electrophoresis MS-system of intact mAbs

The etched fused silica separation capillary had a length of 60 cm and was coated with SMIL according to Dhellemmes et al.[147] and Höchsmann et al..[30] Briefly, the capillary is prepared by flushing with 1 M sodium hydroxide (10 min), UPW (5 min), and 20 mM aqueous HEPES solution (pH 7.4; 10 min). The coating is established by alternate flushing of DEAED and PSS solution (3 g/L in 20 mM HEPES solution; pH 7.4; 7 min), including a rinsing step with HEPES solution for 3 min after each polymer layer. After five layers have been applied a waiting step (5 min), a flushing step with UPW (3 min), and a final flushing step with BGE (4 M HAc;10 min) complete the coating procedure. All coating steps were performed at 2 bar external pressure. For measurement samples were hydrodynamically injected (40 mbar,5 seconds) and the separation was executed in 4 M HAc at −20 kV for 60 min. BGE was exchanged after two measurements to prevent contamination and capillaries were stored overnight in BGE.

Capillary zone electrophoresis MS-system of subunit mAbs

The detailed method can be found elsewhere.[34] Briefly, an etched 60 cm PEO-coated capillary was used. First, capillaries were etched with HF (40% (v/v)) for 1 hour followed by PEO coating of the capillary. For

the PEO coating, the capillary was prepared with 1 M NaOH, water, and 1 M HCl for 5 min, respectively, followed by the PEO coating solution for 10 min, water, and BGE for 5 min, respectively. The solutions were flushed using an external pressure of three bar. The BGE consisted of 10% IPA in water containing 1 M FA. Sample injection was done hydrodynamically using 50 mbar pressure for 10 seconds. A 20 kV voltage was applied for the separation.

MS instrumentation

CEX-MS coupling

Native CEX was coupled to a maXis Q-TOF from Bruker Daltonics (Bremen, Germany) using an ESI source. The integrated valve at the MS was used to direct the flow to the source or the waste. The MS method consisted of three segments adjusted to the mAb elution time. In segments one and three, the valve is in the waste position and the ES voltage is turned off, while in segment two the valve is in the source position and the ES voltage is turned on. After calibrating the MS in the high mass range, measurements were done using a capillary voltage of 4500 V, an endplate offset of 500 V, a nebulizer pressure of 2.5 bar, and a dry gas flow and temperature of 8 L/min and 220°C, respectively. The acquisition was done from 1500 to 8000 m/z.

CIEF-MS coupling

The CIEF was coupled to a maXis Q-TOF from Bruker Daltonics (Bremen, Germany) using the nanoCEasy interface, which was supervised using a digital microscope (Dino-Lite, Almere, The Netherlands). Instead of an outlet CIEF vial the end of the separation capillary is introduced to a glass emitter that was purchased from BioMedical Instruments (Zöllnitz, Germany). The emitter had a 30 µm tip opening and a tip length of 4 mm and was placed 3 mm in front of the MS orifice. The integrated valve at the MS and two syringe pumps were used to switch from catholyte (0.2% ammonium hydroxide) during focusing to sheath liquid (ACN: UPW 1:1 + 0.5% FA) during mobilization. The MS method consisted of two segments. In segment one, during focusing, the ES voltage is turned off, the catholyte is flushed to the emitter and the separation capillary is positioned behind the sheath liquid capillary. In segment two, during mobilization the ES voltage is turned on, the sheath liquid (SL) is flushed to the emitter, and the separation capillary is placed close behind the emitter tip in front of the SL capillary. Here, the 20 kV CIEF voltage can be maintained during focusing and mobilization. Online UV detection was done at 280 nm using an external ECD2600 EX UV detector (ECOM spol. S r.o., Prague, Czech Republic). MS acquisition was done using a capillary voltage of 2000 V, a dry gas flow of 3 L/min, and a dry gas temperature of 200°C in the mass range from 250 to 4500 m/z.

CZE-MS coupling

The CZE was coupled to an Orbitrap Fusion Lumos (Thermo Fisher Scientific, SanJose, CA, USA) using the nanoCEasy interface and a digital microscope (Dino-Lite, Almere, The Netherlands). The same emitters as for the CIEF application were used. IPA: UPW (50:50) + 0.5% FA was utilized as SL. MS acquisition was performed using a capillary voltage of 2000 V, sweep gas of 3 Arb, and 300°C ion transfer tube temperature. The MS was operated in positive ionization mode using a mass range of 700–4000 m/z and a resolution of 30,000. Further MS parameters can be found in the publications of Höchsmann et al.[30] and Schairer et al.,[34] respectively

Data evaluation

Theoretical mAb masses and pI values were calculated sequence-based with ProtPi (https://www.protpi.ch). CEX-UV data were processed with Chromeleon™ 7 (Thermo Fisher Scientific) analysis software. CIEF-UV data were processed with ECOMAC – ECOM Acquisition and Control Version 2.9.5.0 software and CZE-UV was processed with CEval 0.6h9 (available at: https://echmet.natur.cuni.cz/). For variant analysis, the CEX-MS, CIEF-MS, and CZE-MS data were 0.2 min time-sliced and processed using Intact Mass 3.4 (Protein Metrics). Additionally, CEX-MS and CIEF-MS data were evaluated using Data Analysis 6.0 (Bruker Daltonics). CZE-MS data were additionally processed using Freestyle 1.8 (Thermo Fisher Scientific).

Abbreviations

A	Acidic variant
ACN	Acetonitrile
ADCs	Antibody-drug-conjugates
B	Basic variant
BGE	Background electrolyte
BPEs	Base peak electropherograms
CEX	Cation exchange chromatography
(i)CIEF	(imaged) Capillary isoelectric focusing
CZE	Capillary zone electrophoresis
DEAED	Diethylaminoethyl-dextran
EACA	6-aminocaproic acid
EICs	Extracted ion chromatograms
EIEs	Extracted ion electropherograms
EOF	Electroosmotic flow
ES	Electrospray
ESI	Electrospray ionization
FA	Formic acid
HAc	Acetic acid
HCl	Hydrochloric acid
HEPES	4-(2hydroxyethyl)-1-piperazineethanesulfonic acid
HF	Hydrofluoric acid
HPC	Hydroxypropyl cellulose
ID	Inner diameter
IDA	Iminodiacetic acid
IPA	Isopropanol, LPA: Linear polyacrylamide
M	Main variant
mAb	Monoclonal antibody
MES	2-(N-morpholino)ethanesulfonic acid
MS	Mass spectrometry
OD	Outer diameter
pI	Isoelectric point
PSS	Poly(sodium styrene sulfonate)
PVA	Polyvinyl alcohol
R	Resolution
SL	Sheath liquid
SMIL	Successive multiple ionic-polymer layers
TETA	Triethylenetetramine
UPW	Ultrapure water

Acknowledgments

The authors thank Rentschler Biopharma SE for financial support and for providing samples as well as Isabel Schuster for the initial CEX-UV as well as Lea Münzinger and Hanna Ernst for the initial CEX-UV-MS experiments.

Disclosure statement

No potential conflict of interest was reported by the author(s).

Funding

The author(s) reported that there is no funding associated with the work featured in this article.

ORCID

Jasmin Schairer http://orcid.org/0009-0007-3526-1998
Alisa Höchsmann http://orcid.org/0009-0006-3724-9792
Jennifer Römer http://orcid.org/0000-0001-6841-0389
Christian Neusüß http://orcid.org/0000-0003-2404-4924

Data availability statement

The data that support the findings of this study are available from the corresponding author, [CN], upon reasonable request.

References

1. Crescioli S, Kaplon H, Wang L, Visweswaraiah J, Kapoor V, Reichert JM. Antibodies to watch in 2025. Mabs-austin. 2025;17(1):2443538. doi: 10.1080/19420862.2024.2443538. PMID:39711140.
2. Naumann L, Schlossbauer P, Klingler F, Hesse F, Otte K, Neusüß C. High-throughput glycosylation analysis of intact monoclonal antibodies by mass spectrometry coupled with capillary electrophoresis and liquid chromatography. J Sep Sci. 2022;45(12):2034–2044. doi: 10.1002/jssc.202100865. PMID:35044720.
3. Farsang E, Murisier A, Horváth K, Beck A, Kormány R, Guillarme D, Fekete S. Tuning selectivity in cation-exchange chromatography applied for monoclonal antibody separations, part 1: alternative mobile phases and fine tuning of the separation. J Pharm Biomed Anal. 2019;168:138–147. doi: 10.1016/j.jpba.2019.02.024.
4. Fekete S, Beck A, Fekete J, Guillarme D. Method development for the separation of monoclonal antibody charge variants in cation exchange chromatography, part I: salt gradient approach. J Pharm Biomed Anal. 2015;102:33–44. doi: 10.1016/j.jpba.2014.08.035. PMID:25240157.
5. Bailey AO, Han G, Phung W, Gazis P, Sutton J, Josephs JL, Sandoval W. Charge variant native mass spectrometry benefits mass precision and dynamic range of monoclonal antibody intact mass analysis. Mabs-austin. 2018;10(8):1214–1225. doi: 10.1080/19420862.2018.1521131. PMID:30339478.
6. Sankaran PK, Kabadi PG, Honnappa CG, Subbarao M, Pai HV, Adhikary L, Palanivelu DV. Identification and quantification of product-related quality attributes in bio-therapeutic monoclonal antibody via a simple, and robust cation-exchange HPLC method compatible with direct online detection of UV and native ESI-QTOF-MS analysis. J Chromatogr B. 2018;1102-1103:83–95. doi: 10.1016/j.jchromb.2018.10.019.
7. Leblanc Y, Faid V, Lauber MA, Wang Q, Bihoreau N, Chevreux G. A generic method for intact and subunit level characterization of mAb charge variants by native mass spectrometry. J Chromatogr B. 2019;1133:121814. doi: 10.1016/j.jchromb.2019.121814.
8. Goyon A, D'Atri V, Bobaly B, Wagner-Rousset E, Beck A, Fekete S, Guillarme D. Protocols for the analytical characterization of therapeutic monoclonal antibodies. I - Non-denaturing chromatographic techniques. J Chromatogr: B, Analytical Technol Biomed Life Sci. 2017;1058:73–84. doi: 10.1016/j.jchromb.2017.05.010. PMID:28549280.
9. Lingg N, Berndtsson M, Hintersteiner B, Schuster M, Bardor M, Jungbauer A. Highly linear pH gradients for analyzing monoclonal antibody charge heterogeneity in the alkaline range: validation of the method parameters. J Chromatogr A. 2014;1373:124–130. doi: 10.1016/j.chroma.2014.11.021. PMID:25465369.
10. Zhang L, Patapoff T, Farnan D, Zhang B. Improving pH gradient cation-exchange chromatography of monoclonal antibodies by controlling ionic strength. J Chromatogr A. 2013;1272:56–64. doi: 10.1016/j.chroma.2012.11.060. PMID:23253120.
11. Farnan D, Moreno GT. Multiproduct high-resolution monoclonal antibody charge variant separations by pH gradient ion-exchange chromatography. Anal Chem. 2009;81(21):8846–8857. doi: 10.1021/ac901408j. PMID:19795895.
12. Murisier A, Duivelshof BL, Fekete S, Bourquin J, Schmudlach A, Lauber MA, Nguyen JM, Beck A, Guillarme D, D'Atri V. Towards a simple on-line coupling of ion exchange chromatography and native mass spectrometry for the detailed characterization of monoclonal antibodies. J Chromatogr A. 2021;1655:462499. doi: 10.1016/j.chroma.2021.462499. PMID:34487883.
13. Ascione A, Belfiore M, Vesterinen J, Buda M, Holtkamp W, Luciani F. Charge heterogeneity of therapeutic monoclonal antibodies by different cIEF systems: views on the current situation. Mabs-austin. 2024;16(1):2313737. doi: 10.1080/19420862.2024.2313737. PMID:38332713.
14. Wu G, Gao X, Huang Z, Yu X, Du J, Mei Y, Yu C. High sensitivity charge heterogeneity characterization of blinatumomab product by imaged capillary isoelectric focusing with native UV fluorescence detection. J Pharm Biomed Anal. 2025;265:117016. doi: 10.1016/j.jpba.2025.117016. PMID:40483960.
15. Ghizzani V, Ascione A, Gonnella F, Massolini G, Luciani F. Exploring imaged capillary isoelectric focusing parameters for enhanced charge variants quality control. Front Chem. 2025;13:1536222. doi: 10.3389/fchem.2025.1536222. PMID:40084275.

16. Sutton H, Hong F, Han X, Rauniyar N. Analysis of therapeutic monoclonal antibodies by imaged capillary isoelectric focusing (icIEF). Ana Methods. 2024;16(31):5450–5458. doi: 10.1039/D4AY00836G.
17. Cao J, Sun W, Gong F, Liu W. Charge profiling and stability testing of biosimilar by capillary isoelectric focusing. Electrophoresis. 2014;35(10):1461–1468. doi: 10.1002/elps.201300471. PMID:24610636.
18. Lin J, Tan Q, Wang S. A high-resolution capillary isoelectric focusing method for the determination of therapeutic recombinant monoclonal antibody. J Sep Sci. 2011;34(14):1696–1702. doi: 10.1002/jssc.201100067. PMID:21656678.
19. Dai J, Lamp J, Xia Q, Zhang Y. Capillary isoelectric focusing-mass spectrometry method for the separation and online characterization of intact monoclonal antibody charge variants. Anal Chem. 2018;90(3):2246–2254. doi: 10.1021/acs.analchem.7b04608. PMID:29272582.
20. Naghdi E, Reinau ME, Krogh TN, Neusüß C. Chemical mobilization-based capillary isoelectric focusing–mass spectrometry using the nanoCeasy interface for pharmaceutical protein analysis. Anal Chem. 2024;96:12827–12837. doi: 10.1021/acs.analchem.4c02441.
21. Wu G, Yu C, Wang W, Du J, Fu Z, Xu G, Li M, Wang L. Mass spectrometry-based charge heterogeneity characterization of therapeutic mAbs with imaged capillary isoelectric focusing and ion-exchange chromatography as separation techniques. Anal Chem. 2023;95(4):2548–2560. doi: 10.1021/acs.analchem.2c05071. PMID:36656605.
22. Ostrowski MA, Mack S, Ninonuevo M, Yan J, ElNaggar M, Gentalen E, Michels DA. Rapid multi-attribute characterization of intact bispecific antibodies by a microfluidic chip-based integrated icIEF-MS technology. Electrophoresis. 2023;44(3–4):378–386. doi: 10.1002/elps.202200165. PMID:36200174.
23. Kwok T, Chan SL, Xu N, Huang T, Bo T. Advancing protein heterogeneity analysis: nano-flow pressure mobilization for precise icIEF fractionation and online MS detection. Analytical Biochem. 2025;701:115825. doi: 10.1016/j.ab.2025.115825. PMID:40037501.
24. Mack S, Arnold D, Bogdan G, Bousse L, Danan L, Dolnik V, Ducusin M, Gwerder E, Herring C, Jensen M, et al. A novel microchip-based imaged CIEF-MS system for comprehensive characterization and identification of biopharmaceutical charge variants. Electrophoresis. 2019;40(23–24):3084–3091. doi: 10.1002/elps.201900325. PMID:31663138.
25. He Y, Isele C, Hou W, Ruesch M. Rapid analysis of charge variants of monoclonal antibodies with capillary zone electrophoresis in dynamically coated fused-silica capillary. J Of Separation Sci. 2011;34(5):548–555. doi: 10.1002/jssc.201000719. PMID:21265019.
26. Moritz B, Schnaible V, Kiessig S, Heyne A, Wild M, Finkler C, Christians S, Mueller K, Zhang L, Furuya K, et al. Evaluation of capillary zone electrophoresis for charge heterogeneity testing of monoclonal antibodies. J Chromatogr B. 2015;983-984:101–110. doi: 10.1016/j.jchromb.2014.12.024.
27. Meudt M, Pannek M, Glogowski N, Higel F, Thanisch K, Knape MJ. CE methods for charge variant analysis of mAbs and complex format biotherapeutics. Electrophoresis. 2024;45(15–16):1295–1306. doi: 10.1002/elps.202300170. PMID:38233206.
28. Moritz B, Locatelli V, Niess M, Bathke A, Kiessig S, Entler B, Finkler C, Wegele H, Stracke J. Optimization of capillary zone electrophoresis for charge heterogeneity testing of biopharmaceuticals using enhanced method development principles. Electrophoresis. 2017;38(24):3136–3146. doi: 10.1002/elps.201700145. PMID:28887890.
29. Wiesner R, Zagst H, Lan W, Bigelow S, Holper P, Hübner G, Josefsson L, Lancaster C, Lo L, Lößner C, et al. An interlaboratory capillary zone electrophoresis-UV study of various monoclonal antibodies, instruments, and ε-aminocaproic acid lots. Electrophoresis. 2023;44(15–16):1247–1257. doi: 10.1002/elps.202200284. PMID:37079448.
30. Höchsmann A, Dhellemmes L, Leclercq L, Cottet H, Neusüß C. Charge variant analysis of monoclonal antibodies by CZE-MS using a successive multiple ionic-polymer layer coating based on diethylaminoethyl-dextran. Electrophoresis. 2024;46(5–6):279–289. doi: 10.1002/elps.202400084. PMID:39287066.
31. van der Zon AA, Höchsmann A, Bos TS, Neusüß C, Somsen GW, Jooß K, Haselberg R, Gargano AF. Characterization of monoclonal antibody charge variants under near-native separation conditions using nano-flow sheath liquid capillary electrophoresis-mass spectrometry. Analytica (Rome) Acta. 2024;1331:343287. doi: 10.1016/j.aca.2024.343287.
32. Füssl F, Carillo S, Millán-Martín S, Jakes C, Bora K, Liberatori S, Graham J, Bones J. Exploring proteoforms of the IgG2 monoclonal antibody panitumumab using microchip capillary electrophoresis-mass spectrometry. J Pharm Biomed Anal. 2023;234:115494. doi: 10.1016/j.jpba.2023.115494. PMID:37300951.
33. Cageling R, Carillo S, Boumeester AJ, Lubbers-Geuijen K, Bones J, Jooß K, Somsen GW. Microfluidic capillary electrophoresis - mass spectrometry for rapid charge-variant and glycoform assessment of monoclonal antibody biosimilar candidates. J Pharm Biomed Anal. 2024;248:116301. doi: 10.1016/j.jpba.2024.116301. PMID:38901155.
34. Schairer J, Römer J, Lang D, Neusüß C. CE-MS/MS and CE-timsTOF to separate and characterize intramolecular disulfide bridges of monoclonal antibody subunits and their application for the assessment of subunit reduction protocols. Anal Bioanal Chem. 2024;416(7):1599–1612. doi: 10.1007/s00216-024-05161-8. PMID:38296860.

35. Schairer J, Römer J, Neusüß C. CE-MS and CE-MS/MS for the multiattribute analysis of monoclonal antibody variants at the subunit level. J Pharm Biomed Anal. 2025;252:116495. doi: 10.1016/j.jpba.2024.116495.
36. Fekete S, Beck A, Fekete J, Guillarme D. Method development for the separation of monoclonal antibody charge variants in cation exchange chromatography, part II: pH gradient approach. J Pharm Biomed Anal. 2015;102:282–289. doi: 10.1016/j.jpba.2014.09.032. PMID:25459925.
37. Rea JC, Moreno GT, Lou Y, Farnan D. Validation of a pH gradient-based ion-exchange chromatography method for high-resolution monoclonal antibody charge variant separations. J Pharm Biomed Anal. 2011;54(2):317–323. doi: 10.1016/j.jpba.2010.08.030. PMID:20884149.
38. Dakshinamurthy P, Mukunda P, Prasad Kodaganti B, Shenoy BR, Natarajan B, Maliwalave A, Halan V, Murugesan S, Maity S. Charge variant analysis of proposed biosimilar to trastuzumab. Biologicals. 2017;46:46–56. doi: 10.1016/j.biologicals.2016.12.006. PMID:28087106.
39. Kahle J, Zagst H, Wiesner R, Wätzig H. Comparative charge-based separation study with various capillary electrophoresis (CE) modes and cation exchange chromatography (CEX) for the analysis of monoclonal antibodies. J Pharm Biomed Anal. 2019;174:460–470. doi: 10.1016/j.jpba.2019.05.058. PMID:31228849.
40. Rea JC, Freistadt BS, McDonald D, Farnan D, Wang YJ. Capillary ion-exchange chromatography with nanogram sensitivity for the analysis of monoclonal antibodies. J Chromatogr A. 2015;1424:77–85. doi: 10.1016/j.chroma.2015.11.002. PMID:26596872.
41. Goyon A, Excoffier M, Janin-Bussat M-C, Bobaly B, Fekete S, Guillarme D, Beck A. Determination of isoelectric points and relative charge variants of 23 therapeutic monoclonal antibodies. J Chromatogr: B, Analytical Technol Biomed Life Sci. 2017;1065-1066:119–128. doi: 10.1016/j.jchromb.2017.09.033. PMID:28961486.
42. Füssl F, Millán-Martín S, Bones J, Carillo S. Cation exchange chromatography on a monodisperse 3 µm particle enables extensive analytical similarity assessment of biosimilars. J Pharm Biomed Anal. 2023;234:115534. doi: 10.1016/j.jpba.2023.115534. PMID:37343453.
43. Moorhouse K, Nashabeh W, Deveney J, Bjork N, Mulkerrin M, Ryskamp T. Validation of an HPLC method for the analysis of the charge heterogeneity of the recombinant monoclonal antibody IDEC-C2B8 after papain digestion. J Pharm Biomed Anal. 1997;16(4):593–603. doi: 10.1016/S0731-7085(97)00178-7.
44. Gaza-Bulseco G, Bulseco A, Chumsae C, Liu H. Characterization of the glycosylation state of a recombinant monoclonal antibody using weak cation exchange chromatography and mass spectrometry. J Chromatogr B. 2008;862(1–2):155–160. doi: 10.1016/j.jchromb.2007.12.001. PMID:18164669.
45. Griaud F, Denefeld B, Lang M, Hensinger H, Haberl P, Berg M. Unbiased in-depth characterization of CEX fractions from a stressed monoclonal antibody by mass spectrometry. Mabs-austin. 2017;9(5):820–830. doi: 10.1080/19420862.2017.1313367. PMID:28379786.
46. Liu H, Ren W, Zong L, Zhang J, Wang Y. Characterization of recombinant monoclonal antibody charge variants using WCX chromatography, icIEF and LC-MS/MS. Analytical Biochem. 2019;564-565:1–12. doi: 10.1016/j.ab.2018.10.002. PMID:30291836.
47. Ponniah G, Kita A, Nowak C, Neill A, Kori Y, Rajendran S, Liu H. Characterization of the acidic species of a monoclonal antibody using weak cation exchange chromatography and LC-MS. Anal Chem. 2015;87(17):9084–9092. doi: 10.1021/acs.analchem.5b02385. PMID:26222016.
48. Haberger M, Heidenreich A-K, Hook M, Fichtl J, Lang R, Cymer F, Adibzadeh M, Kuhne F, Wegele H, Reusch D, et al. Multiattribute monitoring of antibody charge variants by cation-exchange chromatography coupled to native mass spectrometry. J Am Soc Mass Spectrom. 2021;32(8):2062–2071. doi: 10.1021/jasms.0c00446. PMID:33687195.
49. Wagner-Rousset E, Fekete S, Morel-Chevillet L, Colas O, Corvaïa N, Cianférani S, Guillarme D, Beck A. Development of a fast workflow to screen the charge variants of therapeutic antibodies. J Chromatogr A. 2017;1498:147–154. doi: 10.1016/j.chroma.2017.02.065. PMID:28400066.
50. Verscheure L, Detremmerie S, Stals H, de VJ, Sandra P, Lynen F, Borgions F, Sandra K. Multidimensional LC-MS with 1D multi-method option and parallel middle-up and bottom-up MS acquisition for in-depth characterization of antibodies. J Chromatogr A. 2024;1726:464947. doi: 10.1016/j.chroma.2024.464947. PMID:38724406.
51. Verscheure L, Cerdobbel A, Sandra P, Lynen F, Sandra K. Monoclonal antibody charge variant characterization by fully automated four-dimensional liquid chromatography-mass spectrometry. J Chromatogr A. 2021;1653:462409. doi: 10.1016/j.chroma.2021.462409. PMID:34325295.
52. Gstöttner C, Klemm D, Haberger M, Bathke A, Wegele H, Bell C, Kopf R. Fast and automated characterization of antibody variants with 4D HPLC/MS. Anal Chem. 2018;90(3):2119–2125. doi: 10.1021/acs.analchem.7b04372. PMID:29264912.
53. Talebi M, Nordborg A, Gaspar A, Lacher NA, Wang Q, He XZ, Haddad PR, Hilder EF. Charge heterogeneity profiling of monoclonal antibodies using low ionic strength ion-exchange chromatography and well-controlled pH gradients on monolithic columns. J Chromatogr A. 2013;1317:148–154. doi: 10.1016/j.chroma.2013.08.061. PMID:24011724.
54. Füssl F, Cook K, Scheffler K, Farrell A, Mittermayr S, Bones J. Charge variant analysis of monoclonal antibodies using direct coupled pH gradient cation exchange chromatography to high-resolution native mass spectrometry. Anal Chem. 2018;90(7):4669–4676. doi: 10.1021/acs.analchem.7b05241. PMID:29494133.

55. Yan Y, Liu AP, Wang S, Daly TJ, Li N. Ultrasensitive characterization of charge heterogeneity of therapeutic monoclonal antibodies using strong cation exchange chromatography coupled to native mass spectrometry. Anal Chem. 2018;90(21):13013–13020. doi: 10.1021/acs.analchem.8b03773. PMID:30280893.
56. Füssl F, Trappe A, Cook K, Scheffler K, Fitzgerald O, Bones J. Comprehensive characterisation of the heterogeneity of adalimumab via charge variant analysis hyphenated on-line to native high resolution orbitrap mass spectrometry. Mabs-austin. 2019;11(1):116–128. doi: 10.1080/19420862.2018.1531664. PMID:30296204.
57. Ippoliti S, Schmudlach A, Lauber MA. Online IEX-MS of mAb charge variants using a BioResolve SCX mAb column, IonHance CX-MS pH concentrates, and BioAccord system. Application Note. 2019:1–14.
58. Phung W, Han G, Polderdijk SG, Dillon M, Shatz W, Liu P, Wei B, Suresh P, Fischer D, Spiess C, et al. Characterization of bispecific and mispaired IgGs by native charge-variant mass spectrometry. Int J Mass Spectrom. 2019;446:116229. doi: 10.1016/j.ijms.2019.116229.
59. Füssl F, Trappe A, Carillo S, Jakes C, Bones J. Comparative elucidation of cetuximab heterogeneity on the intact protein level by cation exchange chromatography and capillary electrophoresis coupled to mass spectrometry. Anal Chem. 2020;92(7):5431–5438. doi: 10.1021/acs.analchem.0c00185. PMID:32105056.
60. Ma F, Raoufi F, Bailly MA, Fayadat-Dilman L, Tomazela D. Hyphenation of strong cation exchange chromatography to native mass spectrometry for high throughput online characterization of charge heterogeneity of therapeutic monoclonal antibodies. Mabs-austin. 2020;12(1):1763762. doi: 10.1080/19420862.2020.1763762. PMID:32370592.
61. Rouby G, Tran NT, Leblanc Y, Taverna M, Bihoreau N. Investigation of monoclonal antibody dimers in a final formulated drug by separation techniques coupled to native mass spectrometry. Mabs-austin. 2020;12(1):e1781743. doi: 10.1080/19420862.2020.1781743. PMID:32633190.
62. Shi RL, Xiao G, Dillon TM, Ricci MS, Bondarenko PV. Characterization of therapeutic proteins by cation exchange chromatography-mass spectrometry and top-down analysis. Mabs-austin. 2020;12(1):1739825. doi: 10.1080/19420862.2020.1739825. PMID:32292112.
63. Di Marco F, Berger T, Esser-Skala W, Rapp E, Regl C, Huber CG. Simultaneous monitoring of monoclonal antibody variants by strong cation-exchange chromatography hyphenated to mass spectrometry to assess quality attributes of rituximab-based biotherapeutics. Int J Mol Sci. 2021;22(16):9072. doi: 10.3390/ijms22169072. PMID:34445776.
64. Duivelshof BL, Beck A, Guillarme D, D'Atri V. Bispecific antibody characterization by a combination of intact and site-specific/chain-specific LC/MS techniques. Talanta. 2022;236:122836. doi: 10.1016/j.talanta.2021.122836. PMID:34635226.
65. Liu AP, Yan Y, Wang S, Li N. Coupling anion exchange chromatography with native mass spectrometry for charge heterogeneity characterization of monoclonal antibodies. Anal Chem. 2022;94(16):6355–6362. doi: 10.1021/acs.analchem.2c00707. PMID:35420790.
66. Dai J, Ji C. In-depth size and charge variants characterization of monoclonal antibody with native mass spectrometry. Anal Chim Acta. 2023;1265:341360. doi: 10.1016/j.aca.2023.341360.
67. van Schaick G, Domínguez-Vega E, Castel J, Wuhrer M, Hernandez-Alba O, Cianférani S. Online collision-induced unfolding of therapeutic monoclonal antibody glyco-variants through direct hyphenation of cation exchange chromatography with native ion mobility–mass spectrometry. Anal Chem. 2023;95(8):3932–3939. doi: 10.1021/acs.analchem.2c03163.
68. VanAernum ZL, Sergi JA, Dey M, Toner T, Kilgore B, Lay-Fortenbery A, Wang Y, Bian S, Kochert BA, Bothe JR, et al. Discovery and control of succinimide formation and accumulation at aspartic acid residues in the complementarity-determining region of a therapeutic monoclonal antibody. Pharm Res. 2023;40(6):1411–1423. doi: 10.1007/s11095-022-03462-0.
69. Shah A, Cui W, Harrahy J, Ivanov AR. Characterization of charge variants, including post-translational modifications and proteoforms, of bispecific antigen-binding protein by cation-exchange chromatography coupled to native mass spectrometry. Talanta. 2024;266:125062. doi: 10.1016/j.talanta.2023.125062. PMID:37566926.
70. Zhai Z, Mavridou D, Damian M, Mutti FG, Schoenmakers PJ, Gargano AFG. Characterization of complex proteoform mixtures by online nanoflow ion-exchange chromatography-native mass spectrometry. Anal Chem. 2024;96(22):8880–8885. doi: 10.1021/acs.analchem.4c01760. PMID:38771719.
71. Leblanc Y, Ramon C, Bihoreau N, Chevreux G. Charge variants characterization of a monoclonal antibody by ion exchange chromatography coupled on-line to native mass spectrometry: case study after a long-term storage at +5°C. J Chromatogr: B, Analytical Technol Biomed Life Sci. 2017;1048:130–139. doi: 10.1016/j.jchromb.2017.02.017. PMID:28242492.
72. Beloborodov SS, Schneider BB, Oleschuk RD, Yves Le Blanc JC. Open port interface for coupling capillary electrophoresis and mass spectrometry: performance evaluation for capillary isoelectric focusing. J Am Soc Mass Spectrom. 2023;34(10):2107–2116. doi: 10.1021/jasms.3c00060. PMID:37650584.
73. He X, ElNaggar M, Ostrowski MA, Guttman A, Gentalen E, Sperry J. Evaluation of an icIEF-MS system for comparable charge variant analysis of biotherapeutics with rapid peak identification by mass spectrometry. Electrophoresis. 2022;43(11):1215–1222. doi: 10.1002/elps.202100295. PMID:35286725.

74. Kwok T, Chan SL, Courtney M, Zhou M, Huang T, Bo T, Li V, Chen T. Imaged capillary isoelectric focusing tandem high-resolution mass spectrometry using nano electrospray ionization (ESI) for protein heterogeneity characterization. Analytical Biochem. 2023;680:115312. doi: 10.1016/j.ab.2023.115312. PMID:37683714.
75. Kwok T, Chan SL, Shi J, Zhou M, Schaefer A, Bo T, Li V, Huang T, Chen T. Imaged capillary isoelectric focusing employing fluorocarbon and methylcellulose coated fused silica capillary for characterization of charge heterogeneity of protein biopharmaceuticals. Separ Sci Plus. 2023;6(5). doi: 10.1002/sscp.202200160.
76. Kwok T, Zhou M, Schaefer A, Bo T, Li V, Huang T, Chen T. Fractionation and online mass spectrometry based on imaged capillary isoelectric focusing (icIEF) for characterizing charge heterogeneity of therapeutic antibody. Ana Methods. 2023;15(4):411–418. doi: 10.1039/d2ay01670b. PMID:36537584.
77. Li M, Zhao X, Shen D, Wu G, Wang W, Yu C, Sausen J, Xu H, Wang L. Identification of a monoclonal antibody clipping variant by cross-validation using capillary electrophoresis – sodium dodecyl sulfate, capillary zone electrophoresis – mass spectrometry and capillary isoelectric focusing – mass spectrometry. J Chromatogr A. 2022;1684:463560. doi: 10.1016/j.chroma.2022.463560.
78. Madda R, Nichiporuk R, ElNaggar M. [accessed 2024 Oct 31]. https://sciex.com/tech-notes/biopharma/reproducible-intact-mab-analysis-icief-uv-ms.
79. Madda R, Ding J, ElNaggar M. [accessed 2024 Oct 31]. https://sciex.com/tech-notes/biopharma/icief-uv-ms-characterization-of-deglycosylated-nistmab.
80. Schlecht J, Moritz B, Kiessig S, Neusüß C. Characterization of therapeutic mAb charge heterogeneity by iCIEF coupled to mass spectrometry (iCIEF-MS). Electrophoresis. 2022;44(5–6):540–548. doi: 10.1002/elps.202200170. PMID:36148605.
81. Shen X, Liang Z, Xu T, Yang Z, Wang Q, Chen D, Pham L, Du W, Sun L. Investigating native capillary zone electrophoresis-mass spectrometry on a high-end quadrupole-time-of-flight mass spectrometer for the characterization of monoclonal antibodies. Int J Mass Spectrom. 2021;462:116541. doi: 10.1016/j.ijms.2021.116541. PMID:33642939.
82. Wang L, Bo T, Zhang Z, Wang G, Tong W, Da Yong Chen D. High resolution capillary isoelectric focusing mass spectrometry analysis of peptides, proteins, and monoclonal antibodies with a flow-through microvial interface. Anal Chem. 2018;90(15):9495–9503. doi: 10.1021/acs.analchem.8b02175. PMID:29993237.
83. Wang L, Chen DDY. Analysis of four therapeutic monoclonal antibodies by online capillary isoelectric focusing directly coupled to quadrupole time-of-flight mass spectrometry. Electrophoresis. 2019;40(21):2899–2907. doi: 10.1002/elps.201900195. PMID:31407816.
84. Xu T, Han L, George Thompson AM, Sun L. An improved capillary isoelectric focusing-mass spectrometry method for high-resolution characterization of monoclonal antibody charge variants. Ana Methods. 2021;14(4):383–393. doi: 10.1039/d1ay01556g. PMID:34939625.
85. Zhang X, Chen T, Li V, Bo T, Du M, Huang T. Cutting-edge mass spectrometry strategy based on imaged capillary isoelectric focusing (icIEF) technology for characterizing charge heterogeneity of monoclonal antibody. Analy Biochem. 2023;660:114961. doi: 10.1016/j.ab.2022.114961. PMID:36341769.
86. Zhang X, Kwok T, Zhou M, Du M, Li V, Bo T, Huang T, Chen T. Imaged capillary isoelectric focusing (icIEF) tandem high resolution mass spectrometry for charged heterogeneity of protein drugs in biopharmaceutical discovery. J Pharmaceut Biomed. 2023;224:115178. doi: 10.1016/j.jpba.2022.115178. PMID:36435084.
87. Maeda E, Urakami K, Shimura K, Kinoshita M, Kakehi K. Charge heterogeneity of a therapeutic monoclonal antibody conjugated with a cytotoxic antitumor antibiotic, calicheamicin. J Chromatogr A. 2010;1217(45):7164–7171. doi: 10.1016/j.chroma.2010.09.022. PMID:20932526.
88. Meert CD, Brady LJ, Guo A, Balland A. Characterization of antibody charge heterogeneity resolved by preparative immobilized pH gradients. Anal Chem. 2010;82(9):3510–3518. doi: 10.1021/ac902408r. PMID:20364842.
89. Turner A, Schiel JE. Qualification of NISTmAb charge heterogeneity control assays. Anal Bioanal Chem. 2018;410(8):2079–2093. doi: 10.1007/s00216-017-0816-6. PMID:29423598.
90. Mack S, Cruzado-Park I, Chapman J, Ratnayake C, Vigh G. A systematic study in CIEF: defining and optimizing experimental parameters critical to method reproducibility and robustness. Electrophoresis. 2009;30(23):4049–4058. doi: 10.1002/elps.200800690. PMID:19960469.
91. Wu G, Yu C, Wang W, Zhang R, Li M, Wang L. A platform method for charge heterogeneity characterization of fusion proteins by icIEF. Analytical Biochem. 2022;638:114505. doi: 10.1016/j.ab.2021.114505. PMID:34856184.
92. Hühner J, Neusüß C. CIEF-CZE-MS applying a mechanical valve. Anal Bioanal Chem. 2016;408(15):4055–4061. doi: 10.1007/s00216-016-9498-8.
93. Hühner J, Lämmerhofer M, Neusüß C. Capillary isoelectric focusing-mass spectrometry: coupling strategies and applications. Electrophoresis. 2015;36(21–22):2670–2686. doi: 10.1002/elps.201500185. PMID:26299384.
94. Montealegre C, Neusüß C. Coupling imaged capillary isoelectric focusing with mass spectrometry using a nanoliter valve. Electrophoresis. 2018;39(9–10):1151–1154. doi: 10.1002/elps.201800013. PMID:29469203.
95. Hühner J, Jooß K, Neusüß C. Interference-free mass spectrometric detection of capillary isoelectric focused proteins, including charge variants of a model monoclonal antibody. Electrophoresis. 2017;38(6):914–921. doi: 10.1002/elps.201600457. PMID:27885684.

96. Xu T, Han L, Sun L. Automated capillary isoelectric focusing-mass spectrometry with ultrahigh resolution for characterizing microheterogeneity and isoelectric points of intact protein complexes. Anal Chem. 2022;94 (27):9674–9682. doi: 10.1021/acs.analchem.2c00975. PMID:35766479.
97. [accessed 2024 Oct 31]. https://www.chromatographytoday.com/article/preparative/33/rozingcom-consulting/high-efficiency-preparative-imaged-capillary-isoelectric-focusing-icief-and-icief-ms-protein-charge-variant-characterisation/2950.
98. Wu G, Zhang X, Wang X, Du J, Li M, Xu G, Du M, Yu C. In-depth characterization of a cysteine-linked ADC disitamab vedotin by multiple LC-MS analysis methods and cutting-edge imaged capillary isoelectric focusing coupled with native mass spectrometry. J Chromatogr A. 2024;1736:465353. doi: 10.1016/j.chroma.2024.465353. PMID:39270568.
99. Zhang X, Wu G, Du M, Bo T, Chen T, Huang T. Imaged capillary isoelectric focusing coupled to high-resolution mass spectrometry (icIEF-MS) for cysteine-linked antibody-drug conjugate (ADC) heterogeneity characterization under native condition. Electrophoresis. 2024;45(21–22):1915–1926. doi: 10.1002/elps.202400083. PMID:39347563.
100. Chen H, Qiu D, Shi J, Wang N, Li M, Wu Y, Tian Y, Bu X, Liu Q, Jiang Y, et al. In-depth structure and function characterization of heterogeneous interchain cysteine-conjugated antibody–drug conjugates. ACS Pharmacol Transl Sci. 2024;7(1):212–221. doi: 10.1021/acsptsci.3c00235.
101. Dai J, Zhang Y. A middle-up approach with online capillary isoelectric focusing/mass spectrometry for In-depth characterization of cetuximab charge heterogeneity. Anal Chem. 2018;90(24):14527–14534. doi: 10.1021/acs.analchem.8b04396. PMID:30451489.
102. Hutanu A, Kiessig S, Bathke A, Ketterer R, Riner S, Olaf Stracke J, Wild M, Moritz B. Application of affinity capillary electrophoresis for charge heterogeneity profiling of biopharmaceuticals. Electrophoresis. 2019;40 (22):3014–3022. doi: 10.1002/elps.201900233. PMID:31560789.
103. Kumar R, Sarin D, Rathore AS. High-throughput capillary electrophoresis analysis of biopharmaceuticals utilizing sequential injections. Electrophoresis. 2023;44(9–10):767–774. doi: 10.1002/elps.202200208. PMID:36719057.
104. Kumar R, Vishwakarma G, Rathore AS. Cyclodextrins as modulators for separation of charged variants of mAbs by capillary zone electrophoresis. J Chromatogr Open. 2021;1:100011. doi: 10.1016/j.jcoa.2021.100011.
105. Legrand P, Dembele O, Alamil H, Lamoureux C, Mignet N, Houzé P, Gahoual R. Structural identification and absolute quantification of monoclonal antibodies in suspected counterfeits using capillary electrophoresis and liquid chromatography-tandem mass spectrometry. Anal Bioanal Chem. 2022;414(8):2699–2712. doi: 10.1007/s00216-022-03913-y.
106. Wheeler TD, Sun JL, Pleiner S, Geier H, Dobberthien P, Studts J, Singh R, Fathollahi B. Microchip zone electrophoresis for high-throughput analysis of monoclonal antibody charge variants. Anal Chem. 2014;86 (11):5416–5424. doi: 10.1021/ac500497n. PMID:24786229.
107. Goyon A, Francois YN, Colas O, Beck A, Veuthey JL, Guillarme D. High-resolution separation of monoclonal antibodies mixtures and their charge variants by an alternative and generic CZE method. Electrophoresis. 2018;39(16):2083–2090. doi: 10.1002/elps.201800131. PMID:29774560.
108. Biacchi M, Gahoual R, Said N, Beck A, Leize-Wagner E, François Y-N. Glycoform separation and characterization of cetuximab variants by middle-up off-line capillary zone electrophoresis-UV/Electrospray ionization-MS. Anal Chem. 2015;87(12):6240–6250. doi: 10.1021/acs.analchem.5b00928. PMID:25970692.
109. Biacchi M, Said N, Beck A, Leize-Wagner E, François Y-N. Top-down and middle-down approach by fraction collection enrichment using off-line capillary electrophoresis – mass spectrometry coupling: application to monoclonal antibody F c/2 charge variants. J Chromatogr A. 2017;1498:120–127. doi: 10.1016/j.chroma.2017.02.064. PMID:28259456.
110. François Y-N, Biacchi M, Said N, Renard C, Beck A, Gahoual R, Leize-Wagner E. Characterization of cetuximab Fc/2 dimers by off-line CZE-MS. Analytica (Rome) Acta. 2016;908:168–176. doi: 10.1016/j.aca.2015.12.033. PMID:26826699.
111. Han H, Livingston E, Chen X. High throughput profiling of charge heterogeneity in antibodies by microchip electrophoresis. Anal Chem. 2011;83(21):8184–8191. doi: 10.1021/ac201741w. PMID:21928854.
112. Shi Y, Li Z, Qiao Y, Lin J. Development and validation of a rapid capillary zone electrophoresis method for determining charge variants of mAb. J Chromatogr: B, Analytical Technol Biomed Life Sci. 2012;906:63–68. doi: 10.1016/j.jchromb.2012.08.022. PMID:22954968.
113. Jooß K, Hühner J, Kiessig S, Moritz B, Neusüß C. Two-dimensional capillary zone electrophoresis–mass spectrometry for the characterization of intact monoclonal antibody charge variants, including deamidation products. Anal Bioanal Chem. 2017;409(26):6057–6067. doi: 10.1007/s00216-017-0542-0.
114. Schlecht J, Jooß K, Neusüß C. Two-dimensional capillary electrophoresis-mass spectrometry (CE-CE-MS): coupling MS-interfering capillary electromigration methods with mass spectrometry. Anal Bioanal Chem. 2018;410(25):6353–6359. doi: 10.1007/s00216-018-1157-9.
115. Schlecht J, Jooß K, Moritz B, Kiessig S, Neusüß C. Two-dimensional capillary zone electrophoresis-mass spectrometry: intact mAb charge variant separation followed by peptide level analysis using In-capillary digestion. Anal Chem. 2023;95(8):4059–4066. doi: 10.1021/acs.analchem.2c04578. PMID:36800441.

116. Belov AM, Zang L, Sebastiano R, Santos MR, Bush DR, Karger BL, Ivanov AR. Complementary middle-down and intact monoclonal antibody proteoform characterization by capillary zone electrophoresis – mass spectrometry. Electrophoresis. 2018;39(16):2069–2082. doi: 10.1002/elps.201800067. PMID:29749064.
117. Belov AM, Viner R, Santos MR, Horn DM, Bern M, Karger BL, Ivanov AR. Analysis of proteins, protein complexes, and organellar proteomes using sheathless capillary zone electrophoresis - native mass spectrometry. J Am Soc Mass Spectrom. 2017;28(12):2614–2634. doi: 10.1007/s13361-017-1781-1. PMID:28875426.
118. Cao L, Fabry D, Lan K. Rapid and comprehensive monoclonal antibody characterization using microfluidic CE-MS. J Pharm Biomed Anal. 2021;204:114251. doi: 10.1016/j.jpba.2021.114251. PMID:34265486.
119. Carillo S, Jakes C, Bones J. In-depth analysis of monoclonal antibodies using microfluidic capillary electrophoresis and native mass spectrometry. J Pharm Biomed Anal. 2020;185:113218. doi: 10.1016/j.jpba.2020.113218. PMID:32193040.
120. Chen C-H, Feng H, Guo R, Li P, Laserna AKC, Ji Y, Ng BH, Li SFY, Khan SH, Paulus A, et al. Intact NIST monoclonal antibody characterization—proteoforms, glycoforms—using CE-MS and CE-LIF. Cogent Chem. 2018;4(1):1480455. doi: 10.1080/23312009.2018.1480455.
121. Giorgetti J, Beck A, Leize-Wagner E, François Y-N. Combination of intact, middle-up and bottom-up levels to characterize 7 therapeutic monoclonal antibodies by capillary electrophoresis - mass spectrometry. J Pharm Biomed Anal. 2020;182:113107. doi: 10.1016/j.jpba.2020.113107. PMID:32004767.
122. Giorgetti J, Lechner A, Del Nero E, Beck A, François Y-N, Leize-Wagner E. Intact monoclonal antibodies separation and analysis by sheathless capillary electrophoresis-mass spectrometry. Eur J Mass Spectrom (chichester). 2019;25(3):324–332. doi: 10.1177/1469066718807798. PMID:30351978.
123. Gstöttner C, Nicolardi S, Haberger M, Reusch D, Wuhrer M, Domínguez-Vega E. Intact and subunit-specific analysis of bispecific antibodies by sheathless CE-MS. Anal Chim Acta. 2020;1134:18–27. doi: 10.1016/j.aca.2020.07.069. PMID:33059862.
124. Gstöttner C, Vergoossen DLE, Wuhrer M, Huijbers MGM, Domínguez-Vega E. Sheathless CE-MS as a tool for monitoring exchange efficiency and stability of bispecific antibodies. Electrophoresis. 2021;42(1–2):171–176. doi: 10.1002/elps.202000166. PMID:32901958.
125. Gstöttner C, Lippold S, Hook M, Yang F, Haberger M, Wuhrer M, Falck D, Schlothauer T, Domínguez-Vega E. Benchmarking glycoform-resolved affinity separation - mass spectrometry assays for studying FcγRIIIa binding. Front Immunol. 2024;15:1347871. doi: 10.3389/fimmu.2024.1347871. PMID:38469305.
126. Gstöttner C, Hook M, Christopeit T, Knaupp A, Schlothauer T, Reusch D, Haberger M, Wuhrer M, Domínguez-Vega E. Affinity capillary electrophoresis-mass spectrometry as a tool to unravel proteoform-specific antibody-receptor interactions. Anal Chem. 2021;93(45):15133–15141. doi: 10.1021/acs.analchem.1c03560. PMID:34739220.
127. Han M, Rock BM, Pearson JT, Rock DA. Intact mass analysis of monoclonal antibodies by capillary electrophoresis—mass spectrometry. J Chromatogr: B, Analytical Technol Biomed Life Sci. 2016;1011:24–32. doi: 10.1016/j.jchromb.2015.12.045. PMID:26751590.
128. Haselberg R, de Vijlder T, Heukers R, Smit MJ, Romijn EP, Somsen GW, Domínguez-Vega E. Heterogeneity assessment of antibody-derived therapeutics at the intact and middle-up level by low-flow sheathless capillary electrophoresis-mass spectrometry. Anal Chim Acta. 2018;1044:181–190. doi: 10.1016/j.aca.2018.08.024. PMID:30442400.
129. Jooß K, McGee JP, Melani RD, Kelleher NL. Standard procedures for native CZE-MS of proteins and protein complexes up to 800 kDa. Electrophoresis. 2021;42(9–10):1050–1059. doi: 10.1002/elps.202000317. PMID:33502026.
130. Le-Minh V, Tran NT, Makky A, Rosilio V, Taverna M, Smadja C. Capillary zone electrophoresis-native mass spectrometry for the quality control of intact therapeutic monoclonal antibodies. J Chromatogr A. 2019;1601:375–384. doi: 10.1016/j.chroma.2019.05.050. PMID:31160095.
131. Redman EA, Batz NG, Mellors JS, Ramsey JM. Integrated microfluidic capillary electrophoresis-electrospray ionization devices with online MS detection for the separation and characterization of intact monoclonal antibody variants. Anal Chem. 2015;87(4):2264–2272. doi: 10.1021/ac503964j. PMID:25569459.
132. Srzentić K, Fornelli L, Tsybin YO, Loo JA, Seckler H, Agar JN, Anderson LC, Bai DL, Beck A, Brodbelt JS, et al. Interlaboratory study for characterizing monoclonal antibodies by top-down and middle-down mass spectrometry. J Am Soc Mass Spectrom. 2020;31(9):1783–1802. doi: 10.1021/jasms.0c00036.
133. Sun Q, Wang L, Li N, Shi L. Characterization and monitoring of charge variants of a recombinant monoclonal antibody using microfluidic capillary electrophoresis-mass spectrometry. Analytical Biochem. 2021;625:114214. doi: 10.1016/j.ab.2021.114214. PMID:33915116.
134. Elektroforéza K. [accessed 2021 June 8]. https://lcms.labrulez.com/paper/12173.
135. Wu Z, Wang H, Wu J, Huang Y, Zhao X, Nguyen JB, Rosconi MP, Pyles EA, Qiu H, Li N. High-sensitivity and high-resolution therapeutic antibody charge variant and impurity characterization by microfluidic native capillary electrophoresis-mass spectrometry. J Pharm Biomed Anal. 2023;223:115147. doi: 10.1016/j.jpba.2022.115147. PMID:36399907.
136. Wu Z, Wang H, Zhao X, Gong C, Sidnam S, Cantero-Tubilla B, Nedjic-Dugic B, Li M, Wu J, Su Y, et al. Characterization of therapeutic antibody charge heterogeneity under stress conditions by microfluidic capillary

electrophoresis coupled with mass spectrometry. J Pharm Sci. 2024;113(8):2170–2177. doi: 10.1016/j.xphs.2024.05.022. PMID:38796156.
137. Xu T, Zhang F, Chen D, Sun L, Tomazela D, Fayadat-Dilman L. Interrogating heterogeneity of cysteine-engineered antibody-drug conjugates and antibody-oligonucleotide conjugates by capillary zone electrophoresis-mass spectrometry. Mabs-austin. 2023;15(1):2229102. doi: 10.1080/19420862.2023.2229102. PMID:37381585.
138. Suresh Babu CV, Gudihal R. [accessed 2025 Jan 28]. https://hpst.cz/sites/default/files/oldfiles/5991-5212en.pdf .
139. Biacchi M, Bhajun R, Saïd N, Beck A, François YN, Leize-Wagner E. Analysis of monoclonal antibody by a novel CE-UV/MALDI-MS interface. Electrophoresis. 2014;35(20):2986–2995. doi: 10.1002/elps.201400276. PMID:25070377.
140. Schwenzer A-K, Kruse L, Jooß K, Neusüß C. Capillary electrophoresis-mass spectrometry for protein analyses under native conditions: current progress and perspectives. Proteomics. 2024;24(3–4):e2300135. doi: 10.1002/pmic.202300135. PMID:37312401.
141. Madren S, Yi L. Microchip electrophoresis separation coupled to mass spectrometry (MCE–MS) for the rapid monitoring of multiple quality attributes of monoclonal antibodies. Electrophoresis. 2022;43(23–24):2453–2465. doi: 10.1002/elps.202200129.
142. Faid V, Leblanc Y, Berger M, Seifert A, Bihoreau N, Chevreux G. C-terminal lysine clipping of IgG1: impact on binding to human FcγRIIIa and neonatal Fc receptors. Eur J Pharm Sci. 2021;159:105730. doi: 10.1016/j.ejps.2021.105730.
143. Lu X, Machiesky LA, de Mel N, Du Q, Xu W, Washabaugh M, Jiang X-R, Wang J. Characterization of IgG1 Fc deamidation at asparagine 325 and its impact on antibody-dependent cell-mediated cytotoxicity and FcγRIIIa binding. Sci Rep. 2020;10(1):383. doi: 10.1038/s41598-019-57184-2. PMID:31941950.
144. Höcker O, Montealegre C, Neusüß C. Characterization of a nanoflow sheath liquid interface and comparison to a sheath liquid and a sheathless porous-tip interface for CE-ESI-MS in positive and negative ionization. Anal Bioanal Chem. 2018;410(21):5265–5275. doi: 10.1007/s00216-018-1179-3.
145. Leng C, Sun S, Lin W, Pavon JA, Gennaro L, Gunawan RC, Bu X, Yang T, Li S. Imaged capillary isoelectric focusing method development for charge variants of high DAR ADCs. Analytica (Rome) Acta. 2024;1328:343176. doi: 10.1016/j.aca.2024.343176. PMID:39266202.
146. Schlecht J, Stolz A, Hofmann A, Gerstung L, Neusüß C. nanoCeasy: an easy, flexible, and robust nanoflow sheath liquid capillary electrophoresis-mass spectrometry interface based on 3D printed parts. Anal Chem. 2021;93(44):14593–14598. doi: 10.1021/acs.analchem.1c03213. PMID:34719920.
147. Dhellemmes L, Leclercq L, Höchsmann A, Neusüß C, Biron J-P, Roca S, Cottet H. Critical parameters for highly efficient and reproducible polyelectrolyte multilayer coatings for protein separation by capillary electrophoresis. J Of Chromatography A. 2023;1695:463912. doi: 10.1016/j.chroma.2023.463912. PMID:36972664.